Title
Structural Diversification of Saturated Cyclic Amines Through Photo- and Metal-Mediated Ring Opening

Author
Soro, David Martin

Publication Date
2023

Peer reviewed|Thesis/dissertation

Structural Diversification of Saturated Cyclic Amines Through Photo- and Metal-Mediated Ring Opening

by

David Martin Soro

A dissertation submitted in partial satisfaction of the

requirements for the degree of

Doctor of Philosophy

in

Chemistry

in the

Graduate Division

of the

University of California, Berkeley

Committee in charge:

Professor Richmond Sarpong, Chair
Professor John F. Hartwig
Professor Roberto Zoncu

Summer 2023

Structural Diversification of Saturated Cyclic Amines Through Photo- and Metal-Mediated Ring Opening

Abstract

Structural Diversification of Saturated Cyclic Amines Through Photo- and Metal-Mediated Ring Opening

by

David Martin Soro

Doctor of Philosophy in Chemistry

University of California, Berkeley

Professor Richmond Sarpong, Chair

This dissertation describes studies toward the core modification of cyclic aliphatic amines aimed at late-stage structural diversification. The main strategy involves oxidative C–N and/or C–C bond cleavage to open the cyclic amine core, and this work explores mild methods for ring opening in order to provide wide functional group tolerance, as well as opportunities for bond formation following ring opening. These investigations are contingent on the use of peroxydisulfate (persulfate) as a versatile oxidant that can be paired with metal or non-metal oxidative mediators for a set of distinct outcomes involving transformation of the cyclic amine framework. Specifically, Chapter 1 discusses mild, oxidative ring opening of cyclic amines to access linear aldehydes using flavin-derived photoredox catalysis. Linear carboxylic acids are also accessed with copper salts as a mediator. The mechanisms of these two reactions are investigated by computation. The computations suggest that the flavin-mediated oxidation is initiated by hydrogen-atom transfer from the cyclic amine to the photocatalyst, whereas the copper-mediated process begins instead with single-electron oxidation of the cyclic amine with concomitant reduction of persulfate. Chapter 2 describes ring opening of cyclic amines and subsequent C–C and C–O bond formation in one-pot reactions, enabled by the intermediacy of a primary alkyl radical. Ring opening followed by radical decarboxylation with Ag(I) and persulfate enables a Minisci-type Csp^3–Csp^2 coupling to form alkylamine-substituted pyridines. Additionally, Cu(II) oxidation of the alkyl radical arising from N-acylated cyclic amines leads to a C–O bond-forming cyclization event producing oxazines, constituting a heterocycle replacement of the cyclic amine core. While Cu(II) oxidations of radicals typically favor elimination pathways leading to olefins, computational studies into the cyclization indicate that cyclization is kinetically preferred over elimination in this instance.

Contents

List of Figures

List of Tables

List of Schemes

Acknowledgments

I would like to thank Professor Richmond Sarpong for providing me with space to work on my research, feedback and ideas for my projects, and advice for my time as a graduate student and beyond. I never thought that I would be receiving my doctoral degree having been a student in your research group, but I am grateful that you made the time to meet with me several years ago when I expressed my interest in graduate school. I was challenged in many ways being in your research group, and I learned so much from the experience. The knowledge I have now will be instrumental in my future.

I am also fortunate to have worked with several others during my time in graduate school, both from UC Berkeley as well as other institutions. I would like to thank Jose Roque, Jonas Rackl, Stefan Payer, Shelby McCowen, and Hélöise Colombano who were all members of the Sarpong research group and collaborators on various projects. I am also thankful to have worked with Dr. Yuan Shi and Dr. J. Craig Ruble from Eli Lilly, Professor Djamaladdin Musaev and Dr. Alexey Kaledin from Emory University, as well as Bohyun Park and Professor Mookie Baik from KAIST. I am also grateful for my cohort members with whom I started my degree: William Kayitare, Kerry Jones, Jin Su Ham, and Brandon Wright. They were all immensely helpful as I adjusted to organic chemistry research during my first year.

I would like to give a special thanks to Dr. Xing Gao, with whom I have now spent almost a decade in academia. I could not have imagined where our futures would take us after our chemistry class together during our first year of college. Though we never had another class together since then, I am so glad that we still were part of each other's academic trajectory. It meant so much to be able to spend time together on good days and bad, share our fears and triumphs, and grow with one another both personally and as scholars. In the times that I was not sure that I could see myself through to the end of the degree, the encouragement I received from her helped me make it past those tough times. I would not have gotten to where I am without her there. Though our time together as students in academia is ending, I am excited to see where our post-academic lives take us (and who knows, maybe we will be back?).

Finally, I would like to thank my family, Nancy, Tenena, and Jackie. Even though we were practically on opposite sides of the country, I still felt their support during my time at Berkeley. No matter what I was going through, they always had my back and were there to give me their wisdom and advice.

Chapter 1

Development of Mild Conditions for Oxidative Ring-Opening of Cyclic Amines*

1.1 Introduction

Modern drug discovery has benefited from advancements in chemical reaction development.[1] For example, the development of selective C–H functionalization has changed how synthetic chemists approach the retrosynthetic analysis of bioactive compounds.[2] Largely, disconnections of molecules to simpler precursors through a retrosynthesis exercise focuses on removal of peripheral groups.[3,4] As a result, in the forward sense, syntheses and late-stage diversification of molecules have mostly focused on peripheral modification. Alternatively, an emerging approach to access novel chemical space has been centered around making modifications to the core framework of molecules, in contrast to traditional molecular structural diversification approaches.[5,6] Recognizing a need for more methods to accomplish modification of the core framework of molecules (skeletal editing) to access unique chemical and functional space, we have initiated a program aimed at the deconstructive functionalization (i.e., breaking of traditionally strong bonds, such as C–C and C–N bonds, and functionalization of their constituent atoms) of saturated cyclic amines in order to access new chemical space. We have primarily focused on saturated azacycles, especially piperidines, given their prevalence in pharmaceuticals,[7] as well as agrochemicals.[8] Our previous studies have identified ring opening,[9] ring contraction,[10] as well as heterocycle replacement methods[11] for achieving skeletal diversity (Figure 1.1A).

We have found oxidative pathways to be particularly effective for the deconstructive functionalization of cyclic aliphatic amines (saturated azacycles).[9,10] In complementary approaches, others have demonstrated oxidative bond cleavage of cyclic amines under aerobic conditions,[12–14] as well as through the use of metal-oxo species.[15–17] While these strategies

*This chapter is adapted from previously published work: *J. Am. Chem. Soc.* **2023**, *145*, 11245–11257.

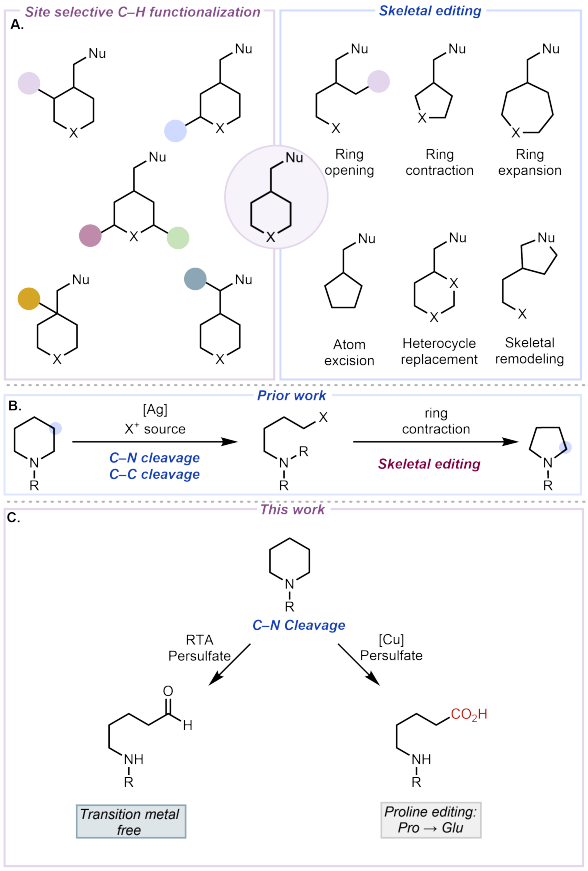

Figure 1.1: A. Site selective C–H functionalization and skeletal editing; B. Prior work; C. This work.

provide effective ways to achieve diversity in cyclic amine transformations, metal-oxo catalysts tend to favor oxidative pathways leading to imide products;[18] peripheral modification is favored over core modification for these catalysts. Our goal was to develop a straightforward, distinct approach that would achieve a reconfiguration of the cyclic amine skeleton through structural transformations beyond ring opening. Peroxydisulfate (persulfate) has been shown to serve as a versatile oxidant in various contexts. Given its high oxidation potential (2.01 V in aqueous solution),[19,20] the redox reactivity of persulfate with transition metals or organic substrates can lead to different outcomes. In particular, persulfate has been used in the oxidative functionalization of amines, providing access to α-amino radicals and iminium intermediates.[21] On this basis, our lab previously reported the deconstructive diversification of cyclic amines using a Ag(I)-persulfate combination (Figure 1.1B).[9,10] With the goal of increasing the diversity of scaffolds that could be accessed, we envisioned that persulfate might serve a key role in the deconstructive functionalization of saturated cyclic

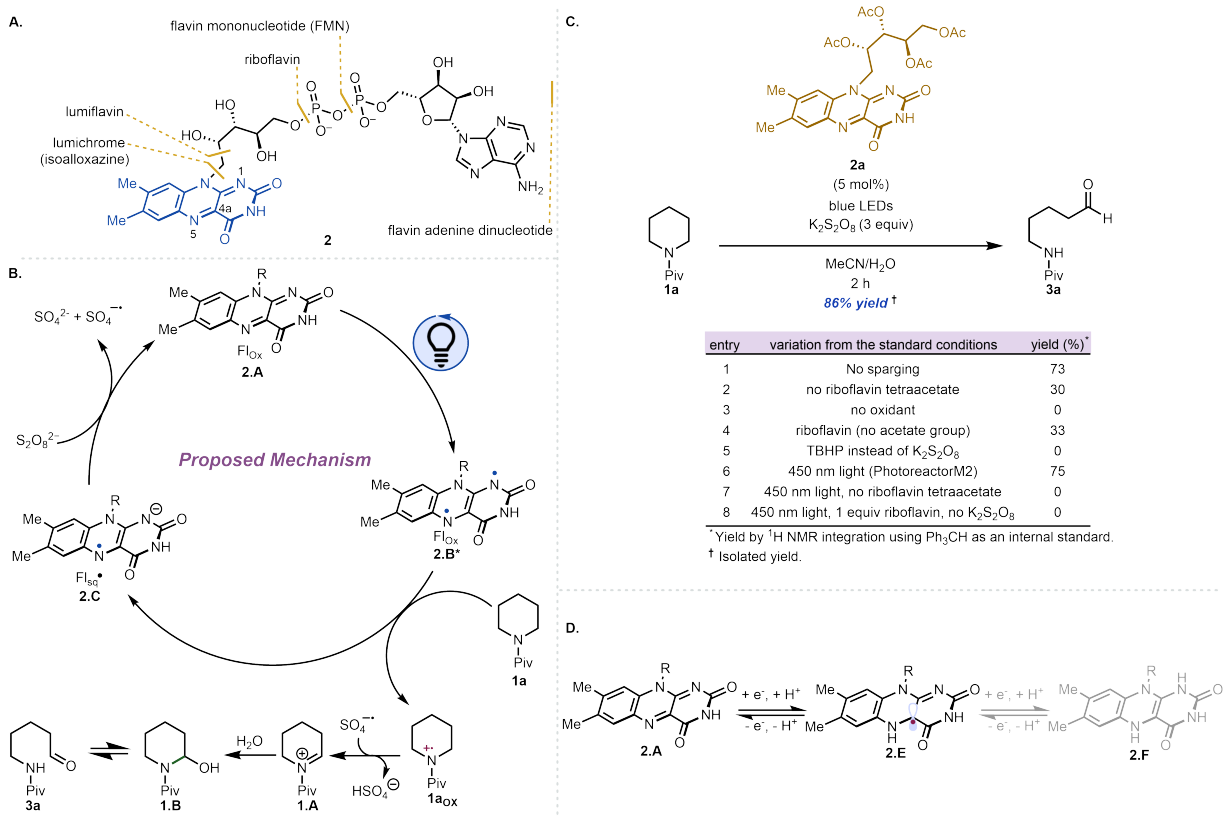

Figure 1.2: A. Flavin derivatives; B. Proposed reaction mechanism for the ring-opening oxidation of cyclic amines using riboflavin tetraacetate; C. Selected reaction optimization experiments (see Section 1.4 for full details); D. Typical redox states of flavin molecules.

amines by mediating the cleavage of the C–N bond to provide novel acyclic structures. By pairing the persulfate oxidant with various redox-active co-reagents, we anticipated tuning the deconstructive process in order to access a broad range of scaffolds.

Herein, we present complementary efforts that achieve saturated azacycle diversification. Specifically, we report two mild oxidative ring opening methods using riboflavin-persulfate and copper-persulfate combinations that generate aldehydes and acyclic alkyl carboxylic acids, respectively (Figure 1.1C).

1.2 Results and Discussion

Bio-inspired deconstructive functionalization

Flavins, a set of molecules featuring an isoalloxazine core (Figure 1.2A), are key facilitators in a subset of biological electron transfer processes including the oxidation of amines

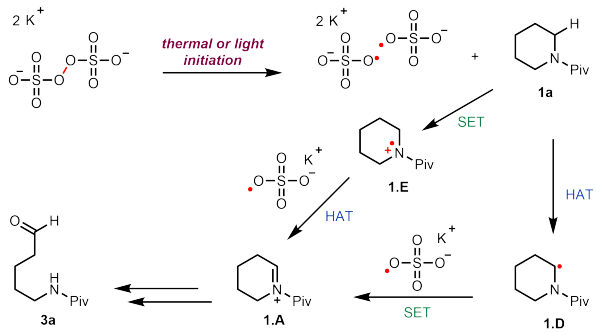

Scheme 1.1: Light or thermal driven homolysis of persulfate leading to cyclic amine oxidation.

by monoamine oxidases (MAOs).[22] They have also been used in non-biological contexts for similar purposes.[23] As such, we wondered whether they could effect non-biological oxidative diversification of cyclic aliphatic amines. A general mechanism for our proposed transformation of saturated cyclic amines using the riboflavin-persulfate system is depicted in Figure 1.2B. Excitation of an isoalloxazine derivative (**2.A**) was expected to generate an excited state photocatalyst (**2.B***). This excited state species should then oxidize cyclic amine **1a** via photoinduced electron transfer (PET) to produce an amidyl radical cation ($\mathbf{1a}_{ox}$) and reduced photocatalyst (**2.C**). Oxidation of the reduced photocatalyst by a persulfate ion would regenerate quinone **2.A** as well as a sulfate radical anion. The sulfate radical anion was anticipated to effect α-amino C–H abstraction of $\mathbf{1a}_{ox}$ to generate iminium ion **1.A**. As previously proposed by our group using the combination of Ag(I) and persulfate,[9,10] the resulting iminium ion (**1.A**) would then be trapped by H_2O to give hemi-aminal **1.B**, which would suffer heterolytic C–N bond cleavage to furnish aldehyde **3a**. A pivaloyl group on the nitrogen atom was identified previously to be optimal in favoring the open-chain aminoaldehyde product (**3a**).[10]

We commenced our investigations of the oxidative C–N bond cleavage by evaluating a broad range of photoredox catalysts, oxidants, and solvent combinations (See Section 1.4 for details). After extensive optimization, we identified the conditions shown in Figure 1.2C that employ 5 mol% of riboflavin tetraacetate, 3 equivalents of $K_2S_2O_8$ in a 1:1 (v/v) mixture of MeCN/H_2O, and irradiation with blue light-emitting diodes (Kessil brand A160WE Tuna Blue LED 40 W lamp).

We considered whether the quinone state of the riboflavin photocatalyst (see **2.A** in Figure 1.2D) might oxidize the cyclic amine substrate and form its one-electron-reduced semiquinone state (**2.E**). **2.E** might be subsequently oxidized without reaching the fully reduced hydroquinone state (**2.F**), although that remained to be fully supported by additional studies. We hypothesized that upon generation of semiquinone **2.E**, oxidation by persulfate occurs to regenerate **2.A**, the corresponding sulfate dianion, and sulfate radical anion. Furthermore, the sulfate radical anion can also oxidize semiquinone **2.E**.

To investigate our mechanistic hypothesis, we investigated the outcome of the reaction under a series of altered conditions. Performing the reaction without sparging the reaction mixture (entry 1, Figure 1.2C) led to a slightly diminished yield, presumably due to some catalyst deactivation by molecular oxygen. In the absence of riboflavin tetraacetate, only a 30% yield of product is obtained (entry 2). Likely, in this case, the product arises from light or thermal activation in which homolytic O–O cleavage of the persulfate leads to two sulfate radical anions which effect α-amino C–H abstraction leading to **1.D** followed by single-electron oxidation to generate **1.A** (Scheme 1.1). An alternative productive pathway, given the oxidizing strength of sulfate radical anions (+2.4 V vs. SCE), could proceed through an initial oxidation of the substrate, forming radical cation **1.E**, prior to α-amino C–H abstraction.[24] The light-driven homolysis of persulfate has been previously reported.[20] Unfortunately, increased loadings of $K_2S_2O_8$ along with increased temperature and/or longer reaction times did not improve the yield, leading instead to undesired reactivity such as over-oxidation. The use of riboflavin instead of riboflavin tetraacetate also led to diminished yields (entry 4). Riboflavin has been reported to undergo rapid photodegradation upon irradiation,[25,26] which might contribute to the decreased yields. The acetylation of the ribose side chain (i.e., riboflavin $\rightarrow$ riboflavin tetraacetate) presumably prevents competing intramolecular hydrogen atom transfer from the T_1 excited state.[27]

In our studies, persulfate emerged as the superior oxidant as other oxidants led to lower yields (entry 5). Control studies confirmed the importance of both the oxidant and light source as the desired product was not observed when either component was excluded from the reaction conditions. Irradiation with 450 nm blue LEDs (Penn PhD Photoreactor M2) in the absence of riboflavin tetraacetate led to recovered starting material (entry 7). Presumably, O–O bond homolysis does not occur with irradiation at 450 nm;[28] this is also supported by our calculated UV–Vis spectrum of $K_2S_2O_8$ (see Section 1.4). Additionally, the use of one equivalent of riboflavin tetraacetate as the sole oxidant in the reaction led only to recovery of the starting material without any observed product formation. However, upon the combination of 5 mol% of riboflavin tetraacetate with persulfate, a 75% yield of aldehyde **3a** was obtained (entry 6). These experiments, as well as the low yields obtained using $K_2S_2O_8$ alone, suggest the major pathway for product formation is not light- or thermal-driven O–O bond homolysis followed by SET. Rather, it is driven by the combined action of the photocatalyst and oxidant. Furthermore, no correlation was observed between the excited state triplet energies of the photocatalysts examined and starting material consumption (see Section 1.4 for details). These experiments imply triplet energy transfer pathways are not operating in these oxidative ring-opening reactions.

Following our identification of an efficient set of conditions, we investigated the scope of the transition metal-free oxidative C–N cleavage protocol (Figure 1.3). Various substitution patterns on the piperidine ring were tolerated, providing access to the corresponding acyclic amines in moderate to good yields (43–95%). For example, 4-subsituted piperidines (**1b**–**1f**) led to β-substituted aliphatic aldehydes (**3b**–**3f**). Notably, piperidines containing benzylic sites that are susceptible to oxidation afforded the corresponding aldehydes (**3b** and **3c**) in 62% and 43% yield, respectively. Piperidines bearing ester functional groups on the satu-

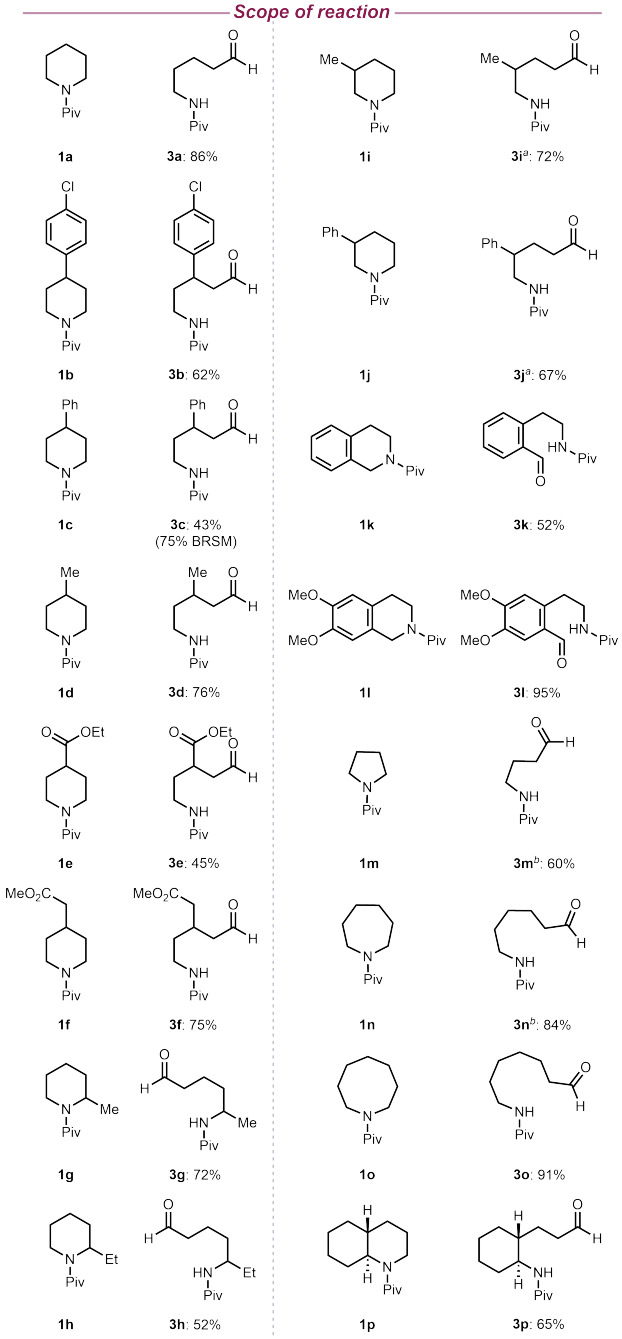

Figure 1.3: **Cyclic amine scope.** Only isolated yields are shown. Reaction conditions: Cyclic amine (0.2 mmol), RTA (5 mol%), $K_2S_2O_8$ (3 equivalents), MeCN: H_2O (1:1), blue LEDs, 2 hours. All reactions were conducted using a Kessil lamp for irradiation. [a]Major isolated constitutional isomer shown. [b]Isolated yield of acid product: **3m**: 2.5%, **3n**: 13%).

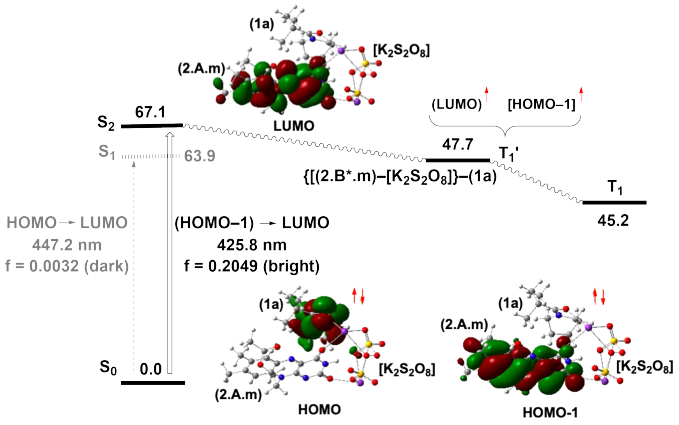

Figure 1.4: Schematic presentation of radiative generation of the S_2 excited state of the riboflavin-persulfate-substrate adduct (**2.A.m**)–[$K_2S_2O_8$]–**1a**. All energies are shown in kcal/mol.

rated azacycle backbone (e.g., **1e** and **1f**) also worked well. Complete positional selectivity was observed when 2-substituted piperidines (**1g**, **1h**) were subjected to the oxidative ring opening protocol. Presumably, the selectivity that is observed is dictated by sterics in accordance with literature precedent.[9,10,29] However, 3-substituted piperidines (**3i**, **3j**) gave a mixture of constitutional isomers.

Our transition metal-free oxidative protocol is not limited to piperidines. For example, skeletal diversification of the tetrahydroisoquinoline skeleton, which is present in a significant number of pharmaceuticals and natural products,[30,31] is also possible. *N*-Pivaloyltetrahydroisoquinoline **1k** underwent oxidative ring opening to provide aldehyde **3k** in 52% yield. Notably, the C–N bond proximal to the arene ring was selectively cleaved. Furthermore, competing α-C–H abstraction was not observed despite the presence of two ether functional groups in **1l**; benzaldehyde **3l** was obtained in 95% yield. The α-arylation of ethers has been recently reported featuring open-shell alkyl radical intermediates which add to heteroarenes (i.e., Minisci reaction).[32] In these cases, the participating radicals were generated by hydrogen atom abstraction with persulfate.

Saturated azacycles of various ring sizes underwent oxidative ring opening to provide the corresponding aliphatic aldehydes in moderate to good yield (60%–91%). However, in the case of **3m** and **3n**, the aldehyde groups underwent subsequent oxidation to the corresponding carboxylic acids, resulting in a mixture of products that was easily separated (see Section 1.4 for details).

In order to gain insight into the transition metal-free oxidative C–N cleavage protocol, we turned to density functional theory (DFT) and time-dependent DFT (TD-DFT) calcu-

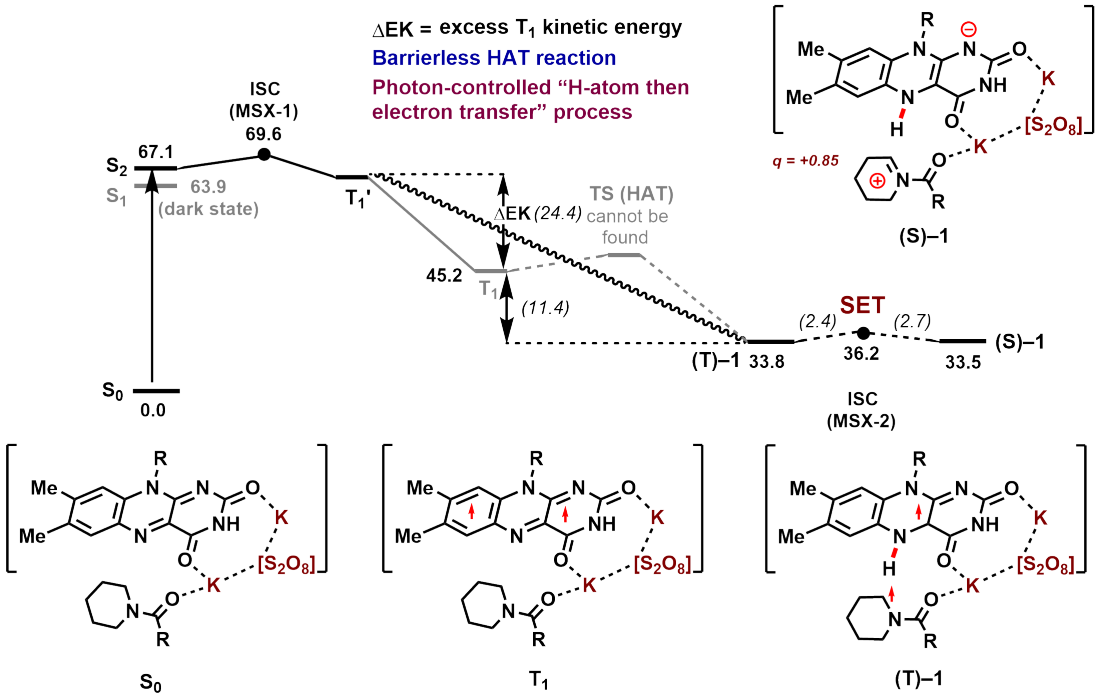

Figure 1.5: Computed reaction pathways for the oxidation of **1a** to **1.A**. All energies are Gibbs free energies listed in kcal/mol (energy differences are shown in parentheses).

lations.[†] Following a series of computations to validate our models (see Section 2.4), we selected riboflavin monoacetate (**2.A.m**, where "**m**" stands for monoacetate) as a model for riboflavin tetraacetate (**2.A**), which was used in our experiments. The calculations show that the formation of (**2.A.m**)–[$K_2S_2O_8$] adduct is exergonic by 5.9 kcal/mol. Since the coordination of **1a** to (**2.A.m**)–[$K_2S_2O_8$] that leads to the (**2.A.m**)–[$K_2S_2O_8$]–(**1a**) adduct, $\mathbf{S_0}$, is also exergonic (by 3.2 kcal/mol), we selected the $\mathbf{S_0}$ adduct as the photon-absorbing species which aligns with precedent demonstrating prior coordination of persulfate to the photocatalyst.[33] Here, we discuss only the energetically lowest conformers of every calculated structure and the corresponding Gibbs free energies unless otherwise stated—full computational details are described in Section 1.4.

Our calculated reaction mechanism for the oxidation of **1a** is described in Figure 1.5. Irradiation of $\mathbf{S_0}$ with blue light (see Section 1.4 for the computed UV–Vis spectra of $\mathbf{S_0}$, (**2.A.m**)–[$K_2S_2O_8$], and **2.A.m**) results in excitation to its S_2 bright state (see Figure 1.4). Its energetically lower-lying S_1 state is a largely dark state that is unlikely to contribute to the reaction (see Section 1.4). The bright S_0/S_2 transition is the (HOMO–1)–LUMO (i.e.,

[†]Calculations were performed by Djamaladdin G. Musaev and Alexey L. Kaledin at the Cherry L. Emerson Center for Scientific Computation and Department of Chemistry, Emory University, 1515 Dickey Drive, Atlanta, GA, United States.

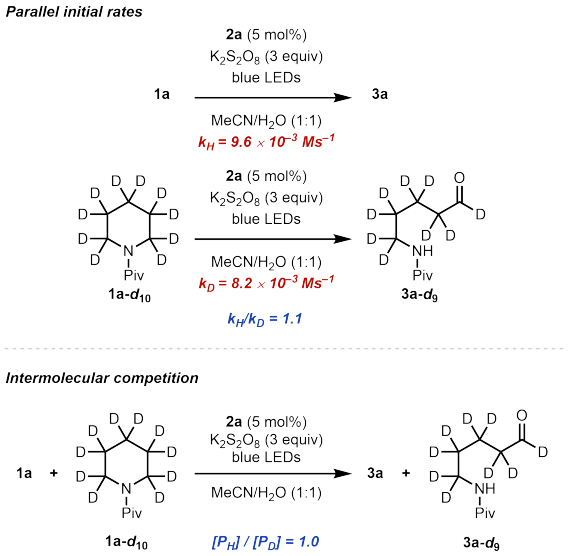

Figure 1.6: Initial rates for **1a** and **1a-d$_{10}$**; $k_H/k_D = 1.1$. Intermolecular competition experiments (0.05 mmol **1a** + 0.05 mmol **1a-d$_{10}$**); $[P_H]/[P_D] = 1.0$. See Section 1.4 for full details.

π–π^*) transition associated with the riboflavin fragment (see Section 1.4). The excited S_2 state of this system quenches to the optically dark triplet state T_1 (through the T_1' state, see Figures 1.4 and 1.5) through the S_0/T_1 seam of crossing (MSX), which was determined to have a minimum point of 3.02 eV. Thus, the photoinitiated $S_0 \rightarrow T_1$ transition is controlled by the minimum on the S_0/T_1 seam of crossing (MSX), which is energetically easily accessible at the wavelengths used in our experiments. The MSX serves as an interfacial "funnel", which can also be described as intersystem crossing (ISC), from the optically bright singlets to the reactive T_1 potential energy surface. The calculated 1.06 eV energy difference between the MSX point and the T_1 minimum of the complex is internal energy that is available to complete the hydrogen atom transfer (HAT) from cyclic amine **1a** to the excited state riboflavin-persulfate complex. This process has no associated energy barrier and forms the triplet state intermediate **(T)-1**. This conclusion is consistent with parallel reaction KIE studies using Piv-protected piperidine-d_{10} (**1a-*d*$_{10}$**). The results of the parallel experiments and intermolecular competition experiments do not support rate-limiting C–H bond cleavage (see Figure 1.6). Additionally, while we could not rule out radical chain pathways,[34] a light on/off study revealed that any chain processes are short-lived, and irradiation is required for continued product formation (See Section 1.4).

Calculations show that the formation of intermediate **(T)-1** is exergonic by 11.4 kcal/mol, relative to the optimized T_1 state. Our computational analyses show that **(T)-1** possesses one less α-amino H-atom and has almost one full α-spin. Another unpaired α-spin is located in the riboflavin fragment. The subsequent SET from the α-amino radical (i.e., **1a'**) to (**2.E.m**)–$[K_2S_2O_8]$ in **(T)-1** is almost thermoneutral. In the resulting singlet state interme-

diate **(S)–1**, the isoalloxazine is fully reduced and iminium ion **1.A** has formed. Extensive analyses show that the **(T)-1→(S)-1** transition occurs through the triplet-to-singlet seam of crossing (MSX), which has a minimum point located only 2.4 kcal/mol higher than **(T)-1**; therefore, the SET in **(T)-1** is a facile process and the **(T)-1→(S)-1** transition is exergonic by only 0.3 kcal/mol. Dissociation of iminium ion **1.A** from **(S)–1**, requires only 10.4 kcal/mol and completes the formation of the iminium ion and intermediate **(S)–2** (see Section 1.4 for subsequent reactions from the **(S)–2** intermediate).

In summary, our calculations show that irradiation of a mixture of riboflavin tetraacetate, modeled as riboflavin monoacetate (**2.A.m**), potassium persulfate, and *N*-Piv-piperidine **1a** with blue light generates the triplet state intermediate $\mathbf{T_1}$ through the S_0/T_1 seam of crossing (MSX), which is energetically accessible at the wavelengths used in our experiments. The iminium ion (**1.A**) generation from the T_1 intermediate is a barrierless, photon-controlled process and occurs by a stepwise "H-atom then electron transfer" mechanism. This conclusion is the opposite of our initial hypothesis involving "electron then H-atom transfer" but is consistent with our experimental KIE studies.

Copper-mediated deconstructive functionalization

During our investigation of the photocatalytic oxidative ring opening of cyclic amines, we noted, in some cases, subsequent oxidation of the generated aldehyde products to the corresponding carboxylic acids. Given the potential of these readily accessed carboxylic acids in subsequent derivatizations, we also explored complementary transition metal-mediated processes that would achieve oxidation of the aldehyde and provide access to alkyl carboxylic acids. Given the mild oxidation properties of copper salts (Cu(II)/Cu(I): –0.09 V vs. SCE;[35] Flavins: +1.67 V vs. SCE;[36] N-acyl cyclic amines: +1.13 V vs. SCE[9]), we envisaged a process in which a Cu(I) salt is oxidized by persulfate to Cu(II), forming a sulfate ion and a sulfate radical anion as by-products. Under these conditions, oxidation of cyclic amine substrates through a HAT/SET process analogous to that depicted in Scheme 1.1 was expected. Upon formation of the open chain aldehyde, a second oxidation to the carboxylic acid would be achieved through a Cu(II)/Cu(I) cycle.

Following optimization of the reaction conditions, N-Piv-piperidine was converted to carboxylic acid **4a** in 55% yield using 25 mol% $Cu(MeCN)_4BF_4$ and 4 equivalents of sodium persulfate in an acetone/water mixture. Cyclic amines of various ring sizes (**1m**–**1o**, Figure 1.7) also underwent ring opening to form carboxylic acids with a range of chain lengths in moderate yield (53–61%). Piperidines bearing an α-methyl substituent (**1g**), analogous to our observations described above using riboflavin tetraacetate (Figure 1.3), exhibited selective ring opening on the less substituted side of the ring, giving the corresponding product in 49% yield. Other piperidine derivatives with various substitution patterns (**1c**–**1e**, **1q**) also participated in the ring opening. Esters and other substituents that possess activated benzylic hydrogens were tolerated and resulted in moderate yields (48–54%). The Cu(I)-mediated ring opening reaction was also extended to other medicinally relevant saturated azacycles including perhydroquinoline (**1p**), pipecolic acid methyl ester (**1r**), and proline

methyl ester (**1s**) in 52%, 62%, and 60% yield, respectively. Interestingly, a cyclic amine bearing an α-phenyl substituent resulted in the formation of a linear aryl ketone product (**4t**) along with a small amount (9%; 21%, based on recovered starting material; brsm) of a δ-keto acid product resulting from a second set of oxidations at the α-position of the amine (see Section 1.4 for details). Spiro-fused cyclopropyl piperidine **1u** was also converted to the corresponding carboxylic acid (**4u**; 55% yield) without competing opening of the cyclopropane, which may have occurred under more forcing conditions.

This mild, oxidative ring-opening process can also be applied to the selective modification of amino acid sequences. Since polypeptides contain N-acylated cyclic amines in the form of proline residues, this method may provide a route for their modification.[37,38] The copper-mediated oxidative ring-opening of a proline residue effectively transforms it to a glutamate residue through this direct core modification method. As is well recognized, the cyclic structure of proline imparts unique structural characteristics to peptide sequences because of its dihedral angle.[39–41] As such, transforming a proline residue into a glutamate residue may not only impact the primary structure of a protein through a change in the amino acid sequence, but could also have implications on larger scale structures by influencing protein folding. While the transformation of a proline residue into glutamate has been reported previously,[12,17] the existing methods require the use of catalysts that are either expensive or not commercially available, and therefore these reaction conditions might be difficult to translate into industrial processes. Our method makes use of a cheap, commercially available catalyst that does not require difficult-to-access ligands.

We demonstrated the potential for modification of peptide sequences by performing a ring-opening oxidation on two dipeptides, Pro-Thr **5a** and Pro-Val **5b** (Figure 1.8). The resulting glutamate-bearing edited dipeptides were obtained in moderate yield (56% and 74%, respectively). Since the newly formed glutamate residue should serve as a reactive handle in esterification, amidation, and decarboxylation processes, we also briefly investigated subsequent transformations of the Glu-Val dipeptide. For example, esterification of the dipeptide with N-hydroxyphthalimide (NHPI) resulted in the corresponding NHPI ester (**7a**) in 80% yield. Given the emerging methods for engaging NHPI esters in cross-couplings,[42] **7a** may be used in a range of decarboxylative coupling reactions. The glutamic acid side chain could also be engaged in simple peptide couplings. For example, an amide coupling using valine led to branched peptide **7b** in 50% yield.

Computational Study of the Cu(I)-mediated deconstructive C–H functionalization of *1a* using sodium-persulfate as an oxidant

In order to gain further insight into the Cu(I)-mediated oxidative opening of aliphatic amines derivatives (e.g., **1a**) to form ring-opened carboxylic acids, we initiated DFT studies using $CuBF_4$ to model Cu(I), N-Piv-piperidine **1a** as a substrate, and sodium persulfate ($Na_2S_2O_8$)

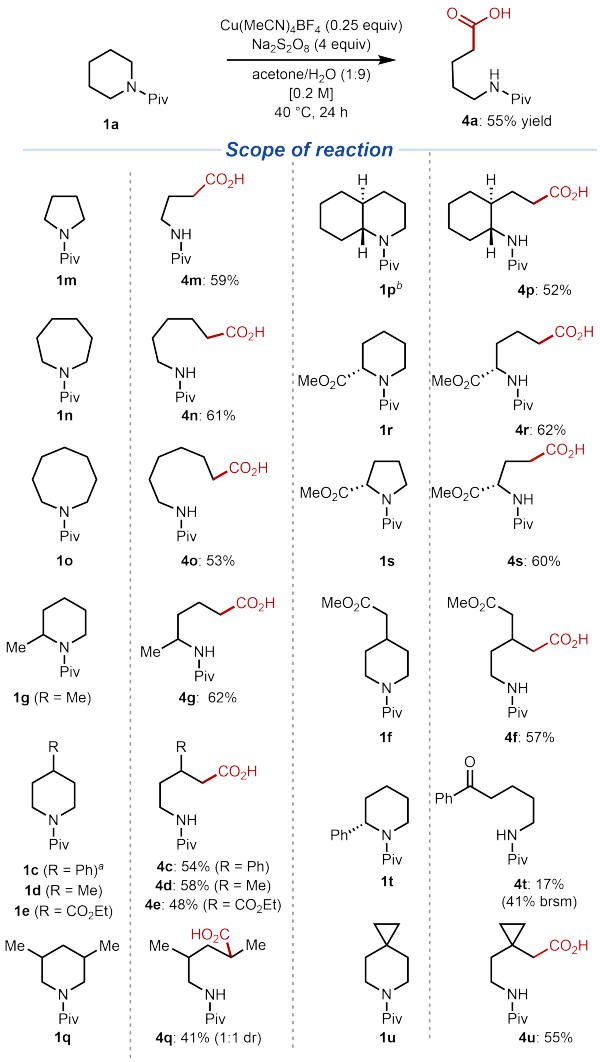

Figure 1.7: **Copper mediated oxidative ring opening of cyclic amines: Reaction scope.** Only isolated yields are shown. Reaction conditions: cyclic amine (0.2 mmol), $Cu(MeCN)_4BF_4$ (25 mol%), $Na_2S_2O_8$ (4 equivalents), acetone:H_2O (1:9), 24 h. [a]Reaction performed in acetone:H_2O (1:1). [b]Reaction performed with 1 equivalent of $Cu(MeCN)_4BF_4$.

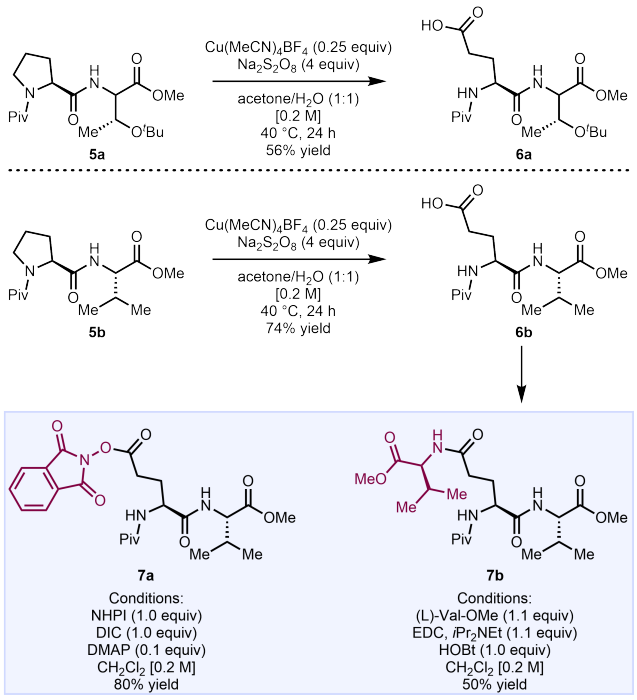

Figure 1.8: **Peptide diversification.** Only isolated yields are shown. See Section 1.4 for full experimental details.

as an oxidant (see Section 1.4 for details).[‡] Similar to our previously reported Ag(I)-mediated C–C deconstructive fluorination of N-benzoylated cyclic amines using Selectfluor,[9,43] one would expect either **1a** (represented as **LH** in Figure 1.9 to highlight and closely follow the anticipated H-atom transfer) or sodium persulfate coordination to the Cu(I)-center as a first step. Our calculations show that sodium persulfate coordination to $CuBF_4$ is thermodynamically more favorable by 2.9 kcal/mol (26.2 vs 29.1 kcal/mol for the direct H-atom transfer) and leads to the singlet state adduct $[CuBF_4]$–$[Na_2S_2O_8]$ (see Section 1.4 for more details).

From singlet state adduct $[CuBF_4]$–$[Na_2S_2O_8]$, SET could occur either prior to or after substrate coordination to the Cu(I)-center. In either case, SET from the Cu(I) center to sodium persulfate leads to O–O bond cleavage and formation of sodium sulfate and a sulfate radical anion. Should the SET occur prior to substrate coordination to the Cu(I) center, the ring-opened aldehyde product (**3a**) will form through a radical pathway initiated by H-atom abstraction by the sulfate radical anion (shown in Scheme 1.1). However, our calculations show that the SET most likely occurs upon substrate coordination to the Cu(I) center since the formation of the triplet state Cu(II) intermediate $[(\mathbf{LH})$–$(NaSO_4)]$–$[NaSO_4$–$Cu(II)BF_4]$ is

[‡]Calculations were performed by Djamaladdin G. Musaev and Alexey L. Kaledin at the Cherry L. Emerson Center for Scientific Computation and Department of Chemistry, Emory University, 1515 Dickey Drive, Atlanta, GA, United States.

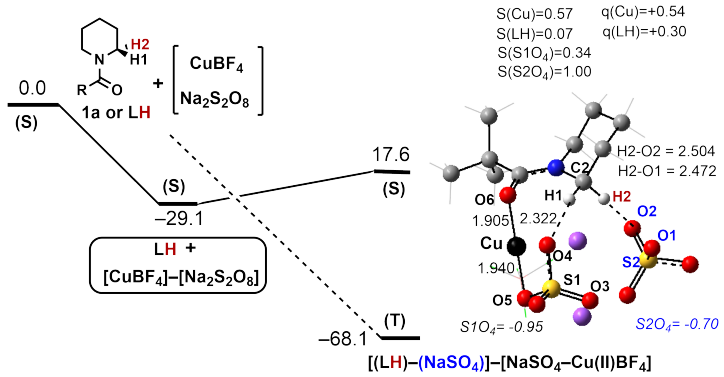

Figure 1.9: Computed reaction mechanism for the formation of intermediate [(**LH**)–($NaSO_4$)]– $NaSO_4$–Cu(II)BF_4] upon reaction of $CuBF_4$, LH and sodium persulfate ($Na_2S_2O_8$). Here, Gibbs free energies are in kcal/mol. Labels (S) and (T) represent the singlet and triplet electronic states, respectively. Spin densities, S(X), and Mulliken charges, q(X), are given in |e|. Geometries are in Å. BF_4 anions are omitted for clarity.

highly favored relative to the dissociation limit of (**LH**) + [$CuBF_4$]–[$Na_2S_2O_8$]. Interestingly, as shown in Figure 1.9, in the Cu(II) intermediate [(**LH**)–($NaSO_4$)]–[$NaSO_4$–Cu(II)BF_4], the $S1O_4$ sulfate anion (left side of the structure, each SO_4 unit here is denoted as $S1O_4$ or $S2O_4$ for distinction) is coordinated to the Cu(II)-center (Cu–O5 bond length = 1.940 Å). The second sulfate anion ($S2O_4$) is weakly associated with the Cu-coordinated substrate (H2–O2 = 2.504 Å and H2–O1 = 2.472 Å). These sulfate anions are bridged by the two sodium cations. Since the SET is expected to be very fast and occur through the singlet-to-triplet seam of crossing for the [$CuBF_4$]–[$Na_2S_2O_8$] complex, it should not impact the rate of reaction or reaction outcome. Therefore, here, an in-depth analysis of this path was not conducted.[44,45] The next step of the reaction, H-atom abstraction from the C2-position of the N-acylated piperidine substrate by the $S2O_4$ sulfate anion, is illustrated in Figure 1.10a. This step is a two-state reactivity event (i.e., starts from a triplet state pre-reaction complex and results in a singlet state product) that has a small free energy barrier of 4.1 kcal/mol at the triplet state transition state **TS(H-transf.)**. The net process is highly exergonic (by 56.0 kcal/mol). Interestingly, IRC calculations show that while this process begins with abstraction of a H-atom from C2 by the O2-atom of the $S2O_4$ sulfate anion at **TS(H-transf.)**, it culminates in a product where the abstracted H-atom has been transferred to the second sulfate anion (i.e., $S1O_4$) and the O2-atom of the $S2O_4$ sulfate anion is coordinated to the piperidine ring at the C2-position. Overall, this H-atom abstraction event leads to the formation of a singlet state product [L-OSO_3Na]–[$NaHSO_4$–$CuBF_4$] which is a complex of the [L-OSO_3Na] and [$NaHSO_4$–$CuBF_4$] fragments. Charge density analyses show that the [L-OSO_3Na] unit possesses an overall +0.57 |e| charge.

Calculations show that in the presence of water molecules (see Figure 1.10b), in-

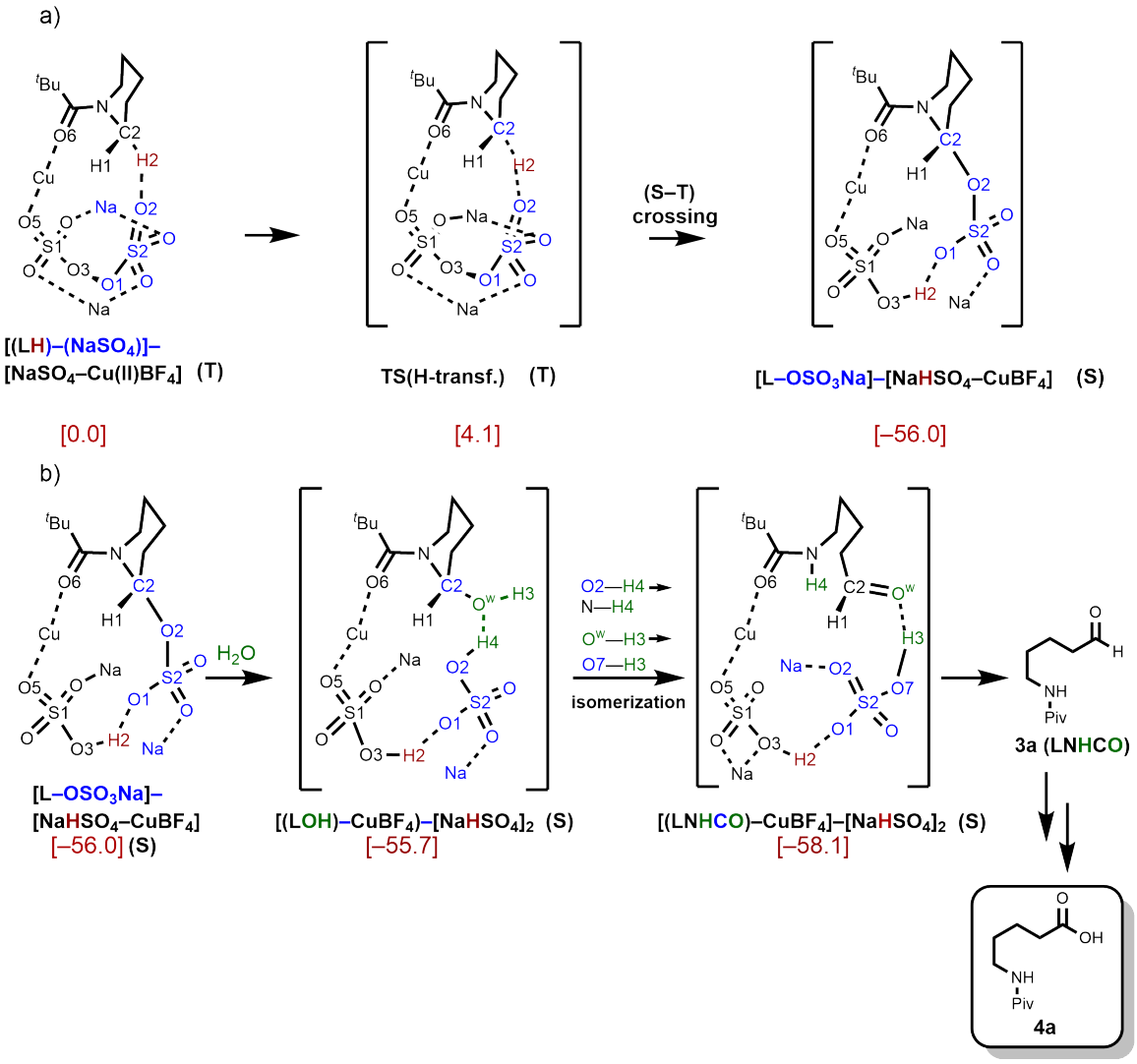

Figure 1.10: Computed ring opening mechanism for intermediate [(**LH**)–($NaSO_4$)]–[$NaSO_4$–Cu(II)BF_4]. Gibbs free energies are reported in kcal/mol. Label (S) represents a singlet electronic state. Bond lengths are reported in Å. For simplicity, the BF_4 fragment is omitted.

termediate [L-OSO_3Na]–[NaHSO4–CuBF4] is in equilibrium with the hemiaminal (i.e., [(LOH)–$CuBF_4$]–[$NaHSO_4$]$_2$). The hemiaminal is the product of H–O_wH hydrolysis of the L–OSO_3Na bond. Multiple proton-shuttles occur between the N-center of the substrate and HSO4– unit, as well as be-tween the LOH and HSO_4– units, which leads to formation of intermediate [(**LNHCO**)–$CuBF_4$]–[$NaHSO_4$]$_2$. Calculations show that [(**LNHCO**)–$CuBF_4$]–[$NaHSO_4$]$_2$ is only 2.4 kcal/mol lower in free energy than the [(LOH)–$CuBF_4$]–[$NaHSO_4$]$_2$ complex. At this time, we cannot rule out the formation of [(**LNHCO**)–$CuBF_4$]–[$NaHSO_4$]$_2$ through outer-sphere protonation-deprotonation by other molecules of water from the solvent.

Dissociation of **LNHCO** from [(**LNHCO**)–$CuBF_4$]–[$NaHSO_4$]$_2$ leads to free aldehyde **3a**. The computational data presented above shows that the overall reaction (**LH**) + $CuBF_4$ + $Na_2S_2O_8$ → (**LNHCO**) + [$CuBF_4$]–[$NaHSO_4$]$_2$ is highly exergonic (by 126.2 kcal/mol) and will proceed spontaneously without a significant energy barrier. Under the oxidative reaction conditions, it is likely that the resulting aldehyde (**3a**) is oxidized to the corresponding carboxylic acid **4a** (see Figure 1.10B).[46]

1.3 Conclusion

In summary, we have developed deconstructive functionalizations of cyclic aliphatic amines to achieve skeletal diversification that build on our previous reports.[9–11] We developed two methods for ring-opening transformations, achieving an organo-photocatalytic formation of linear aldehydes with riboflavin tetraacetate and a Cu(I)-mediated oxidation to access amine derivatives bearing carboxylic acid groups. Our calculations of the photoinduced oxidation of piperidines by riboflavin tetraacetate suggest that the oxidation is initiated by a photon-driven HAT. For the Cu-mediated oxidation of cyclic amines, the oxidation is instead initiated by a SET resulting in peroxy bond homolysis of persulfate.

1.4 Experimental Section

Solvents and Reagents

Tetrahydrofuran (THF) and triethylamine (Et_3N) were sparged with argon and dried by passing through alumina columns using argon in a Glass Contour solvent purification system. Dichloromethane (CH_2Cl_2) was freshly distilled over calcium hydride under a N_2 atmosphere prior to each use. DMF was purchased in Aldrich Sure/Seal™ bottles. N-Boc-piperidine (**1a.a**) was obtained from Aldrich and used as received. Reagents were purchased from commercial vendors as follows: Riboflavin (RTA, 98%) was purchased from Alfa Aesar. Silver nitrate ($AgNO_3$, ≥99%) was purchased from Sigma-Aldrich. Ammonium persulfate ($(NH_4)_2S_2O_8$, ACS Reagent) was purchased from J. T. Baker Chemicals, potassium persulfate ($K_2S_2O_8$, ACS Reagent) was purchased from Fisher Scientific, and sodium persulfate ($Na_2S_2O_8$, 98+%) was purchased from Acros Organics. Acetonitrile (HPLC), acetone (HPLC) and water (HPLC) were purchased from Fisher Scientific.

Experimental Procedures

Unless otherwise noted in the experimental procedures, reactions were carried out in flame or oven-dried glassware under a positive pressure of N_2 in anhydrous solvents using standard Schlenk techniques. Reaction temperatures above room temperature (22–23 °C) were controlled by an IKA® temperature modulator and monitored using glass thermometers. Reaction progress was monitored using a combination of LC/MS analysis (using a Shimadzu LCMS-2020 (UFLC) equipped with the LC-20AD solvent delivery system, a SPD-20AV prominence UV/Vis detector (SPD-M20A Photo Diode Array), and a Thermo Scientific Hypersil GOLD HPLC column (5 µm particle size, 4.6 × 50 mm)), and thin-layer chromatography (TLC) on Macherey-Nagel (MN) silica gel plates (glass backed, 60 Å, 0.25 mm thickness, UV254 manganese-activated zinc silicate fluorescence indicator). Visualization of the developed plates was performed under UV-light (254 nm) irradiation, and then gently heated with *p*-anisaldehyde or cerium ammonium molybdate (CAM) stain. Flash column chromatography was performed with either glass columns using Silicycle silica gel (40–63 μm particle size) or using a Yamazen Smart Flash EPCLC W-Prep 2XY (dual channel) automated flash chromatography system on prefilled, premium, universal columns using ACS grade solvents. Preparative thin layer chromatography was performed on SiliCycle Siliaplates (glass backed, extra hard layer, 60 Å, 250 μm thickness, F254 indicator).

Analytical Instrumentation

^{1}H NMR and ^{13}C NMR data were recorded on Bruker AVQ-400, AVB-400, AV-600, and AV-700 spectrometers using $CDCl_3$ as solvent, typically at 20–23 °C. Chemical shifts (δ) are reported in ppm relative to the residual solvent signal (δ 7.26 for ^{1}H NMR, δ 77.16 for ^{13}C NMR in $CDCl_3$). ^{19}F NMR spectra were acquired on an AVQ-400 spectrometer and internally referenced to $CFCl_3$ (δ 0.00). Data for ^{1}H and ^{13}C spectroscopy are reported as follows; chemical shift (δ ppm), multiplicity (s = singlet, d = doublet, t = triplet, q = quartet, quint = quintet, hept = heptet, m = multiplet, br = broad), coupling constant (Hz), integration. High-resolution mass spectra (HRMS) were analyzed as MeOH solutions (30–50 μM) using a Finnigan LTQ FT mass spectrometer (Thermo). Solutions were injected

directly into the ion source via syringe pump with 5 uL/min flow rate. Xcalibur software (version 2.0.7, Thermo) was used for both spectra acquisition and data analysis.

Preparation of *N*-Protected Cyclic Amines

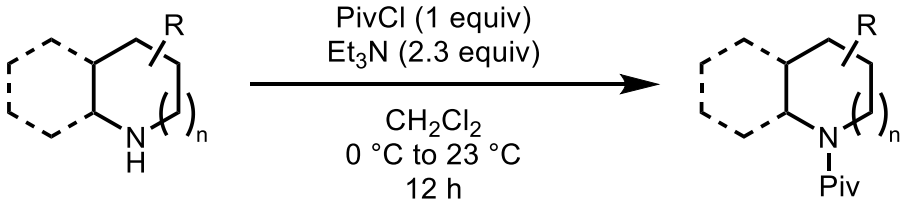

A 25 mL round-bottomed flask was charged with a solution of the cyclic amine (500 mg, 1.0 equiv) and Et_3N (2.3 equiv) in CH_2Cl_2 (20 mL) and cooled to 0 °C. Pivaloyl chloride (1.1 equiv) was added dropwise. The resulting mixture was allowed to warm to room temperature and stirred for 12 h, after which the reaction mixture was quenched with HCl (1M, 5 mL). The phases were separated, and the aqueous phase was extracted with CH_2Cl_2 (3 x 5–10 mL). The combined organic layers were washed with brine (5–10 mL), dried over Na_2SO_4, filtered, and concentrated under reduced pressure.

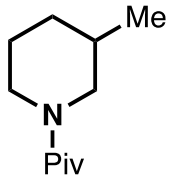

1i

2,2-Dimethyl-1-(3-methylpiperidin-1-yl)propan-1-one (**1i**): The title compound was prepared according to the general procedure using 3-methylpiperidine to give **1i** (644mg, 81%) as a colorless to slight yellowish liquid.

^{1}H NMR (400 MHz, $CDCl_3$): δ 4.28 (dd, J = 30.5, 13.2 Hz, 2H), 2.72 (t, J = 12.1 Hz, 1H), 2.41 (t, J = 12.0 Hz, 1H), 1.9 – 1.74 (m, 1H), 1.73 – 1.61 (m, 1H), 1.61 – 1.37 (m, 2H), 1.27 (s, 9H), 1.13 – 1.05 (m, 1H), 0.89 (d, J = 6.6 Hz, 3H);

^{13}C NMR (126 MHz, $CDCl_3$) δ 176.2, 38.9, 38.5, 33.44, 31.7, 28.6, 27.2, 25.8, 19.2;

HRMS (ESI): Calc'd for $C_{11}H_{22}NO$ $[M+H]^+$: 184.1696, found: 186.1695.

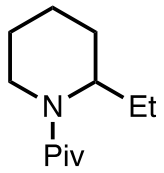

1h

1-(2-ethylpiperidin-1-yl)-2,2-dimethylpropan-1-one (**1h**): The title compound was prepared according to the general procedure using 2-ethylpiperidine to give **1h** (854 mg, 98%) as a slight yellowish liquid.
^{1}H NMR (400 MHz, $CDCl_3$): δ 4.67 (s, 1H), 4.01 (s, 1H), 2.98 (s, 1H), 1.70 – 1.51 (m, 6H), 1.49 – 1.31 (m, 2H), 1.25 (s, 9H), 0.83 (t, $J = 7.3$ Hz, 3H);
^{13}C NMR (126 MHz, $CDCl_3$) δ 176.6, 39.0, 28.7, 27.3, 26.3, 22.5, 19.2, 10.7
(*Two ^{13}C signals are missing due to peak broadening*);
HRMS (ESI): Calc'd for $C_{12}H_{24}NO$ $[M+H]^+$: 198.1852, found: 198.1852.

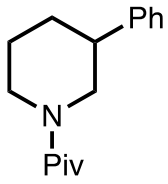

1j

2,2-dimethyl-1-(3-phenylpiperidin-1-yl)propan-1-one (**1j**): The title compound was prepared according to the general procedure using 3-phenylpiperidine (250 mg, 1.55 mmol, 1 equiv) to give **1j** (378 mg, 99%) as a slight yellowish liquid.
^{1}H NMR (400 MHz, $CDCl_3$): δ 7.37 – 7.29 (m, 2H), 7.27 – 7.20 (m, 3H), 4.52 (t, $J = 15.3$ Hz, 2H), 2.85 – 2.62 (m, 3H), 2.11 – 2.00 (m, 1H), 1.88 – 1.77 (m, 1H), 1.76 – 1.67 (m, 1H), 1.66 – 1.53 (m, 1H), 1.30 (s, 9H);
^{13}C NMR (126 MHz, $CDCl_3$) δ 176.4, 143.4, 128.8, 127.2, 126.9, 43.4, 39.00, 32.1, 28.6, 26.1
(*Two ^{13}C signals are missing due to peak broadening*);
HRMS (ESI): Calc'd for $C_{16}H_{24}NO$ $[M+H]^+$: 246.1852, found: 246.1852.

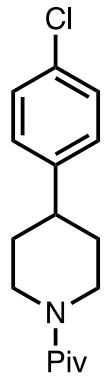

1b

1-(4-(4-chlorophenyl)piperidin-1-yl)-2,2-dimethylpropan-1-one (**1b**): The title compound was prepared according to the general procedure using 4-(4-chlorophenyl)piperidine (250 mg, 1.28 mmol, 1 equiv) to give **1b** (300 mg, 84%) as a slight brownish-yellowish liquid.

^{1}H NMR (400 MHz, $CDCl_3$): δ 7.32 – 7.24 (m, 3H), 7.17 – 7.09 (m, 2H), 4.57 (d, J = 13.3 Hz, 2H), 2.86 (t, J = 13.0 Hz, 2H), 2.74 (tt, J = 12.1, 3.8 Hz, 1H), 1.87 (d, J = 13.5 Hz, 2H), 1.66 – 1.51 (m, 2H), 1.31 (s, 9H);

^{13}C NMR (126 MHz, $CDCl_3$) δ 176.5, 149.6, 129.2, 125.5, 117.8, 49.7, 45.0, 28.5. (*Three ^{13}C signals are missing due to peak broadening*);

HRMS (ESI): Calc'd for $C_{16}H_{23}NOCl$ $[M+H]^+$: 280.1463, found: 280.1461.

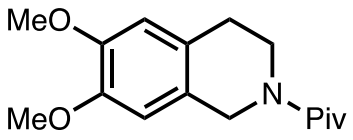

1l

1-(6,7-dimethoxy-3,4-dihydroisoquinolin-2(1*H*)-yl)-2,2-dimethylpropan-1-one (**1l**): The title compound was prepared according to the general procedure using 6,7-dimethoxy-1,2,3,4-tetrahydroisoquinoline (250 mg, 1.55 mmol, 1 equiv) to give **1l** (378 mg, 99%) as a slight yellowish liquid.

^{1}H NMR (500 MHz, $CDCl_3$) δ 6.61 (s, 1H), 6.59 (s, 1H), 4.67 (s, 1H), 4.09 – 3.68 (m, 8H), 2.80 (t, J = 6.1 Hz, 2H), 1.31 (s, 9H).

^{13}C NMR (126 MHz, $CDCl_3$) δ 176.8, 147.9, 147.8, 126.3, 125.5, 111.5, 109.2, 56.1, 56.1, 47.2, 43.6, 38.9, 28.6, 28.5.

HRMS (ESI): Calc'd for $C_{16}H_{24}NO_3$ $[M+H]^+$: 278.1751, found: 278.1750.

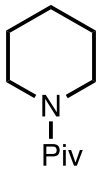

1a

2,2-dimethyl-1-(piperidin-1-yl)propan-1-one (**1b**) was prepared according to a published procedure.[47] Spectral data were in full agreement with the reported literature values.

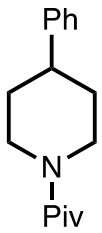

1c

2,2-dimethyl-1-(4-phenylpiperidin-1-yl)propan-1-one (**1e**) was prepared according to a published procedure.[48] Spectral data were in full agreement with the reported literature values.

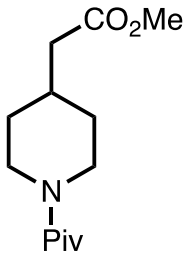

1f

Methyl 2-(1-pivaloylpiperidin-4-yl)acetate (**1f**) was prepared according to a published procedure. Spectral data were in full agreement with the reported literature values.[10]

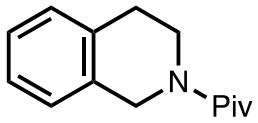

1k

1-(3,4-dihydroisoquinolin-2(1H)-yl)-2,2-dimethylpropan-1-one (**1k**) was prepared according to a published procedure.[49] Spectral data were in full agreement with the reported literature values.

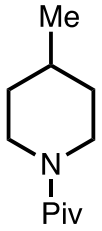

1d

2,2-dimethyl-1-(4-methylpiperidin-1-yl)propan-1-one (**1d**) was prepared according to a published procedure.[10] Spectral data were in full agreement with the reported literature values.

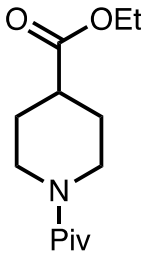

1e

Ethyl 1-pivaloylpiperidine-4-carboxylate (**1e**) was prepared according to a published procedure.[10] Spectral data were in full agreement with the reported literature values.

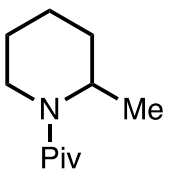

1g

2,2-dimethyl-1-(2-methylpiperidin-1-yl)propan-1-one (**1g**) was prepared according to a published procedure.[10] Spectral data were in full agreement with the reported literature values.

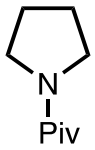

1m

2,2-dimethyl-1-(pyrrolidin-1-yl)propan-1-one (**1m**) was prepared according to a published procedure.[50] Spectral data were in full agreement with the reported literature values.

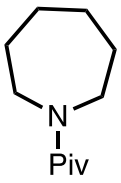

1n

1-(azepan-1-yl)-2,2-dimethylpropan-1-one (**1n**) was prepared according to a published procedure.[10] Spectral data were in full agreement with the reported literature values.

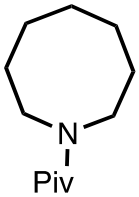

1o

1-(azocan-1-yl)-2,2-dimethylpropan-1-one (**1o**) was prepared according to a published procedure.[10] Spectral data were in full agreement with the reported literature values.

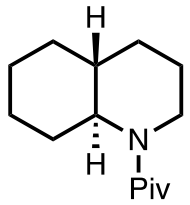

1p

2,2-dimethyl-1-((4a*R*,8a*S*)-octahydroquinolin-1(2*H*)-yl)propan-1-one (**1p**) was prepared according to a published procedure.[10] Spectral data were in full agreement with the reported literature values.

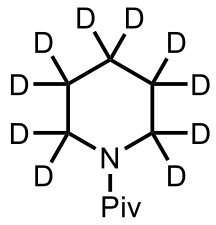

1a-*d*$_{10}$

2,2-dimethyl-1-(piperidin-1-yl-*d*$_{10}$)propan-1-one (**1a-*d*$_{10}$**): The title compound was prepared according to the general procedure using piperidine-d_{11} to give **1a-*d*$_{10}$** (881 mg, 95%) as a colorless liquid.

^{1}H NMR (500 MHz, $CDCl_3$) δ 1.24 (s, 9H);

^{13}C NMR (126 MHz, $CDCl_3$) δ 176.2, 45.8 – 45.0 (m), 38.7, 28.5, 25.7 – 24.7 (m), 23.8 – 23.2 (m).

HRMS (ESI): Calc'd for $C_{16}H_{24}NO_2$ $[M+H]^+$: 180.2168, found: 180.2167.

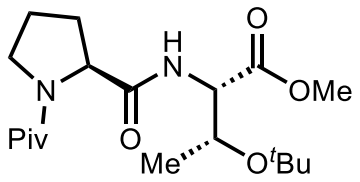

5a

Methyl O-(tert-butyl)-N-(pivaloyl-L-prolyl)-L-threoninate (**5a**) was prepared according to a published procedure.[10] Spectral data were in full agreement with the reported literature values.

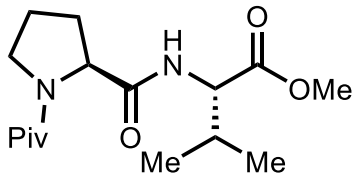

5b

Methyl pivaloyl-L-prolyl-L-valinate (**5b**) was prepared according to a published procedure.[10] Spectral data were in full agreement with the reported literature values.

Preparation of Photocatalyst 2a (Riboflavin Tetraacetate, RTA)

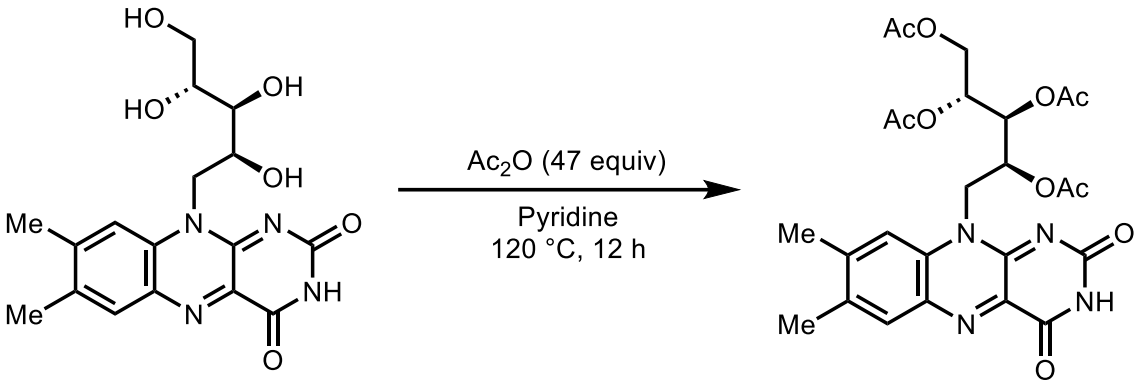

S1 **2a**

(2*R*,3*S*,4*S*)-5-(7,8-dimethyl-2,4-dioxo-3,4-dihydrobenzo[*g*]pteridin-10(2*H*)-yl)pentane-1,2,3,4-tetrayl tetraacetate (**2a**): (–)-Riboflavin (**S1**) (10.0 g, 26.6 mmol, 1 equiv) was dissolved in pyridine (120 mL) and acetic anhydride (118 mL, 47 equiv) was added. The resulting reaction mixture was stirred at reflux (120 °C) over night (12 h) and then cooled to room temperature, diluted with CH_2Cl_2 (200 mL) and poured into ice cold HCl (aq., 1M, 200 mL). The aqueous and organic layer were separated, the aqueous phase extracted with CH_2Cl_2 (3 x 100 mL) and the combined organic layers washed with HCl (aq., 1 M, 100 mL) and water (100 mL), dried over Na_2SO_4 and concentrated in *vacuo*. Purification of the crude product via column chromatography (10% MeOH/CH_2Cl_2) afforded the title compound (**2a**) as yellow-brown solid (5.30 g, 37%).

Spectral data were in full agreement with the reported literature values.[51]

Experimental Setup of Photoreactor

Photochemical reactions were performed either in an air-cooled photobox lined with aluminum foil using a blue Kessil brand A160WE Tuna Blue LED 40 W lamp (Figure 1.4.1), or the commercially marketed *Penn PhD Photoreactor M2* (450 nm).

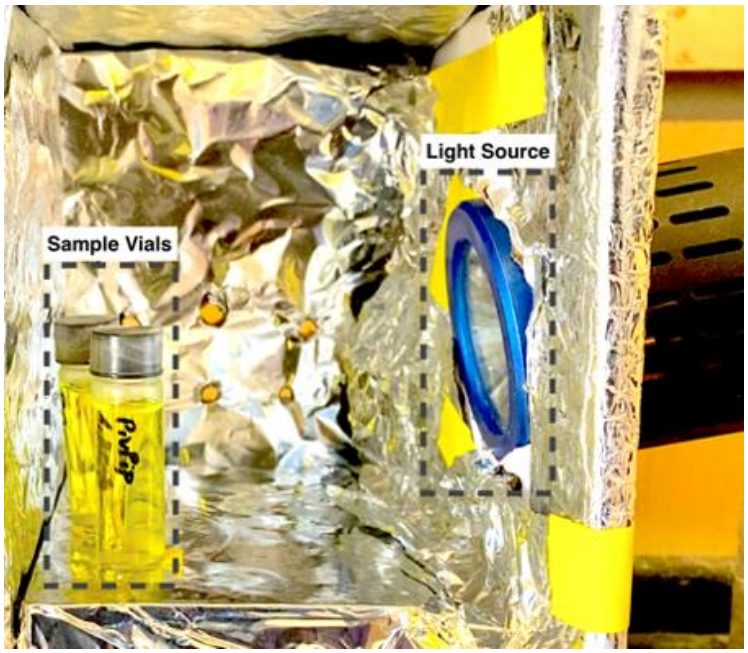

Figure 1.4.1: Photoreactor setup using a blue Kessil brand A160WE Tuna Blue LED 40 W lamp.

Photochemical Method Optimization

Representative Procedure for Photocatalyst Screening

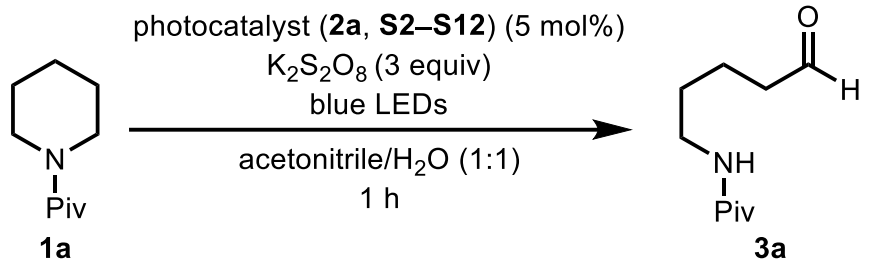

To a 2-dram vial was added sequentially piperidine **1a** (50.7 mg, 0.30 mmol, 1 equiv), potassium persulfate (243 mg, 0.60 mmol, 3 equiv), photocatalyst **(2a, S1 – S11)** (5 mol%) and 15 ml of a 1:1 acetonitrile:H_2O solution. The resulting mixture was sparged with nitrogen for 10 min and subsequently transferred to the photoreactor, exposed to a blue Kessil brand A160WE Tuna Blue LED 40 W lamp and cooled with an airstream. After 1 h, the reaction mixture was partitioned with DCM (5 ml) and the phases were separated. The aqueous phase was extracted with DCM (4 X 5 ml) and the combined organic layers dried over Na_2SO_4 and concentrated under nitrogen. $(C_6H_5)_3CH$ (0.1 mmol, 24.4 mg) was added as NMR standard to the crude reaction product and the yield and conversion determined using ^{1}H-NMR.

Table 1.4.1: Results of photocatalyst screening.

entry	catalyst	yield [%]#	conv. [%]#
1	**2a**	70 (4)	79
2	**S2**	9 (0)	28
3	**S3**	10 (1)	86
4	**S4**	7 (0)	23
5	**S5**	30 (9)	93
6	**S6**	5 (0)	48
7	**S7**	36 (9)	74
8	**S8**	10 (2)	35
9	**S9**	34 (17)	69
10	**S10**	29 (11)	91
11	**S11**	25 (3)	37
12	**S12**	38 (10)	71

Yield and conversion by ^{1}H integration using Ph_3CH as internal standard. Yield of carboxylic acid shown in parentheses.

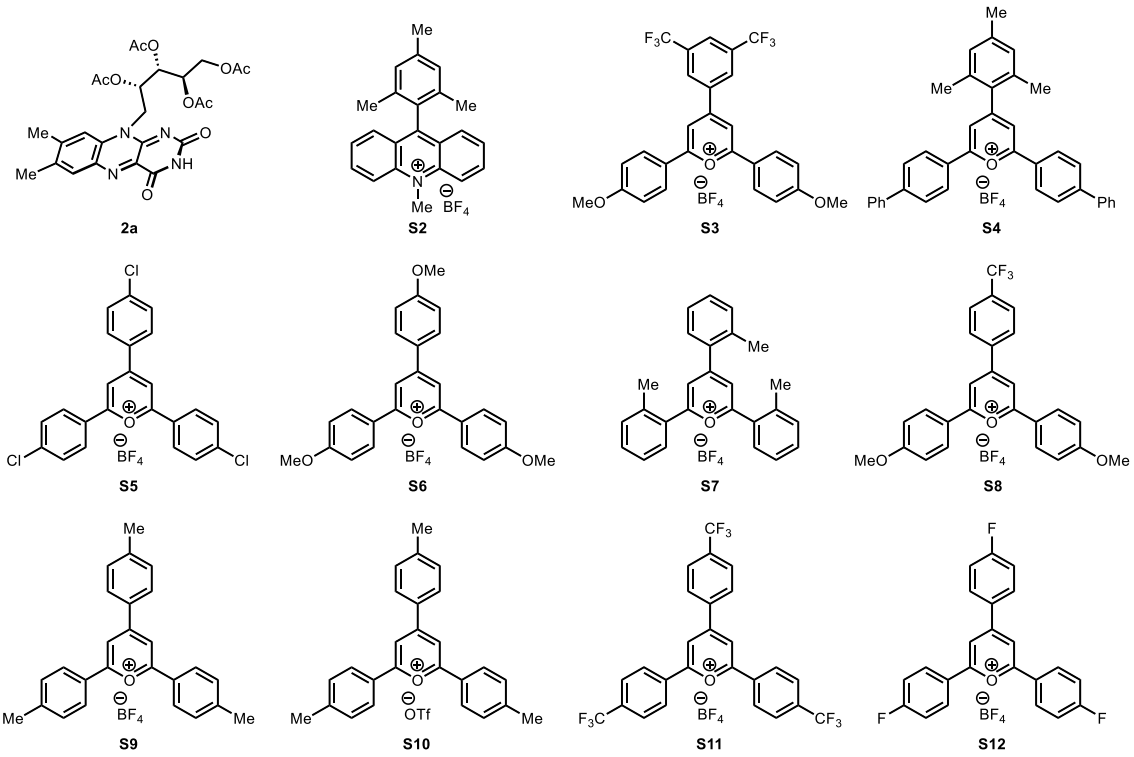

Figure 1.4.2: Photocatalysts used for optimization studies.

Photochemical Method – Optimization of Reaction Time

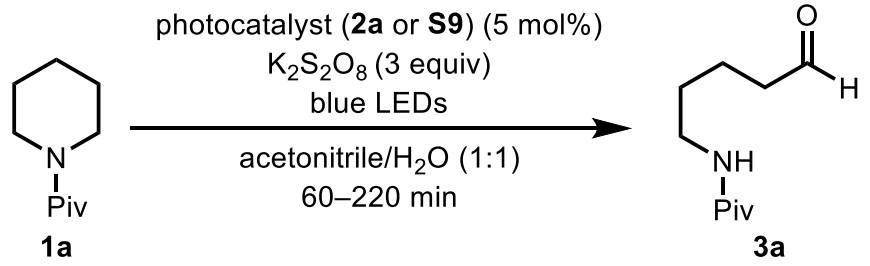

To a 2-dram vial was added, sequentially, piperidine **1a** (50.7 mg, 0.30 mmol, 1 equiv), potassium persulfate (243 mg, 0.60 mmol, 3 equiv), photocatalyst **2a** or **S9** (5 mol%) and 15 ml of a 1:1 acetonitrile/H_2O solution. The resulting mixture was sparged with nitrogen for 10 min, placed in a photoreactor, and irradiated with a blue Kessil brand A160WE Tuna Blue LED 40 W lamp cooled with an airstream. After the set duration (see Table 1.4.2 below), the reaction mixture was partitioned with DCM (5 ml) and the phases were separated. The aqueous phase was extracted with DCM (4 X 5 ml) and the combined organic layers dried over Na_2SO_4 and concentrated under nitrogen. $(C_6H_5)_3CH$ (0.1 mmol, 24.4 mg) was added as

NMR standard to the crude reaction product and the yield and conversion determined via ^{1}H-NMR.

Table 1.4.2: Optimization of reaction time for photochemical method.

entry	catalyst	time [min]	yield [%]#	conv. [%]#
1	**S9**	60	34 (17)	69
2	**S9**	120	11 (51)	>99
3	**2a**	60	70 (4)	79
4	**2a**	120	83 (13)	99
5	**2a**	220	59 (33)	>99

Yield and conversion by ^{1}H integration using Ph_3CH as internal standard. Yield of carboxylic acid shown in parentheses.

Photochemical Method – Optimization of Catalyst Loading

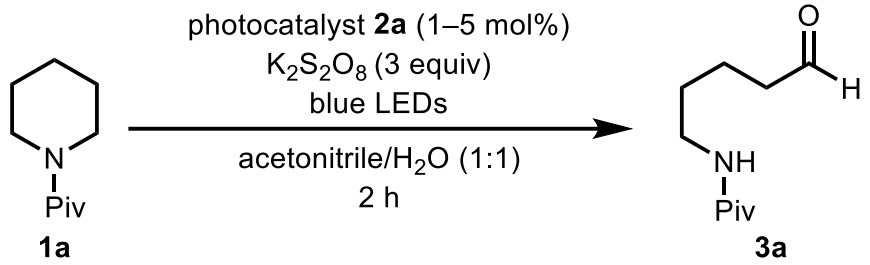

To a 2-dram vial was added, sequentially, piperidine **1a** (50.7 mg, 0.30 mmol, 1 equiv), potassium persulfate (243 mg, 0.60 mmol, 3 equiv), photocatalyst **2a** (1, 2.5, or 5 mol%) and 15 ml of a 1:1 acetonitrile:H_2O solution. The resulting mixture was sparged with nitrogen for 10 min and placed in a photoreactor, irradiated with a blue Kessil brand A160WE Tuna Blue LED 40 W lamp and cooled with an airstream. After 2 h, the reaction mixture was partitioned with DCM (5 ml) and the phases were separated. The aqueous phase was extracted with DCM (4 X 5 ml) and the combined organic layers dried over Na_2SO_4 and concentrated under nitrogen. $(C_6H_5)_3CH$ (0.1 mmol, 24.4 mg) was added as NMR standard to the crude reaction product and the yield as well as conversion determined by ^{1}H-NMR.

Table 1.4.3: Optimization of catalyst loading for RTA (**2a**).

entry	cat. loading [mol%]	yield [%]#	conv. [%]#
1	1	37 (9)	97
2	2.5	63 (24)	96
3	5	83 (13)	99

Yield and conversion by ^{1}H integration using Ph_3CH as internal standard. Yield of carboxylic acid shown in parentheses.

Photochemical Method – Optimization of Oxidant and Solvent

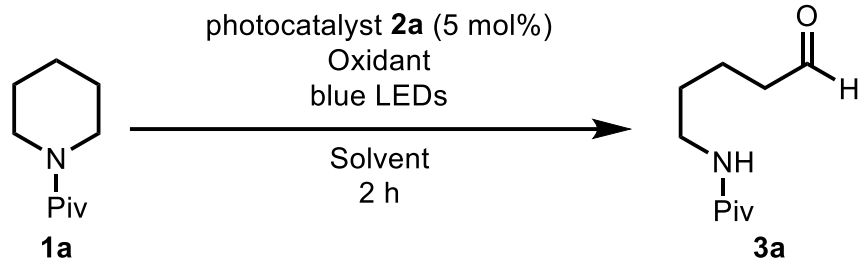

To a 2-dram vial was added, sequentially, piperidine **1a** (50.7 mg, 0.30 mmol, 1 equiv), oxidant (0.60 mmol, 3 equiv; or 1.20 mmol, 6 equiv), photocatalyst **2a** (5 mol%) and 15 ml of a 1:1 solvent solution. The resulting mixture was sparged with nitrogen for 10 min and placed in a photoreactor, exposed to a blue Kessil brand A160WE Tuna Blue LED 40 W lamp and cooled with an airstream. After 2 h, the reaction mixture was partitioned with DCM (5 ml) and the phases were separated. The aqueous phase was extracted with DCM (4 X 5 ml) and the combined organic layers dried over Na_2SO_4 and concentrated under nitrogen. $(C_6H_5)_3CH$ (0.1 mmol, 24.4 mg) was added as NMR standard to the crude reaction product and the yield and conversion determined using ^{1}H-NMR.

Table 1.4.4: Optimization of oxidant for photochemical method.

entry	**oxidant**	**equiv.**	**yield** [%]#	**conv.** [%]#
1	$K_2S_2O_8$	3	83 (13)	99
2	$(NH_4)_2S_2O_8$	3	18 (1)	98
3	$Na_2S_2O_8$	3	70 (24)	>99
4	Oxone	3	47 (31)	87
5	H_2O_2 (30%)	3	0	35
6	TBHP	3	0	20

Yield and conversion by ^{1}H integration using Ph_3CH as internal standard. Yield of carboxylic acid shown in parentheses.

Table 1.4.5: Optimization of solvent for photochemical method.

entry	**solvent**	**M** [mol/L]	**yield** [%]#	**conv.** [%]#
1	MeCN/H_2O (1:1)	0.02	83 (13)	99
2	Acetone/H_2O (1:1)	0.02	67 (18)	96
3	DCE/H_2O (1:1)	0.02	3 (0)	44

Yield and conversion by ^{1}H integration using Ph_3CH as internal standard. Yield of carboxylic acid shown in parentheses.

Photochemical Method – Variation of Reaction Parameters

Any variation to the reaction conditions is listed as a change to the standard reaction parameters listed below.

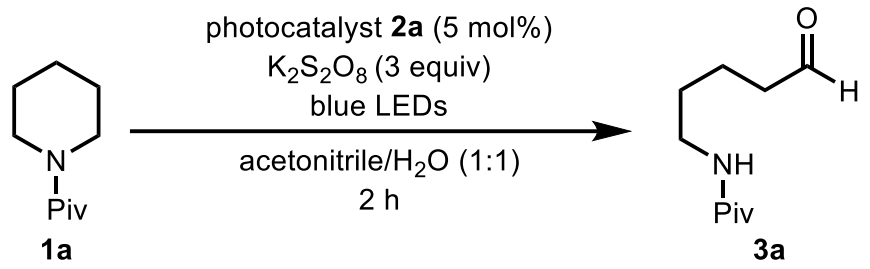

To a 2-dram vial was added, sequentially, piperidine **1a** (50.7 mg, 0.30 mmol, 1 equiv), potassium persulfate (243 mg, 0.60 mmol, 3 equiv), photocatalyst **2a** (8.1 mg, 5 mol%) and 15 ml of a 1:1 acetonitrile:H_2O solution. The resulting mixture was sparged with nitrogen for 10 min and placed in a photoreactor, exposed to a blue Kessil brand A160WE Tuna Blue LED 40 W lamp and cooled with an an airstream. After 2 h, the reaction mixture was partitioned with DCM (5 ml) and the phases were separated. The aqueous phase was extracted with DCM (4 X 5 ml) and the combined organic layers dried over Na_2SO_4 and concentrated under nitrogen. $(C_6H_5)_3CH$ (0.1 mmol, 24.4 mg) was added as an NMR standard to the crude reaction product and the yield and conversion determined using ^1H NMR.

Table 1.4.6: Variation of the reaction parameters with respect to the standard conditions.

entry	variation from the standard conditions	yield [%]
1	no sparging, open to air	73 (19)[#]
2	no riboflavin tetraacetate	29 (12)[#]
3	riboflavin (**S1**) (without acetate groups)	31 (4)[#]
4	no oxidant	0[#]
6	no light source	0[#]
7	450 nm	45 (34)[#]

[#] Yield and conversion by ^1H integration using Ph_3CH as internal standard. Yield of carboxylic acid shown in parentheses.

Photochemical Method – N-Protecting Group Screening

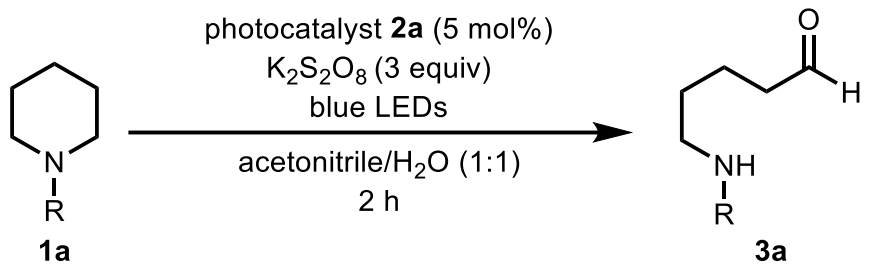

Piperidine derivatives bearing different substituents on nitrogen were subjected to the standard reaction conditions according to the representative procedure. The result obtained for N-Boc piperidine is representative of the observations made under the standard conditions. For the quantification of the reaction outcome, $(C_6H_5)_3CH$ (0.1 mmol, 24.4 mg) was added as NMR standard to the crude reaction product and the yield and conversion determined using ^1H NMR integration.

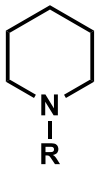

	R	yield[#]	conv.[#]
1a:	**Piv**	96%	99%
1a.a:	**Boc**	18%	86%
1a.b:	**Bz**	41%	54%

[#] Yield by ^1H integration using Ph_3CH as internal standard.

Figure 1.4.3: Results for N-protecting group screening.

Experiments to Probe Triplet Energy Transfer Mechanism

Some recent reports[52] of photochemical transformations have implicated excited-state triplet energy transfer from the photocatalyst to the substrate or oxidant as a key process in the reaction mechanism. In order to determine the viability of such a reaction pathway in our photoinitiated riboflavin tetraacetate oxidation method, photocatalysts of varying triplet energies were explored in place of riboflavin tetraacetate (**2a**), and the conversion of substrate **1a** was assessed for a correlation between the photocatalyst triplet energy and substrate conversion (see Table 1.4.7 below). The excited state triplet energy of the photocatalyst does not appear to have an effect on substrate conversion, so it is unlikely that triplet energy transfer is an operable pathway for oxidation.

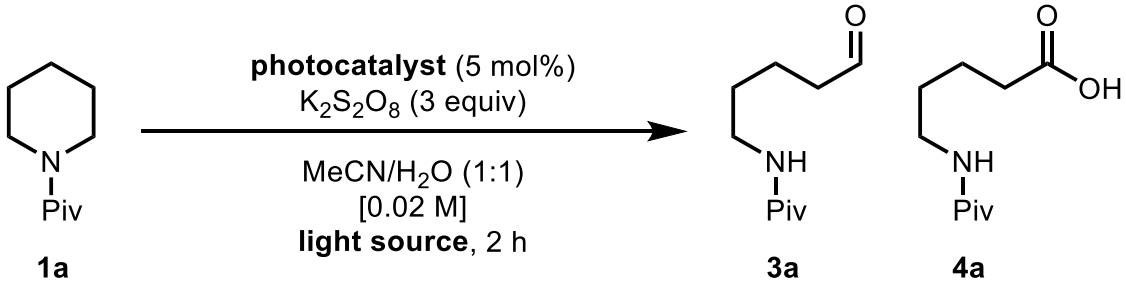

Table 1.4.7: Results of triplet energy transfer mechanistic experiments.

catalyst	λ [nm]	triplet energy [kcal/mol]	conv. [%]#	3a yield [%]#	4a yield [%]#
$(Ir[dF(CF_3)ppy]_2(dtbpy))PF_6$	400	61	61	22	0
	450		63	21	0
9-fluorenone	400	53	34	2	0
	450		51	0	0
$Ru(bpy)_3Cl \cdot H_2O$	400	47	99	0	46
	450		98	0	54

Yield and conversion by ^1H integration using Ph_3CH as internal standard.

Kinetics Experiments

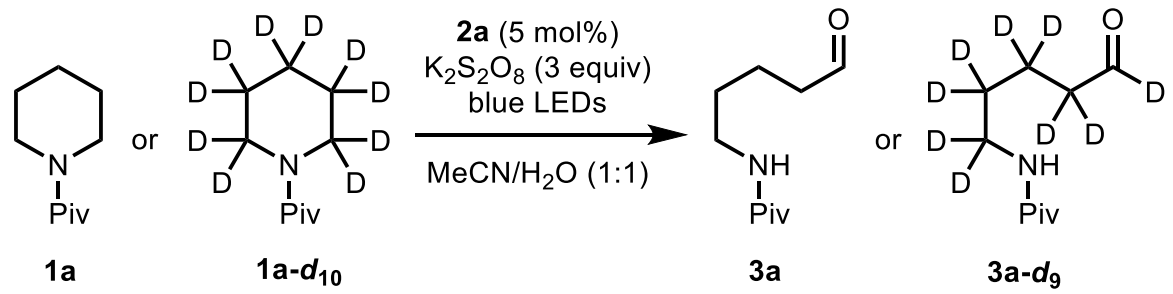

Kinetic Isotope Effect

Absolute rates: **1a** (169 mg, 1.00 mmol, 1 equiv) or **1a-*d*$_{10}$** (179 mg, 1.00 mmol, 1 equiv), potassium persulfate (811 mg, 3.00 mmol, 3 equiv), and **2a** (27.2 mg, 50.0 µmol, 0.05 equiv) were combined in a 30 mL vial with a magnetic stir bar, dissolved in 20 mL of 1:1 MeCN/H_2O, and the mixture was sparged with N_2. The mixture was allowed to stir under irradiation from a Kessil brand A160WE Tuna Blue LED 40 W lamp. Every 5 minutes, the lamp was quickly turned off, a 0.25 mL aliquot was taken from the mixture, the reaction vessel was placed back into the photobox, and irradiation was resumed. The aliquot was diluted with DI H_2O and extracted with 3 x 1 mL DCM. The combined organic layers were dried over Na_2SO_4, filtered, and concentrated. The resulting crude samples were analyzed by ^{1}H NMR using Ph_3CH as a standard to assess yield of **3a** or **3a-*d*$_9$**. $k_H/k_D = 1.1$

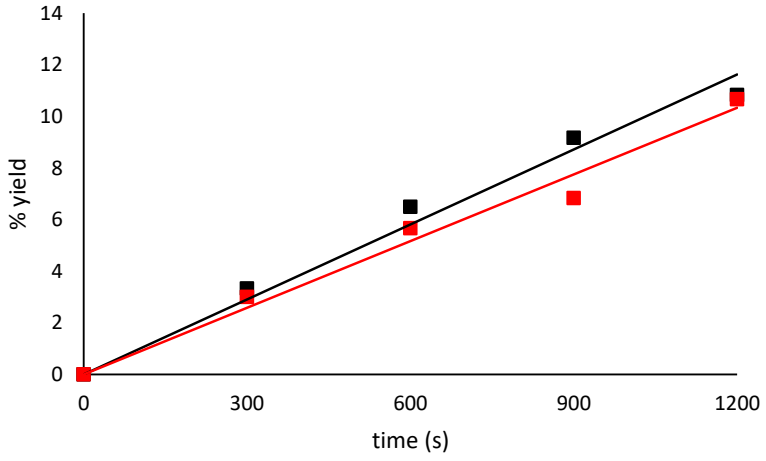

Figure 1.4.4: Initial rates for **1a** (black, 9.6 × 10^{-3} M/s) and **1a-*d*$_{10}$** (red, 8.2 × 10^{-3} M/s), $k_H/k_D = 1.1$.

Intermolecular competition: **1a** (8.5 mg, 50.0 μmol, 1 equiv) and **1a-*d*$_{10}$** (8.9 mg, 50.0 μmol, 1 equiv), potassium persulfate (81.1 mg, 0.300 mmol, 6 equiv), and **2a** (2.7 mg, 5.0 μmol, 0.1 equiv) were combined in a 2 dram vial with a magnetic stir bar, dissolved in 5 mL of 1:1 MeCN/H_2O, and the mixture was sparged with N_2. The mixture was allowed to stir under irradiation from a Kessil brand A160WE Tuna Blue LED 40 W lamp for 15 minutes. The mixture was extracted with 3 x 3 mL DCM. The combined organic layers were dried over Na_2SO_4, filtered, and concentrated. The aldehyde products were isolated by preparative thin-layer chromatography (1:1 hexanes/EtOAc). The resulting mixture of **3a** and **3a-*d*$_9$** was analyzed by ^{1}H NMR using Ph_3CH as a standard to assess yields. $[P_H]/[P_D] = 1.0$ (average of three trials)

Light On/Off Experiment

1a (169 mg, 1.00 mmol, 1 equiv), potassium persulfate (811 mg, 3.00 mmol, 3 equiv), and **2a** (27.2 mg, 50.0 μmol, 0.05 equiv) were combined in 30 mL vial with a magnetic stir bar, dissolved in 20 mL of 1:1 MeCN/H_2O, and the mixture was sparged with N_2. The reaction mixture was irradiated with a Kessil brand A160WE Tuna Blue LED 40 W lamp and kept in the dark for alternating 20 min periods. At the start/end of each period, a 0.25 mL aliquot was taken from the mixture. The aliquot was diluted with DI H_2O and extracted with 3 x 1 mL DCM. The combined organic layers were dried over Na_2SO_4, filtered, and concentrated. The resulting crude samples were analyzed by ^{1}H NMR using Ph_3CH as a standard to assess yield of **3a**.

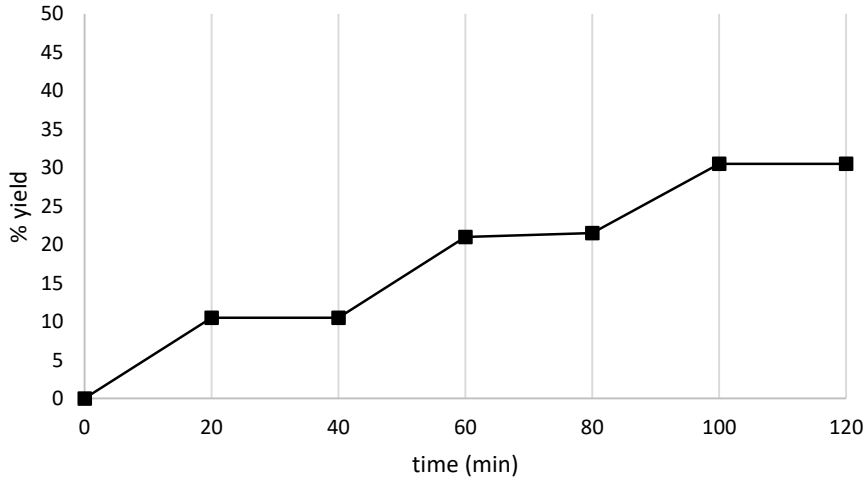

Figure 1.4.5: Light on/off experiment.

Procedure for Riboflavin Tetraacetate-mediated Ring Opening

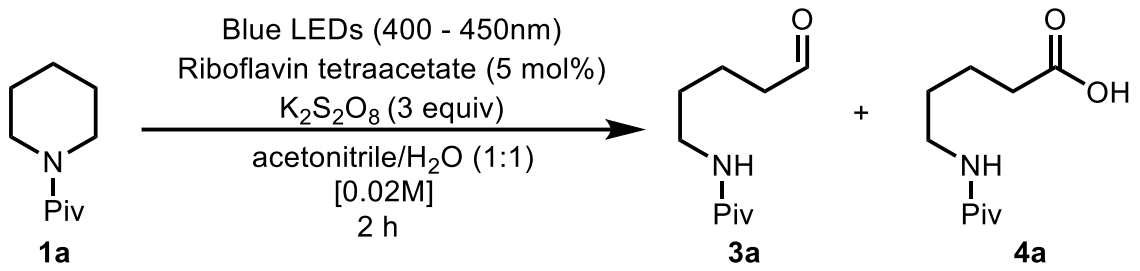

To a 2-dram vial was added, sequentially, piperidine **1a** (50.7 mg, 0.30 mmol, 1 equiv), potassium persulfate (243 mg, 0.60 mmol, 3 equiv), photocatalyst riboflavin tetraacetate (8.1 mg, 5 mol%) and 15 ml of a 1:1 acetonitrile:H_2O solution. The resulting mixture was sparged with nitrogen for 10 min and placed in a photoreactor, exposed to a blue Kessil brand A160WE Tuna Blue LED 40 W lamp and cooled with an airstream. After 2 h, the reaction mixture was partitioned with DCM (5 ml) and the phases were separated. The aqueous phase was extracted with DCM (4 X 5 ml) and the combined organic layers dried over Na_2SO_4 and concentrated under nitrogen to afford a mixture of *N*-(5-oxopentyl)pivalamide (**3a**) and 5-pivalamidopentanoic acid (**4a**). The mixture was subjected to an acid-base extraction using sodium bicarbonate (sat. solution) and HCl (5N) to give the major aldehyde product (**3a**) (47.6 mg, 86%) as a dark yellow brownish oil and the minor acid product (**4a**) (1.9 mg, 3%) as a yellowish oil.

Aldehyde (**3a**):

^{1}H NMR (500 MHz, $CDCl_3$): δ 9.73 (t, J = 1.5 Hz, 1H), 5.83 (s, 1H), 3.20 (td, J = 7.0, 5.8 Hz, 2H), 2.46 (td, J = 7.0, 1.4 Hz, 2H), 1.65 – 1.55 (m, 2H), 1.54 – 1.45 (m, 2H), 1.15 (s, 9H);

^{13}C NMR (126 MHz, $CDCl_3$): δ 202.4, 178.6, 43.4, 39.0, 38.7, 29.1, 27.7, 19.1;

HRMS (ESI): Calc'd for $C_{10}H_{20}NO_2$ $[M+H]^+$: 186.1489, found: 186.1488.

Acid (**4a**):

^{1}H NMR (500 MHz, $CDCl_3$): δ 5.76 (s, 1H), 3.26 (qd, J = 7.1, 5.8 Hz, 2H), 2.40 (t, J = 7.1 Hz, 2H), 1.70 – 1.49 (m, 4H), 1.20 (d, J = 1.8 Hz, 9H);

^{13}C NMR (126 MHz, $CDCl_3$): δ 178.9, 177.0, 39.0, 38.8, 33.2, 29.1, 27.7, 21.9.

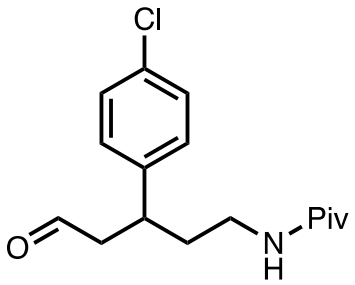

3b

***N*-(3-(4-chlorophenyl)-5-oxopentyl)pivalamide** (**3b**): The title compound was prepared according to the representative procedure using 1-(4-(4-chlorophenyl)piperidin-1-yl)-2,2-dimethylpropan-1-one to give **3b** (9.1 mg, 62%) as a colorless oil.
^{1}H NMR (500 MHz, $CDCl_3$): δ 9.67 (t, J = 1.5 Hz, 1H), 7.31 – 7.24 (m, 2H), 7.17 – 7.11 (m, 2H), 5.63 (s, 1H), 3.26 – 3.13 (m, 2H), 3.05 (ddt, J = 11.6, 7.5, 5.9 Hz, 1H), 2.84 – 2.69 (m, 2H), 1.92 – 1.73 (m, 2H), 1.14 (s, 9H);
^{13}C NMR (101 MHz, $CDCl_3$): δ 200.9, 178.6, 141.8, 132.8, 129.2, 128.9, 50.6, 38.7, 37.9, 37.1, 36.2, 27.6;
HRMS (ESI): Calc'd for $C_{16}H_{23}NO_2Cl$ $[M+H]^+$: 296.1412, found: 296.1411.

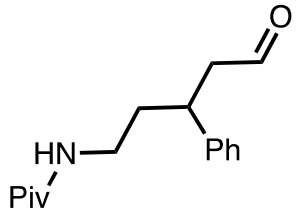

3c

***N*-(5-Oxo-3-phenylpentyl)pivalamide** (**3c**): The title compound was prepared according to the representative procedure using 2,2-dimethyl-1-(4-phenylpiperidin-1-yl)propan-1-one. Purification by preparative thin-layer chromatography (50% EtOAc/hexanes) provided (**3c**) (11.24 mg, 43%, 75% BRSM) as a colorless oil.
^{1}H NMR (600 MHz, $CDCl_3$) δ 9.68 (t, J = 1.7 Hz, 1H), 7.34 – 7.28 (m, 2H), 7.24 – 7.18 (m, 3H), 5.58 (s, 1H), 3.28 – 3.19 (m, 2H), 3.11 – 3.01 (m, 1H), 1.99 – 1.86 (m, 2H), 1.86 – 1.74 (m, 2H), 1.11 (s, 9H);
^{13}C NMR (151 MHz, $CDCl_3$) δ 201.4, 178.6, 143.3, 129.1, 127.5, 50.7, 38.7, 38.0, 36.2, 28.5, 27.6;
HRMS (ESI): Calc'd for $C_{16}H_{24}NO_2$ $[M+H]^+$: 262.1802, found: 262.1802.

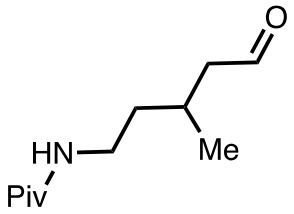

3d

***N*-(3-Methyl-5-oxopentyl)pivalamide** (**3e**): The title compound was prepared according to the representative procedure using 2,2-dimethyl-1-(4-methylpiperidin-1-yl)propan-1-one. Purification by preparative thin-layer chromatography (50% EtOAc/hexanes) provided (**3d**) (15.1 mg, 76%) as a colorless oil.

^{1}H NMR (400 MHz, $CDCl_3$): δ 9.75 (t, J = 1.7 Hz, 1H), 5.83 (s, 1H), 3.34 – 3.13 (m, 2H), 2.56 – 2.24 (m, 2H), 2.10 (dq, J = 13.5, 6.7 Hz, 1H), 1.55 – 1.38 (m, 2H), 1.19 (s, 9H), 0.99 (d, J = 6.8 Hz, 3H);

^{13}C NMR (101 MHz, $CDCl_3$): δ 202.6, 178.7, 51.1, 38.8, 37.5, 36.6, 27.7, 25.5, 20.2;

HRMS (ESI): Calc'd for $C_{11}H_{21}NO_2Na$ $[M+Na]^+$: 222.1465, found: 222.1466.

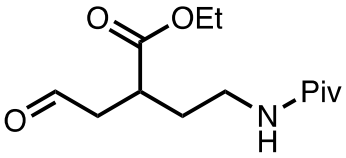

3e

Ethyl 4-oxo-2-(2-pivalamidoethyl)butanoate (**3e**): The title compound was prepared according to the representative procedure using ethyl 1-pivaloylpiperidine-4-carboxylate. Purification by preparative thin-layer chromatography (50% EtOAc/hexanes) provided (**3e**) (34.7 mg, 45%) as a colorless oil.

^{1}H NMR (500 MHz, $CDCl_3$): δ 9.74 (d, J = 1.0 Hz, 1H), 6.03 – 5.97 (m, 1H), 4.14 (q, J = 7.1 Hz, 2H), 3.37 – 3.15 (m, 2H), 2.96 – 2.84 (m, 2H), 2.70 – 2.60 (m, 1H), 1.90 – 1.66 (m, 2H), 1.24 (t, J = 7.1 Hz, 3H), 1.17 (s, 9H);

^{13}C NMR (126 MHz, $CDCl_3$): δ 200.0, 178.8, 174.5, 61.2, 45.4, 38.8, 37.3, 36.7, 31.4, 31.3, 27.6, 14.3;

HRMS (ESI): Calc'd for $C_{13}H_{24}NO_4$ $[M+H]^+$: 258.1700, found: 257.1699.

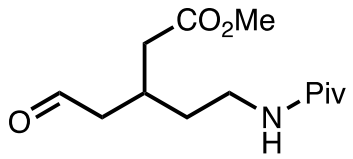

3f

Methyl 5-oxo-3-(2-pivalamidoethyl)pentanoate (**3f**): The title compound was prepared according to the representative procedure using methyl 2-(1-pivaloylpiperidin-4-yl)acetate. However, the catalyst loading was increased to 10 mol%. Purification by preparative thin-layer chromatography (70% EtOAc/hexanes) provided (**3f**) (9.62 mg, 75%) as a colorless oil.
^{1}H NMR (500 MHz, $CDCl_3$): δ 9.76 (d, J = 1.3 Hz, 1H), 6.04 (s, 1H), 3.67 (s, 3H), 3.25 (tdd, J = 6.8, 5.5, 1.6 Hz, 2H), 2.57 (dd, J = 6.3, 1.3 Hz, 2H), 2.52 – 2.43 (m, 1H), 2.42 – 2.31 (m, 2H), 1.55 (m, 2H), 1.20 (s, 9H);
^{13}C NMR (126 MHz, $CDCl_3$): δ 201.4, 178.8, 172.9, 51.7, 48.2, 38.2, 36.9, 34.0, 28.3, 27.6, 26.7;
HRMS (ESI): Calc'd for $C_{13}H_{23}NO_4Na$ $[M+Na]^+$: 280.1519, found: 280.1519.

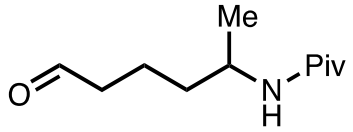

3g

***N*-(6-oxohexan-2-yl)pivalamide** (**3g**): The title compound was prepared according to the representative procedure on a 300 µmol scale using 2,2-dimethyl-1-(2-methylpiperidin-1-yl)propan-1-one. Purification by preparative thin-layer chromatography (50% EtOAc/hexanes) provided (**3g**) (43.3 mg, 72%) as a colorless oil.
^{1}H NMR (500 MHz, $CDCl_3$): δ 9.76 (t, J = 1.4 Hz, 1H), 5.41 (s, 1H), 4.04 – 3.92 (m, 1H), 2.56 – 2.40 (m, 2H), 1.62 – 1.38 (m, 4H), 1.19 (d, J = 3.6 Hz, 9H), 1.12 (d, J = 6.6 Hz, 3H);
^{13}C NMR (126 MHz, $CDCl_3$): δ 202.42, 178.1, 44.7, 43.6, 38.8, 36.4, 27.7, 21.1, 18.5;
HRMS (ESI): Calc'd for $C_{11}H_{22}NO_2$ $[M+H]^+$: 200.1645, found: 200.1646.

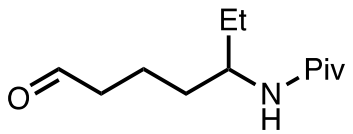

3h

***N*-(7-oxoheptan-3-yl)pivalamide** (**3h**): The title compound was prepared according to the representative procedure on a 300 µmol scale using 1-(2-ethylpiperidin-1-yl)-2,2-dimethylpropan-1-one. Purification by preparative thin-layer chromatography (50% EtOAc/hexanes) provided (**3h**) (33.4 mg, 52%) as a colorless oil.
^{1}H NMR (500 MHz, $CDCl_3$) δ 9.72 (t, J = 1.5 Hz, 1H), 5.35 (d, J = 9.0 Hz, 1H), 3.82 (dtd, J = 12.3, 8.7, 4.5 Hz, 1H), 2.54 – 2.34 (m, 2H), 1.68 – 1.41 (m, 4H), 1.34 (m, 2H), 1.17 (s, 9H), 0.85 (t, J = 7.5 Hz, 3H);
^{13}C NMR (126 MHz, $CDCl_3$) δ 202.4, 178.3, 49.9, 43.6, 34.3, 28.2, 27.8, 18.4, 10.3;
HRMS (ESI): Calc'd for $C_{12}H_{24}NO_2$ $[M+H]^+$: 214.1802, found: 214.1800.

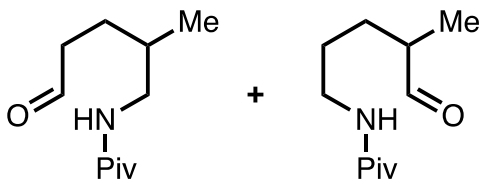

3i.a **3i.b**

***N*-(2-methyl-5-oxopentyl)pivalamide** (**3i.a**) and ***N*-(4-methyl-5-oxopentyl)pivalamide** (**3i.b**): The title compound was prepared according to the representative procedure using 2,2-dimethyl-1-(3-methylpiperidin-1-yl)propan-1-one. Purification by preparative thin-layer chromatography (50% EtOAc/hexanes) provided a mixture of **3i.a** and **3i.b** (14.4 mg, 72%; ratio **3i.a**:**3i.b** 1:0.78) as a colorless oil.
^{1}H NMR (400 MHz, $CDCl_3$): δ 9.76 (t, J = 1.3 Hz, 1H), 9.59 (d, J = 1.7 Hz, 1H), 5.89 (s, 1H), 5.78 (s, 1H), 3.29 – 3.00 (m, 4H), 2.60 – 2.42 (m, 2H), 2.36 (hd, J = 7.0, 1.7 Hz, 1H), 1.77 – 1.28 (m, 6H), 1.18 (d, J = 6.0 Hz, 18H), 1.09 (d, J = 7.1 Hz, 2H), 0.88 (d, J = 6.5 Hz, 3H);
^{13}C NMR (126 MHz, $CDCl_3$): δ 204.9, 202.5, 178.7, 178.6, 46.0, 44.7, 41.5, 39.4, 38.9, 38.8, 33.1, 27.7, 27.7, 27.5, 27.2, 25.9, 17.6, 13.5;
HRMS (ESI): Calc'd for $C_{11}H_{22}NO_2$ $[M+H]^+$: 200.1645, found: 200.1644.

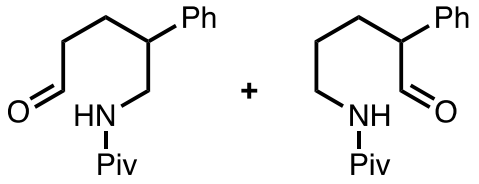

3j.a **3j.b**

***N*-(5-Oxo-2-phenylpentyl)pivalamide** (**3j.a**) and ***N*-(5-Oxo-4-phenylpentyl)pivalamide** (**3j.b**): The title compounds were prepared according to the representative procedure using 2,2-dimethyl-1-(3-phenylpiperidin-1-yl)propan-1-one. Purification by preparative thin-layer chromatography (50% EtOAc/hexanes) provided a mixture of **3j.a** and **3j.b** (52.40 mg, 67%; ratio **3j.a**:**3j.b** 1:0.5) as colorless oils.
^{1}H NMR (500 MHz, $CDCl_3$): δ 9.67 (t, J = 1.3 Hz, 1H), 9.66 (d, J = 1.6 Hz, 1H), 7.39 – 7.22 (m, 7H), 7.18 – 7.11 (m, 4H), 5.73 (s, 1H), 5.54 (s, 1H), 3.73 – 3.60 (m, 2H), 3.54 (ddd, J = 8.1, 6.4, 1.6 Hz, 1H), 3.28 – 3.16 (m, 3H), 2.86 – 2.76 (m, 2H), 2.44 – 2.27 (m, 3H), 2.14 – 1.98 (m, 3H), 1.91 – 1.79 (m, 2H), 1.76 – 1.66 (m, 1H), 1.53 – 1.39 (m, 1H), 1.17 (s, 6H), 1.06 (s, 14H);
^{13}C NMR (126 MHz, $CDCl_3$): δ 201.9, 200.6, 178.6, 178.5, 141.6, 136.1, 129.3, 129.0, 128.9, 127.9, 127.8, 127.3, 58.7, 45.1, 44.9, 41.8, 39.1, 38.7, 38.7, 27.7, 27.5, 27.3, 26.8, 25.5;
HRMS (ESI): Calc'd for $C_{16}H_{24}NO_2$ $[M+H]^+$: 262.1802, found: 262.1801.

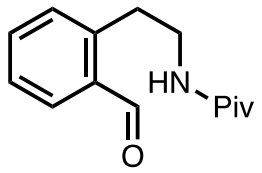

3k

***N*-(2-Formylphenethyl)pivalamide** (**3k**): The title compound was prepared according to the representative procedure using 1-(3,4-dihydroisoquinolin-2(1*H*)-yl)-2,2-dimethylpropan-1-one. Purification by preparative thin-layer chromatography (50% EtOAc/hexanes) provided the title compound (**3k**) (12.13 mg, 52%) as a yellow-brown oil.
^{1}H NMR (500 MHz, $CDCl_3$) δ 10.17 (s, 1H), 7.80 (dd, J = 7.6, 1.6 Hz, 1H), 7.53 (td, J = 7.5, 1.5 Hz, 1H), 7.43 (td, J = 7.5, 1.2 Hz, 1H), 7.31 (dd, J = 7.7, 1.2 Hz, 1H), 5.99 (s, 1H), 3.51 (td, J = 6.9, 5.6 Hz, 2H), 3.25 (t, J = 6.9 Hz, 2H), 1.12 (s, 9H).

^{13}C NMR (126 MHz, $CDCl_3$) δ 193.8, 178.8, 141.7, 134.4, 134.1, 134.0, 132.1, 127.3, 41.2, 38.8, 32.4, 27.7;

HRMS (ESI): Calc'd for $C_{14}H_{20}NO_2$ $[M+H]^+$: 234.1489, found: 234.1489.

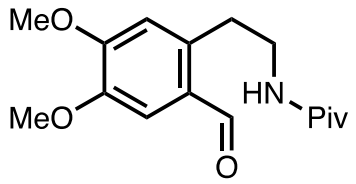

3l

***N*-(2-Formyl-4,5-dimethoxyphenethyl)pivalamide** (**3l**): The title compound was prepared according to the representative procedure using 1-(6,7-dimethoxy-3,4-dihydroisoquinolin-2(1*H*)-yl)-2,2-dimethylpropan-1-one. Purification by preparative thin-layer chromatography (50% EtOAc/hexanes) provided the title compound (**3l**) (27.9 mg, 95%) as a yellow-brown oil.

^{1}H NMR (500 MHz, $CDCl_3$) δ 10.08 (s, 1H), 7.30 (s, 1H), 6.75 (s, 1H), 5.98 (t, J = 5.9 Hz, 1H), 3.93 (d, J = 9.4 Hz, 6H), 3.49 (td, J = 7.0, 5.8 Hz, 2H), 3.19 (t, J = 7.0 Hz, 2H), 1.13 (s, 9H).

^{13}C NMR (126 MHz, $CDCl_3$) δ 191.0, 178.9, 153.9, 148.0, 137.0, 127.3, 113.8, 113.6, 56.3, 56.2, 41.7, 38.8, 31.7, 27.7;

HRMS (ESI): Calc'd for $C_{16}H_{24}NO_4$ $[M+H]^+$: 294.1700, found: 294.1700.

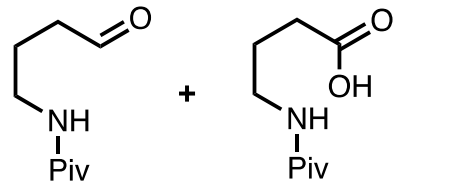

3m **4m**

***N*-(4-oxobutyl)pivalamide** (**3m**) and **4-pivalamidobutanoic acid** (**4m**): The title compounds were prepared according to the representative procedure using *N*-(4-oxobutyl)pivalamide--2,2-dimethyl-1-(pyrrolidin-1-yl)propan-1-one. Evaporation of the organic solvent afforded a mixture of the products (**3m**) and (**4m**). The mixture was subjected to an acid-base extraction using sodium bicarbonate (sat. solution) and HCl (5N) to give the major aldehyde product (**3m**) (30.9 mg, 60%) as a dark yellow-brown oil and the minor acid product (**4m**) (1.4 mg, 2.5%) as a yellowish oil.

Aldehyde (**3m**):

^{1}H NMR (500 MHz, $CDCl_3$): δ 9.77 (t, J = 1.2 Hz, 1H), 5.89 (s, 1H), 3.25 (td, J = 6.8, 5.6 Hz, 2H), 2.51 (td, J = 6.9, 1.2 Hz, 2H), 1.83 (p, J = 6.9 Hz, 2H), 1.16 (s, 9H);

^{13}C NMR (126 MHz, $CDCl_3$): δ 202.2, 178.8, 41.7, 39.1, 38.7, 27.6, 22.0;
HRMS (ESI): Calc'd for $C_9H_{18}NO_2$ $[M+H]^+$: 172.1332, found: 172.1334.
Acid (**4m**):
^{1}H NMR (700 MHz, $CDCl_3$) δ 6.05 (s, 1H), 3.35 – 3.29 (m, 2H), 2.39 (t, J = 6.9 Hz, 2H), 1.85 (p, J = 6.8 Hz, 2H), 1.19 (s, 9H);
^{13}C NMR (176 MHz, $CDCl_3$) δ 179.6, 177.5, 81.5, 39.2, 38.9, 31.7, 27.7, 24.8;
HRMS (ESI): Calc'd for $C_9H_{18}NO_3$ $[M+H]^+$: 188.1281, found: 188.1282.

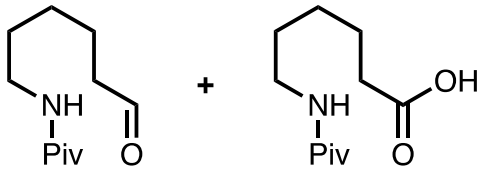

3n **4n**

***N*-(6-oxohexyl)pivalamide** (**3n**) and **6-pivalamidohexanoic acid** (**4n**): The title compounds were prepared according to the representative procedure using 1-(azepan-1-yl)-2,2-dimethylpropan-1-one. Evaporation of the organic solvent afforded a mixture of the products (**3n**) and (**4n**). The mixture was treated with an acid-base extraction using sodium bicarbonate (sat. solution) and HCl (5N) to give the major aldehyde product (**3n**) (16.8 mg, 84%) as a colorless oil and the minor acid product (**4n**) (2.8 mg, 13%) as a yellowish oil.
Aldehyde (**3n**):
^{1}H NMR (500 MHz, $CDCl_3$) δ 9.75 (t, J = 1.7 Hz, 1H), 5.68 (s, 1H), 3.23 (td, J = 7.2, 5.8 Hz, 2H), 2.44 (td, J = 7.2, 1.7 Hz, 2H), 1.64 (p, J = 7.3 Hz, 2H), 1.51 (ddd, J = 14.8, 7.8, 6.6 Hz, 2H), 1.38 – 1.30 (m, 2H), 1.18 (s, 9H);
^{13}C NMR (101 MHz, $CDCl_3$) δ 202.6, 178.7, 43.8, 39.3, 38.8, 29.5, 27.7, 26.4, 21.7;
HRMS (ESI): Calc'd for $C_{11}H_{22}NO_2$ $[M+H]^+$: 200.1645, found: 200.1646.
Acid (**4n**):
^{1}H NMR (500 MHz, $CDCl_3$) δ 5.67 (s, 1H), 3.25 (td, J = 7.2, 5.8 Hz, 2H), 2.36 (t, J = 7.4 Hz, 2H), 1.66 (p, J = 7.4 Hz, 2H), 1.57 – 1.47 (m, 2H), 1.42 – 1.32 (m, 2H), 1.19 (s, 9H);
^{13}C NMR (126 MHz, $CDCl_3$) δ 178.7, 177.7, 39.4, 38.8, 33.7, 29.4, 27.7, 26.3, 24.4;
HRMS (ESI): Calc'd for $C_{11}H_{22}NO_3$ $[M+H]^+$: 216.1594, found: 216.1595.

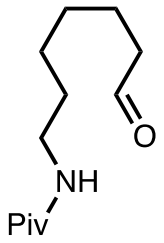

3o

***N*-(7-oxoheptyl)pivalamide** (**3o**): The title compound was prepared according to the representative procedure using 1-(azocan-1-yl)-2,2-dimethylpropan-1-one. Purification by preparative thin-layer chromatography (50% EtOAc/hexanes) provided (**3o**) (19.4 mg, 91%) as a colorless oil.

^{1}H NMR (500 MHz, $CDCl_3$): δ 9.75 (t, J = 1.7 Hz, 1H), 5.64 (s, 1H), 3.21 (td, J = 7.3, 5.7 Hz, 2H), 2.42 (td, J = 7.3, 1.8 Hz, 2H), 1.62 (p, J = 7.2 Hz, 2H), 1.49 (p, J = 7.2 Hz, 2H), 1.32 (qd, J = 6.8, 5.8, 3.6 Hz, 4H), 1.18 (s, 9H);

^{13}C NMR (126 MHz, $CDCl_3$): δ 202.8, 178.5, 43.9, 39.5, 38.8, 29.6, 28.9, 27.7, 26.7, 22.0;

HRMS (ESI): Calc'd for $C_{12}H_{24}NO_2$ $[M+H]^+$: 214.1802, found: 214.1803.

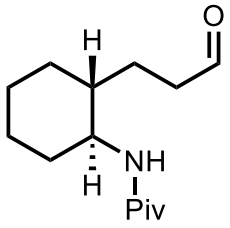

3p

***N*-((1*S*,2*R*)-2-(3-oxopropyl)cyclohexyl)pivalamide** (**3p**): The title compound was prepared according to the representative procedure using 2,2-dimethyl-1-((4a*R*,8a*S*)-octahydroquinolin-1(2*H*)-yl)propan-1-one. Purification by preparative thin-layer chromatography (80% EtOAc/hexanes) provided (**3p**) (15.5 mg, 65%) as a colorless oil.

^{1}H NMR (500 MHz, $CDCl_3$) δ 9.75 (d, J = 1.4 Hz, 1H), 5.62 (d, J = 8.7 Hz, 1H), 3.56 (tdd, J = 11.0, 8.8, 4.1 Hz, 1H), 2.60 – 2.50 (m, 1H), 2.49 – 2.39 (m, 1H), 2.04 – 1.93 (m, 1H), 1.89 – 1.83 (m, 1H), 1.83 – 1.75 (m, 1H), 1.74 – 1.64 (m, 2H), 1.38 – 1.27 (m, 3H), 1.21 (s, 9H), 1.15 – 0.95 (m, 3H);

^{13}C NMR (126 MHz, $CDCl_3$): δ 202.9, 178.1, 51.9, 42.7, 41.0, 38.9, 33.9, 31.1, 27.8, 25.8, 25.3, 24.4;

HRMS (ESI): Calc'd for $C_{14}H_{26}O_2N$ $[M+H]^+$: 240.1958, found: 240.1958;

Calc'd for $C_{14}H_{26}NO_2Na$ $[M+Na]^+$: 262.1778, found: 262.1778.

Procedure for Copper-Mediated Ring Opening

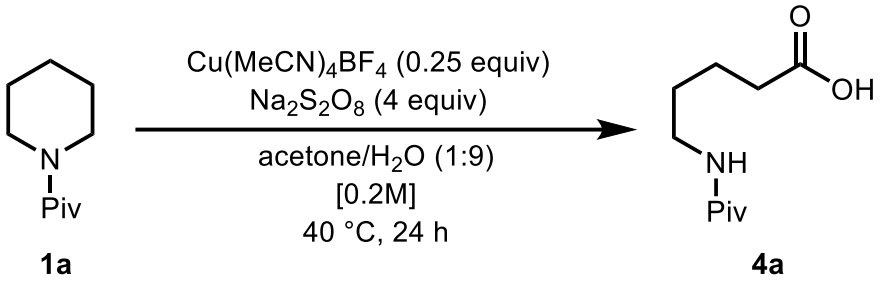

1a **4a**

A 1-dram vial was charged with piperidine **1a** (16.9 mg, 0.10 mmol) and 0.50 mL of a 1:9 acetone:H_2O solution. Sodium persulfate (95 mg, 0.40 mmol) and tetrakis(acetonitrile)copper(I) tetrafluoroborate (7.9 mg, 0.025 mmol) were added to the solution, and the resulting mixture was allowed to stir at 40 °C for 24 h. The reaction mixture was basified with sat. sodium bicarbonate to approx. pH 9, extracted with EtOAc (3 x 3 mL), subsequently acidified to ~pH 4 with 5N HCl and extracted with CH_2Cl_2 (3 x 3 mL). The combined CH_2Cl_2 extracts were dried over Na_2SO_4, filtered, and concentrated under reduced pressure to provide 5-pivalamidopentanoic acid **4a** (10.9 mg, 54%) as a colorless liquid.
^{1}H NMR and ^{13}C NMR spectral data were in full agreement with those for **4a** reported above.
HRMS (ESI): Calc'd for $C_{10}H_{19}NO_3$ $[M+H]^+$: 202.1438, found: 202.1439.

NOTE: Substrates typically show full conversion after a 24 h reaction period. Some over-oxidation can be observed, leading to reduced yields of the desired carboxylic acid.

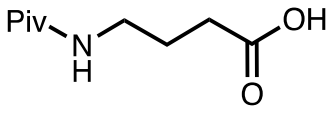

4m

4-Pivalamidobutanoic acid (4m): The title compound was prepared according to the representative procedure on a 200 µmol scale using 2,2-dimethyl-1-(pyrrolidin-1-yl)propan-1-one. Purification by acid-base extraction provided the title compound (**4m**) (22.1 mg, 59%) as a colorless oil.
^{1}H NMR (700 MHz, $CDCl_3$) δ 6.05 (broad s, 1H), 3.32 (td, J = 6.7, 5.8 Hz, 2H), 2.39 (t, J = 6.9 Hz, 2H), 1.85 (apparent p, J = 6.9 Hz, 2H), 1.19 (s, 9H).
^{13}C NMR (176 MHz, $CDCl_3$) δ 179.6, 177.5, 39.2, 38.8, 31.7, 27.6, 24.8.

HRMS (ESI): Calc'd for $C_9H_{18}NO_3$ $[M+H]^+$: 188.1281, found: 188.1282.

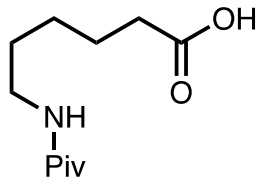

4n

6-Pivalamidohexanoic acid (4n): The title compound was prepared according to the representative procedure on a 200 µmol scale using 1-(azepan-1-yl)-2,2-dimethylpropan-1-one. Purification via acid-base extraction provided the title compound (**4n**) (26.3 mg, 61%) as a colorless oil.

^{1}H NMR (700 MHz, $CDCl_3$) δ 5.74 (broad s, 1H), 3.23 (td, J = 7.2, 5.7 Hz, 2H), 2.34 (t, J = 7.4 Hz, 2H), 1.64 (apparent p, J = 7.4 Hz, 2H), 1.51 (apparent p, J = 7.6 Hz, 2H), 1.44 – 1.33 (m, 2H), 1.18 (s, 9H).

^{13}C NMR (176 MHz, $CDCl_3$) δ 178.9, 178.4, 39.4, 38.8, 33.9, 29.3, 27.7, 26.3, 24.4.

HRMS (ESI): Calc'd for $C_{11}H_{22}NO_3$ $[M+H]^+$: 216.1594, found: 216.1595.

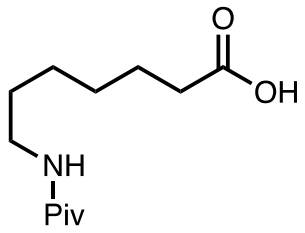

4o

7-Pivalamidoheptanoic acid (4o): The title compound was prepared according to the representative procedure on a 200 µmol scale using 1-(azocan-1-yl)-2,2-dimethylpropan-1-one. Purification using acid-base extraction provided the title compound (**4o**) (24.3 mg, 53%) as a colorless oil.

^{1}H NMR (500 MHz, $CDCl_3$) δ 5.68 (s, 1H), 3.22 (td, J = 7.2, 5.7 Hz, 2H), 2.34 (t, J = 7.4 Hz, 2H), 1.63 (p, J = 7.4 Hz, 2H), 1.50 (p, J = 7.3 Hz, 2H), 1.35 (qtd, J = 16.2, 5.8, 2.8 Hz, 4H), 1.18 (s, 9H);

^{13}C NMR (126 MHz, $CDCl_3$) δ 178.9, 178.8, 39.6, 38.8, 34.0, 29.5, 28.7, 27.7, 26.6, 24.7;

HRMS (ESI): Calc'd for $C_{12}H_{24}NO_3$ $[M+H]^+$: 230.1751, found: 230.1752.

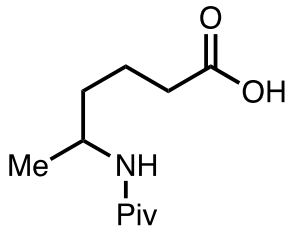

4g

5-Pivalamidohexanoic acid (**4g**): The title compound was prepared according to the representative procedure on a 200 µmol scale using 2,2-dimethyl-1-(2-methylpiperidin-1-yl)propan-1-one. Purification using acid-base extraction provided the title compound (**4g**) (26.7 mg, 62%) as a colorless oil.
^{1}H NMR (500 MHz, $CDCl_3$) δ 5.52 (d, J = 8.3 Hz, 1H), 3.97 (ddd, J = 14.2, 7.9, 6.1 Hz, 1H), 2.43 – 2.28 (m, 2H), 1.69 – 1.54 (m, 2H), 1.54 – 1.39 (m, 2H), 1.17 (s, 9H), 1.11 (d, 3H);
^{13}C NMR (126 MHz, $CDCl_3$) δ 178.4, 178.3, 44.9, 38.7, 38.6, 36.2, 33.7, 27.7, 21.2, 21.0;
HRMS (ESI): Calc'd for $C_{11}H_{22}NO_3$ $[M+H]^+$: 216.1594, found: 216.1595.

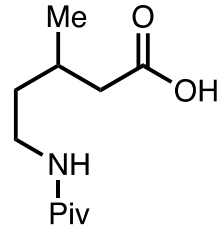

4d

5-Pivalamidoheptanoic acid (4d): The title compound was prepared according to the representative procedure using 1-(2-ethylpiperidin-1-yl)-2,2-dimethylpropan-1-one. Purification using acid-base extraction provided the title compound (**4d**) (25.0 mg, 59%) as a yellow oil.
^{1}H NMR (500 MHz, $CDCl_3$) δ 5.95 (d, J = 5.3 Hz, 1H), 3.27 (td, J = 7.0, 5.4 Hz, 2H), 2.34 (dd, J = 15.6, 7.2 Hz, 1H), 2.23 (dd, J = 15.6, 6.6 Hz, 1H), 1.99 (dq, J = 13.8, 7.0 Hz, 1H), 1.65 – 1.50 (m, 1H), 1.43 (dq, J = 14.2, 7.1 Hz, 1H), 1.17 (s, 9H), 0.99 (d, J = 6.9 Hz, 3H);
^{13}C NMR (126 MHz, $CDCl_3$) δ 179.2, 177.8, 41.3, 38.8, 37.6, 36.2, 27.8, 27.6, 20.1;
HRMS (ESI): Calc'd for $C_{11}H_{22}NO_3$ $[M+H]^+$: 216.1594, found: 216.1595.

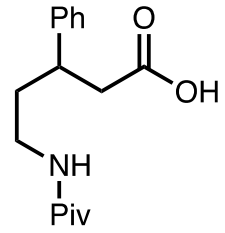

4c

3-phenyl-5-pivalamidopentanoic acid (**4c**): The title compound was prepared according to the representative procedure on a 200 µmol scale using 2,2-dimethyl-1-(4-phenylpiperidin-1-yl)propan-1-one and 1:1 acetone/H_2O solvent. Purification using acid-base extraction provided the title compound (**4c**) (30.2 mg, 54%) as a yellowish oil.
^{1}H NMR (500 MHz, $CDCl_3$) δ 7.33 – 7.27 (m, 2H), 7.24 – 7.16 (m, 3H), 5.64 (t, J = 5.6 Hz, 1H), 3.27 – 3.17 (m, 1H), 3.16 – 2.98 (m, 2H), 2.73 – 2.58 (m, 2H), 2.00 – 1.88 (m, 1H), 1.85 - 1.72 (m, 1H), 1.08 (s, 9H);
^{13}C NMR (126 MHz, $CDCl_3$) δ 178.9, 176.7, 143.3, 129.0, 127.5, 127.1, 41.4, 40.1, 38.7, 38.2, 35.7, 27.5;
HRMS (ESI): Calc'd for $C_{11}H_{24}NO_3$ $[M+H]^+$: 278.1751, found: 278.1751.

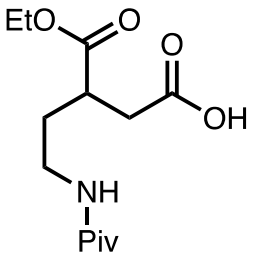

4e

3-(Ethoxycarbonyl)-5-pivalamidopentanoic acid (4e): The title compound was prepared according to the representative procedure on a 200 µmol scale using ethyl 1-pivaloylpiperidine-4-carboxylate. Purification using acid-base extraction provided the title compound (**4e**) (24.9 mg, 46%) as a yellow-orange oil.
^{1}H NMR (500 MHz, $CDCl_3$) δ 6.2 (t, J = 5.8 Hz, 1H), 4.2 (q, J = 7.1 Hz, 2H), 3.5 – 3.1 (m, 2H), 2.9 – 2.8 (m, 2H), 2.5 (dd, J = 16.5, 5.6 Hz, 1H), 1.9 – 1.8 (m, 1H), 1.8 (dtd, J = 14.2, 7.1, 5.3 Hz, 1H), 1.3 (t, J = 7.1 Hz, 3H), 1.2 (s, 9H);
^{13}C NMR (126 MHz, $CDCl_3$) δ 179.4, 175.8, 174.7, 61.2, 39.0, 38.8, 37.6, 35.8, 31.2, 27.6, 14.2;

HRMS (ESI): Calc'd for $C_{13}H_{24}NO_5$ $[M+H]^+$: 274.1649, found: 274.1649.

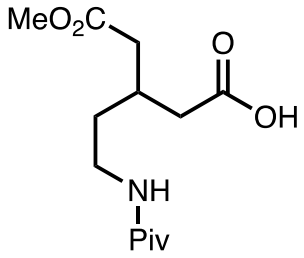

4f

5-methoxy-5-oxo-3-(2-pivalamidoethyl)pentanoic acid (4f): The title compound were prepared according to the representative procedure on a 200 µmol using methyl 2-(1-pivaloylpiperidin-4-yl)acetate. Purification via acid-base extraction provided the title compound (**4f**) (31.2 mg, 57%) as a colorless oil.

^{1}H NMR (500 MHz, $CDCl_3$) δ 6.17 (s, 1H), 3.68 (s, 3H), 3.39 – 3.28 (m, 1H), 3.23 (ddd, J = 14.0, 6.9, 5.5 Hz, 1H), 2.53 – 2.28 (m, 5H), 1.59 (pd, J = 5.8, 2.6 Hz, 2H), 1.20 (s, 9H);

^{13}C NMR (126 MHz, $CDCl_3$) δ 179.6, 176.3, 173.2, 51.9, 38.9, 38.4, 37.2, 33.9, 29.2, 27.63, 27.61;

HRMS (ESI): Calc'd for $C_{13}H_{24}NO_5$ $[M+H]^+$: 274.1649, found: 274.1649.

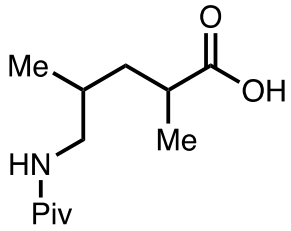

4q

2,4-Dimethyl-5-pivalamidopentanoic acid (4q): The title compound was prepared according to the representative procedure on a 200 µmol scale using 1-(3,5-dimethylpiperidin-1-yl)-2,2-dimethylpropan-1-one. Purification using acid-base extraction provided the title compound (**4q**) (18.8 mg, 41%, mixture of diastereomers 1.0:0.5) as a slight yellowish oil.

^{1}H NMR See ^{1}H NMR spectrum.X

^{13}C NMR (126 MHz, $CDCl_3$) δ 182.1, 181.8, 179.3, 179.0, 45.2, 45.1, 38.9 (corresponding peak for minor diastereomer overlapping), 38.3, 38.2, 37.5, 36.9, 32.0, 31.3, 27.70, 27.68, 18.3, 18.0, 17.9, 17.3;
HRMS (ESI): Calc'd for $C_{12}H_{24}NO_3$ $[M+H]^+$: 230.1751, found: 230.1751.

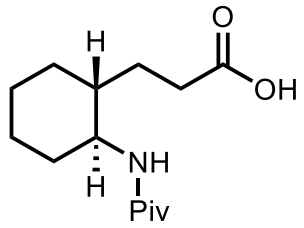

4p

3-(2-Pivalamidocyclohexyl)propanoic acid (4p): The title compound was prepared according to the representative procedure on a 200 µmol scale using 2,2-dimethyl-1-(octahydroquinolin-1(2*H*)-yl)propan-1-one and one equivalent of tetrakis(acetonitrile)copper(I) tetrafluoroborate (63.0 mg, 0.20 mmol). Purification using acid-base extraction provided the title compound (**4p**) (26.5 mg, 52%) as a light orange amorphous solid.
^{1}H NMR (500 MHz, $CDCl_3$) δ 9.74 (br s, 1H), 6.32 (d, J = 7.8 Hz, 1H), 4.59 (td, J = 7.5, 5.0 Hz, 1H), 3.74 (s, 3H), 2.44 – 2.25 (m, 2H), 1.92 – 1.86 (m, 1H), 1.75 – 1.55 (m, 3H), 1.21 (s, 9H);
^{13}C NMR (126 MHz, $CDCl_3$) δ 178.8, 178.6, 51.99, 51.98, 42.6, 38.9, 33.8, 31.0, 27.7, 27.2, 25.7, 25.3;
HRMS (ESI): Calc'd for $C_{14}H_{26}NO_3$ $[M+H]^+$: 256.1907, found: 256.1907.

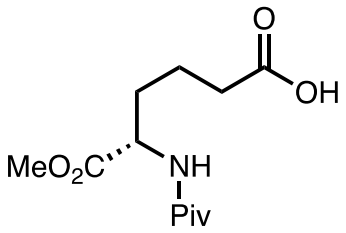

4r

3-(2-Pivalamidocyclohexyl)propanoic acid (4r): The title compound was prepared according to the representative procedure using 2,2-dimethyl-1-(octahydroquinolin-1(2*H*)-

yl)propan-1-one. Purification using acid-base extraction provided the title compound (**4r**) (32.0 mg, 62%) as a yellow oil.

^{1}H NMR (500 MHz, $CDCl_3$) δ 9.73 (br s, 2H), 6.32 (d, J = 7.6 Hz, 1H), 4.59 (apparent td, J = 7.5, 5.1 Hz, 1H), 3.74 (s, 3H), 2.70 – 2.23 (m, 2H), 1.91 (apparent ddt, J = 12.3, 9.5, 5.1 Hz, 1H), 1.78 – 1.52 (m, 3H), 1.21 (s, 9H);

^{13}C NMR (126 MHz, $CDCl_3$) δ 178.8, 178.0, 173.2, 52.6, 51.8, 38.9, 33.3, 31.8, 27.5, 20.5;

HRMS (ESI): Calc'd for $C_{12}H_{22}NO_5$ $[M+H]^+$: 260.1492, found: 260.1493.

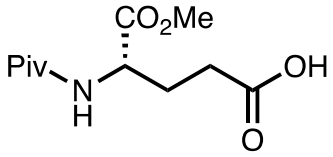

4s

(*S*)-5-Methoxy-5-oxo-4-pivalamidopentanoic acid (4s): The title compound was prepared according to the representative procedure using methyl pivaloyl-*L*-prolinate. Purification using acid-base extraction provided the title compound (**4s**) (29.3 mg, 60%) as a slight yellowish oil.

^{1}H NMR (700 MHz, $CDCl_3$) δ 6.46 (d, J = 7.5 Hz, 1H), 4.62 (td, J = 8.2, 5.1 Hz, 1H), 3.76 (s, 3H), 2.48 – 2.38 (m, 2H), 2.31 – 2.15 (m, 1H), 1.98 (apparent ddt, J = 13.8, 8.5, 6.9 Hz, 1H);

^{13}C NMR (176 MHz, $CDCl_3$) δ 179.2, 176.9, 172.7, 52.8, 51.8, 38.9, 30.3, 27.5, 27.5;

HRMS (ESI): Calc'd for $C_{11}H_{20}NO_5$ $[M+H]^+$: 246.1336, found: 246.1337.

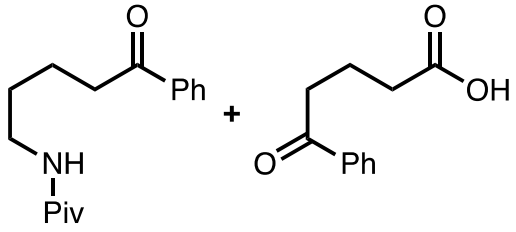

4t **4t.a**

***N*-(5-Oxo-5-phenylpentyl)pivalamide (4t) and 5-oxo-5-phenylpentanoic acid (4t.a):** The title compounds were prepared according to the representative procedure using (*S*)-2,2-dimethyl-1-(2-phenylpiperidin-1-yl)propan-1-one. Purification using acid-base extraction provided the title compounds **4t** (8.9 mg, 17%, 41% brsm) as a colorless oil and **4t.a** (3.5 mg, 9%, 17% brsm) as a white amorphous solid.

4t:

^{1}H NMR (500 MHz, $CDCl_3$) δ 8.14 – 7.86 (m, 2H), 7.64 – 7.51 (m, 1H), 7.46 (dd, J = 8.3, 7.1 Hz, 2H), 5.85 (s, 1H), 3.27 (td, J = 6.9, 5.6 Hz, 2H), 3.02 (t, J = 7.0 Hz, 2H), 1.92 – 1.73 (m, 2H), 1.65 – 1.53 (m, 2H), 1.20 (s, 9H);

^{13}C NMR (126 MHz, $CDCl_3$) δ 200.3, 178.7, 137.0, 133.2, 128.2, 39.2, 38.8, 38.0, 29.2, 27.8;

HRMS (ESI): Calc'd for $C_{16}H_{23}NO_2Na$ $[M+Na]^+$: 284.1621, found: 284.1623.

4t.a:

^{1}H NMR (500 MHz, $CDCl_3$) δ 8.16 – 7.88 (m, 2H), 7.75 – 7.52 (m, 1H), 7.46 (apparent t, J = 7.7 Hz, 2H), 3.09 (t, J = 7.1 Hz, 2H), 2.51 (t, J = 7.1 Hz, 2H), 2.09 (apparent p, J = 7.1 Hz, 2H).

^{13}C NMR (126 MHz, $CDCl_3$) δ 199.5, 178.1, 136.9, 133.3, 128.8, 128.2, 37.4, 33.0, 19.2;

HRMS (ESI): Calc'd for $C_{11}H_{12}O_3Na$ $[M+Na]^+$: 216.0679, found: 216.0677

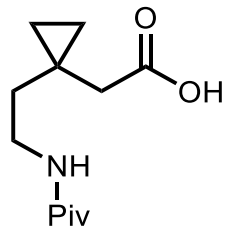

4u

2-(1-(2-pivalamidoethyl)cyclopropyl)acetic acid (4u): The title compound was prepared according to the representative procedure on a 200 µmol scale using 2,2-dimethyl-1-(6-azaspiro[2.5]octan-6-yl)propan-1-one. Purification using acid-base extraction provided the title compound (**4u**) (25.0 mg, 55%) as a yellowish oil.

^{1}H NMR (500 MHz, $CDCl_3$) δ 6.30 (br s, 1H), 3.34 (td, J = 6.8, 5.5 Hz, 2H), 2.31 (s, 2H), 1.57 (t, J = 6.8 Hz, 2H), 1.18 (s, 9H), 0.51 – 0.46 (m, 2H), 0.46 – 0.41 (m, 2H).

^{13}C NMR (126 MHz, $CDCl_3$) δ 179.0, 177.1, 41.0, 38.7, 37.7, 36.3, 27.6, 15.2, 12.3.

HRMS (ESI): Calc'd for $C_{12}H_{22}NO_3$ $[M+H]^+$: 228.1595, found: 228.1595.

Procedures for Peptide Diversification

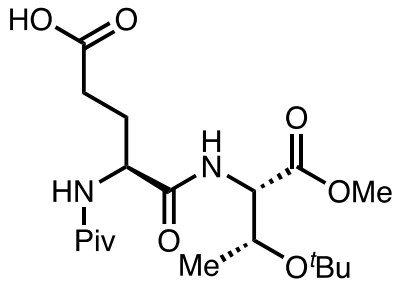

6a

(*S*)-5-(((2*S*,3*R*)-3-(*tert*-Butoxy)-1-methoxy-1-oxobutan-2-yl)amino)-5-oxo-4-pivalamido-pentanoic acid (6a): The title compound was prepared according to the representative procedure using methyl (3*R*)-3-(*tert*-butoxy)-2-((*S*)-1-pivaloylpyrrolidine-2-carboxamido)butanoate (**5a**) with 1:1 acetone/H2O as solvent. Purification using acid-base extraction provided the title compound **6a** (22.5 mg, 56%, mixture of rotamers 1:0.8) as a slightly yellow oil.

^{1}H NMR (500 MHz, $CDCl_3$) δ 7.06 (t, J = 9.3 Hz), 6.92 (d, J = 7.3 Hz), 6.77 (d, J = 7.7 Hz), 4.68 – 4.58 (m), 4.45 (ddd, J = 9.2, 4.4, 1.8 Hz), 4.23 (dtd, J = 12.6, 6.2, 1.8 Hz), 3.70 (d, J = 5.0 Hz), 2.60 – 2.41 (m), 2.26 – 2.14 (m), 2.09 – 1.95 (m), 1.21 (d, J = 9.0 Hz), 1.16 (dd, J = 6.3, 4.9 Hz), 1.10 (d, J = 7.3 Hz);
^{13}C NMR 13C NMR (126 MHz, $CDCl_3$) δ 179.5, 179.3, 176.9, 176.6, 172.24, 172.20, 171.3, 171.1, 74.5, 74.4, 67.4, 67.3, 58.3, 58.1, 52.9, 52.5, 52.3, 39.0, 38.9, 30.5, 30.2, 28.4, 28.2, 27.6, 27.5, 21.09, 21.08;
HRMS (ESI): Calc'd for $C_{18}H_{29}N_9O_2$ $[M+H]^+$: 403.2439, found: 403.2439.

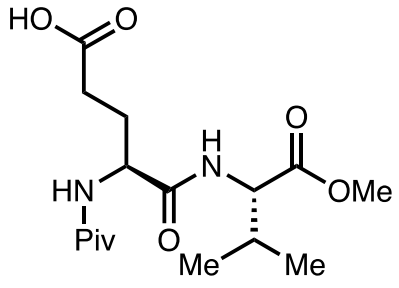

6b

(*S*)-5-(((*S*)-1-Methoxy-3-methyl-1-oxobutan-2-yl)amino)-5-oxo-4-pivalamidopentanoic acid (6b): The title compound was prepared according to the representative procedure using methyl pivaloyl-*L*-prolyl-*L*-valinate (**5b**). Purification using acid-base extraction provided the title compound **6b** (25.5 mg, 74%, mixture of rotamers 1:0.5) as a slightly yellow oil.

^{1}H NMR (500 MHz, $CDCl_3$) δ 7.50 (t, J = 8.2 Hz), 6.84 (d, J = 8.0 Hz), 4.74 – 4.65 (m), 4.45 (dd, J = 8.7, 5.1 Hz), 4.42 (dd, J = 8.3, 5.2 Hz), 3.72 (s), 3.70 (s), 2.48 (qd, J = 5.7, 2.3 Hz), 2.24 – 2.05 (m), 2.01 – 1.88 (m), 1.29 – 1.22 (m), 1.19 (s), 1.18 (s), 0.95 – 0.88 (m);
^{13}C NMR (126 MHz, $CDCl_3$) δ 179.8, 179.7, 176.3, 176.2, 172.2, 172.1, 172.0, 57.9, 57.7, 52.29, 52.28, 52.2, 52.1, 38.94, 38.91, 38.6, 31.0, 30.7, 30.3, 30.1, 27.4, 27.2, 19.2, 19.1, 17.84, 17.83;
HRMS (ESI): Calc'd for $C_{15}H_{23}N_9O$ $[M+H]^+$: 345.2020, found: 345.2019.

Procedures for Peptide Diversification from Dipeptide 6b

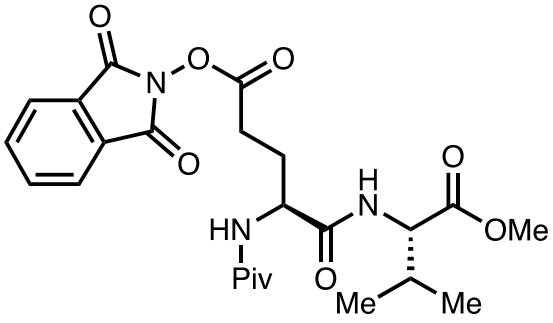

7a

1,3-dioxoisoindolin-2-yl (*S*)-5-(((*S*)-1-methoxy-3-methyl-1-oxobutan-2-yl)amino)-5-oxo-4-pivalamidopentanoate (7a): A 2-dram vial was charged with carboxylic acid **5b** (207 mg, 0.6 mmol), *N*-hydroxyphthalimide (NHPI; 97.9 mg, 0.6 mmol), *N*,*N*'-dicyclohexylcarbodiimide (DCC; 123.8 mg, 0.6 mmol), and dry CH_2Cl_2 (3.0 mL), and the reaction mixture was allowed to stir at room temperature overnight. The mixture was concentrated under reduced pressure, and the resulting crude material was purified by column chromatography (1:2 Hexanes/EtOAc) to provide the title compound **7a** (237 mg, 80%, mixture of rotamers 1:1) as an off-white solid.

^{1}H NMR (500 MHz, $CDCl_3$) δ 7.88 (ddd, J = 5.5, 2.5, 0.9 Hz), 7.79 (ddd, J = 5.5, 3.1, 0.9 Hz), 6.97 (s), 6.44 (d, J = 8.3 Hz), 4.78 – 4.57 (m), 4.47 (ddd, J = 8.5, 4.9, 1.4 Hz), 3.73 (d, J = 0.9 Hz), 3.72 (d, J = 1.1 Hz), 3.04 – 2.83 (m), 2.82 – 2.60 (m), 2.48 – 2.25 (m), 2.18 (dqd, J = 15.0, 6.7, 3.6 Hz), 1.23 (d, J = 0.8 Hz), 1.21 (d, J = 0.7 Hz), 0.94 (dd, J = 10.4, 7.0 Hz), 0.91 (dd, J = 6.9, 1.5 Hz);
^{13}C NMR (126 MHz, $CDCl_3$) δ 179.5, 179.1, 171.9, 171.2, 171.1, 169.69, 169.67, 169.6, 162.0, 161.9, 135.0, 129.0, 124.2, 57.7, 57.6, 52.34, 52.30, 52.2, 52.1, 39.01, 38.95, 31.1, 30.9, 27.8, 27.7, 27.57, 27.55, 27.3, 27.1, 19.2, 19.1, 17.8;
HRMS (ESI): Calc'd for $C_{24}H_{32}NO_8$ $[M+H]^+$: 490.2184, found: 490.2184.

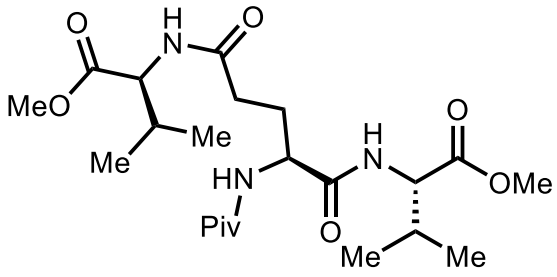

7b

Dimethyl 2,2'-(((S)-2-pivalamidopentanedioyl)bis(azanediyl))(2S,2'S)-bis(3-methylbutanoate) (7b): A 1-dram vial was charged with carboxylic acid **5b** (34.4 mg, 0.1 mmol), *L*-valine methyl ester hydrochloride (18.4 mg, 0.11 mmol), hydroxybenzotriazole (HOBt; 13.5 mg, 0.1 mmol), and dry CH_2Cl_2 (1.5 mL) and cooled to 0 °C in an ice bath. iPr_2Net (23 μL, 0.13 mmol) was added to the mixture dropwise over 5 min, and the resulting mixture was stirred at 0 °C for 10 min. To this mixture was added 1-(3-dimethylaminopropyl)-3-ethylcarbodiimide hydrochloride (EDC; 21.1 mg, 0.11 mmol), and the mixture was allowed to stir and warm to room temperature over 16 h. The reaction mixture was cooled to 0 °C and quenched with 1 M HCl (1 mL). The phases were separated, and the aqueous phase was extracted with CH_2Cl_2 (3 mL × 3). The combined organic layers were washed with brine (1 mL), dried over Na_2SO_4, filtered, and concentrated under reduced pressure. The resulting crude material was purified by column chromatography (1:2 Hexanes/EtOAc) to provide the title compound **7b** (22.9 mg, 50%, mixture of rotamers) as a white amorphous solid.
^{1}H NMR (500 MHz, $CDCl_3$) δ 8.06 (d, J = 8.3 Hz), 7.81 (d, J = 8.8 Hz), 7.30 (d, J = 8.5 Hz), 7.11 (d, J = 9.0 Hz), 6.86 (d, J = 6.8 Hz), 6.46 (d, J = 7.1 Hz), 4.82 (dddd, J = 8.1, 6.9, 2.5, 1.3 Hz), 4.55 (dddd, J = 8.8, 6.4, 5.3, 1.1 Hz), 4.48 – 4.40 (m), 4.28 (ddd, J = 9.3, 7.1, 5.6 Hz), 3.74 (d, J = 0.9 Hz), 3.73 (d, J = 0.8 Hz), 3.73 (d, J = 0.8 Hz), 3.71 (d, J = 0.9 Hz),

2.46 (dd, J = 6.1, 4.3 Hz), 2.43 (dd, J = 6.0, 4.3 Hz), 2.40 – 1.87 (m), 1.18 (d, J = 0.9 Hz), 1.15 (d, J = 0.9 Hz), 1.07 – 0.86 (m);

^{13}C NMR (126 MHz, $CDCl_3$) δ 179.6, 178.3, 174.7, 173.9, 173.8, 173.3, 173.0, 172.4, 172.1, 58.6, 57.7, 57.63, 57.58, 52.7, 52.6, 52.42, 52.41, 52.24, 52.22, 38.8, 38.7, 32.6, 32.4, 30.8, 30.5, 30.4, 29.7, 28.9, 27.53, 27.52, 19.5, 19.3, 19.2, 19.1, 18.1, 18.0, 17.93, 17.90.

HRMS (ESI): Calc'd for $C_{24}H_{32}NO_8$ $[M+H]^+$: 458.2861, found: 458.2864.

Computational Details

General Computational Considerations for Photo- and Copper-Mediated Reactions

Optimization of all reported structures and frequency calculations for the reactions of (a) the riboflavin tetraacetate (**2a**), potassium persulfate, and N-Piv-piperidine (**1a**), as well as the reaction of (b) $CuBF_4$, sodium-persulfate, and N-Piv-piperidine (**1a**) were performed using the Gaussian-16 suite of programs[53] at the B3LYP-D3(BJ)/[6-31G(d,p) + Lanl2dz (Cu)] level of theory with the corresponding Hay-Wadt effective core potential[54–56] for Cu. Therefore, in the calculations described here, we used the B3LYP density functional[57–59] with Grimme's empirical dispersion-correction (D3)[60] and Becke-Johnson (BJ) damping-correction.[61–63] Frequency analyses were used to characterize each minimum and transition state (TS) with zero and one imaginary frequency, respectively. Intrinsic reaction coordinate (IRC) calculations were performed for all TSs to ensure their true nature. Bulk solvent effects were incorporated for all calculations (including geometry optimizations and frequency calculations) using the self-consistent reaction field polarizable continuum model (IEF-PCM).[64,65] Water was chosen as solvent. The reported thermodynamic data were computed at a temperature of 298.15 K and at 1 atm of pressure. Various spin states (including the open-shell singlet states, where that is appropriate) were considered for all key species. All UV-Vis calculations were performed at the TD-DFT [14] level of theory.[66] Previously, we[67,68] and others[69,70] have demonstrated that the B3LYP-D3(BJ) and B3LYP are a reasonable choice for geometry optimization, frequency calculations, as well as for calculation of the relative energies. The role of intersystem crossing (ISC) was examined by locating low energy points on the singlet-triplet crossing surfaces, or seams. These points, which we call minima on the seam of crossing (MSX), were searched using the MECPRO optimize [see: Hamill LA, Snyder JD, Ess DH (**2016**) MECPro Version 1.0.3: Minimum Energy Crossing Program] by starting from each of the triplet and singlet minima along the reaction pathway. We used the xTB's Conformer-Rotamer Ensemble Sampling Tool (CREST) software to identify possible stable conformers of **{(2.A.m)–[$K_2S_2O_8$]}** and **{(2.A.m)–[$K_2S_2O_8$]}–(1a)**. In these calculations, conformers were sampled using the MF-MD-GC workflow. Later, we utilized the outcomes of these conformational analyses in our DFT calculations, and always have validated the related potential conformers. However, here, we discussed only lowest energy structures.

Critical Interactions in {(2.A.m)–[$K_2S_2O_8$]} and {(2.A.m)–[$K_2S_2O_8$]}–(1a)

We wish to emphasize that our initial conformational analyses of **{(2.A.m)–[$K_2S_2O_8$]}** and **{(2.A.m)–[$K_2S_2O_8$]}–(1a)**, performed using the xTB's Conformer-Rotamer Ensemble Sampling Tool (CREST) software, have enabled us to identify several critically important interactions both between (**2.A.m**) and $K_2S_2O_8$ as well as between the **{(2.A.m)–[$K_2S_2O_8$]}** unit and substrate **1a** (See Figure 1.4.6). Over the course of this study, we always have utilized these interactions for design of our DFT calculations. Thus, we always validated the related potential conformers, and we discuss only the lowest energy structures in this Article.

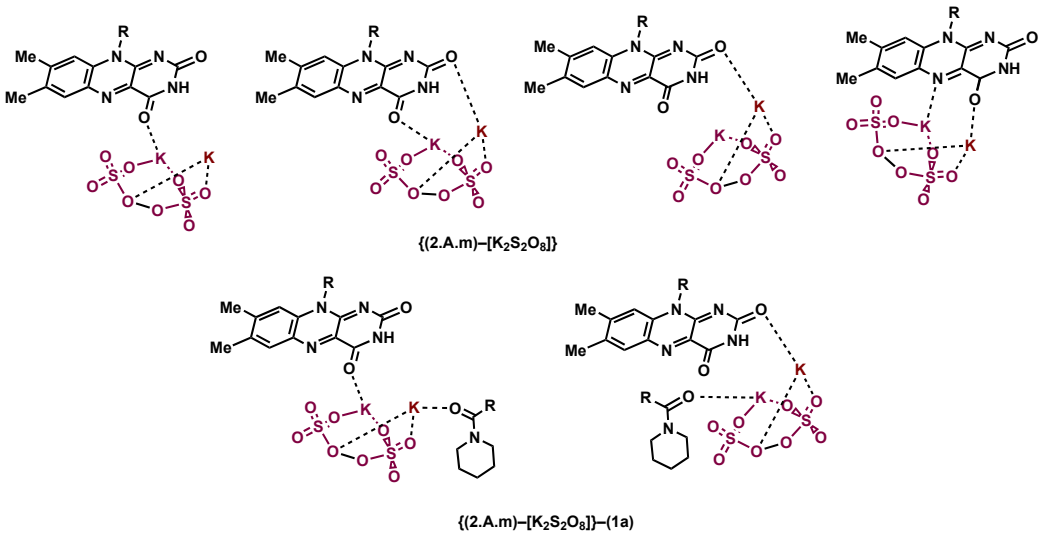

Figure 1.4.6: The validated conformers of the **{(2.A.m)–[$K_2S_2O_8$]}** and **{(2.A.m)–[$K_2S_2O_8$]}–(1a)** structures.

Verification of Photocatalyst Model

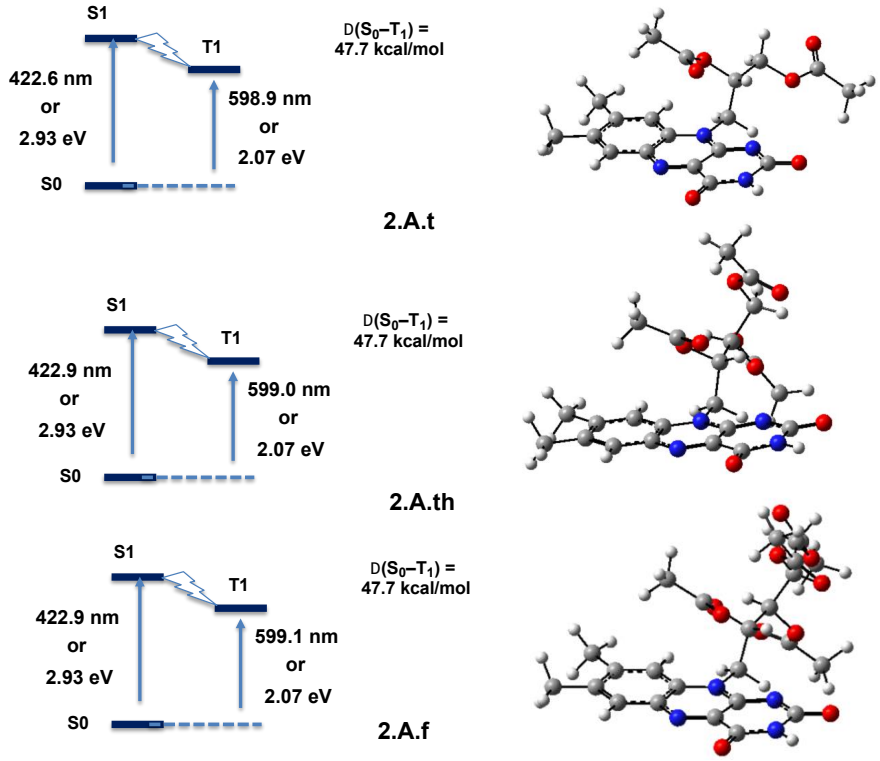

Figure 1.4.7: Validation for the use of the isoalloxazine monoacetate as a model for isoalloxazine tetraacetate.

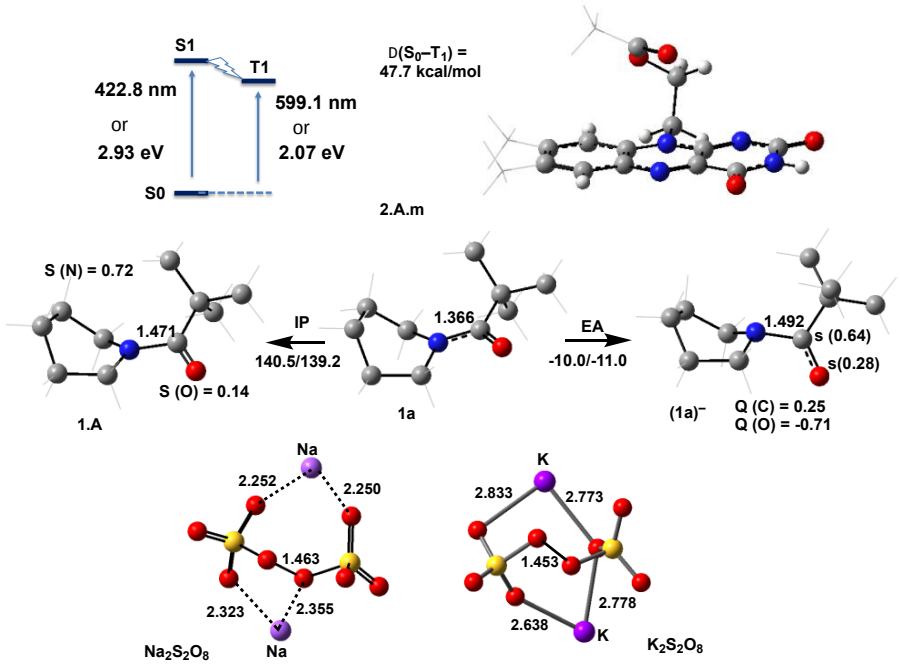

Figure 1.4.8: The calculated geometry parameters and relative energies of isoalloxazine monoacetate, (**2.A.m**), substrate **1a**, iminium ion **1.A**, $Na_2S_2O_8$, and $K_2S_2O_8$.

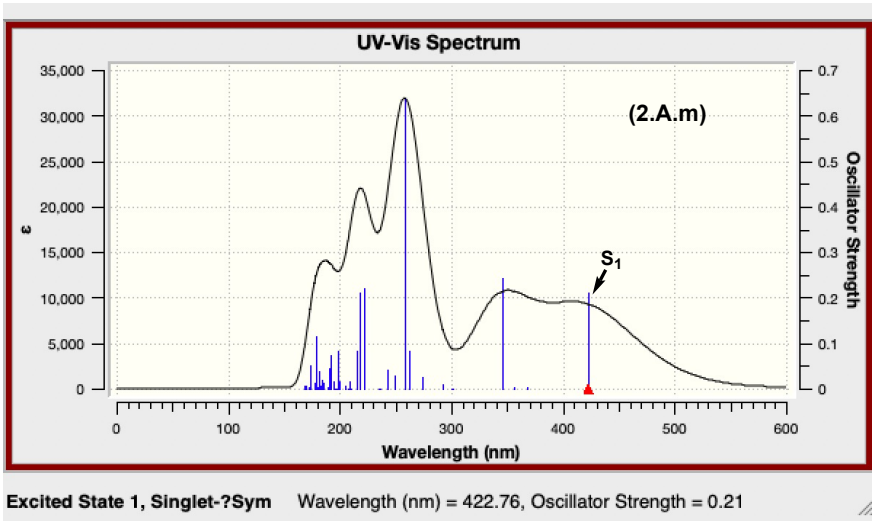

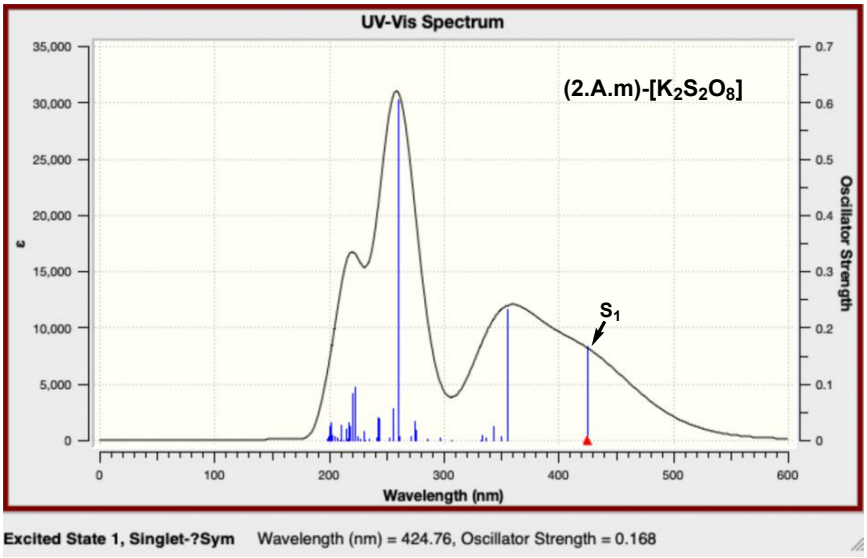

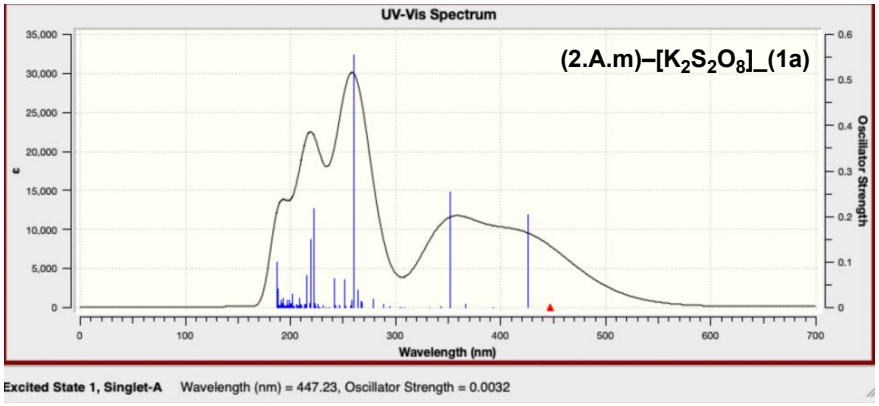

Figure 1.4.9: The calculated UV-vis spectra of isoalloxazine monoacetate, (**2.A.m**, isoalloxazine - persulfate **(2.A.m)**–**[$K_2S_2O_8$]**, and **{(2.A.m)**–**[$K_2S_2O_8$]**–**(1a)}** systems.

Table 1.4.8: Excitation energies (in eV and nm), oscillator strengths (f) for the isoalloxazine monoacetate-persulfate adduct, **{(2.A.m)**–**[$K_2S_2O_8$]**–**(1a)}**, and associated frontier molecular orbitals.

Excited State 1: Singlet-A 2.7723 eV 447.23 nm f=0.0032 (dark)
HOMO -> LUMO 0.70640

Excited State 2: Singlet-A 2.9117 eV 425.81 nm f=0.2049 (bright)
HOMO-3 -> LUMO 0.13122
HOMO-1 -> LUMO 0.68961

Excited State 3: Singlet-A 3.1542 eV 393.08 nm f=0.0002 (dark)
HOMO-2 -> LUMO 0.70468

Excited State 4: Singlet-A 3.3778 eV 367.06 nm f=0.0065 (dark)
HOMO-8 -> LUMO 0.45939
HOMO-6 -> LUMO -0.23666
HOMO-5 -> LUMO 0.45320

Excited State 5: Singlet-A 3.5251 eV 351.72 nm f=0.2539 (bright)
HOMO-3 -> LUMO 0.66806
HOMO-1 -> LUMO -0.11662
HOMO-1 -> LUMO -0.12354

----------MOs----------
LUMO+1 energy = –0.045754 a.u.

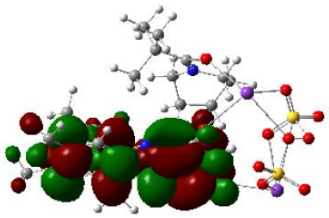

LUMO –0.112529 a.u.

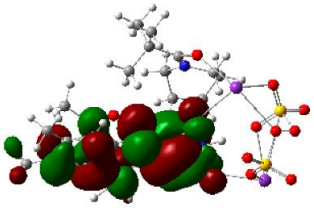

HOMO –0.234451 a.u.

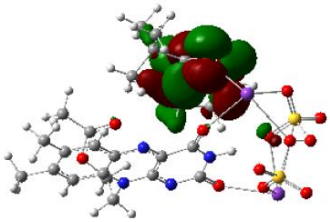

HOMO–1 –0.235775 au.u

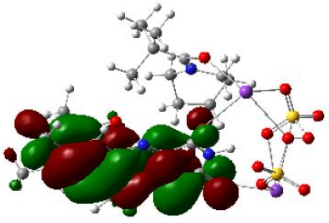

HOMO–2 –0.248124

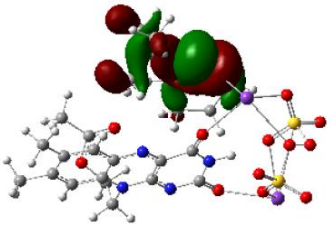

HOMO–3 –0.261656

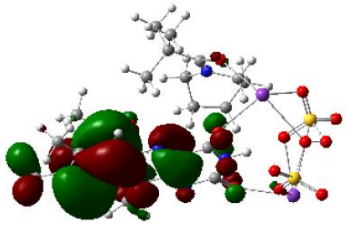

To validate that $K_2S_2O_8$ is not the photocatalyst under blue light irradiation, we have calculated the several lower-lying excited states of $K_2S_2O_8$ at the TD-DFT level. These calculations (see Figure 1.4.10) show that the first feasible excited transition of its UV-Vis spectra is the S_0/S_4 transition at 201.1 nm with a transition dipole of f = 0.0102. This is the HOMO–3 → LUMO transition, where the LUMO is the antibonding orbital of the peroxy O–O bond. Indeed, at 450 nm irradiation, flavin catalysis should lead to substrate oxidation rather than the persulfate homolysis.

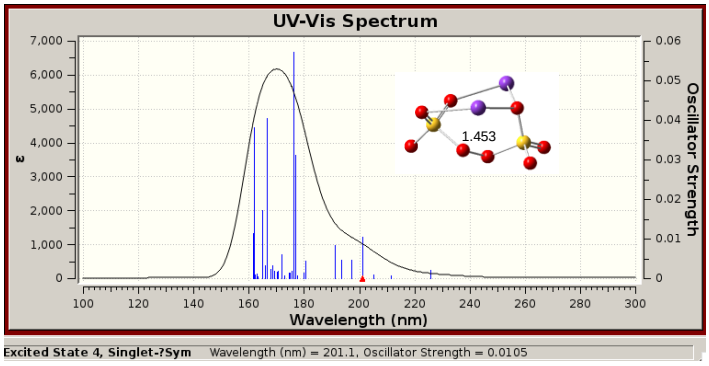

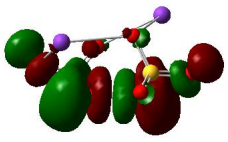

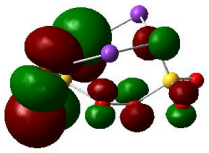

Excited State 1: 5.4885 eV 225.90 nm f=0.0020
65 -> 68 0.51235
66 -> 68 0.35060
67 -> 68 -0.22669

Excited State 2: 5.8605 eV 211.56 nm f=0.0008
65 -> 68 0.16933
66 -> 68 0.16572
67 -> 68 0.64189

Excited State 3: 6.0389 eV 205.31 nm f=0.0009
65 -> 68 -0.39161
66 -> 68 0.55695

Excited State 4: 6.1654 eV 201.10 nm f=0.0105
60 -> 68 0.11249
64 -> 68 0.65696

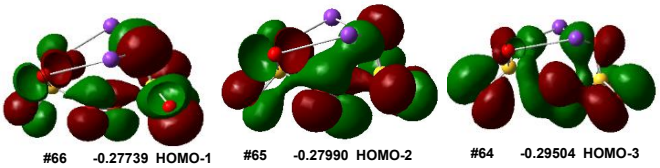

Figure 1.4.10: The calculated UV-Vis spectrum of the $K_2S_2O_8$ oxidant and associated frontier molecular orbitals with their energies (in a.u.). Here, we also show the character of the first four transitions as well as their energies and dipole moments (f).

Computed Reaction Mechanism for Photo-Mediated Reaction

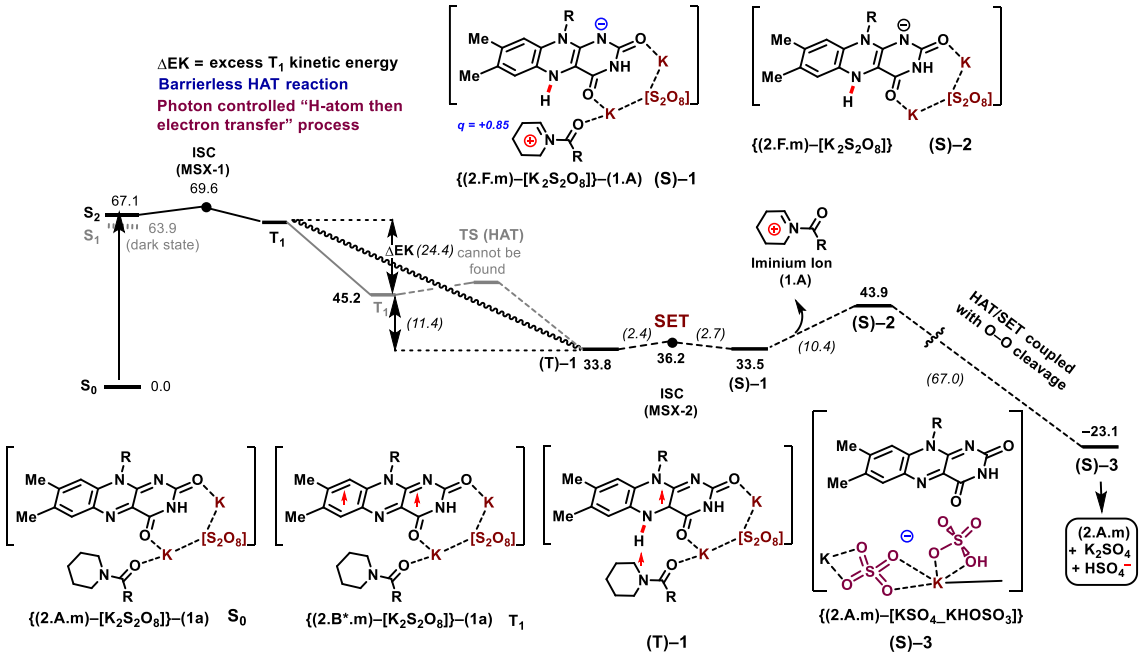

Figure 1.4.11: Computed reaction mechanism for the photocatalytic transformation of *N*-Piv-piperidine (**1a**) to iminium ion **1.A** by the reaction of riboflavin monoacetate (**2.A.m**), **1a**, and $K_2S_2O_8$. All energies are listed in kcal/mol, and energy differences are shown in parentheses. Here, the energies given for the reaction $\mathbf{T}_1$ ® [**(S)-3**] are Gibbs free energies (calculated relative to the $\mathbf{T}_1$ state), except the energy of the **MSX-2** which is an electronic energy (E) calculated relative to that of the **(T)–1** intermediate. The presented energies for the $\mathbf{S}_0$ ®$\mathbf{T}_1$ are electronic energies, calculated relative to the $\mathbf{S}_0$ state.

The processes leading to the formation of iminium ion and **(S)–2** intermediate were presented in main text. From the byproduct **(S)–2** (i.e.,{(**2.F.m**)–[$K_2S_2O_8$]}), the reaction undergoes *SET, HAT, and O–O homolysis* to form the singlet state complex {(**2.A.m**)–[K_2SO_4]–[$HOSO_3^-$], **(S)-3**. This process may proceed in a stepwise or concerted fashion. The conversion **(S)–2 → (S)–3** is calculated to be highly exergonic (by 77.4 kcal/mol). Because of the multi-component nature of this reaction, we failed to locate the associated transition state(s). However, we have established that the first step of this multi-step process is a SET from the fully reduced isoalloxazine-acetate, (**2.F.m**), to the potassium-persulfate.

Optimized Structure Energy Components for Photo-Mediated Reaction

Table 1.4.9: Calculated total electronic (E_{tot}), E_{tot} with zero-point energy corrections (E_{tot} + ZPEC), enthalpy (H), and Gibbs free energies (in Hartrees; all values are negative) of all reported structures for the reaction of the isoalloxazine-acetate, potassium persulfate, and N-Piv-piperidine (**1a**)

Str	$-E_{tot}$	$-E_{tot}$ + ZPEC	−H	−G
(**2.A.m**)_sing	1139.423323	1139.110825	1139.088549	1139.16196
(**2.A.m**)_trip	1139.351508	1139.042038	1139.019378	1139.094658
(**2.A.m**)_1min	1139.540237	1139.230171	1139.20776	1139.281876
(**2.A.m**)_1plus	1139.200118	1138.88866	1138.866161	1138.940735
$K_2S_2O_8$	2598.037921	2598.003612	2597.988744	2598.048963
K_2SO_4	1899.058273	1899.041357	1899.032089	1899.078054
(**2.A.t**), sing	1406.636299	1406.253586	1406.225075	1406.31546
(**2.A.th**), sing	1673.850366	1673.396492	1673.362321	1673.465634
(**2.A.f**), sing	1941.066384	1940.541517	1940.501644	1940.618886
1a, singlet	522.575576	522.29325	522.279314	522.331989
1a, triplet	522.4478571	522.169834	522.155278	522.211105
1a_1plus	522.3498876	522.069779	522.055457	522.110236
1a_1minus	522.5861193	522.309523	522.295276	522.349493
1.A	521.7908303	521.52002	521.506158	521.558656
(**2.A.m**)_ $K_2S_2O_8$ S_0'	3737.498766	3737.150155	3737.112509	3737.2236
(**2.B*.m**)_ $K_2S_2O_8$, $\mathbf{T_1}$'	3737.426034	3737.080619	3737.042464	3737.156538
(**2.A.m**)_ $K_2S_2O_8$_**1a**, $\mathbf{T_1}$	4260.038301	4259.408437	4259.355687	4259.49964
sing	4260.100542	4259.467873	4259.415338	4259.558948
[**2.C.m**]_ $K_2S_2O_8$_1min, doub	3737.618466	3737.272547	3737.234512	3737.348769
quartet	3737.489247	3737.148696	3737.109624	3737.224997
(T)–1	4260.055298	4259.42552	4259.372532	4259.517803
(S)–1	4260.060305	4259.428837	4259.376186	4259.518369
[**2.F.m**]_ $K_2S_2O_8$_1min				
Singlet	3738.225214	3737.867193	3737.828621	3737.943193
Triplet	3738.150189	3737.795498	3737.756296	3737.873933
[**2.A.m**]_$HOSO_3$_K_2SO_4_1min				
3738.352924	3738.225214	3737.993242	3737.955312	3738.066452

Optimized Structures and Energy Components for Copper-Mediated Reaction

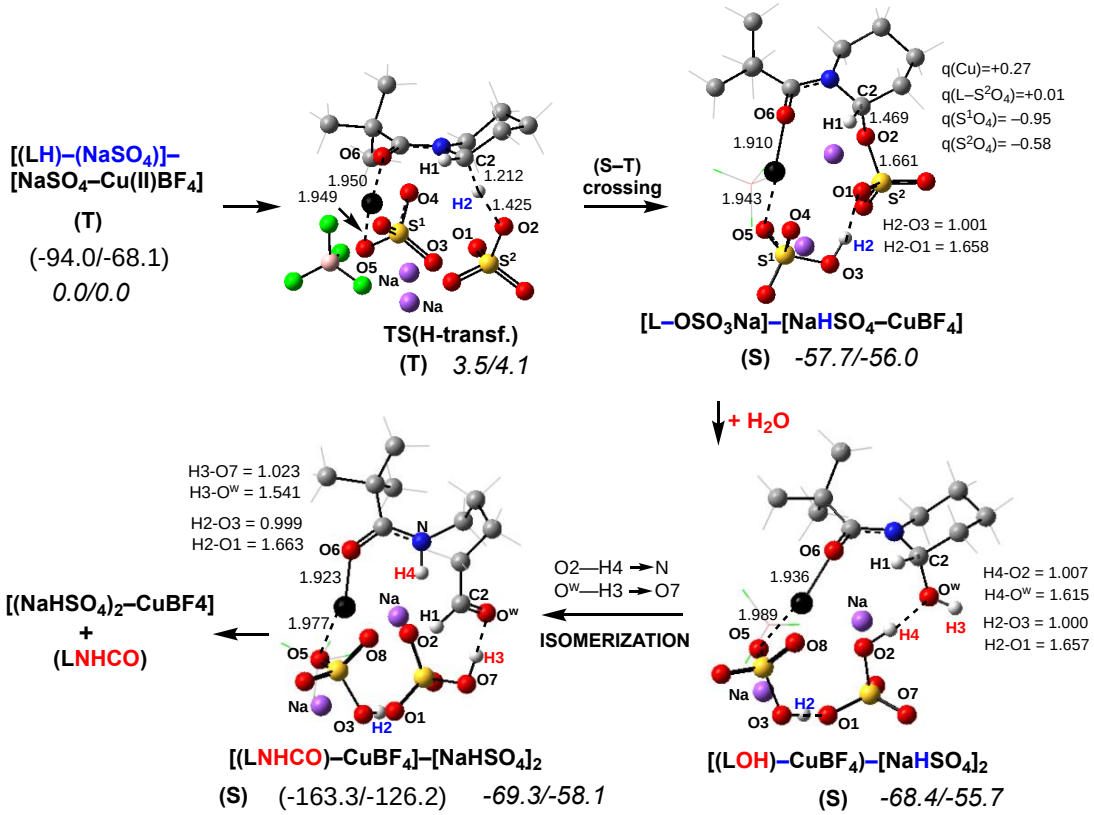

Figure 1.4.12: Computed relevant intermediates along with their geometry parameters (in Å) and relative energies (in kcal/mol) for the reaction of $CuBF_4$, N-Piv-piperidine (**1a** or **LH**) and sodium persulfate ($Na_2S_2O_8$).

Table 1.4.10: Calculated total electronic (E_{tot}), E_{tot} with zero-point energy corrections (E_{tot} + ZPEC), enthalpy (H), and Gibbs free energies (in Hartrees; all values are negative) of all reported structures for the reaction of $CuBF_4$, sodium-persulfate, and N-Piv-piperidine **1a**.

Str	$-E_{tot}$	$-(E_{tot}$ + ZPEC)	–H	–G
SO_4_min	699.1222694	699.108177	699.102801	699.13656
$HOSO_3$, 1min	699.7899769	699.76346	699.757571	699.791896
H_2O	76.4257436	76.40442	76.400641	76.422735
H_2SO_4	700.228991	700.190672	700.184452	700.219072
Na_2SO4	1023.859253	1023.84169	1023.832966	1023.875261
LH, chair	522.575576	522.29325	522.279314	522.331989
CuBF4	620.6138319	620.598672	620.591333	620.630662
$Na_2S_2O_8$	1722.821866	1722.786712	1722.772502	1722.828513
LH_$CuBF_4$	1143.251625	1142.951678	1142.92987	1143.004439
$Na_2S_2O_8$_$CuBF_4$	2343.502843	2343.451628	2343.429223	2343.505589
[(LH)–($NaSO_4$)]–[$NaSO_4$–$CuBF_4$]				
triplet	2866.165074	2865.829466	2865.792933	2865.899653
singlet	2866.134761	2865.798742	2865.761898	2865.871906
TS(H-transf)	2866.152814	2865.823397	2865.787345	2865.893068
[L–OSO_3Na]–[$NaHSO_4$–$CuBF_4$]				
singlet	2866.259207	2865.920586	2865.884829	2865.988907
[(LOH)–$CuBF_4$]–$NaHSO_4$]$_2$				
	2942.705094	2942.340241	2942.302495	2942.411233
[(LNHCO)–$CuBF_4$]–[$NaHSO_4$]$_2$				
singlet	2942.703819	2942.342931	2942.303953	2942.415055
LNHCO	597.8048282	597.521264	597.50508	597.563274
[($NaHSO_4$)$_2$–$CuBF_4$]				
	2344.846166	2344.771362	2344.748954	2344.824479

NMR Spectral Data

Pivaloyl Protected Cyclic Amines

2,2-dimethyl-1-(3-methylpiperidin-1-yl)propan-1-one

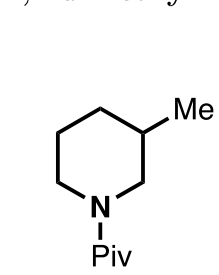

1i

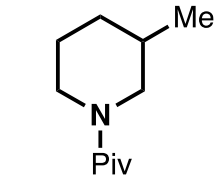

1i

1-(2-ethylpiperidin-1-yl)-2,2-dimethylpropan-1-one

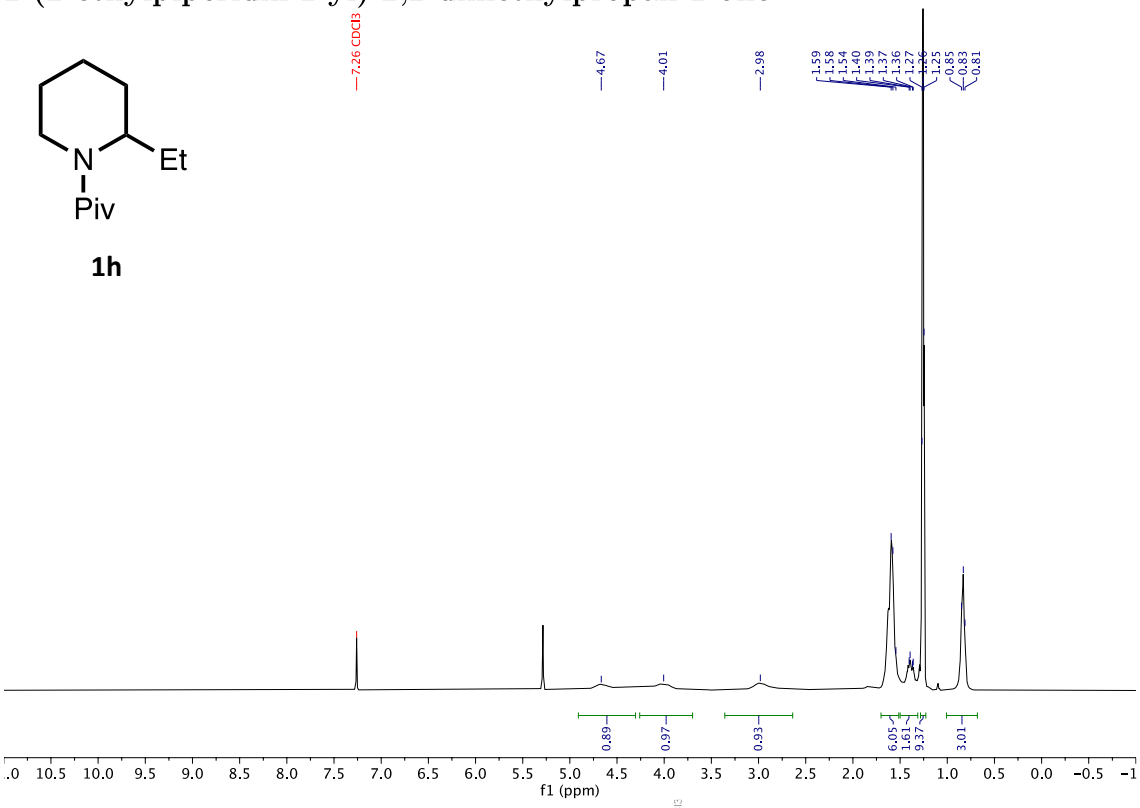

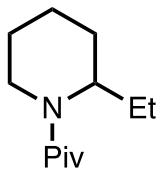

1h

1h

2,2-dimethyl-1-(3-phenylpiperidin-1-yl)propan-1-one

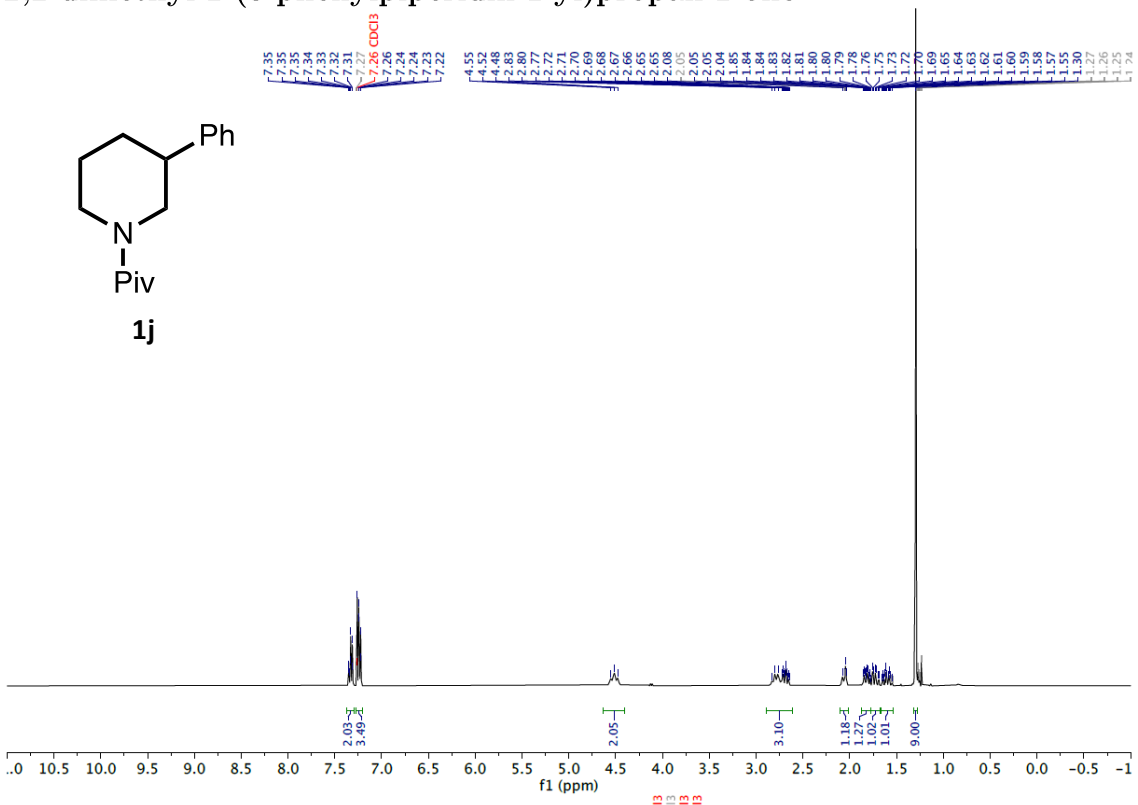

1j

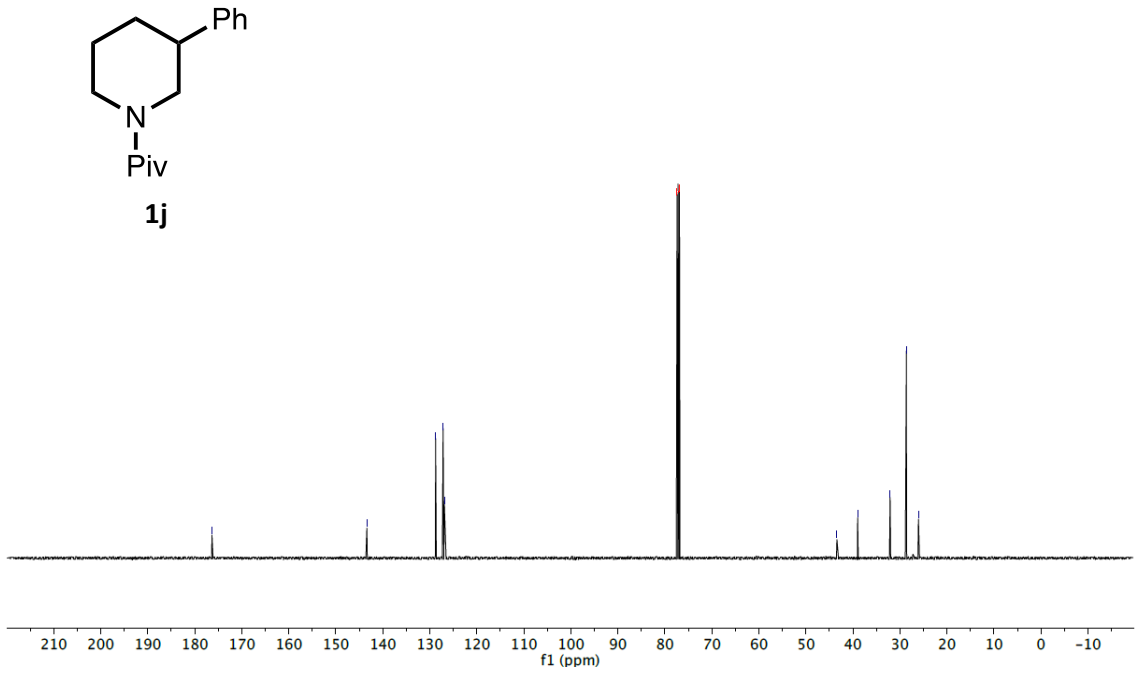

1j

1-(4-(4-chlorophenyl)piperidin-1-yl)-2,2-dimethylpropan-1-one

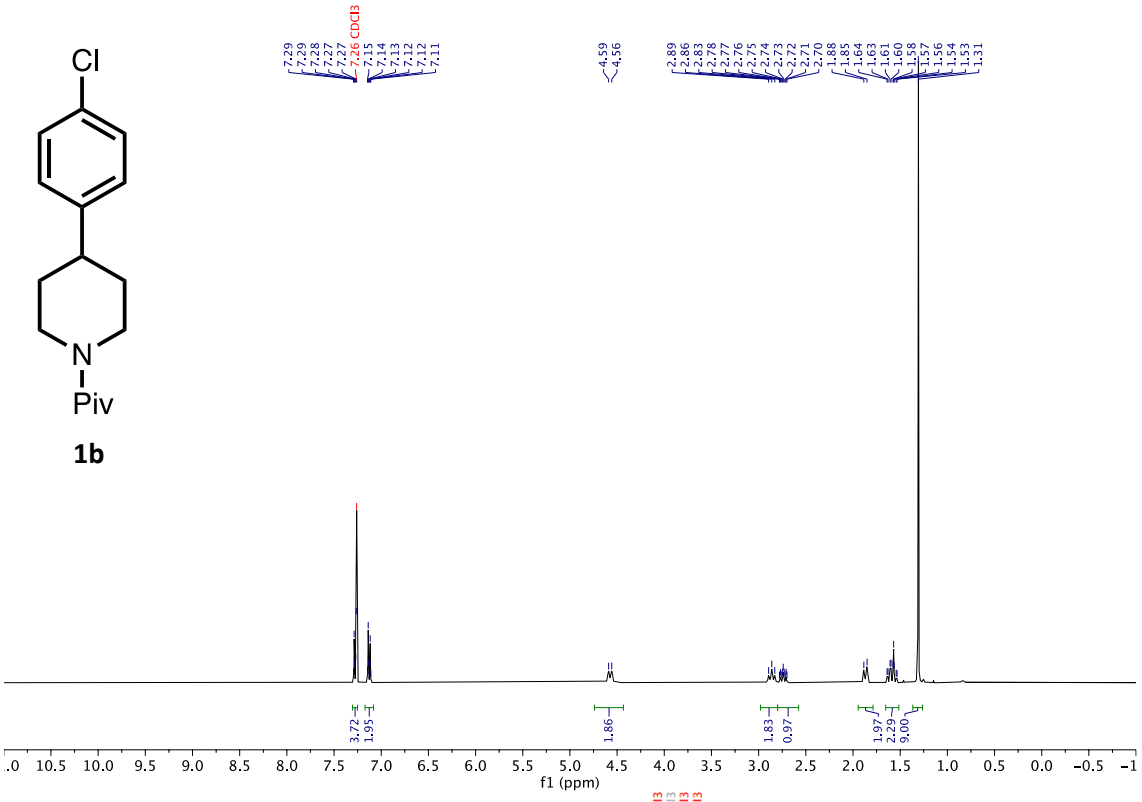

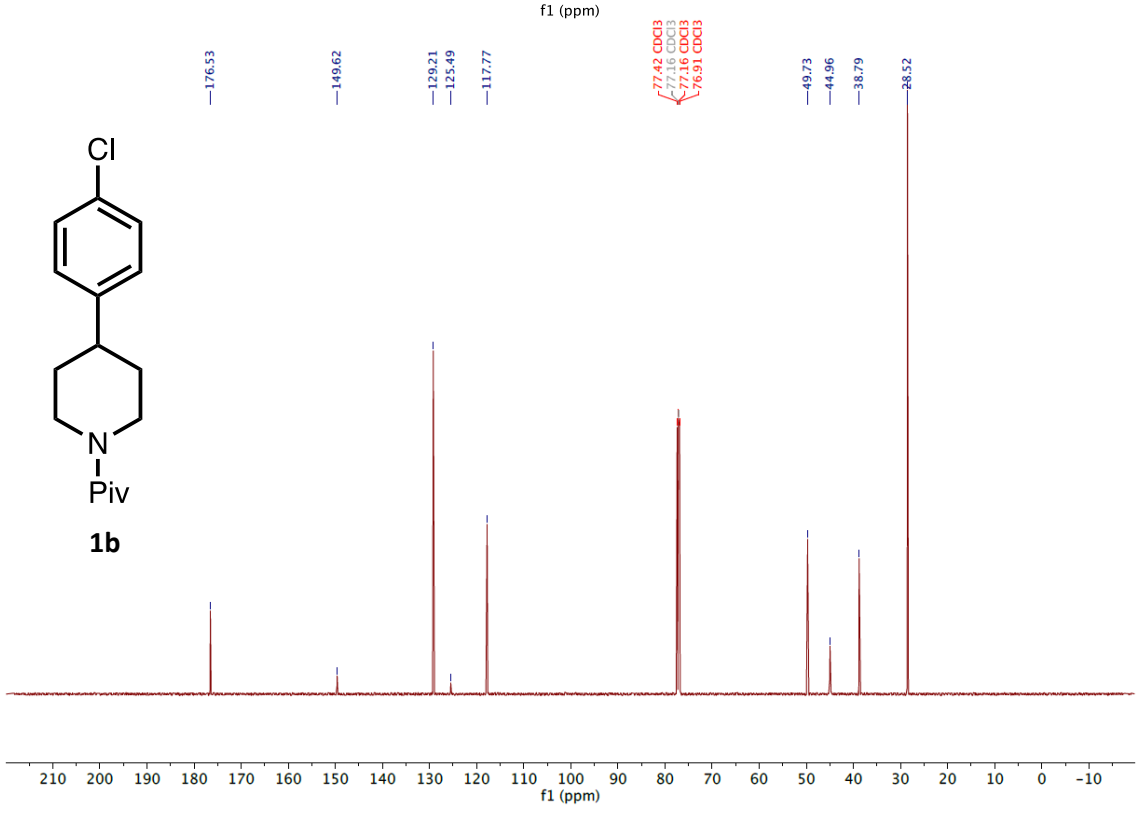

1-(6,7-dimethoxy-3,4-dihydroisoquinolin-2(1*H*)-yl)-2,2-dimethylpropan-1-one

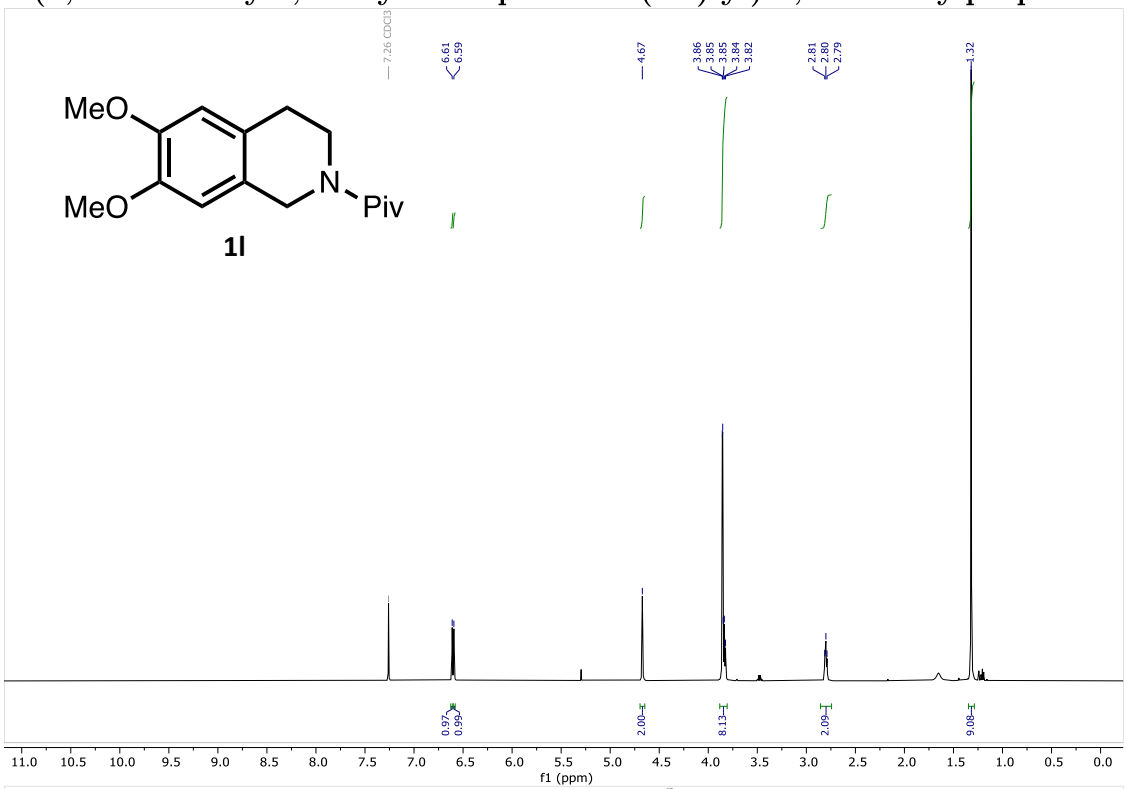

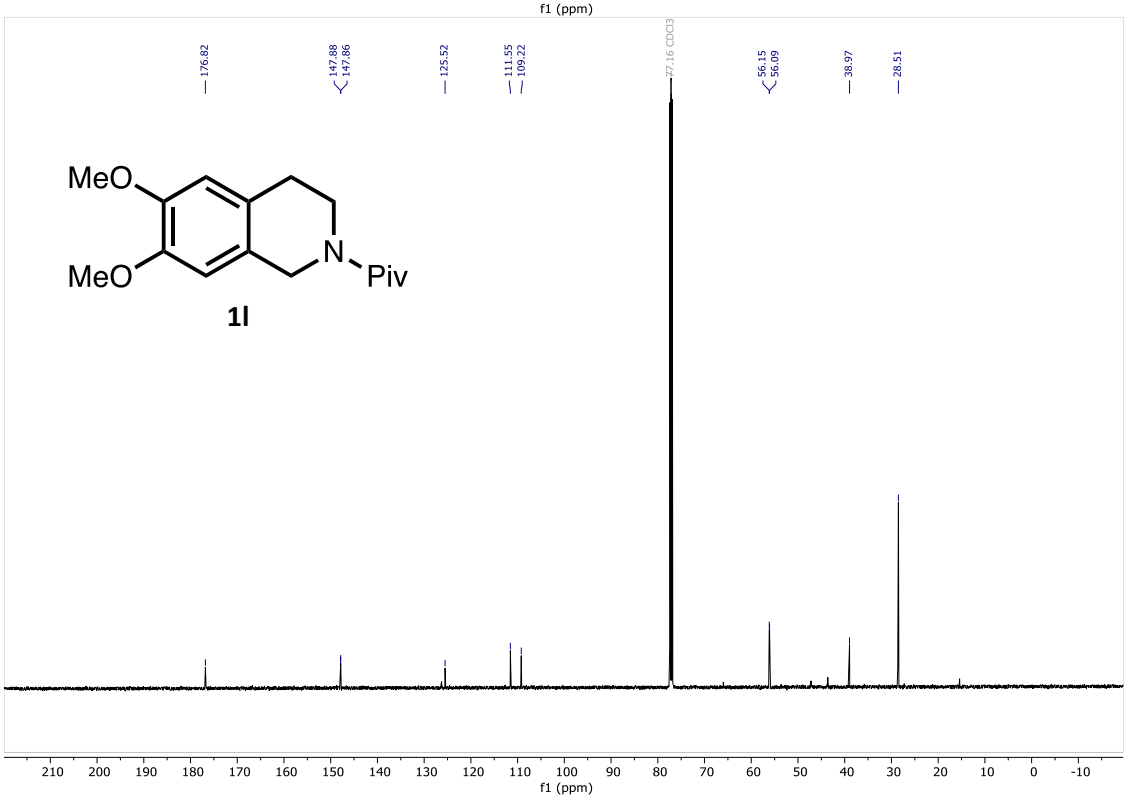

2,2-dimethyl-1-(piperidin-1-yl-d_{10})propan-1-one

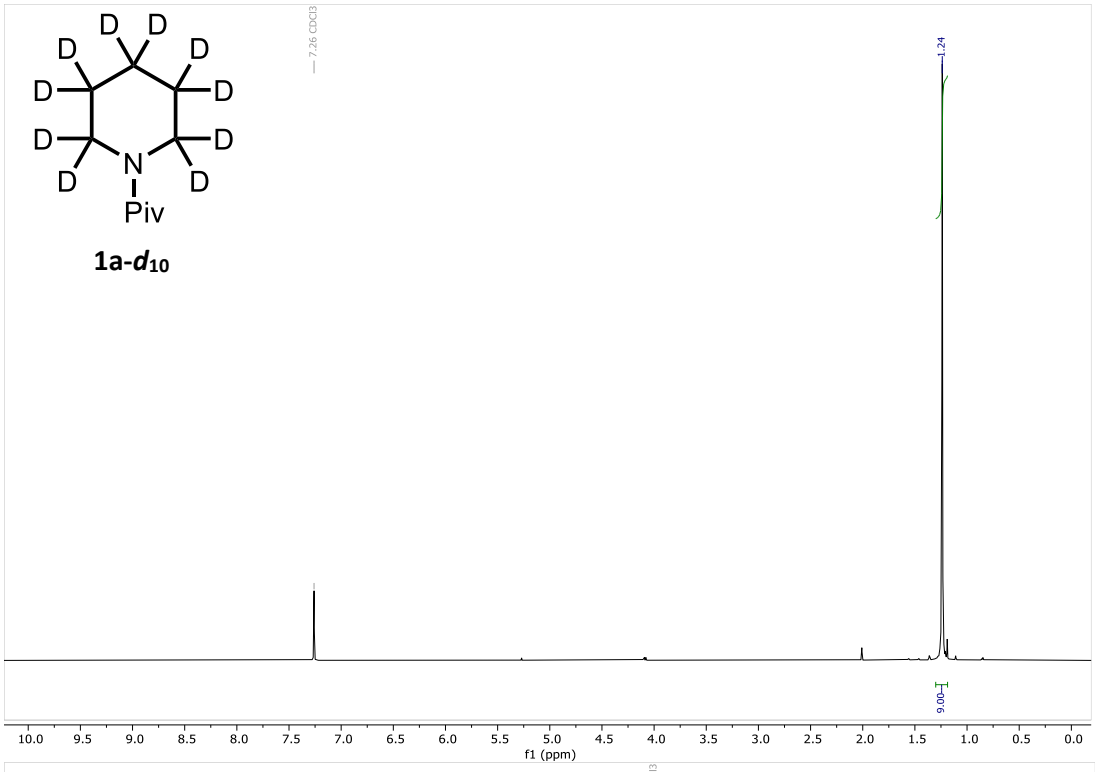

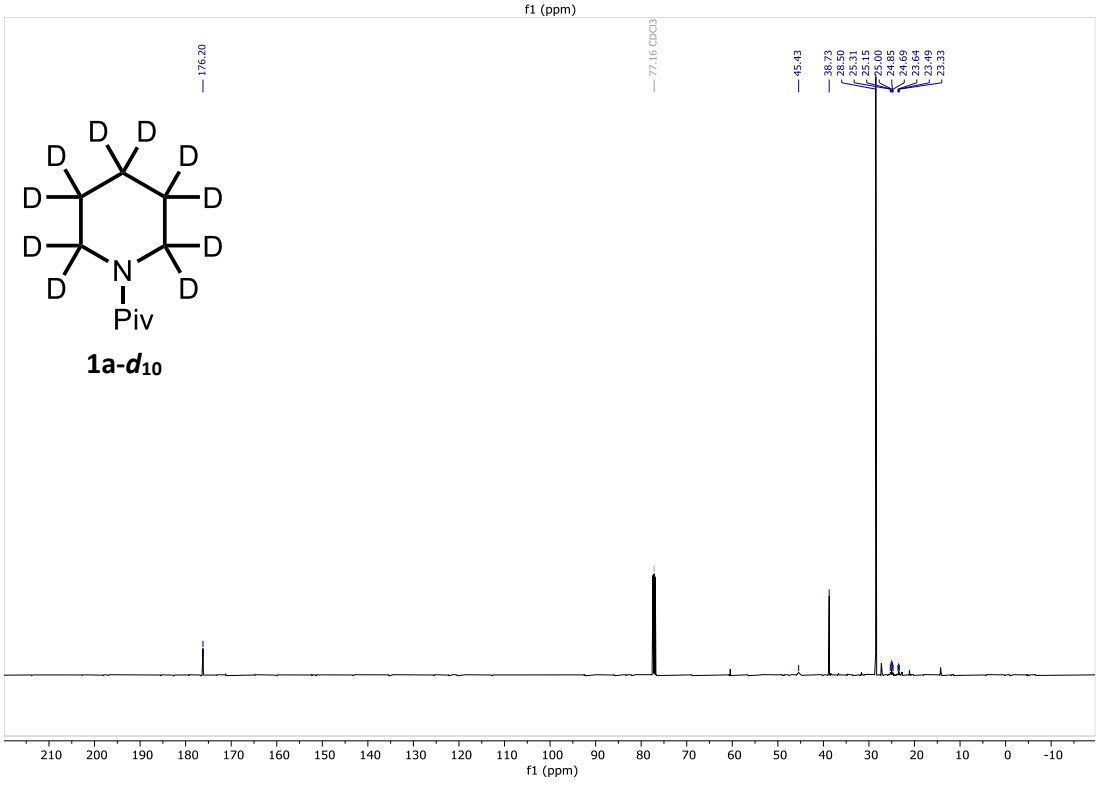

NMR Spectra – Photocatalyst Screening

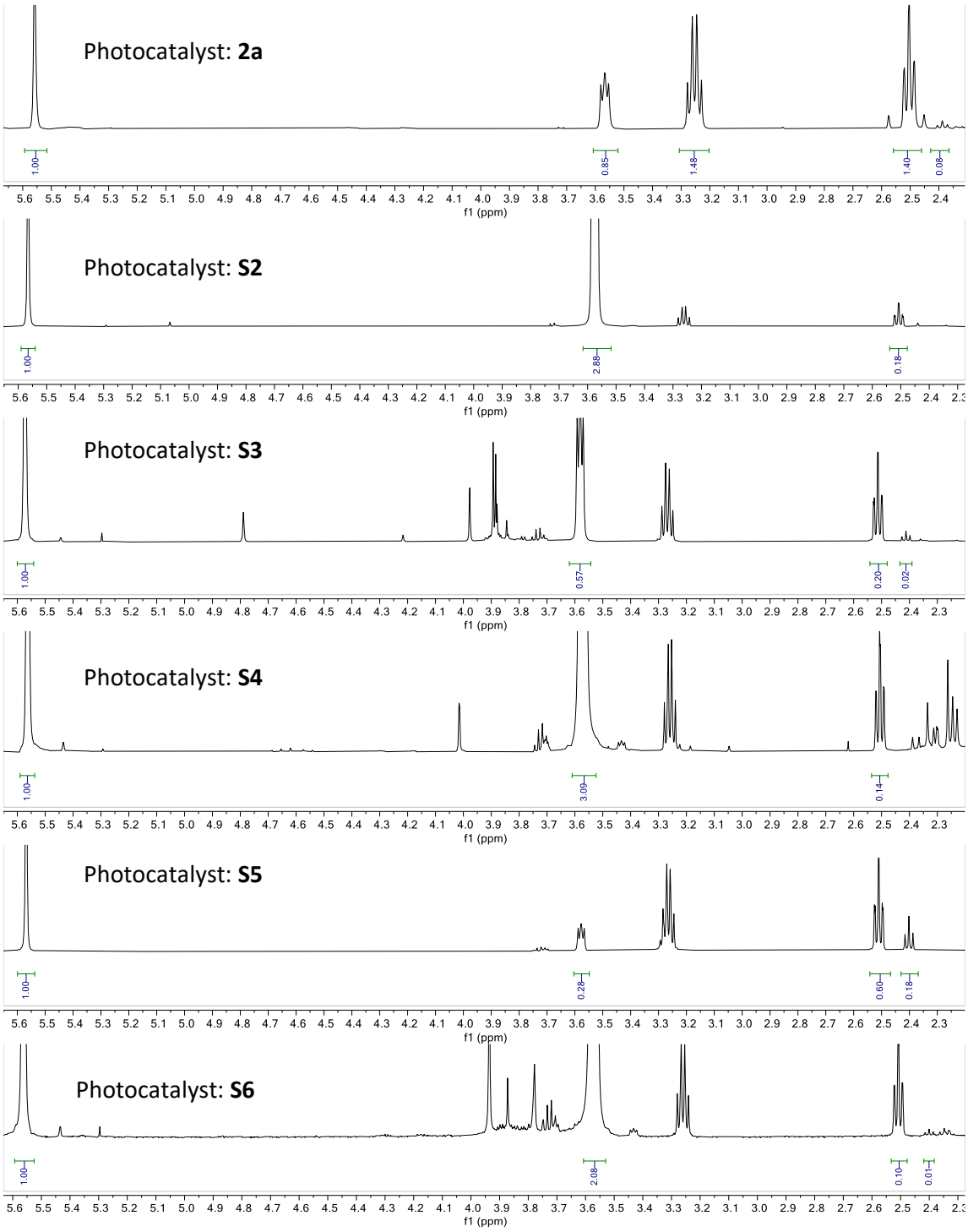

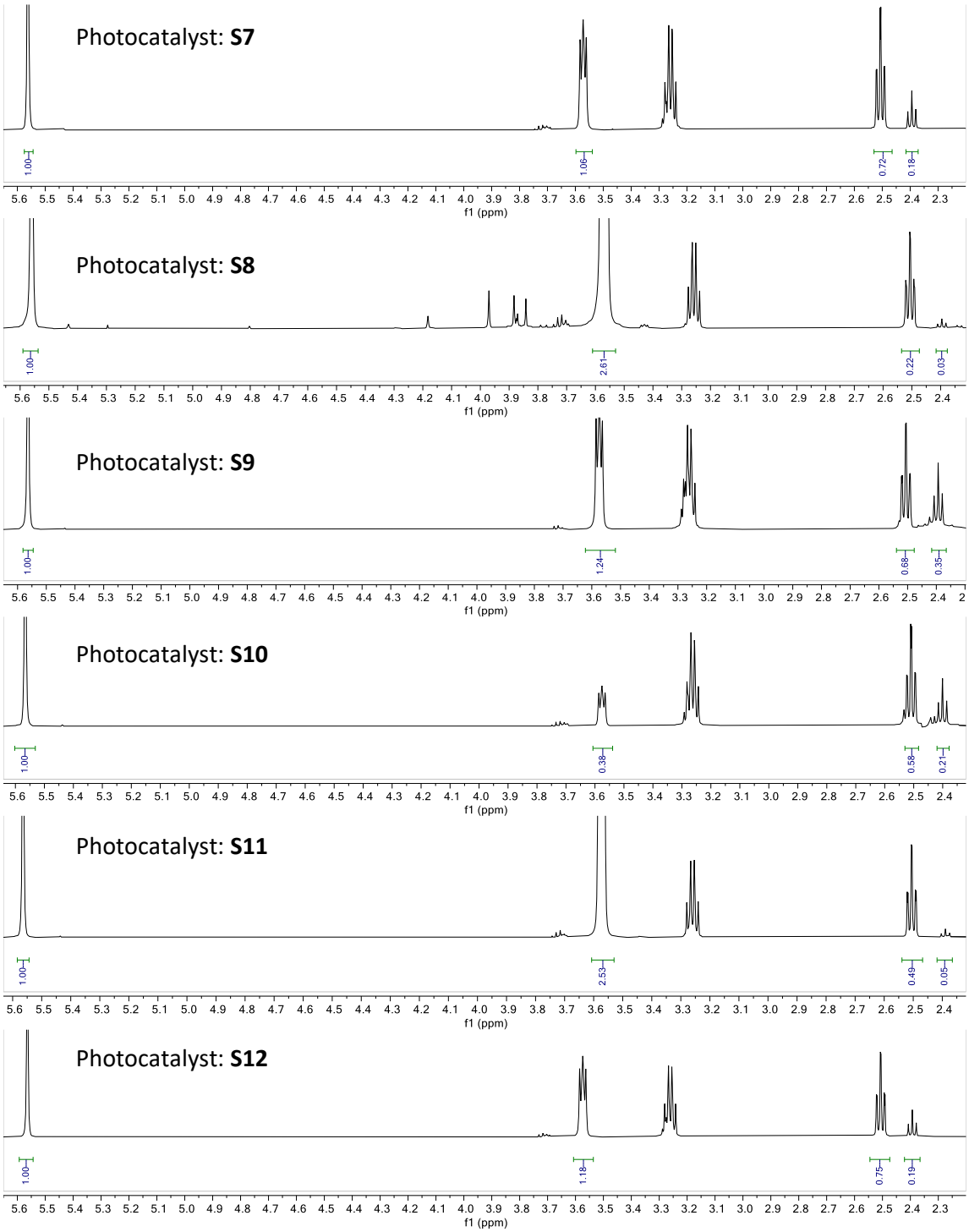
Photocatalyst: **S7**
1.00
1.06
0.72
0.18
Photocatalyst: **S8**
1.00
2.61
0.22
0.03
Photocatalyst: **S9**
1.00
1.24
0.68
0.35
Photocatalyst: **S10**
1.00
0.38
0.58
0.21
Photocatalyst: **S11**
1.00
2.53
0.49
0.05
Photocatalyst: **S12**
1.00
1.18
0.75
0.19
f1 (ppm)

NMR Spectra – Reaction Optimization

Optimization of Reaction Time

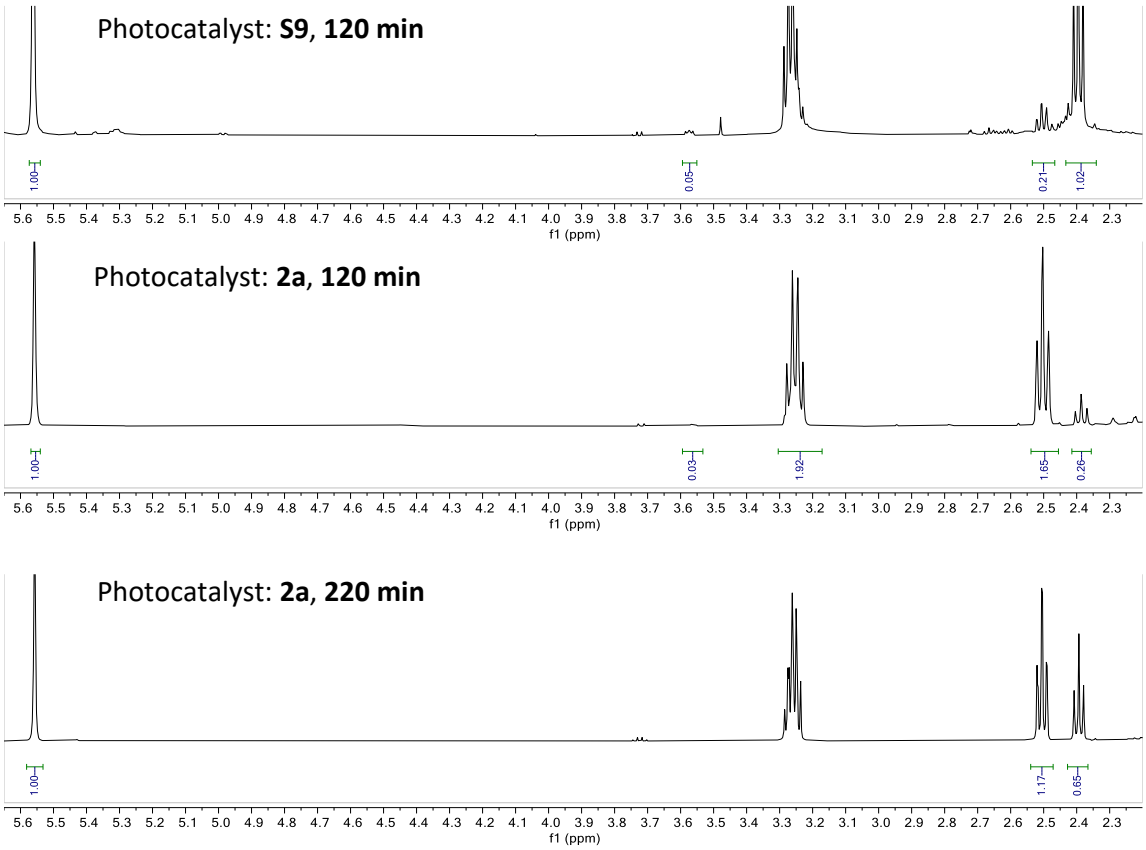

Optimization of Catalyst Loading

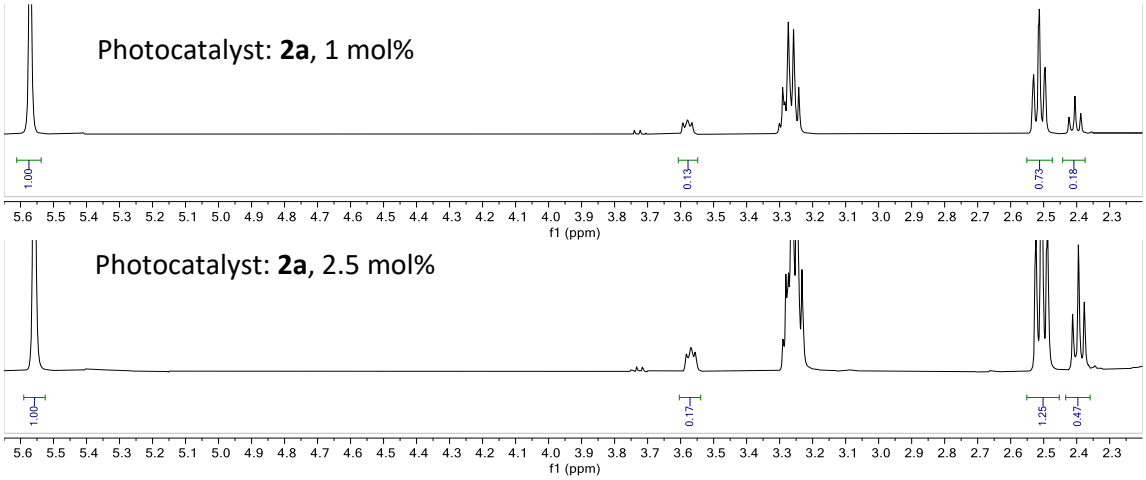

Optimization of Oxidant and Solvent

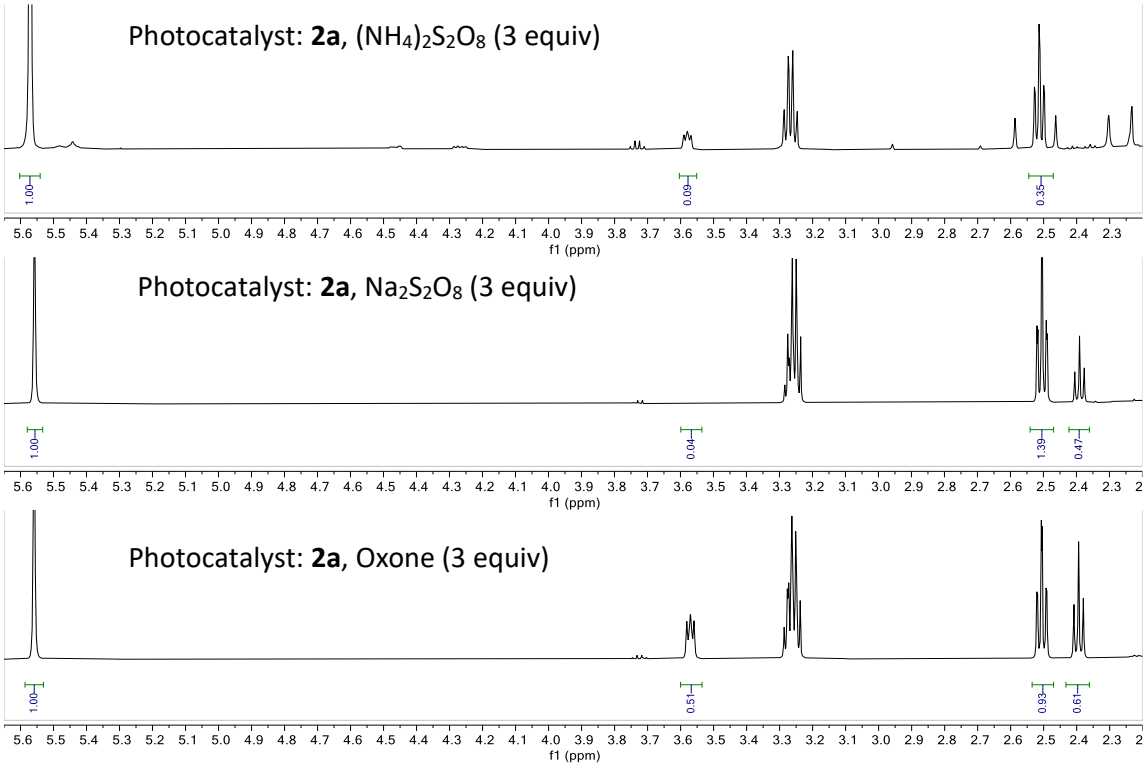

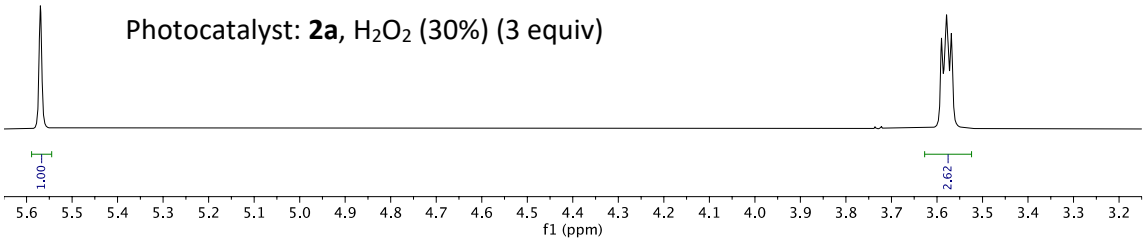
Photocatalyst: **2a**, H_2O_2 (30%) (3 equiv)
1.00
2.62
f1 (ppm)

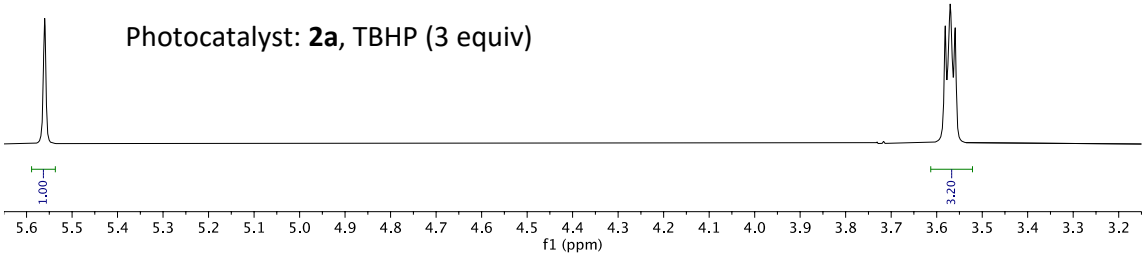
Photocatalyst: **2a**, TBHP (3 equiv)
1.00
3.20
f1 (ppm)

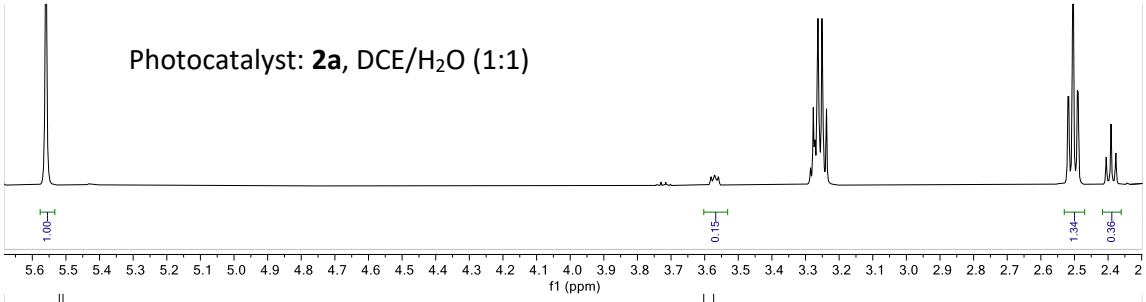
Photocatalyst: **2a**, DCE/H_2O (1:1)
1.00
0.15
1.34
0.36
f1 (ppm)

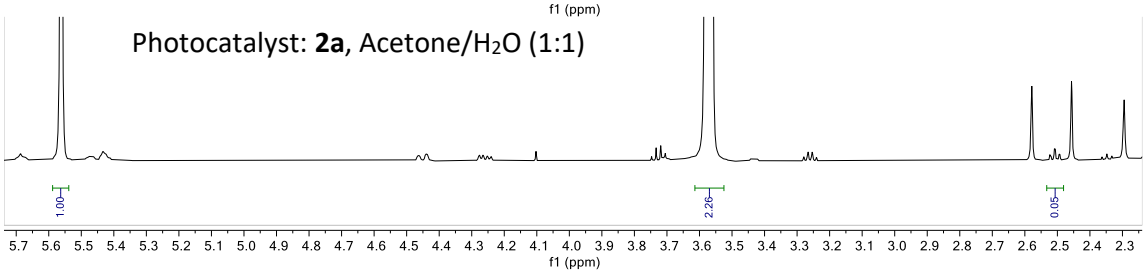
Photocatalyst: **2a**, Acetone/H_2O (1:1)
1.00
2.26
0.05
f1 (ppm)

NMR Spectra – Variation of Reaction Parameters

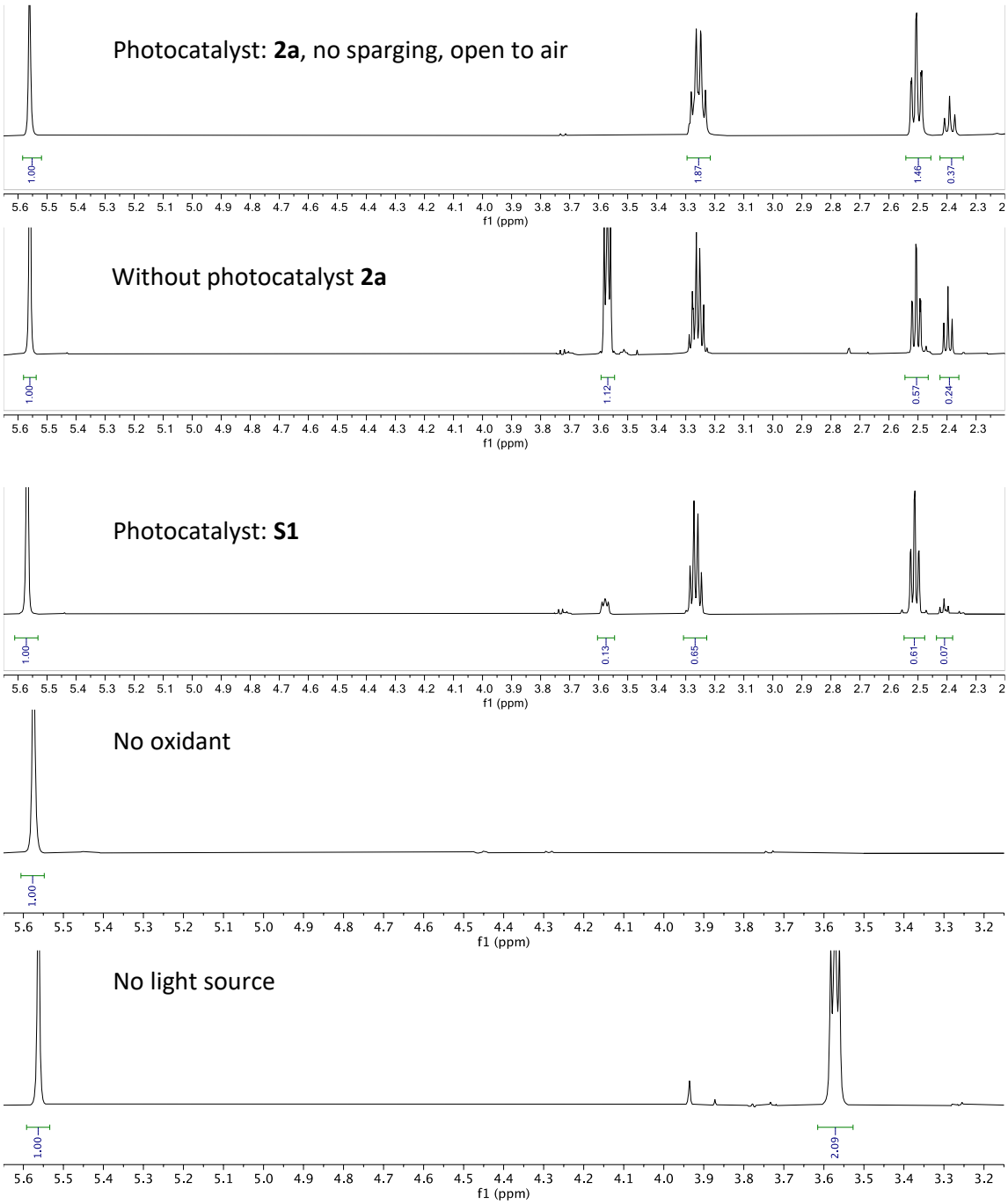

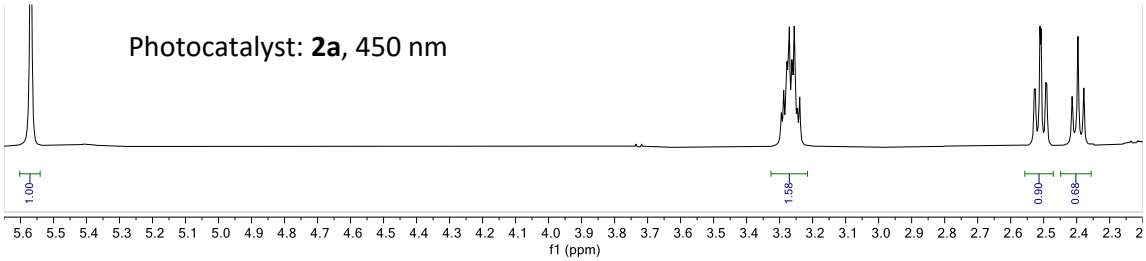

NMR Spectra – N-Protecting Groups

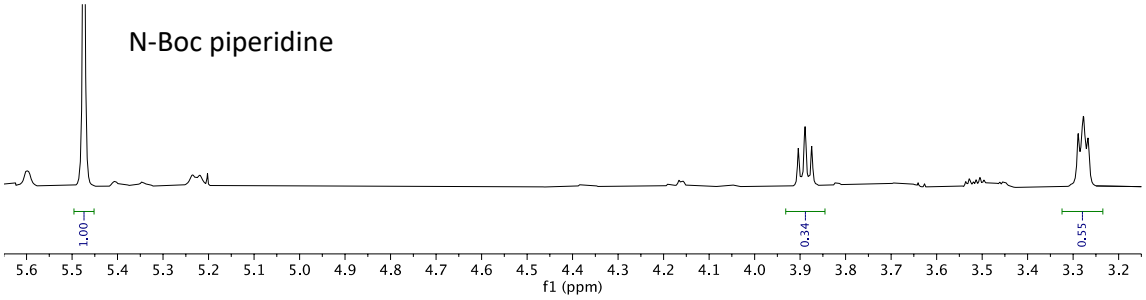

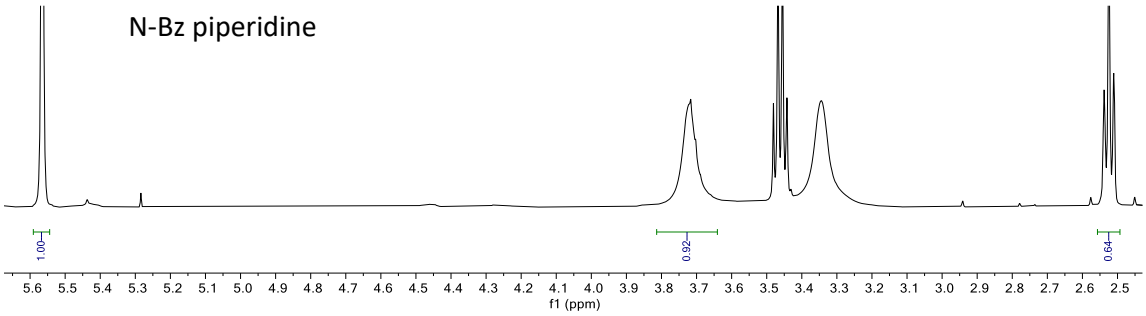

NMR Spectra – Aldehyde Products

N-(5-oxopentyl)pivalamide

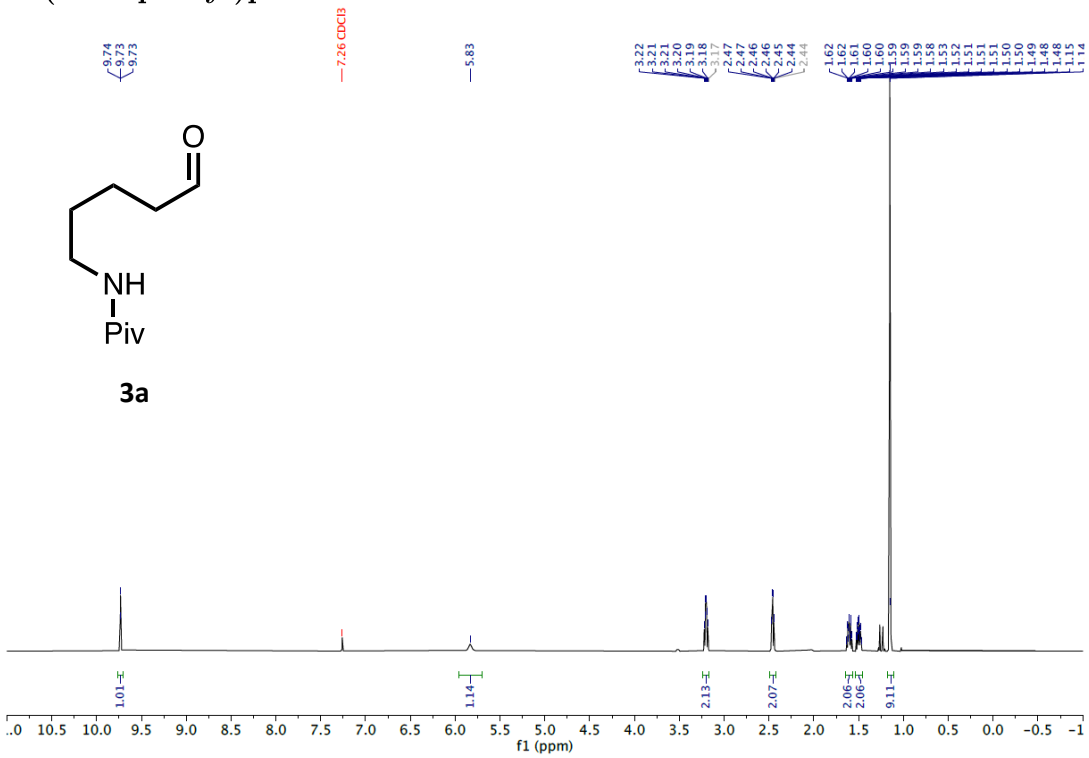

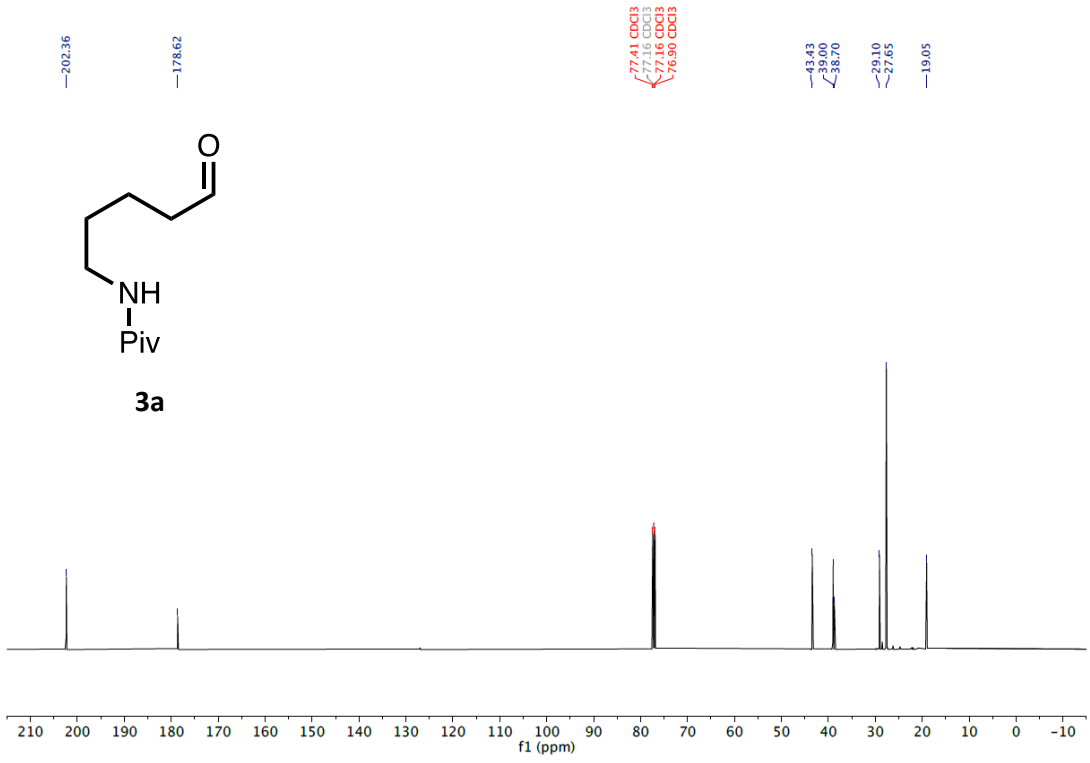

5-pivalamidopentanoic acid

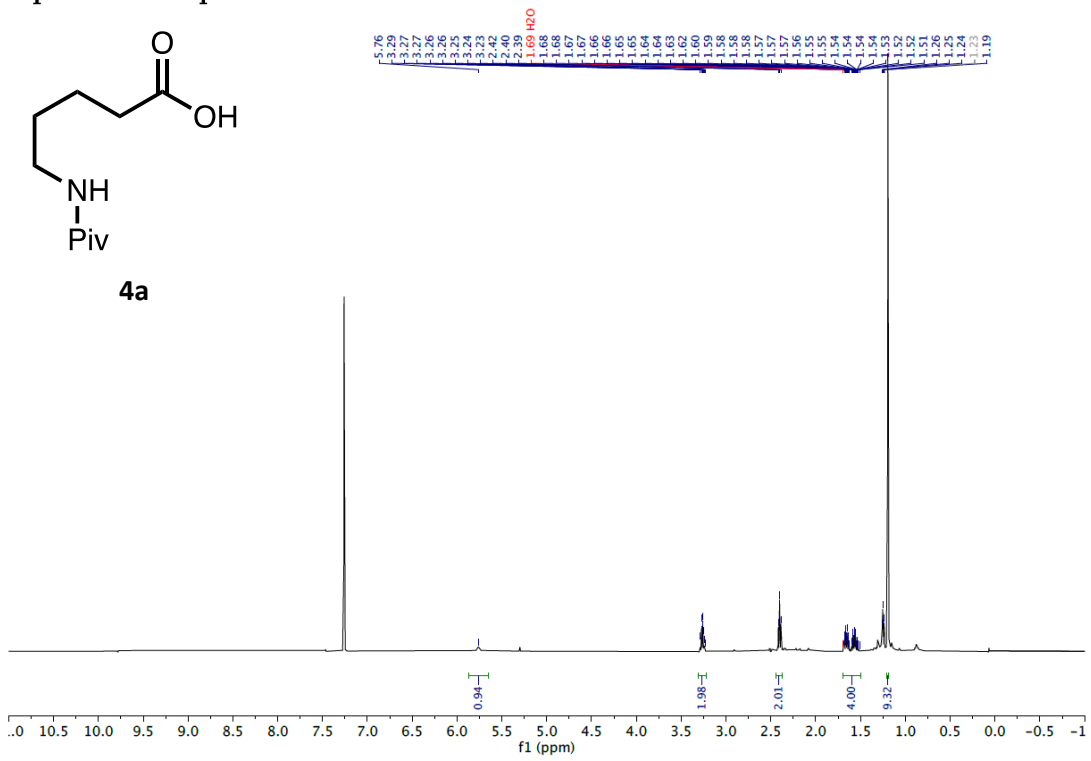

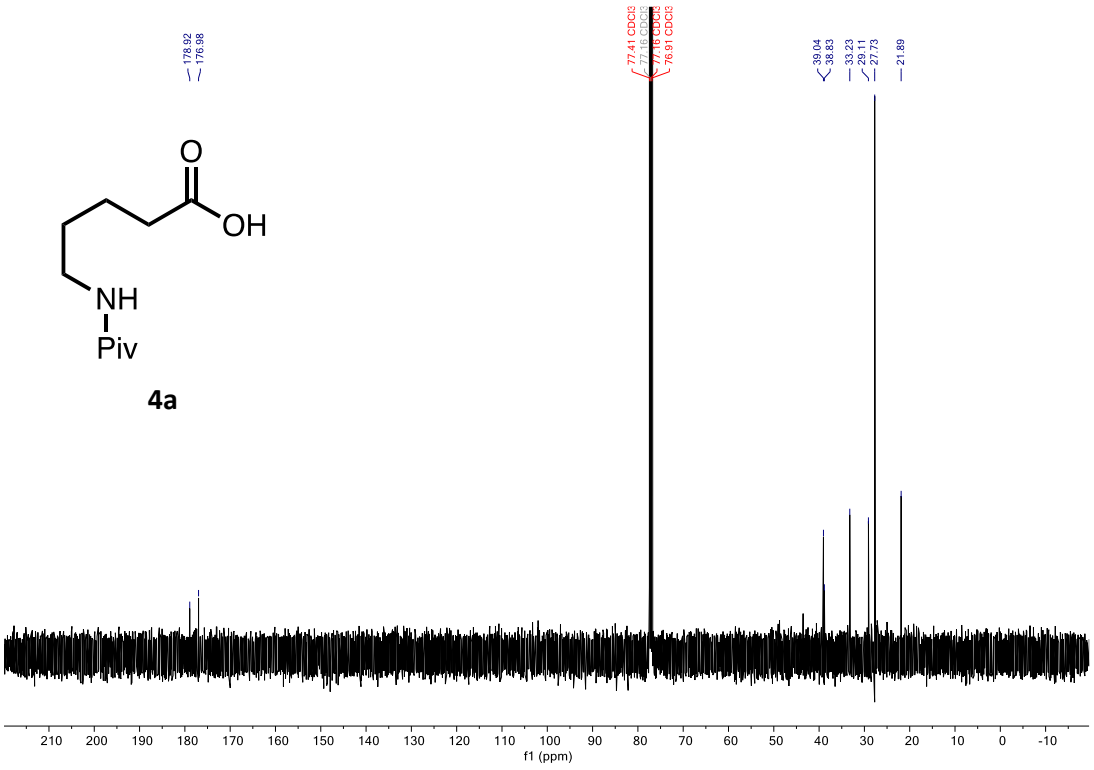

_N_-(4-oxobutyl)pivalamide

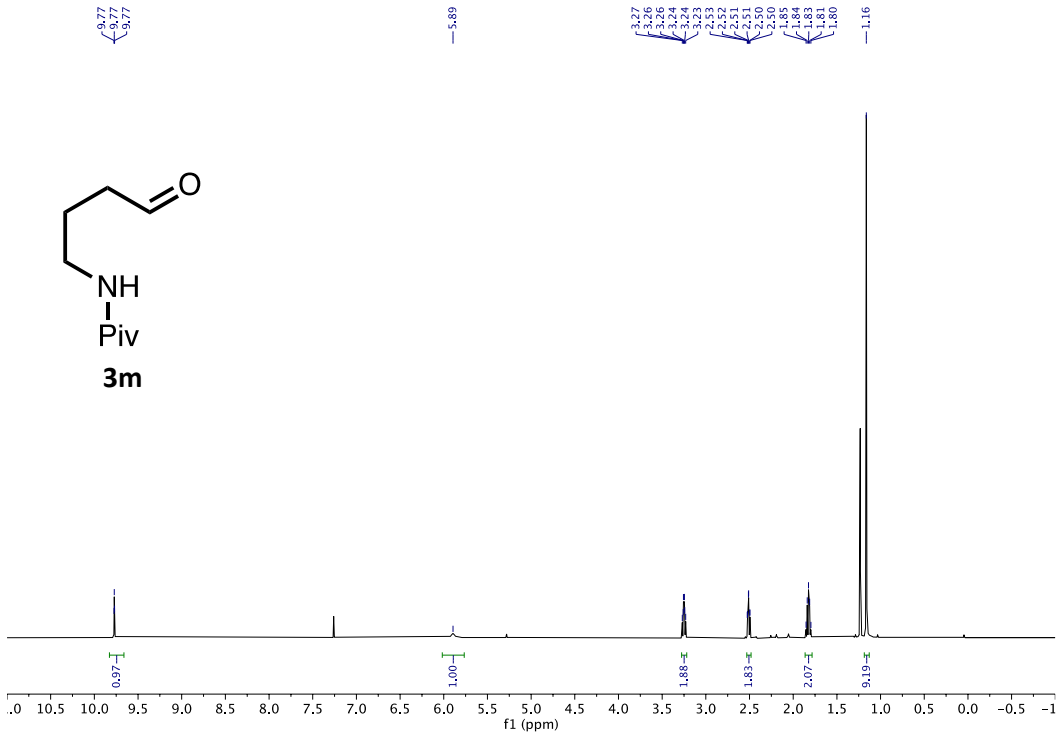

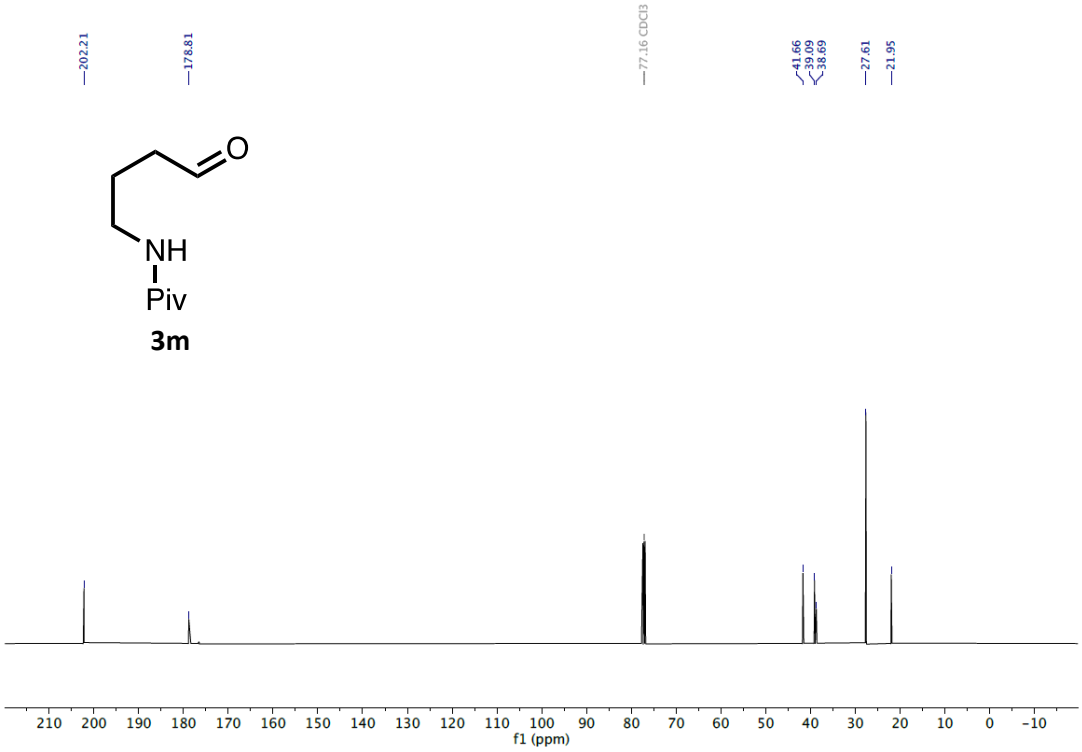

4-pivalamidobutanoic acid

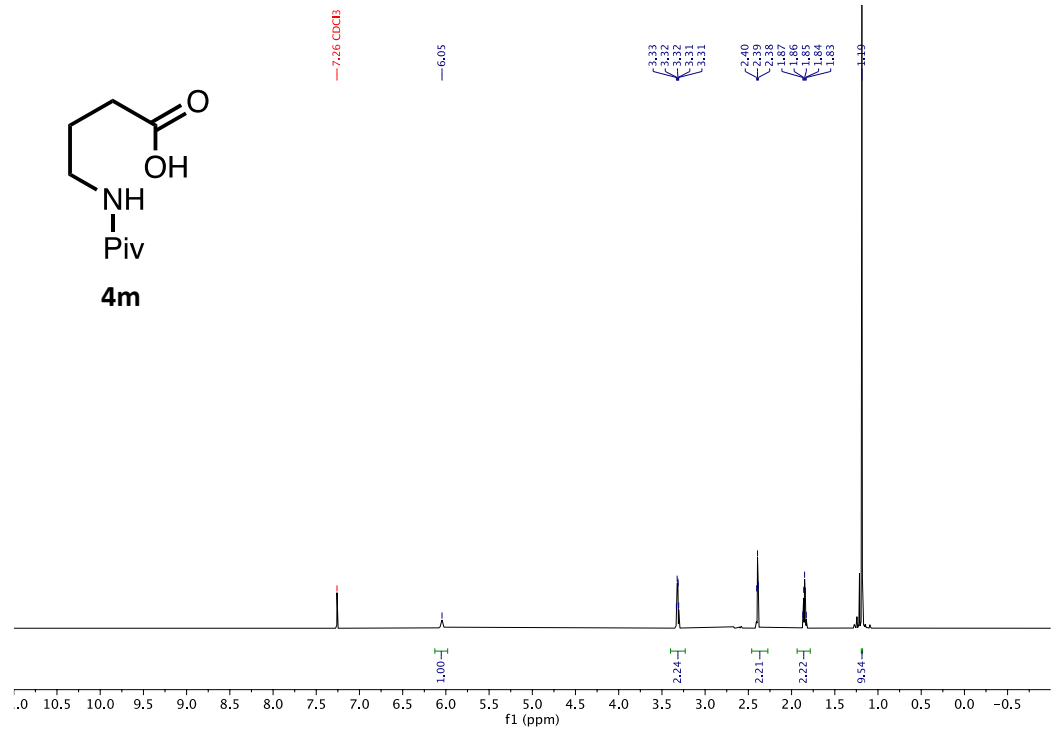

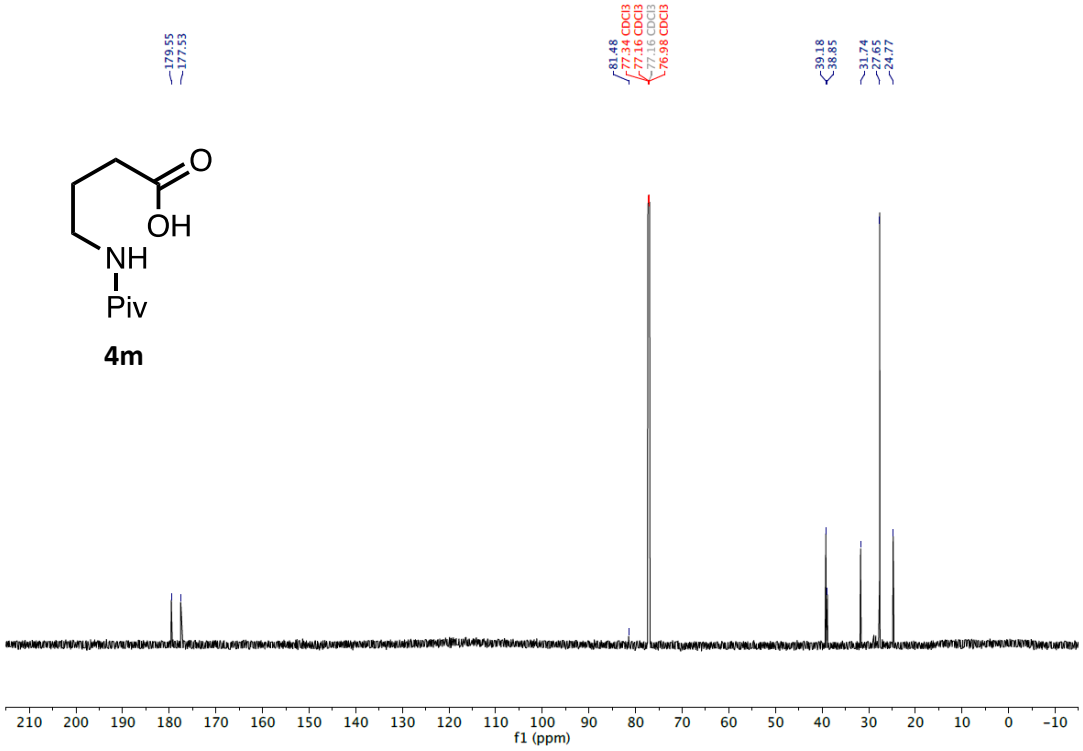

_N_-(6-oxohexyl)pivalamide

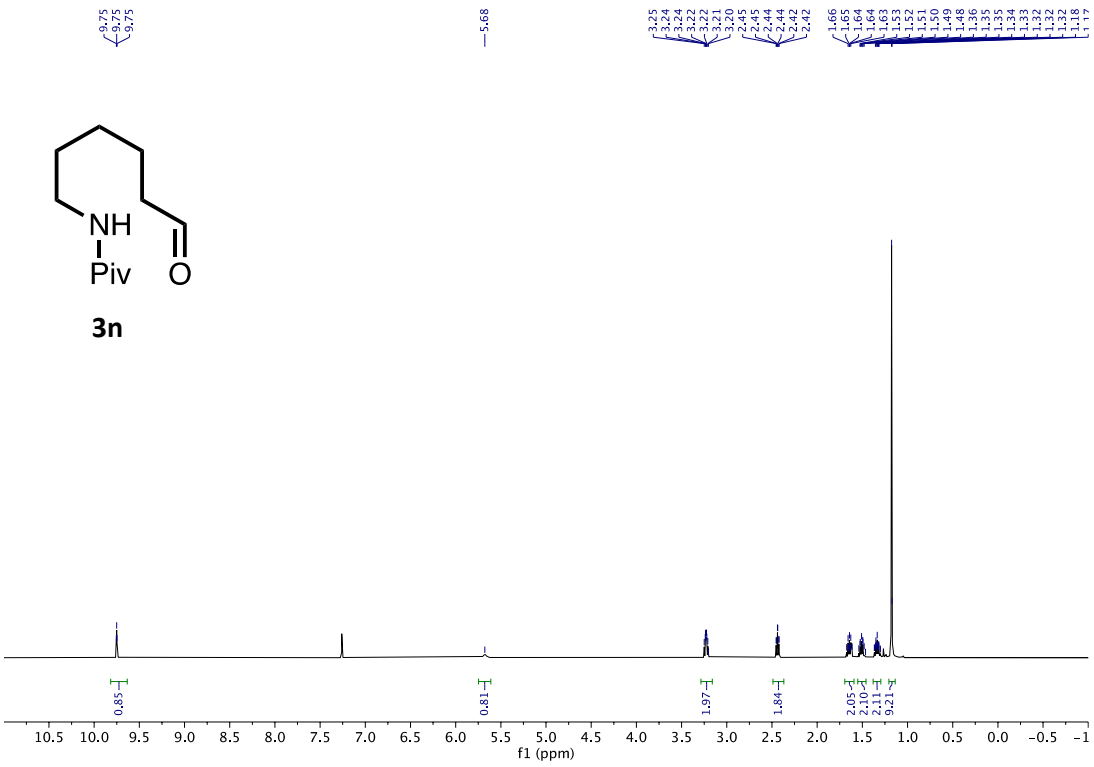

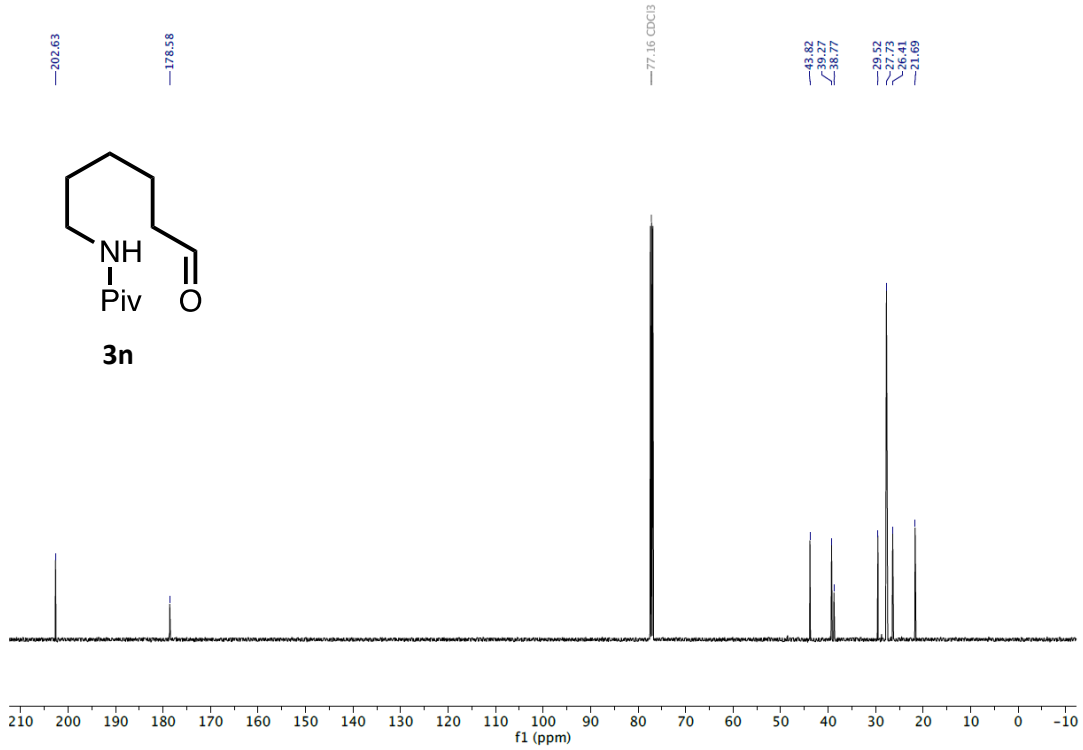

6-pivalamidohexanoic acid

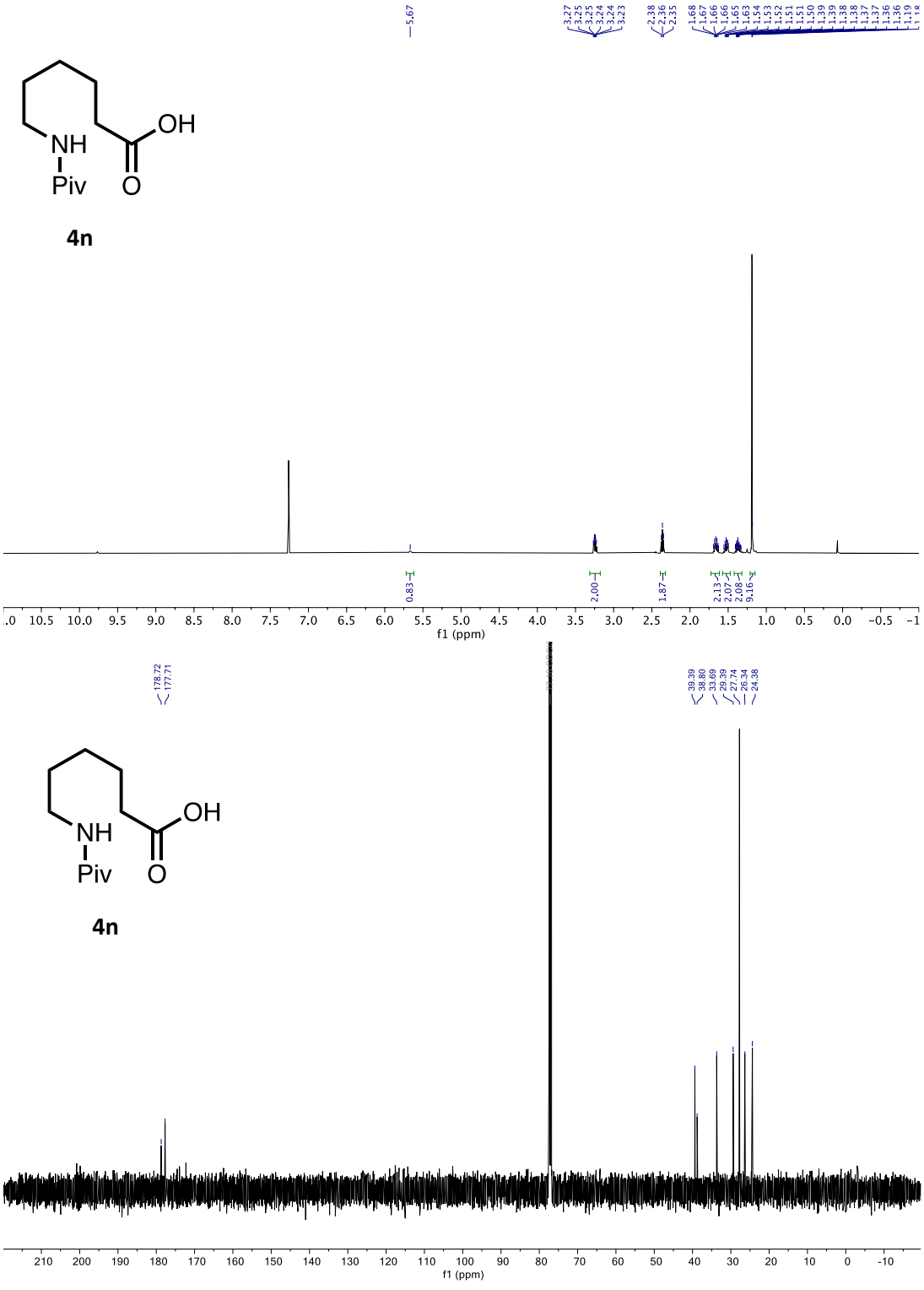

_N_-(7-oxoheptyl)pivalamide

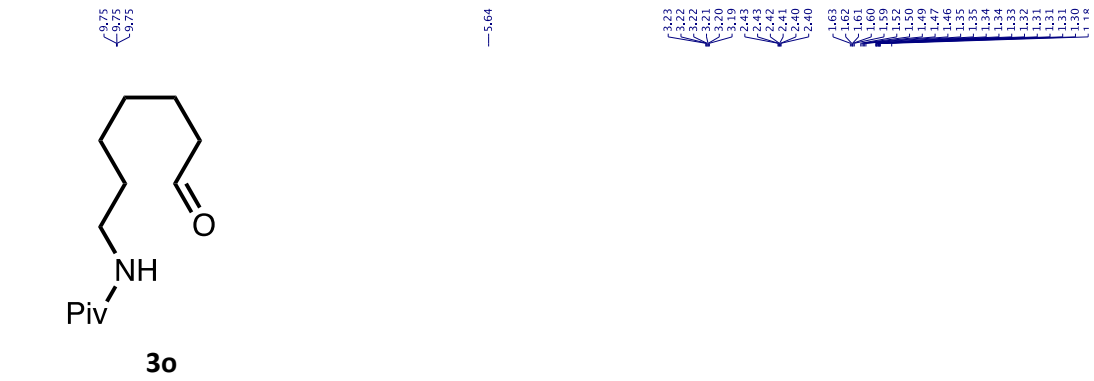

3o

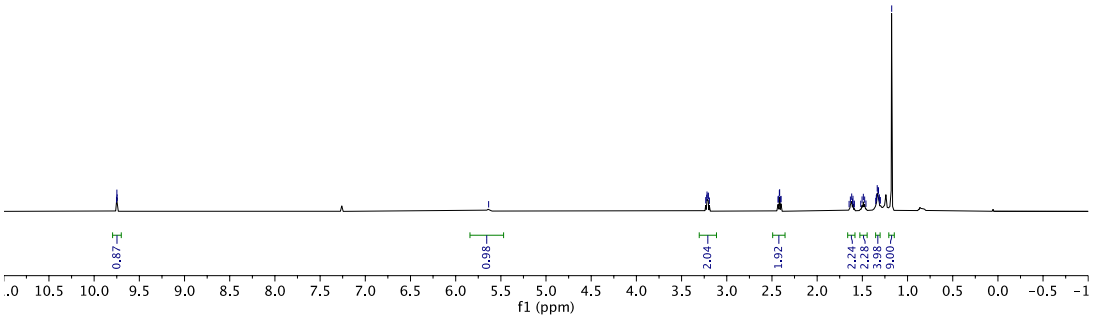

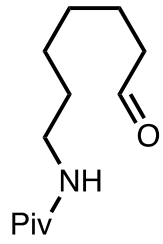

3o

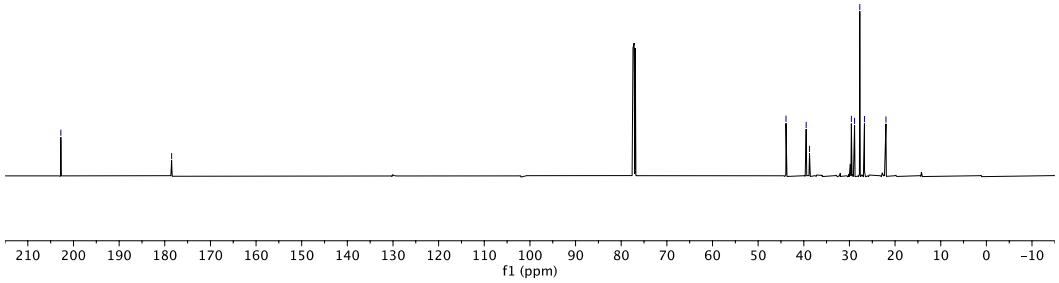

_N_-((1_S_,2_R_)-2-(3-oxopropyl)cyclohexyl)pivalamide

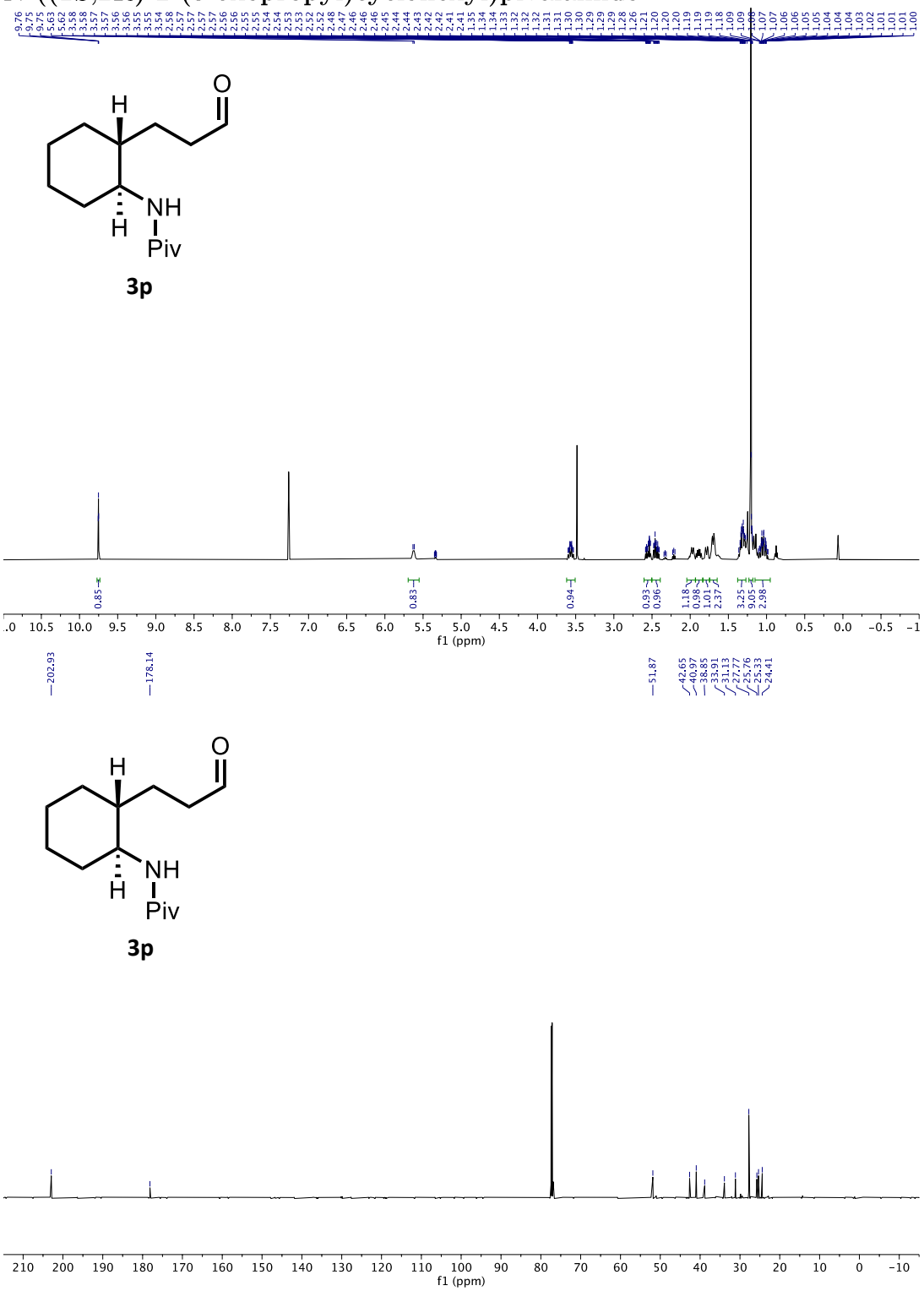

_N_-(3-(4-chlorophenyl)-5-oxopentyl)pivalamide

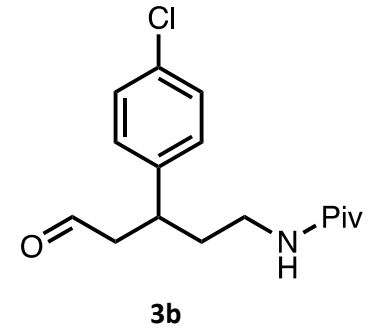

3b

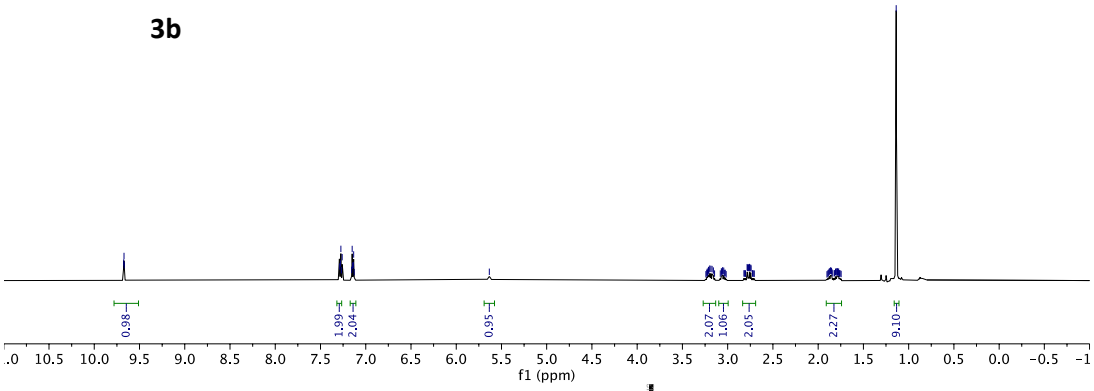

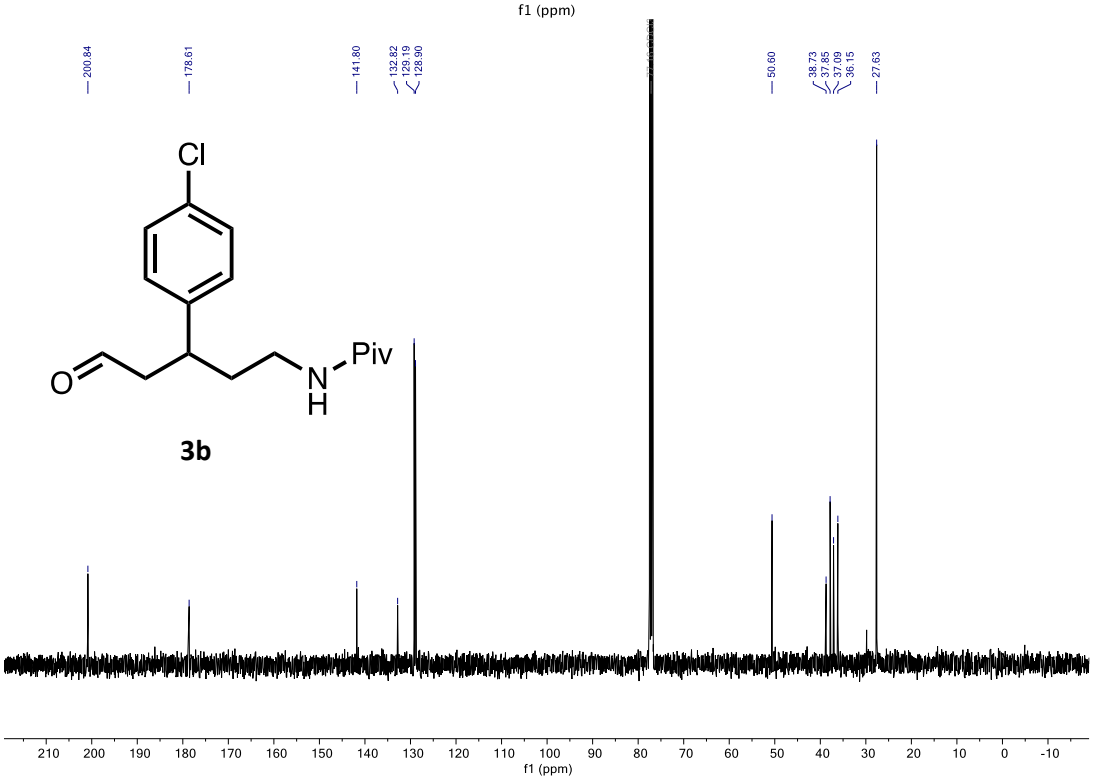

3b

N-(5-oxo-3-phenylpentyl)pivalamide

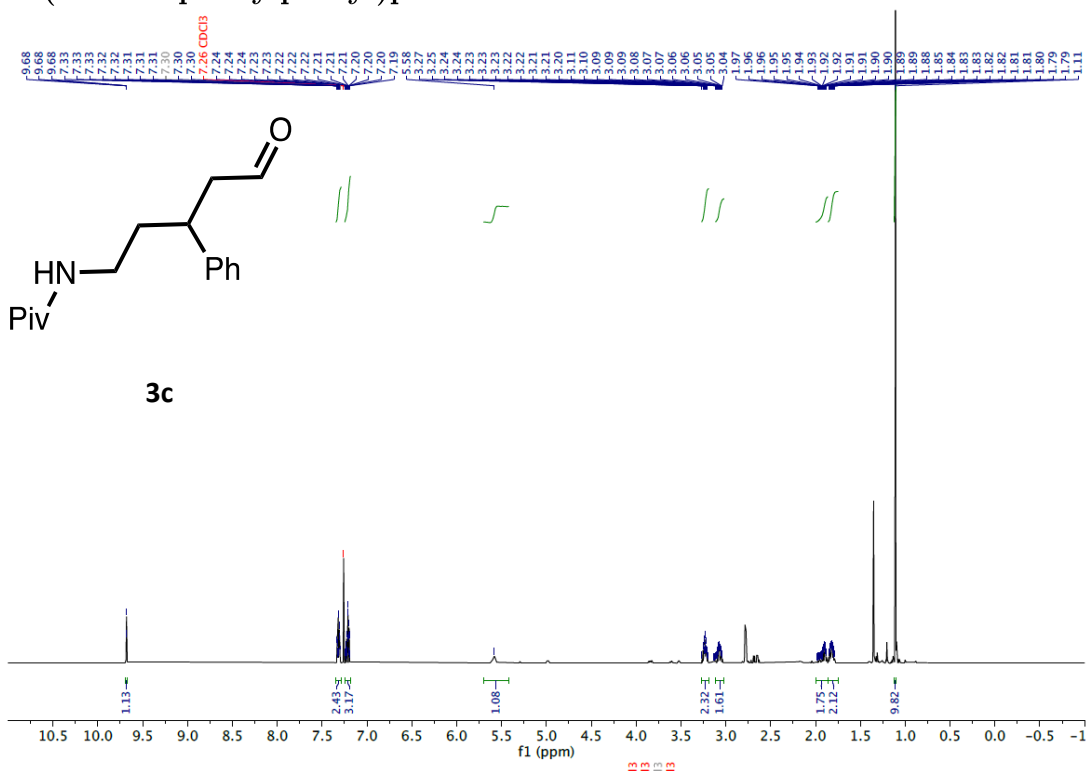

3c

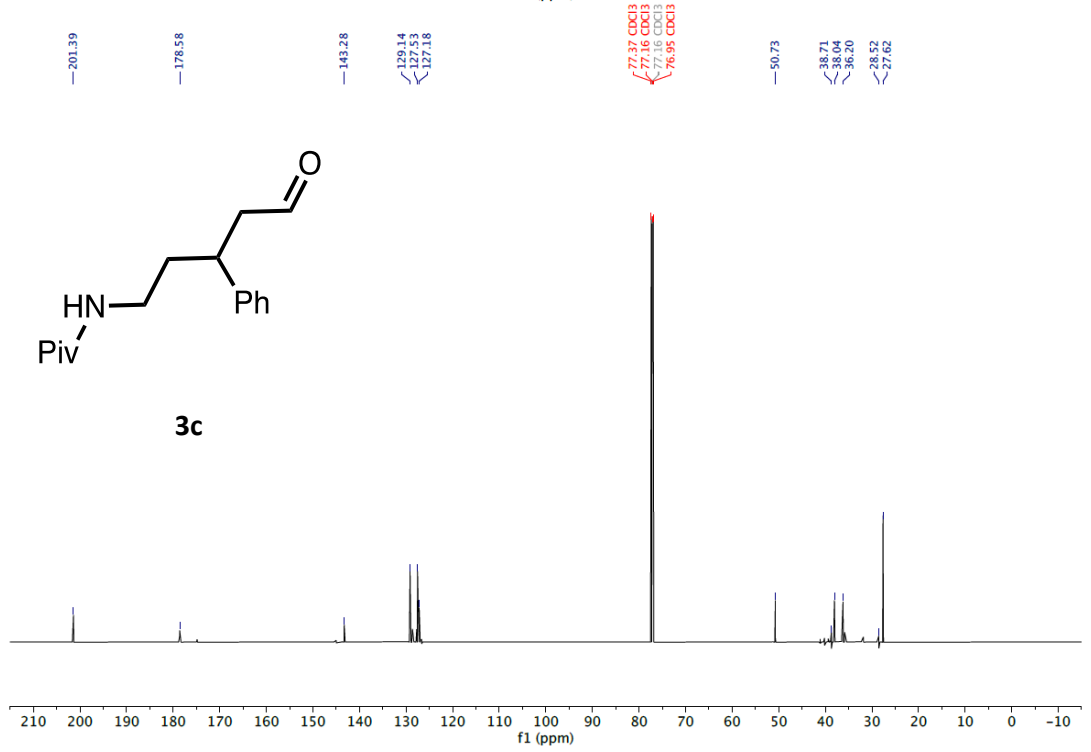

3c

N-(3-methyl-5-oxopentyl)pivalamide

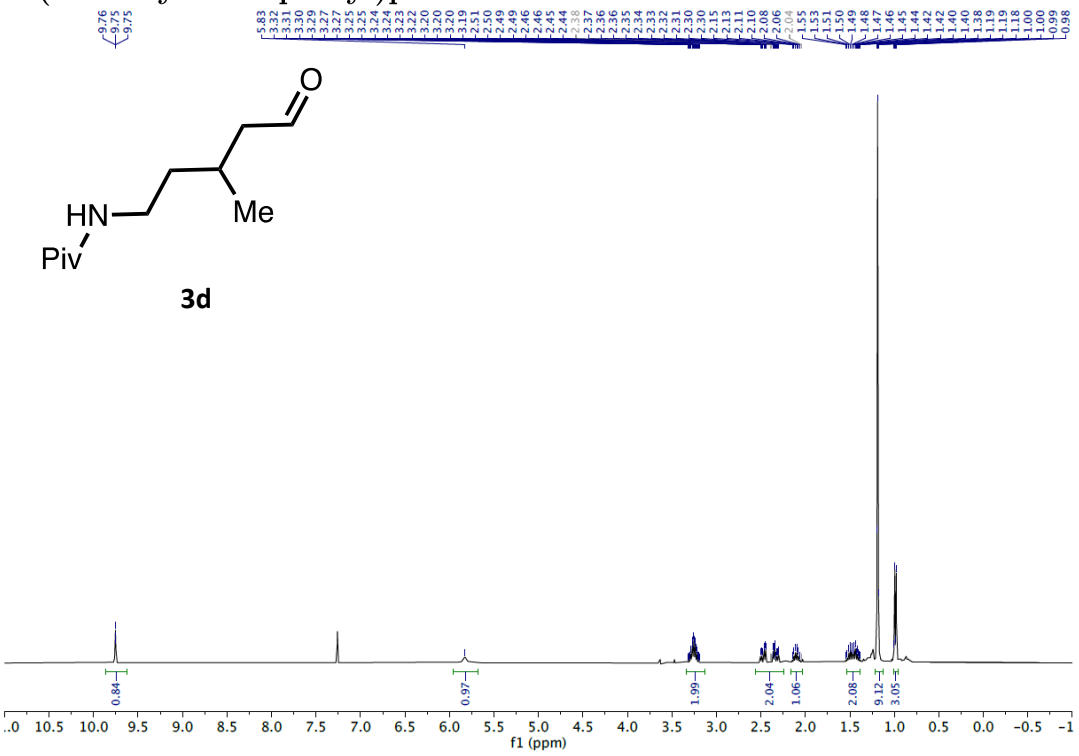

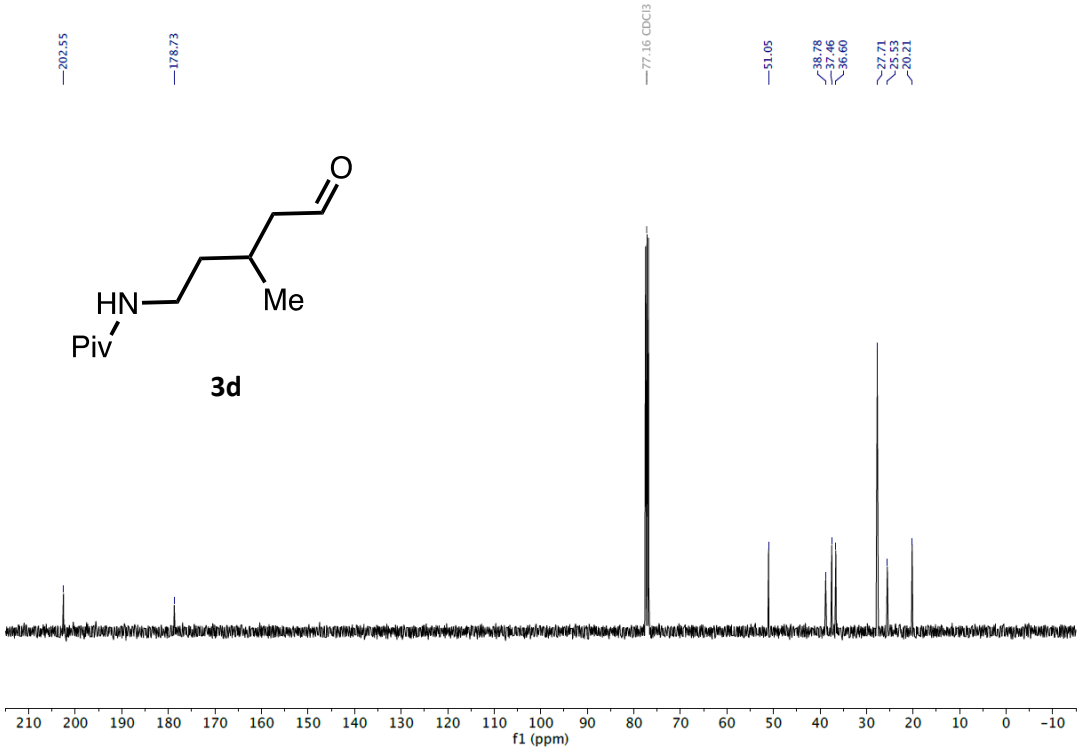

Methyl 5-oxo-3-(2-pivalamidoethyl)pentanoate

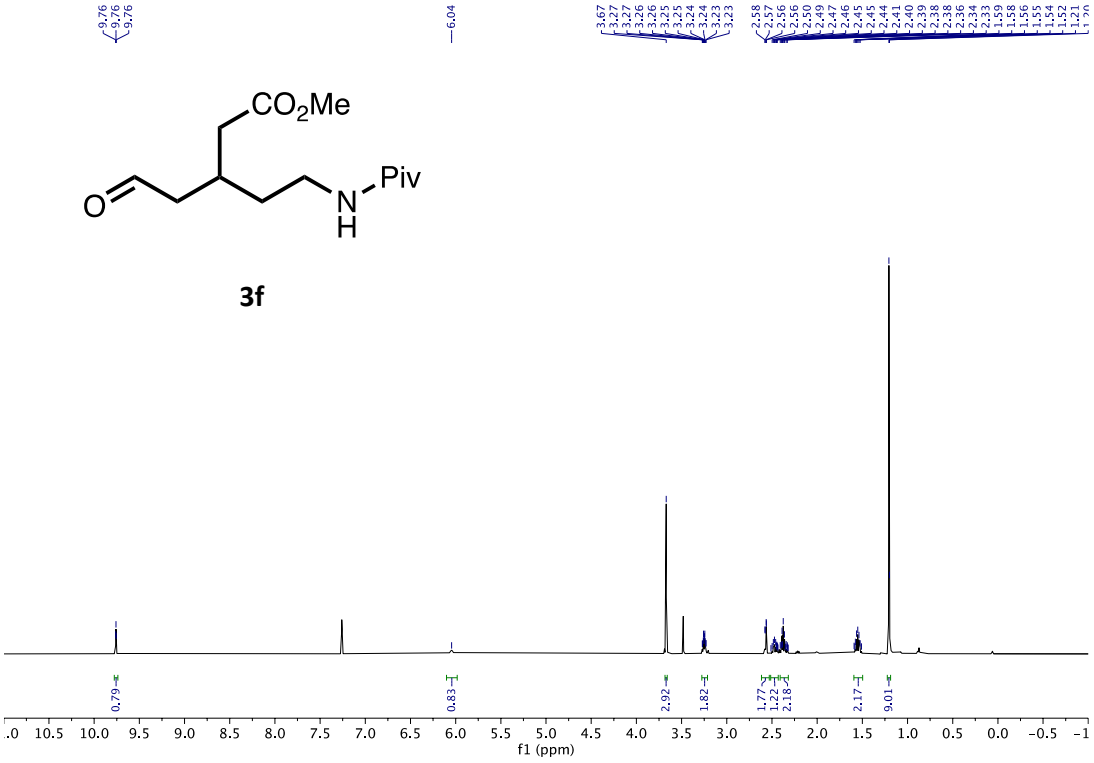

3f

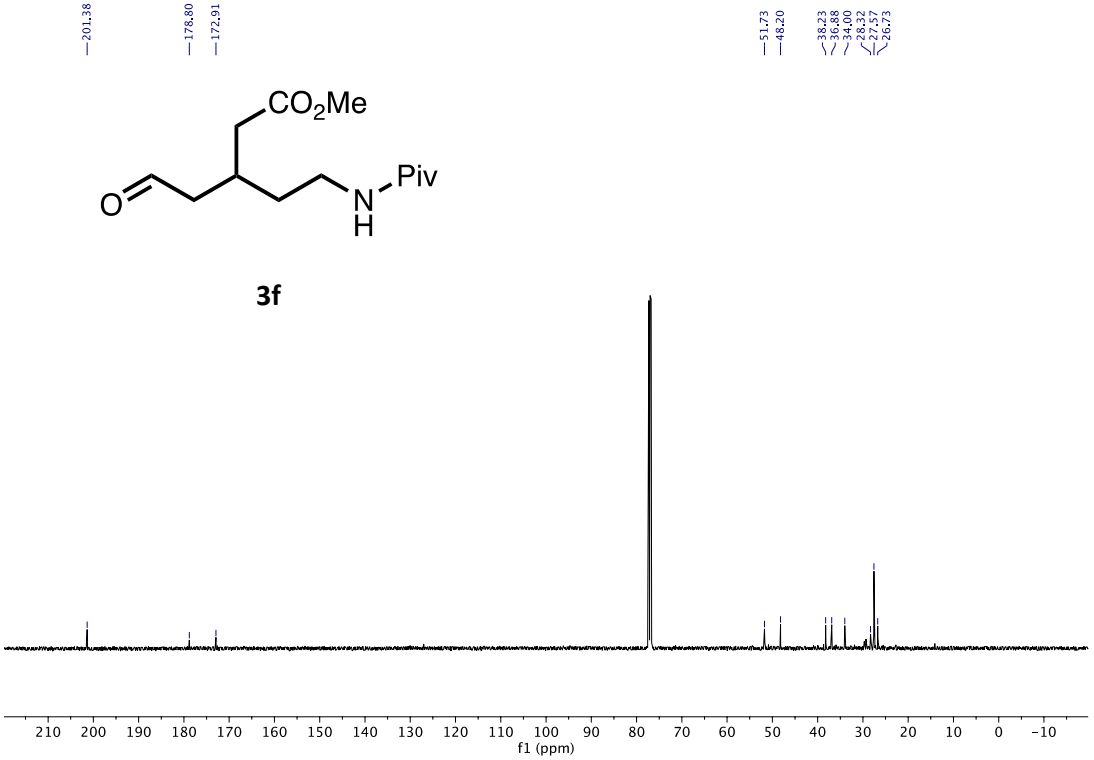

3f

Ethyl 4-oxo-2-(2-pivalamidoethyl)butanoate

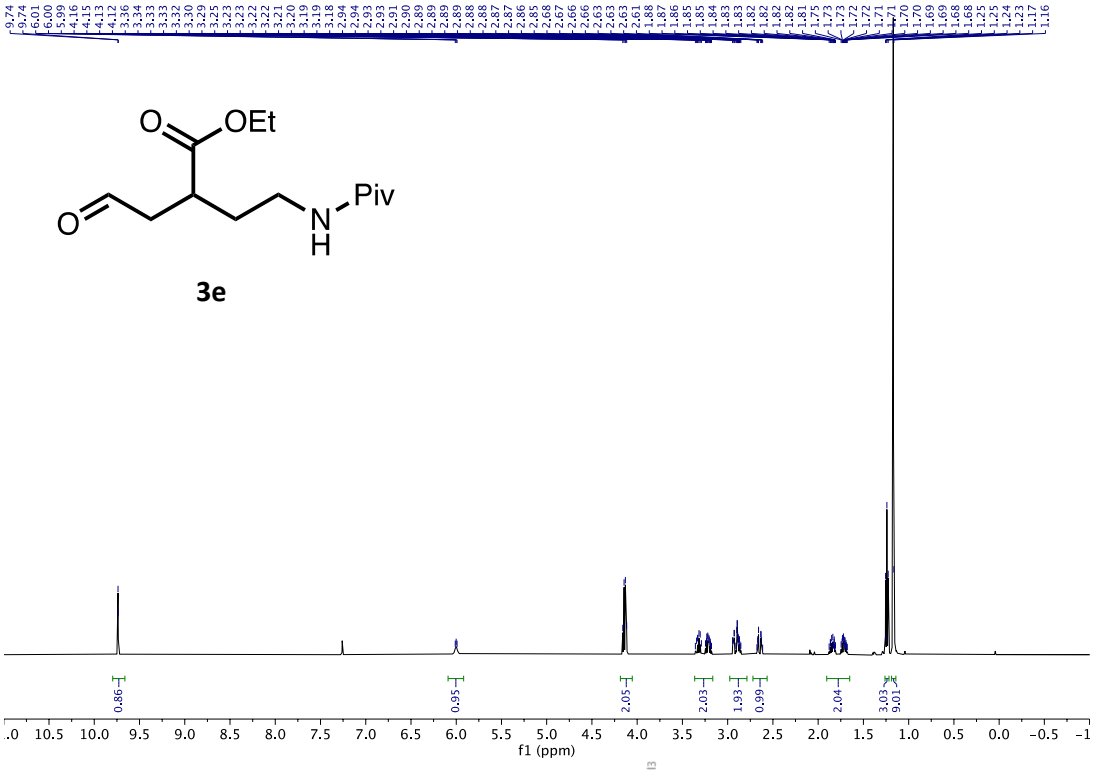

3e

3e

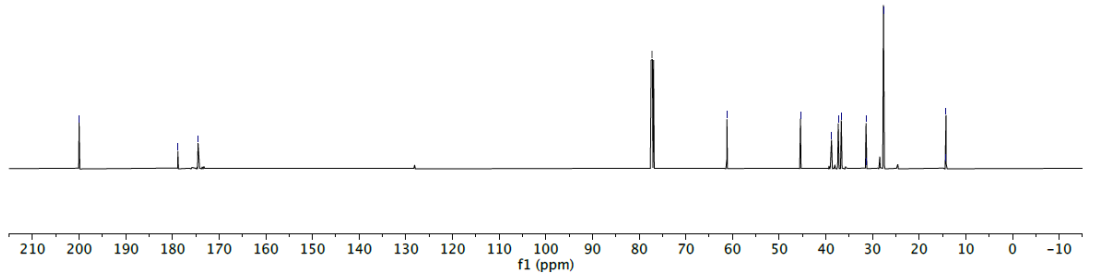

N-(7-oxoheptan-3-yl)pivalamide

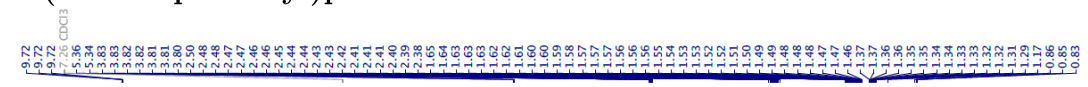

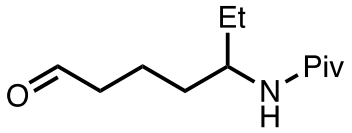

3h

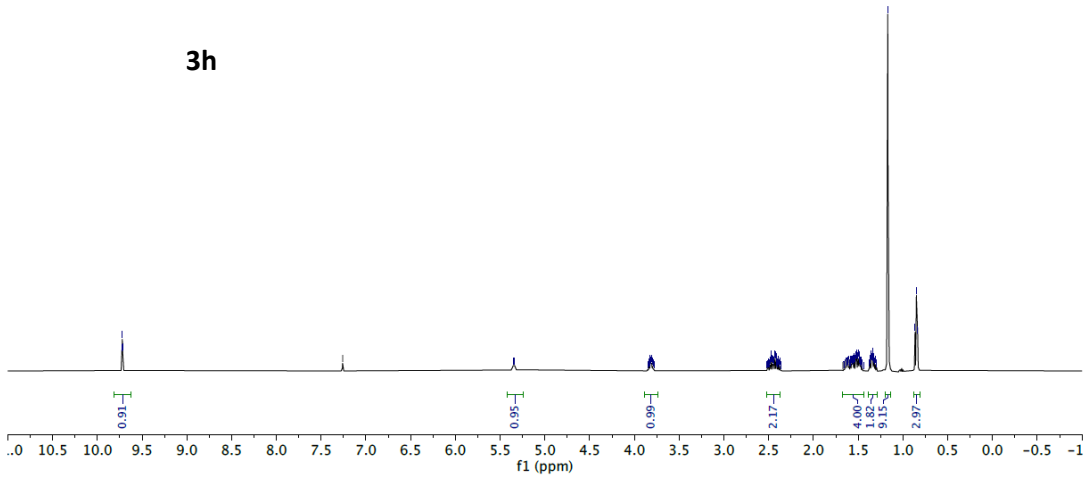

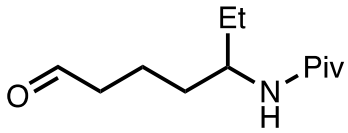

3h

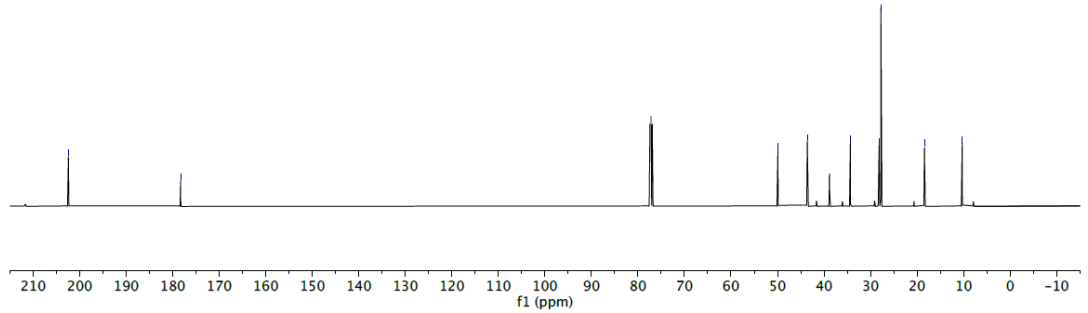

N-(6-oxohexan-2-yl)pivalamide

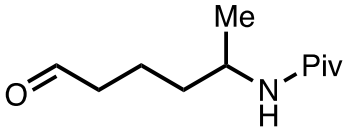

3g

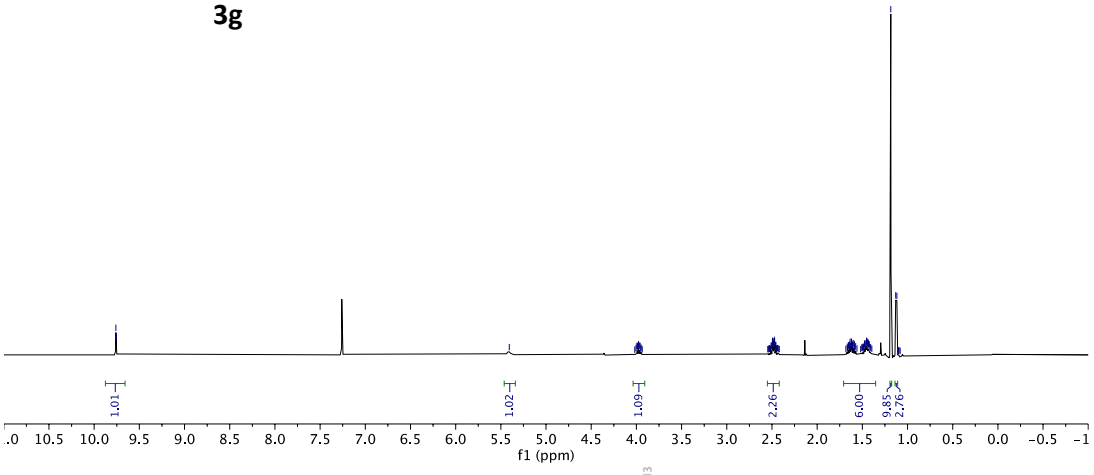

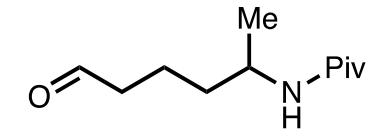

3g

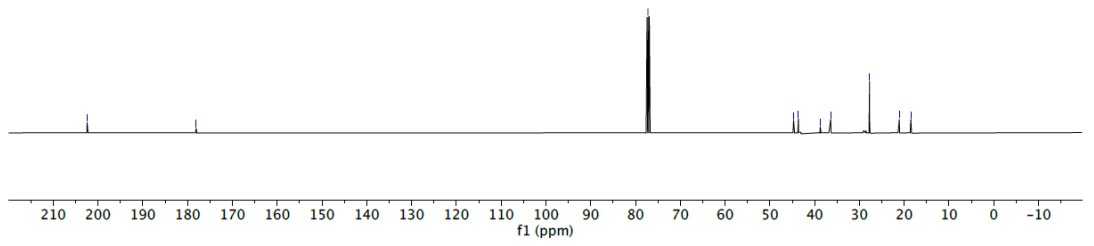

***N*-(2-methyl-5-oxopentyl)pivalamide (3i.a) and *N*-(4-methyl-5-oxopentyl)pivalamide (3i.b)**

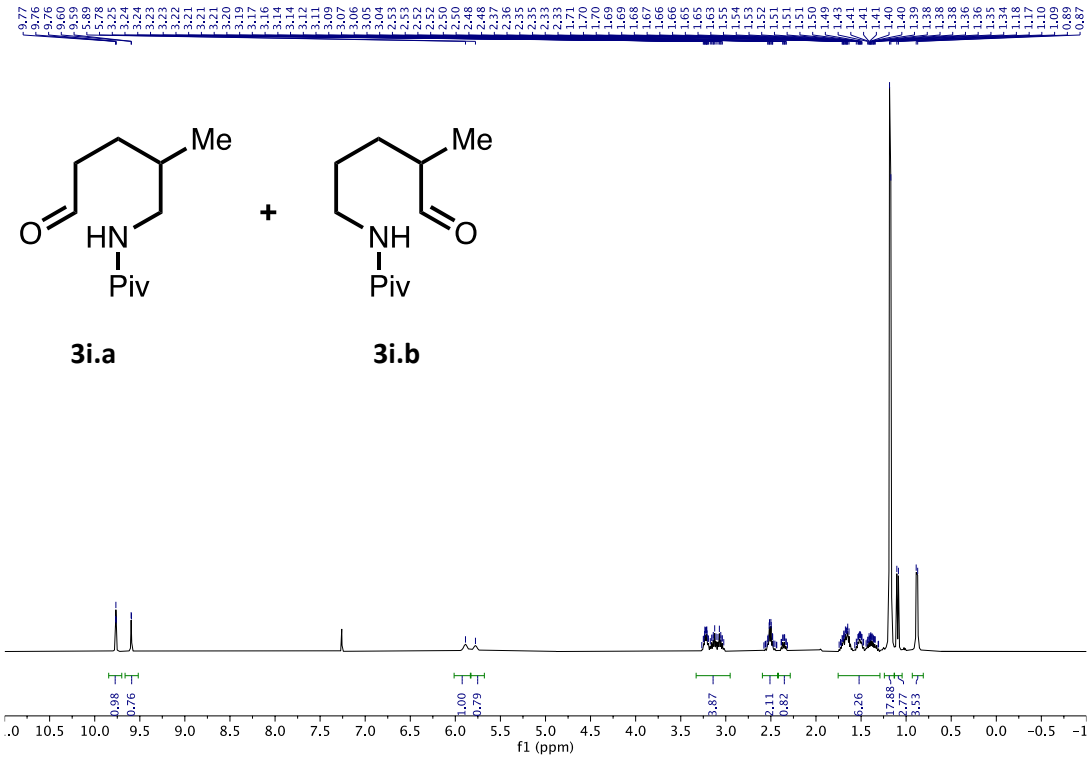

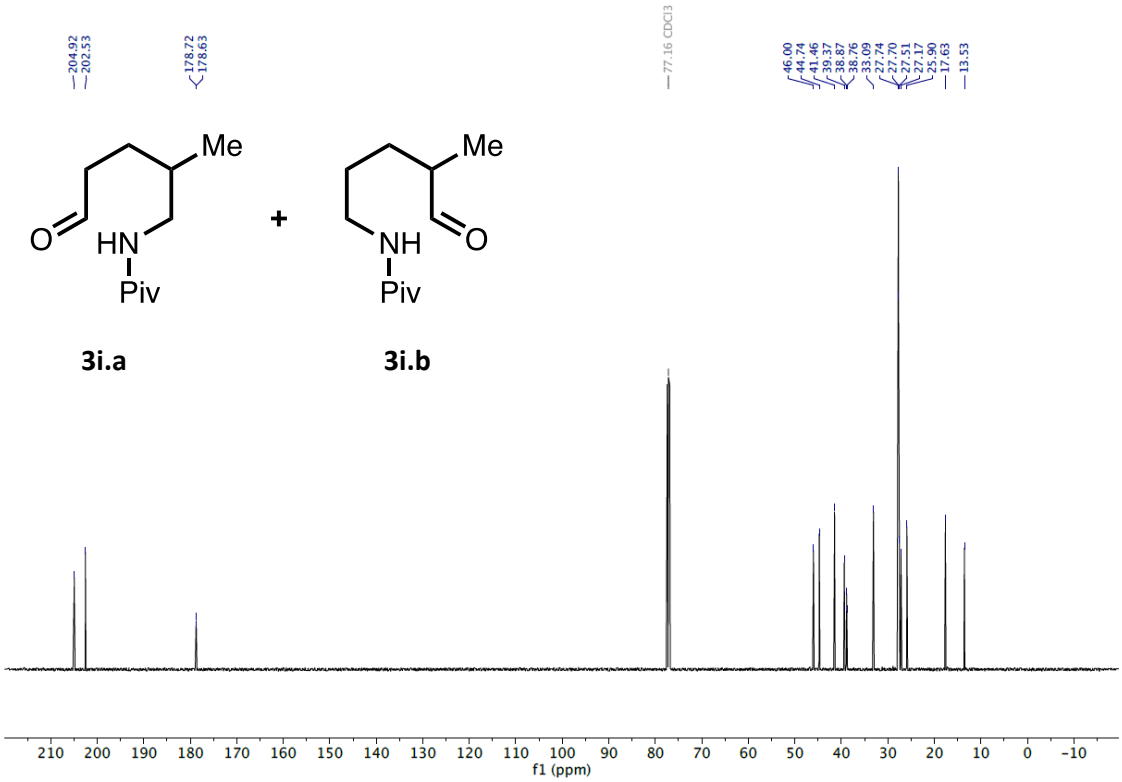
204.92
202.53
178.72
178.63
77.16 CDCl3
46.00
44.74
41.46
39.37
38.87
38.76
33.09
27.74
27.70
27.51
27.17
25.90
17.63
13.53
Me
O
HN
Piv
+
Me
NH
O
Piv
3i.a
3i.b
210 200 190 180 170 160 150 140 130 120 110 100 90 80 70 60 50 40 30 20 10 0 -10
f1 (ppm)

_N_-(5-oxo-2-phenylpentyl)pivalamide and **_N_-(5-oxo-4-phenylpentyl)pivalamide**

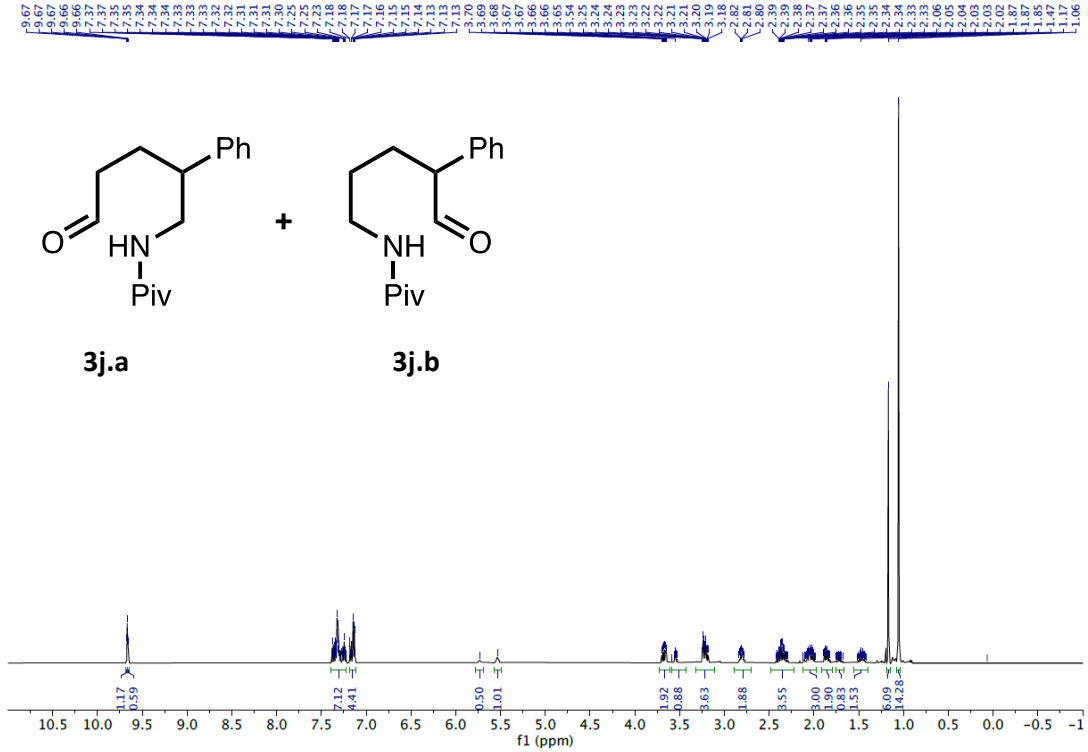

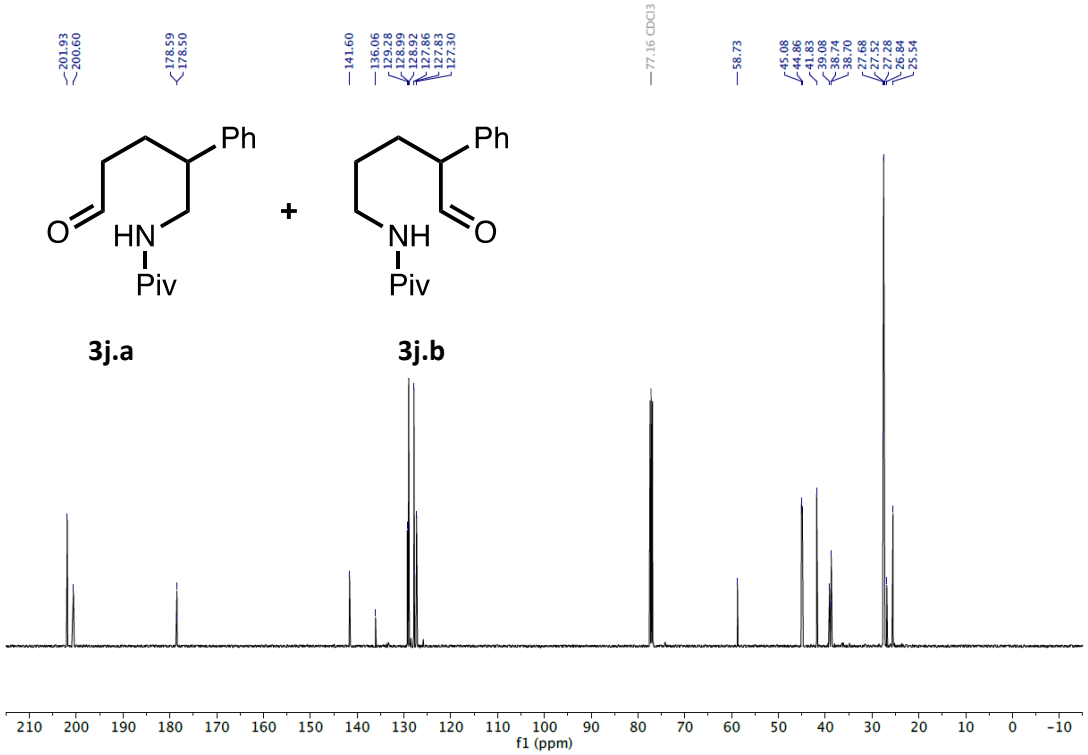

***N*-(2-formylphenethyl)pivalamide**

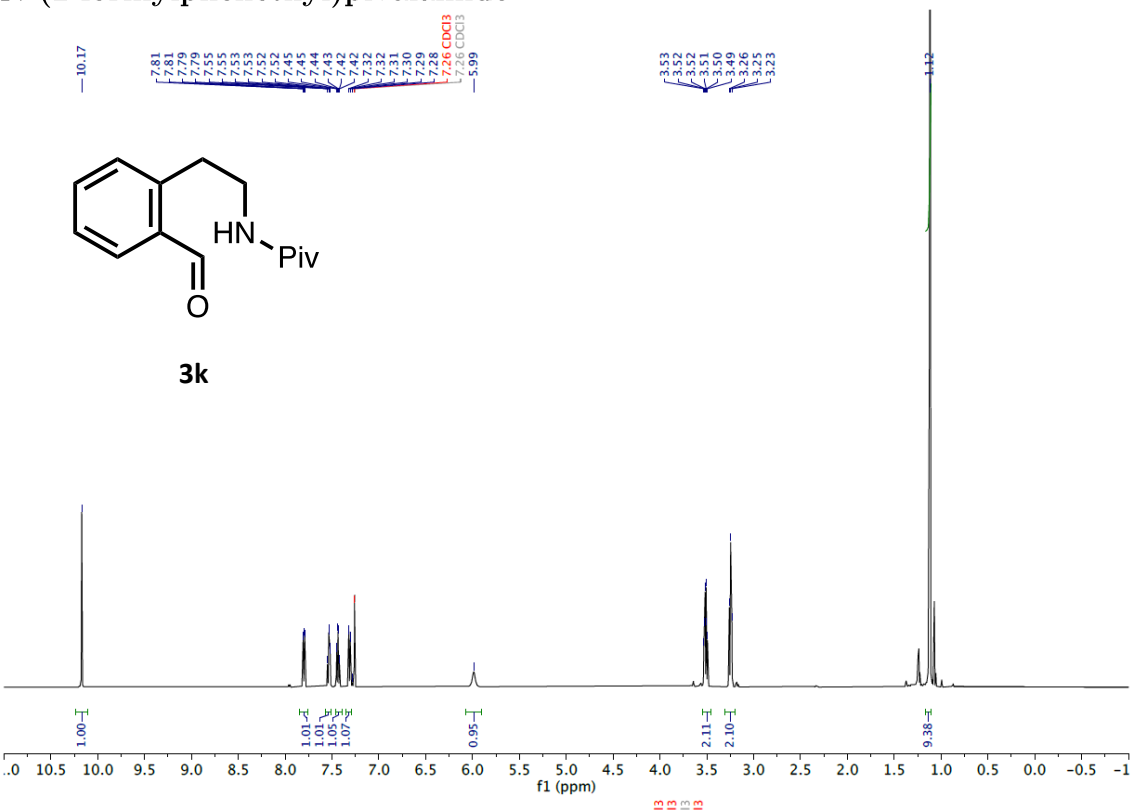

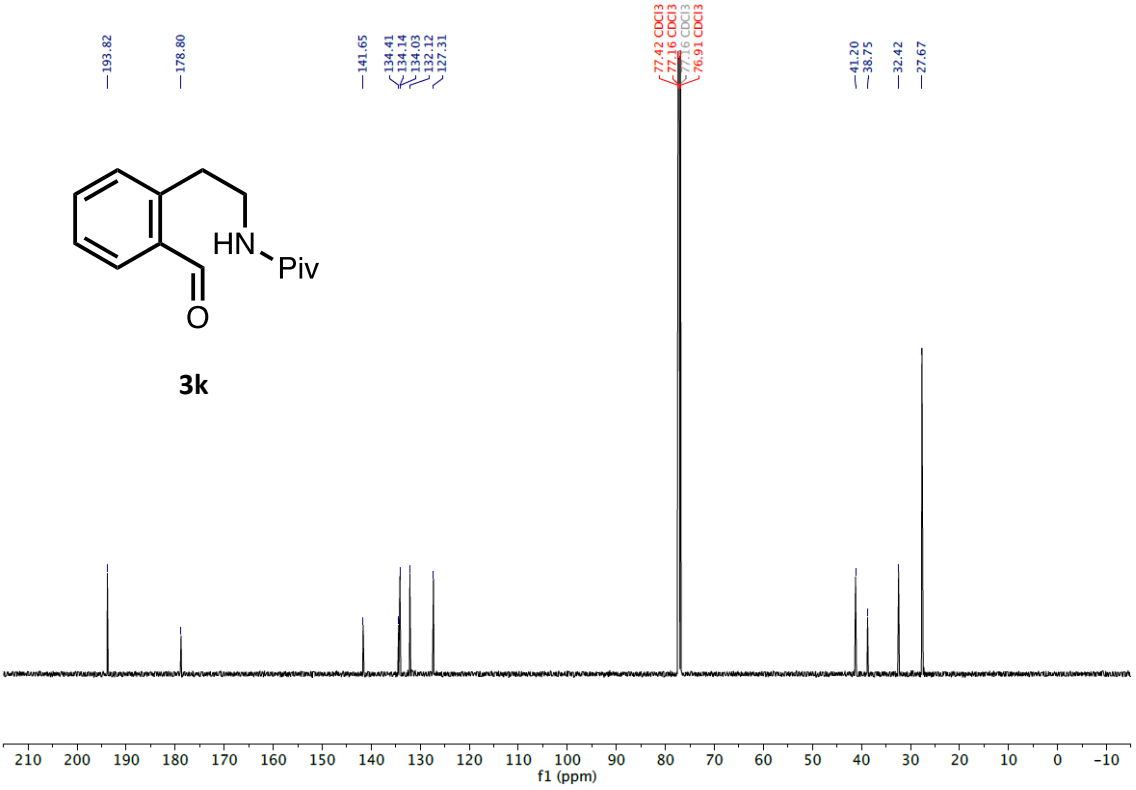

***N*-(2-formyl-4,5-dimethoxyphenethyl)pivalamide**

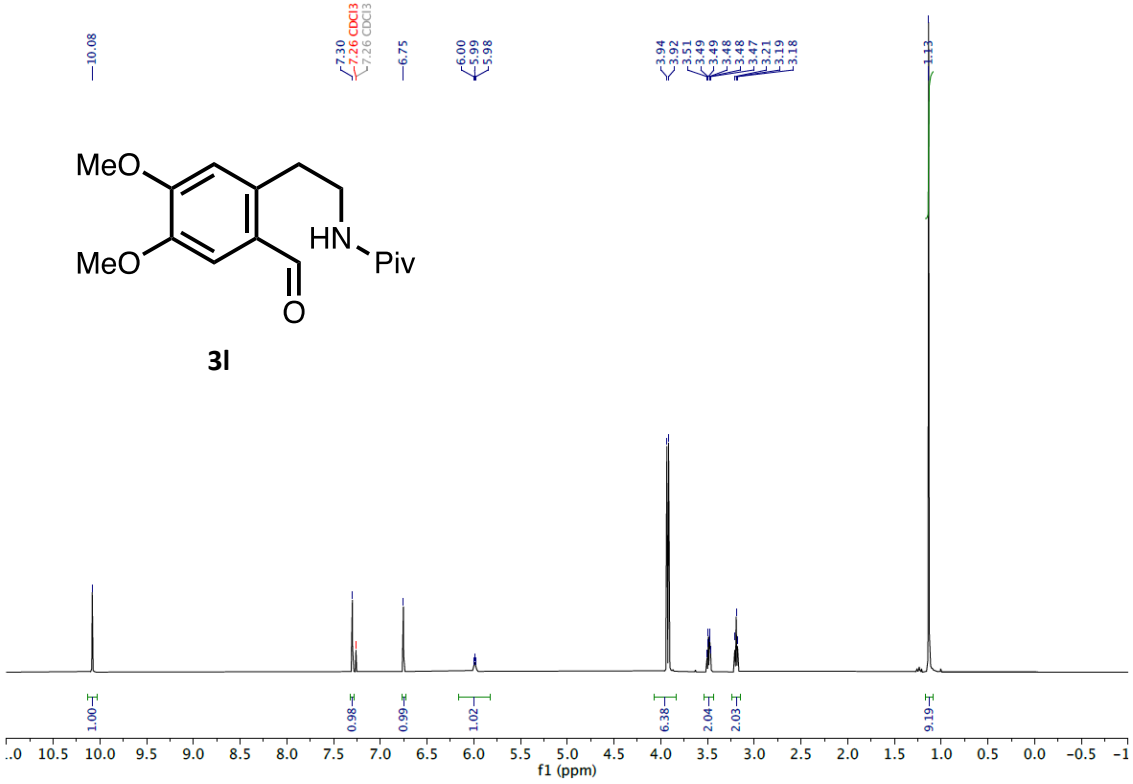

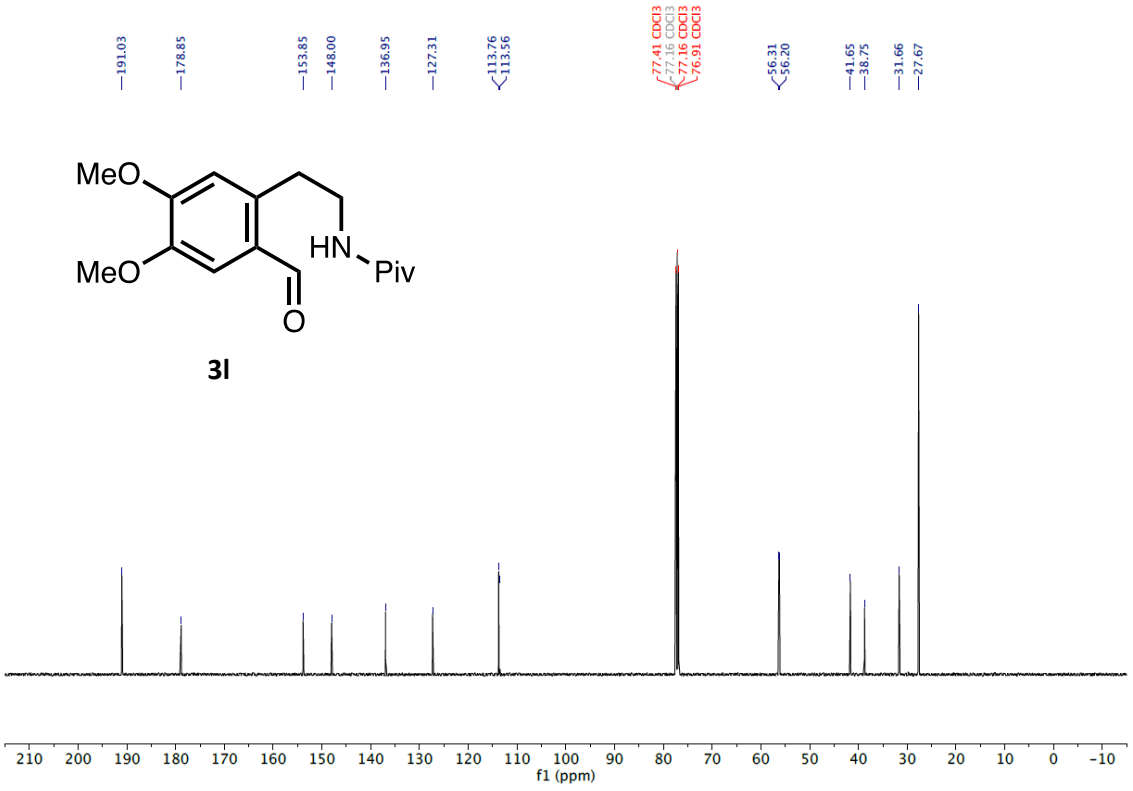

NMR Spectra – Acid Products

7-pivalamidoheptanoic acid

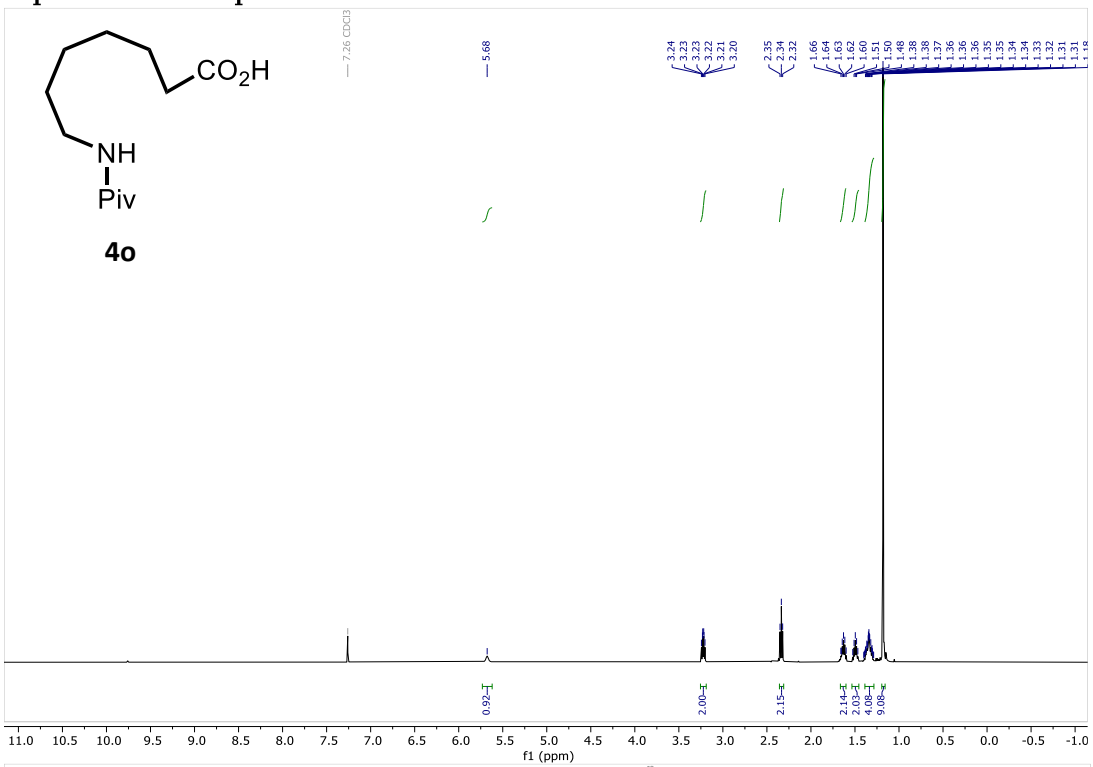

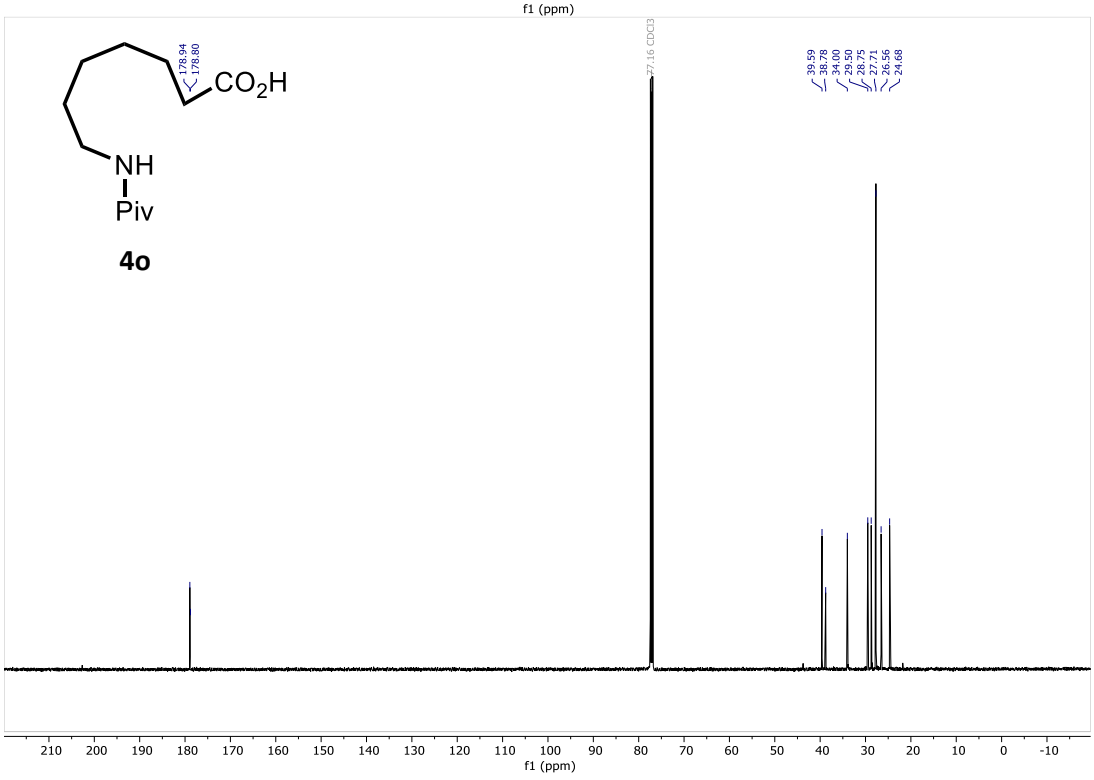

5-pivalamidohexanoic acid

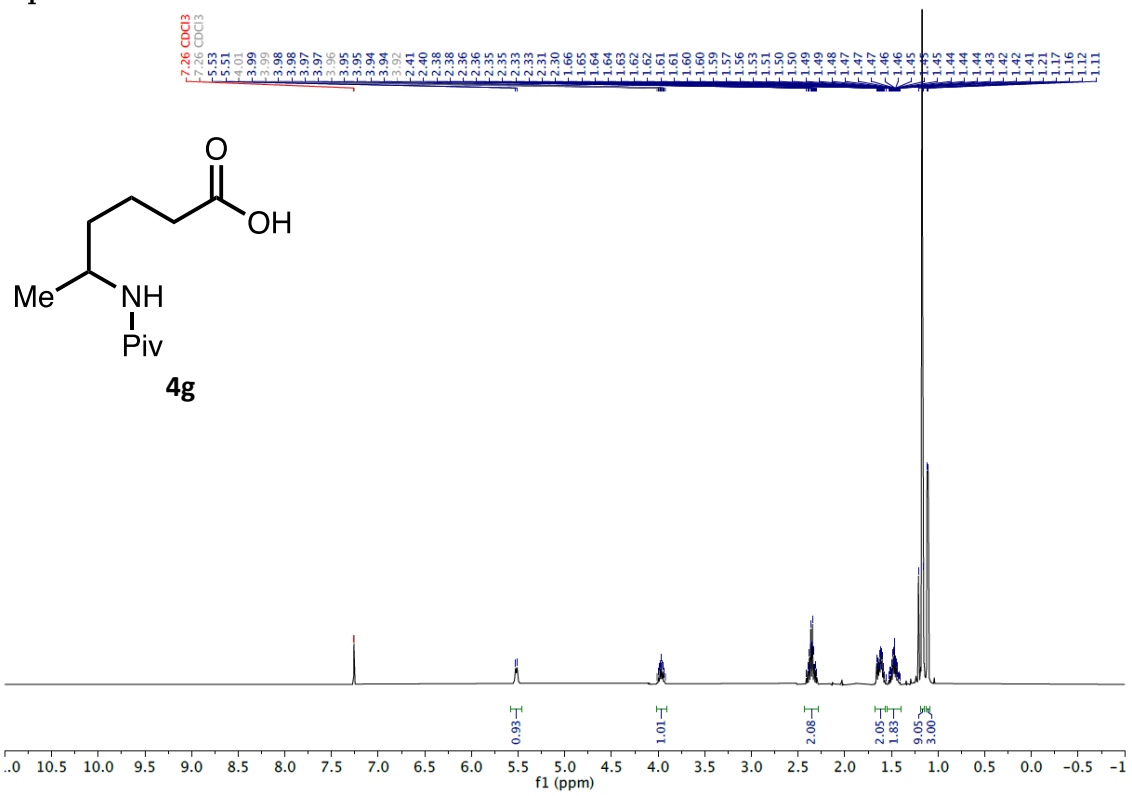

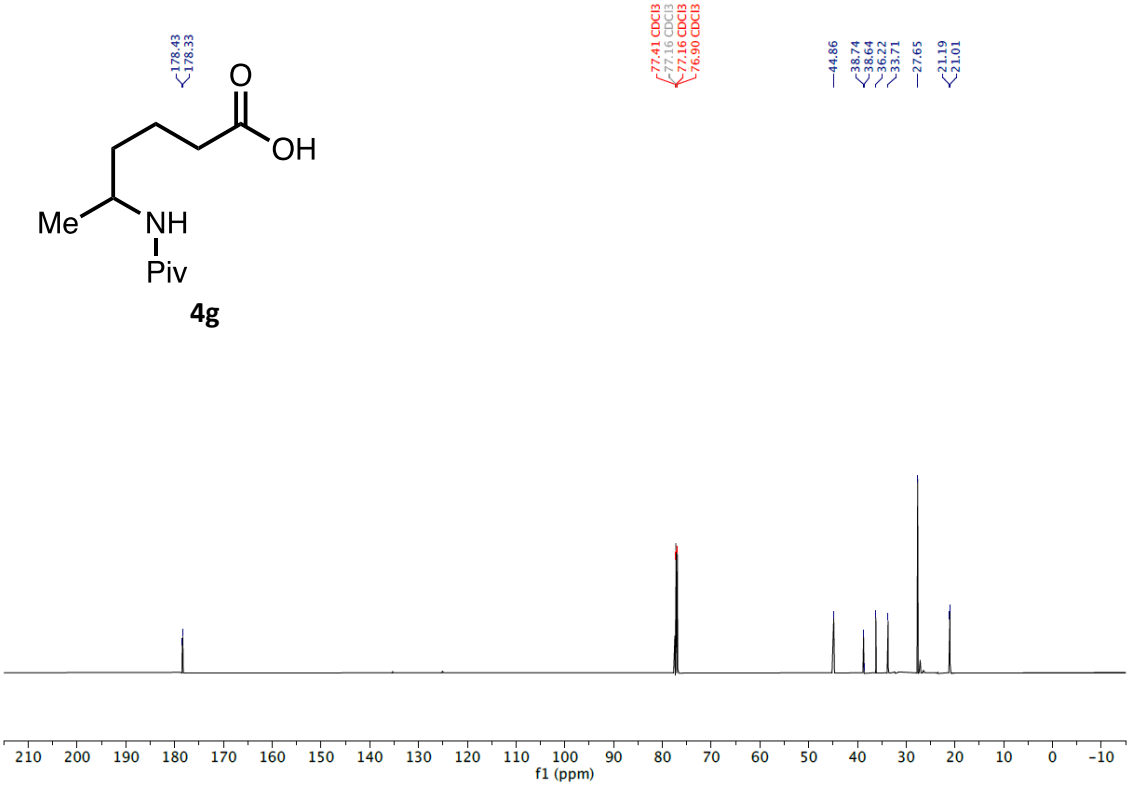

3-phenyl-5-pivalamidopentanoic acid

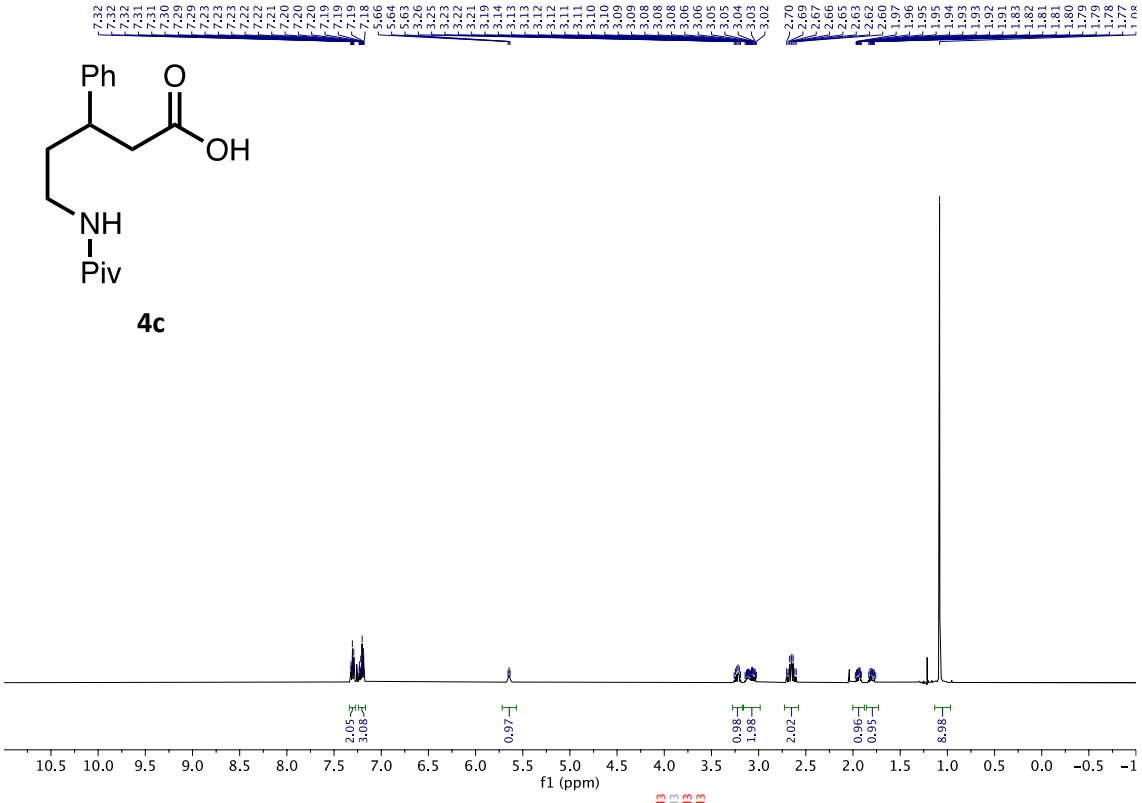

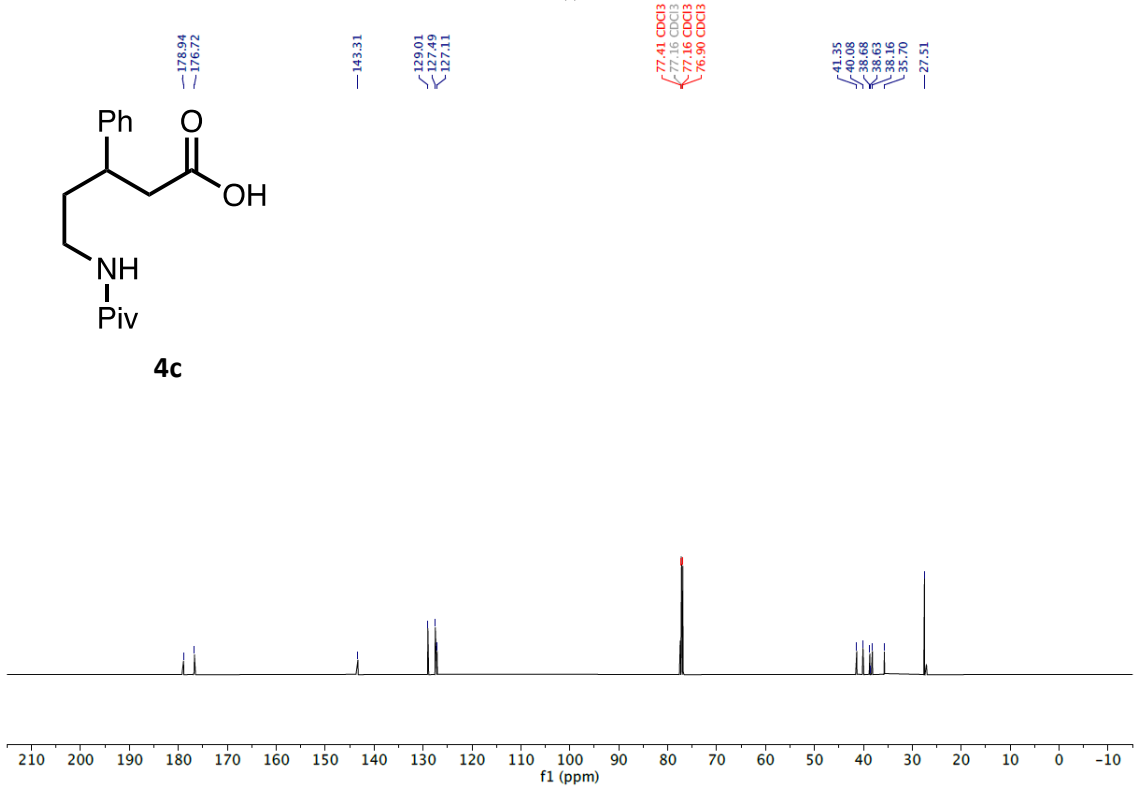

3-methyl-5-pivalamidopentanoic acid

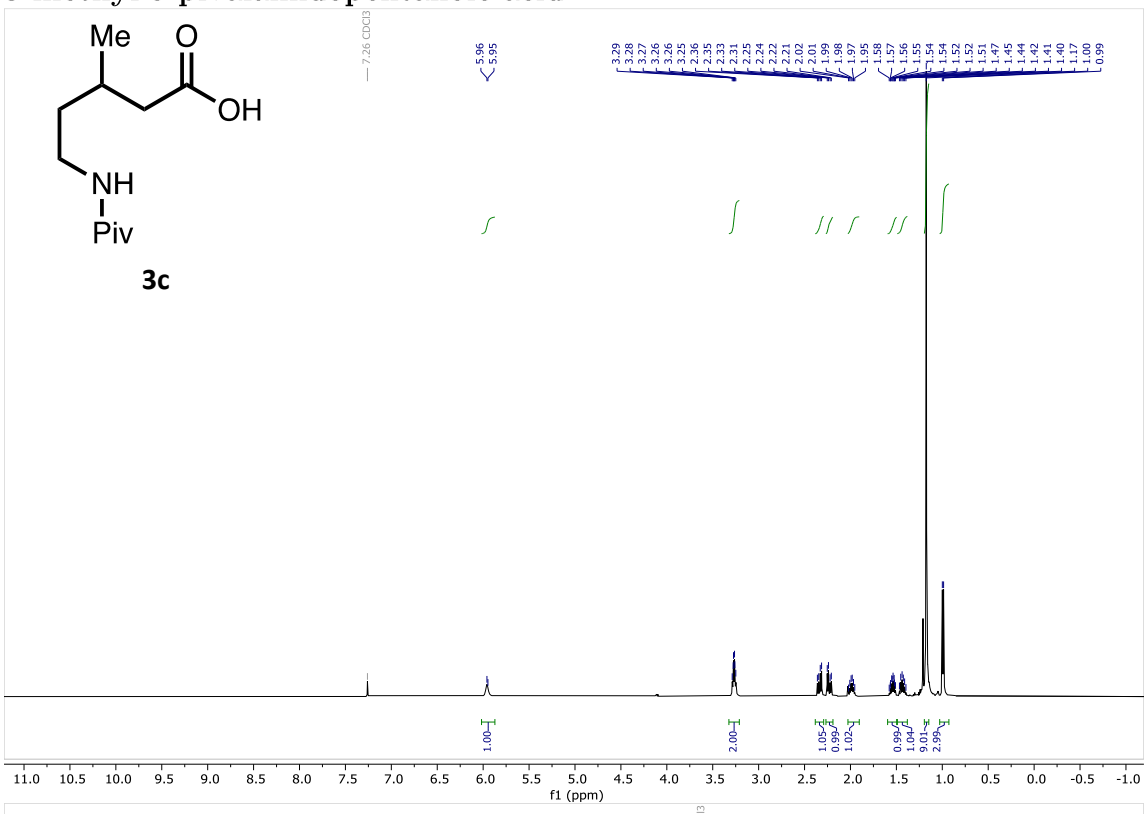

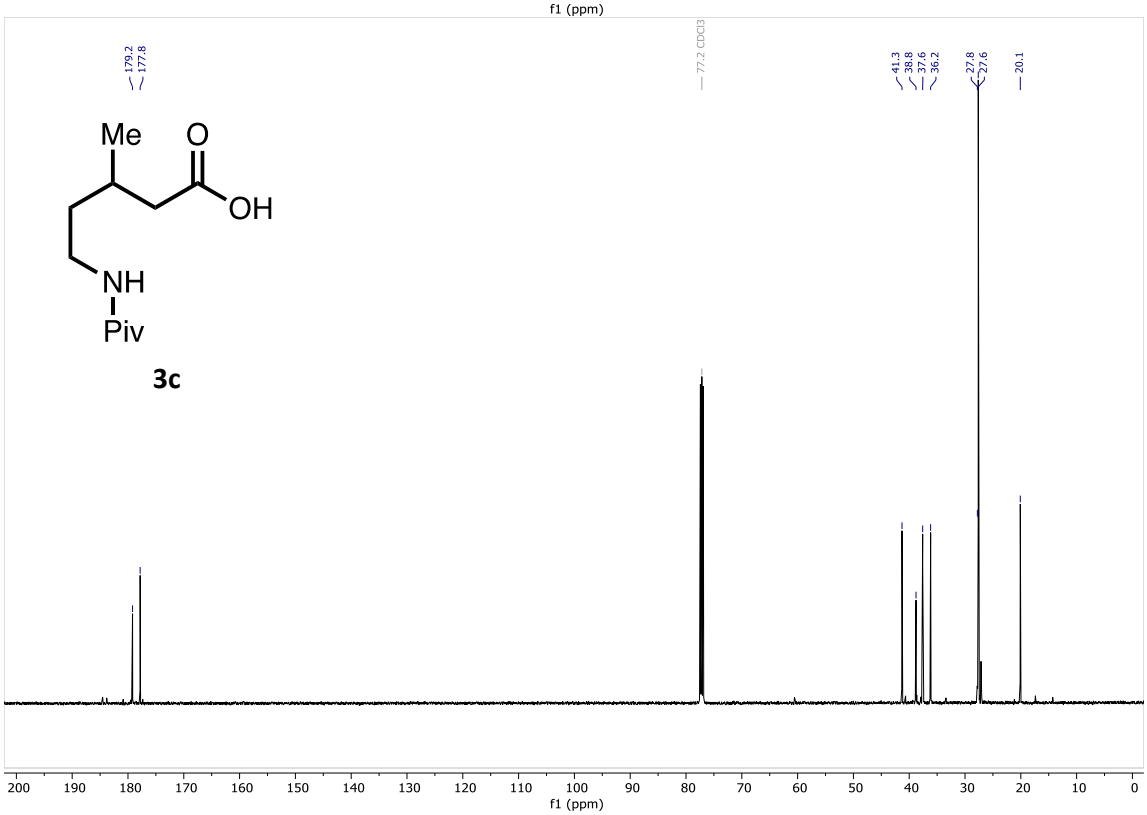

3-(ethoxycarbonyl)-5-pivalamidopentanoic acid

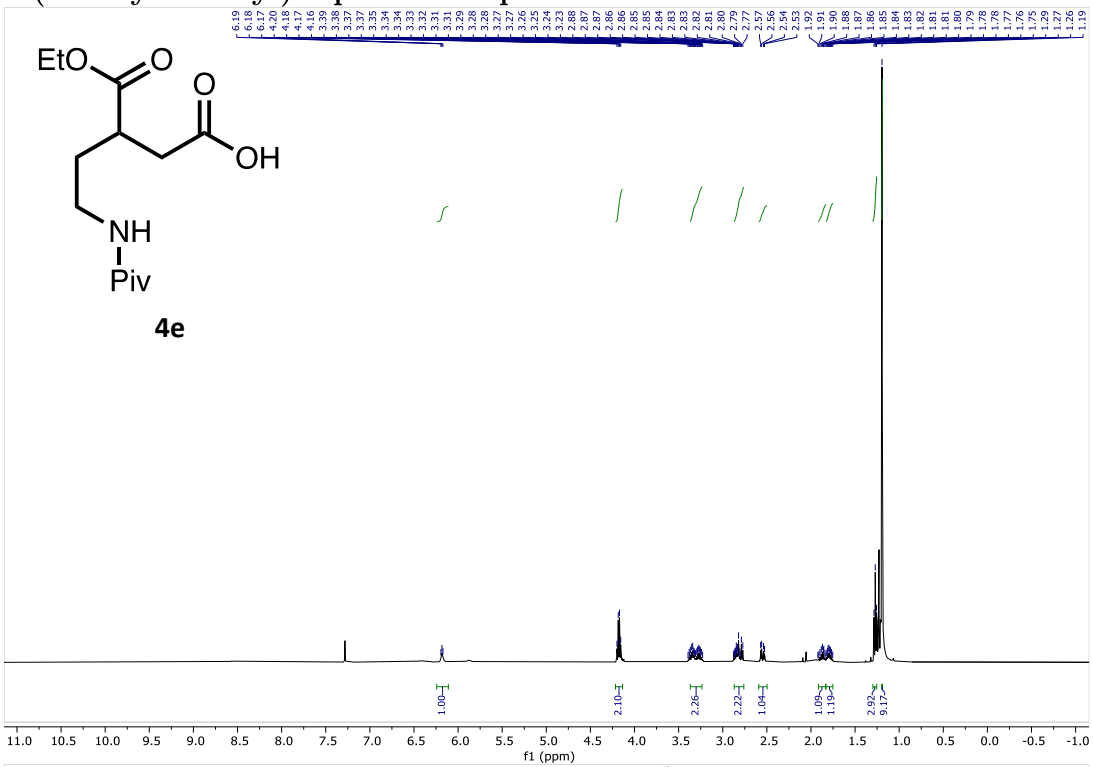

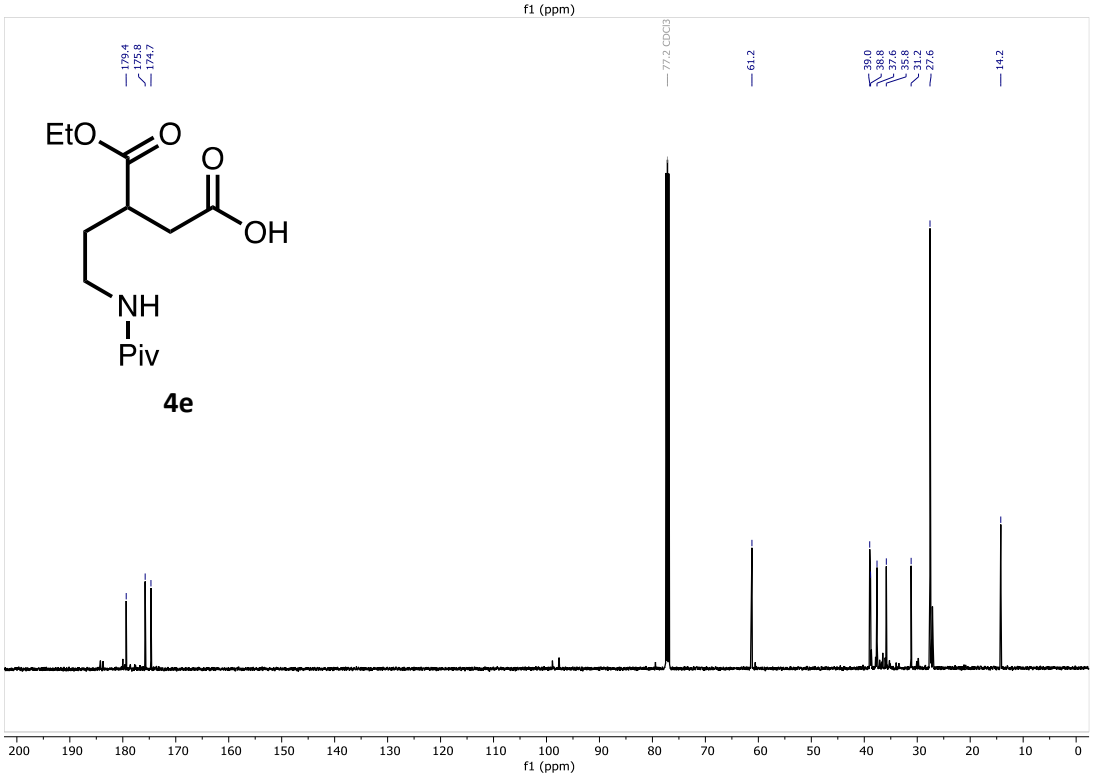

5-methoxy-5-oxo-3-(2-pivalamidoethyl)pentanoic acid

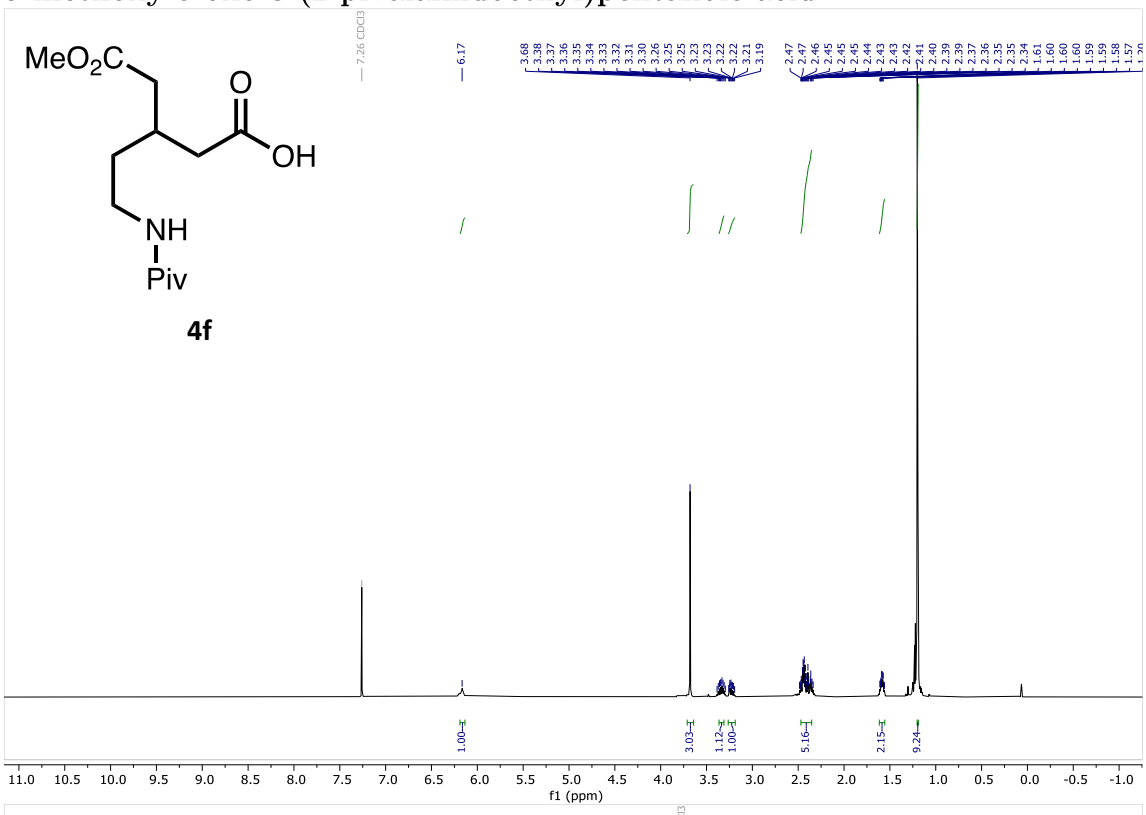

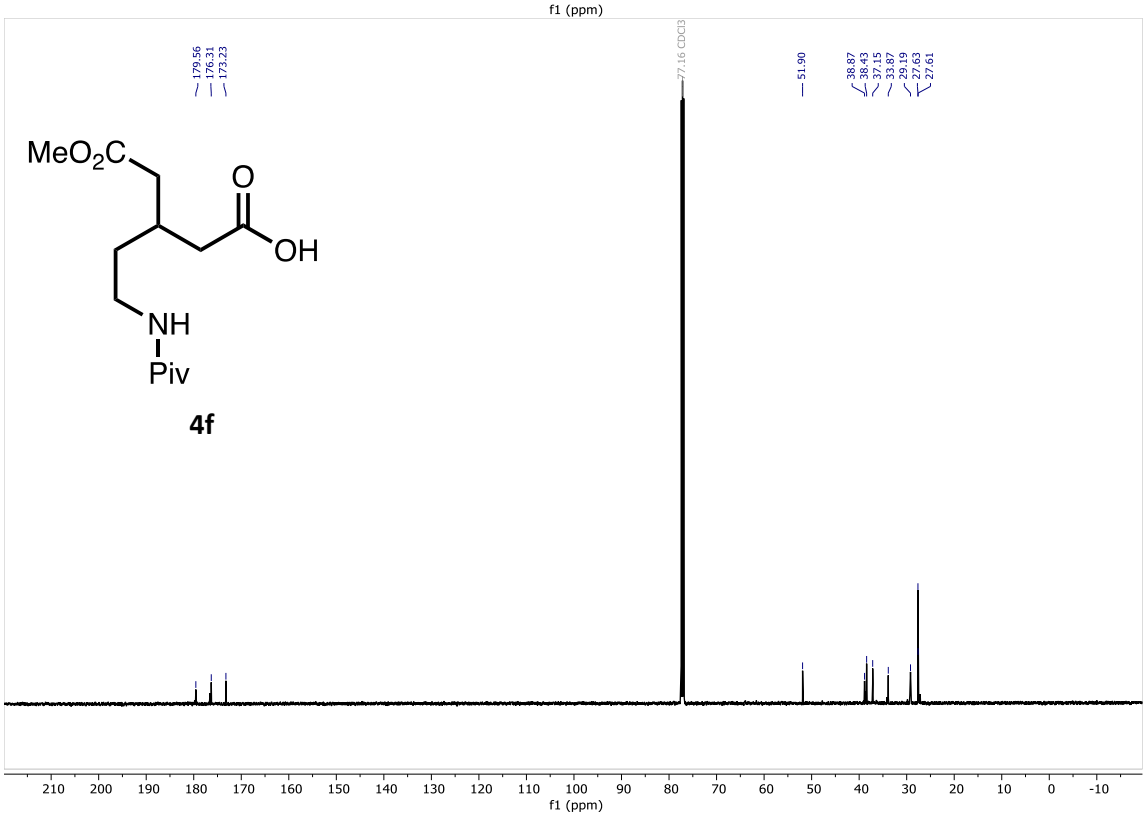

2,4-dimethyl-5-pivalamidopentanoic acid

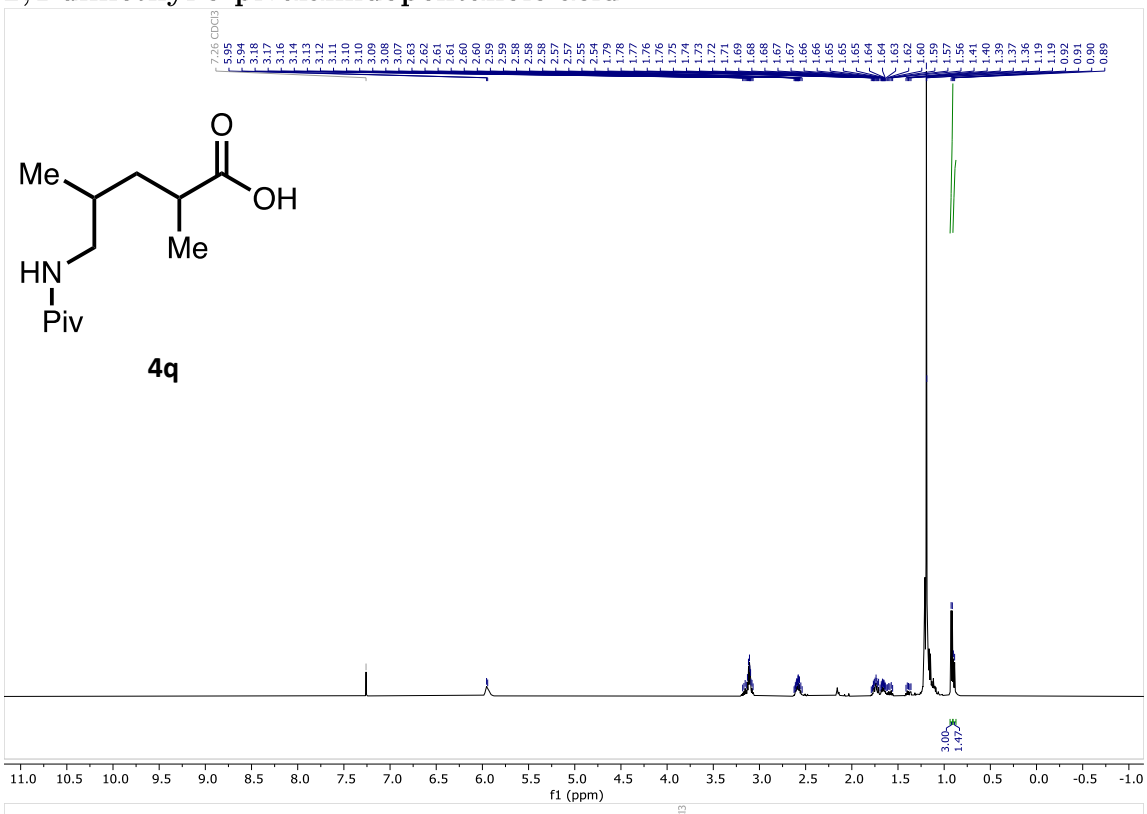

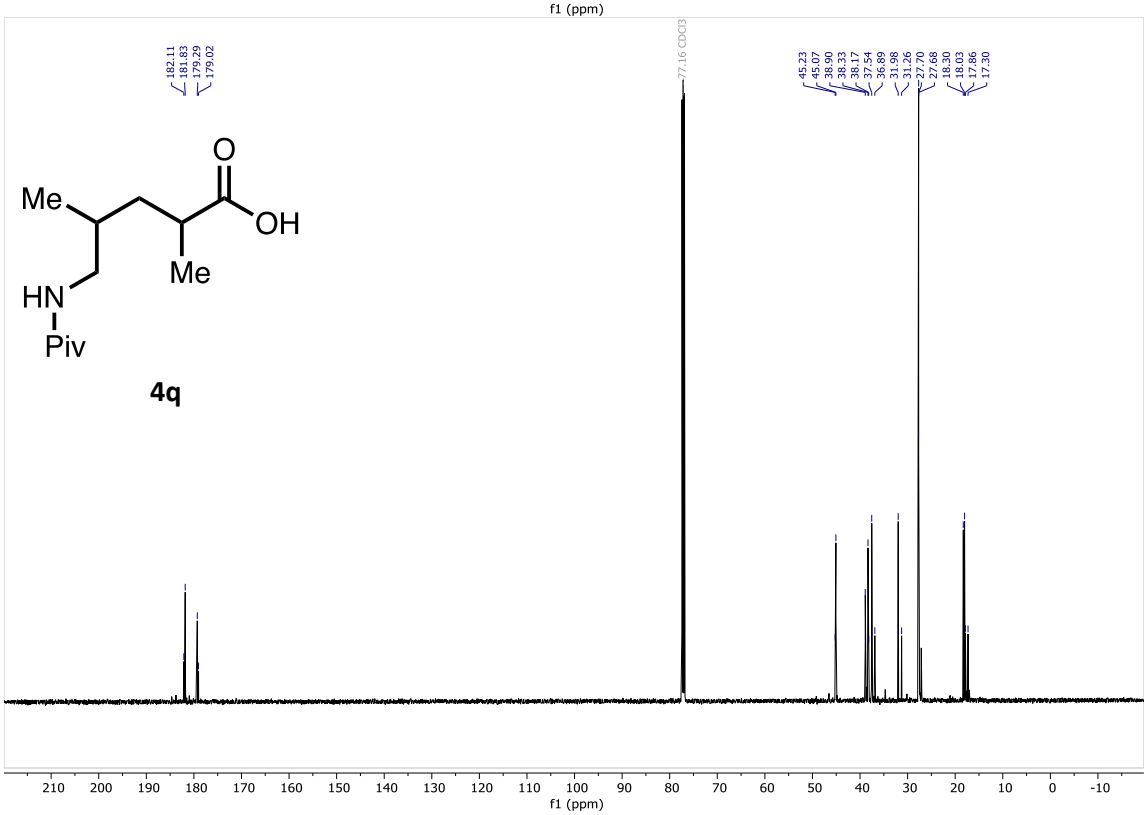

3-(2-pivalamidocyclohexyl)propanoic acid

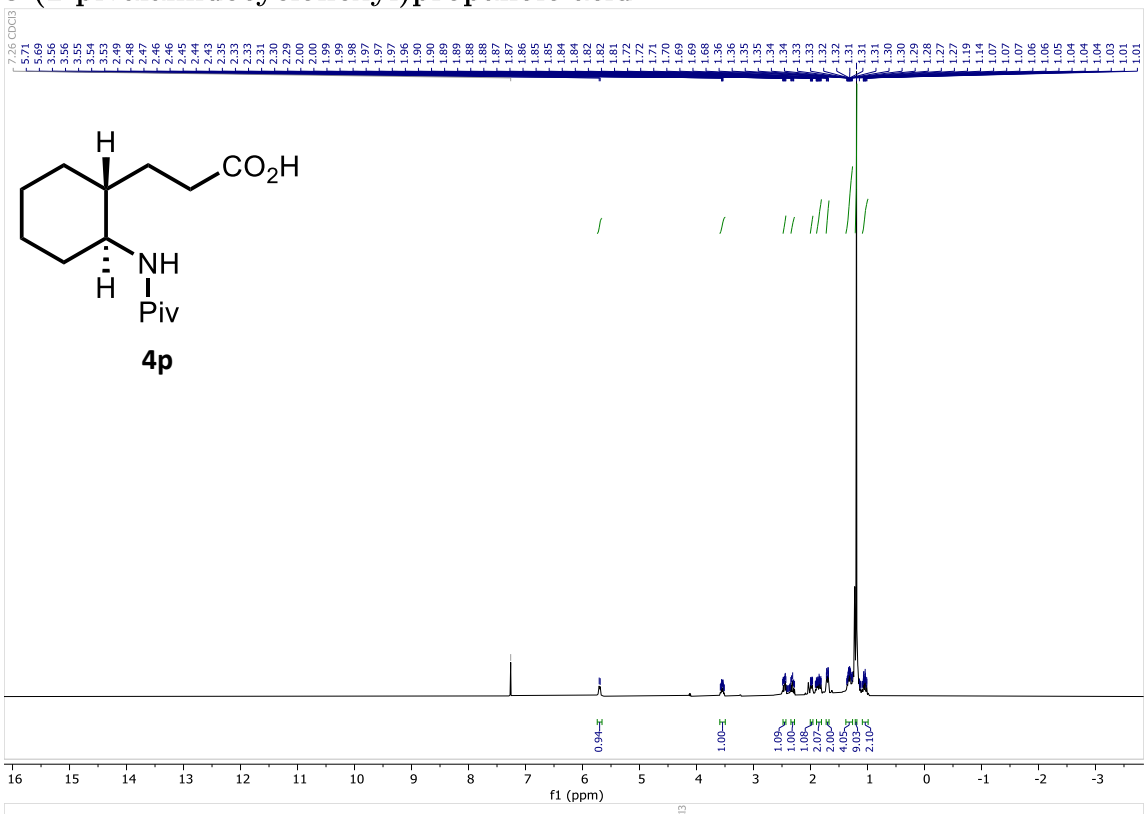

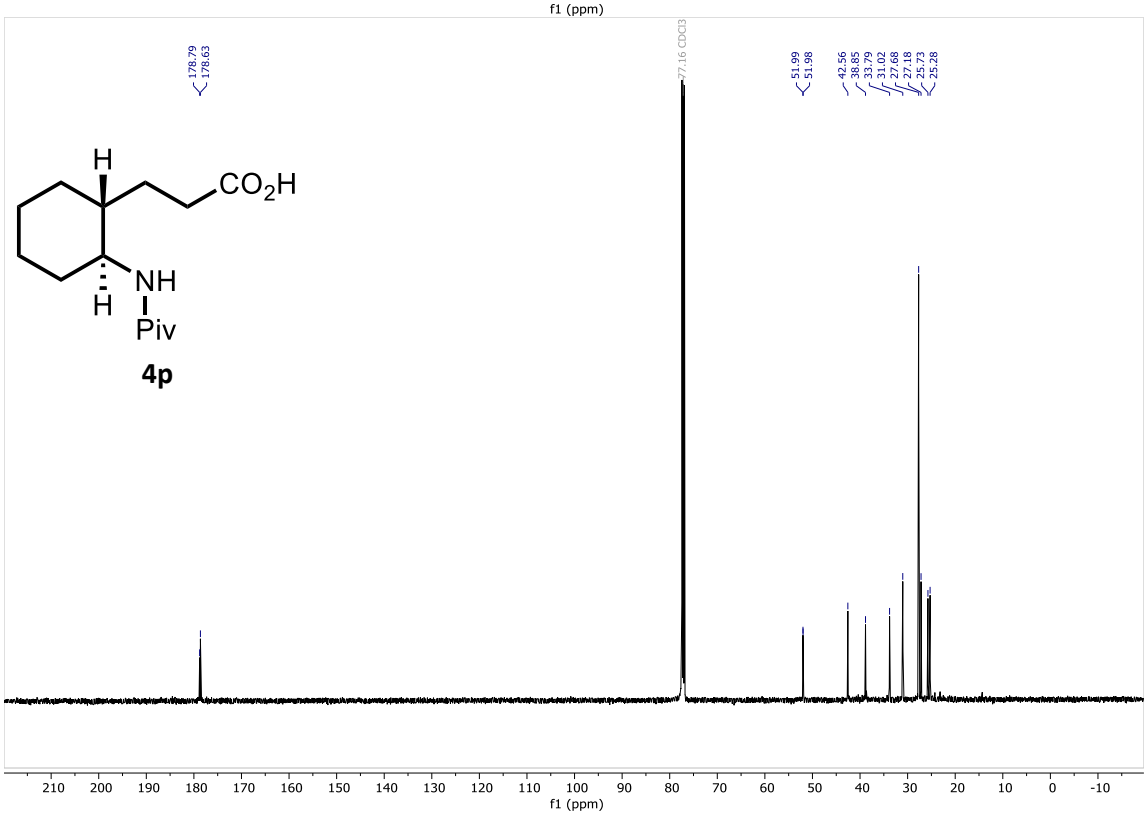

(*S*)-6-methoxy-6-oxo-5-pivalamidohexanoic acid

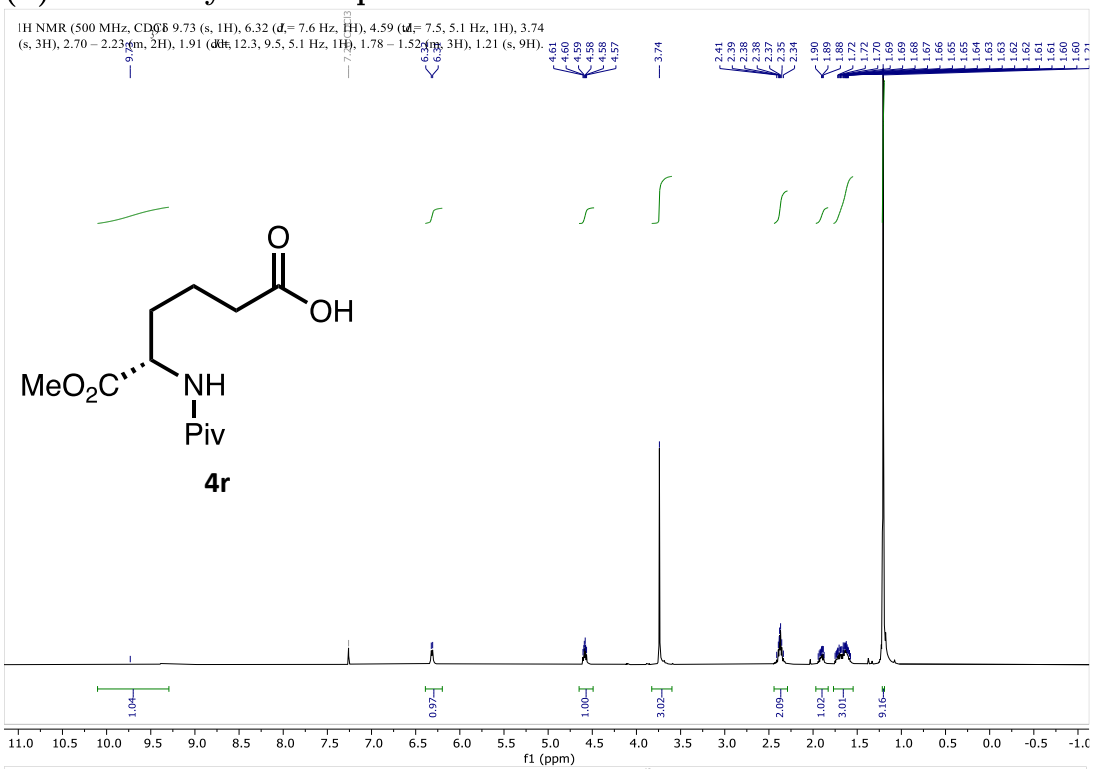

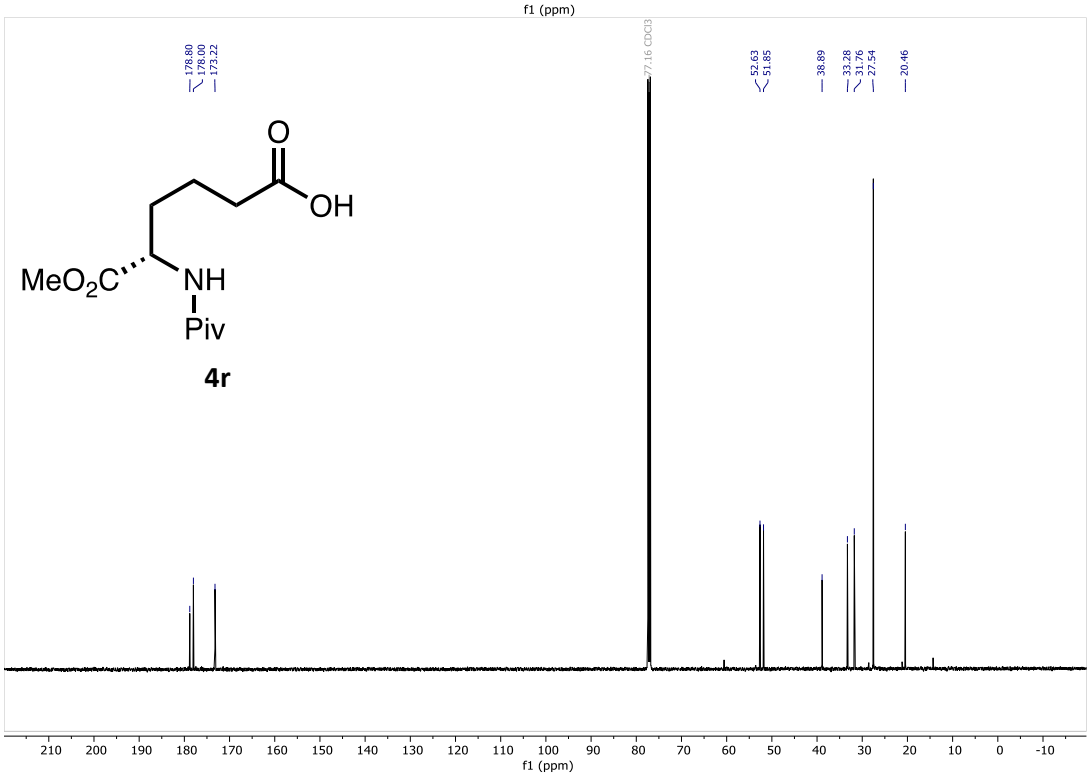

(*S*)-5-methoxy-5-oxo-4-pivalamidopentanoic acid

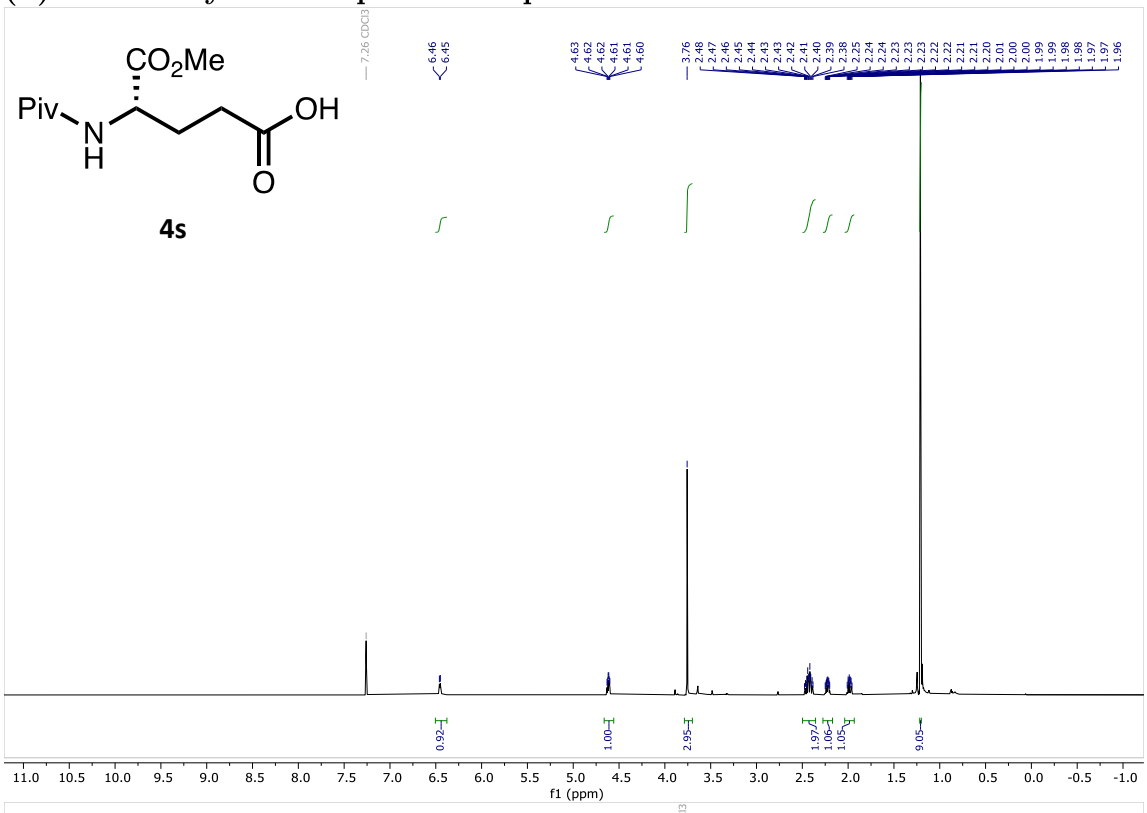

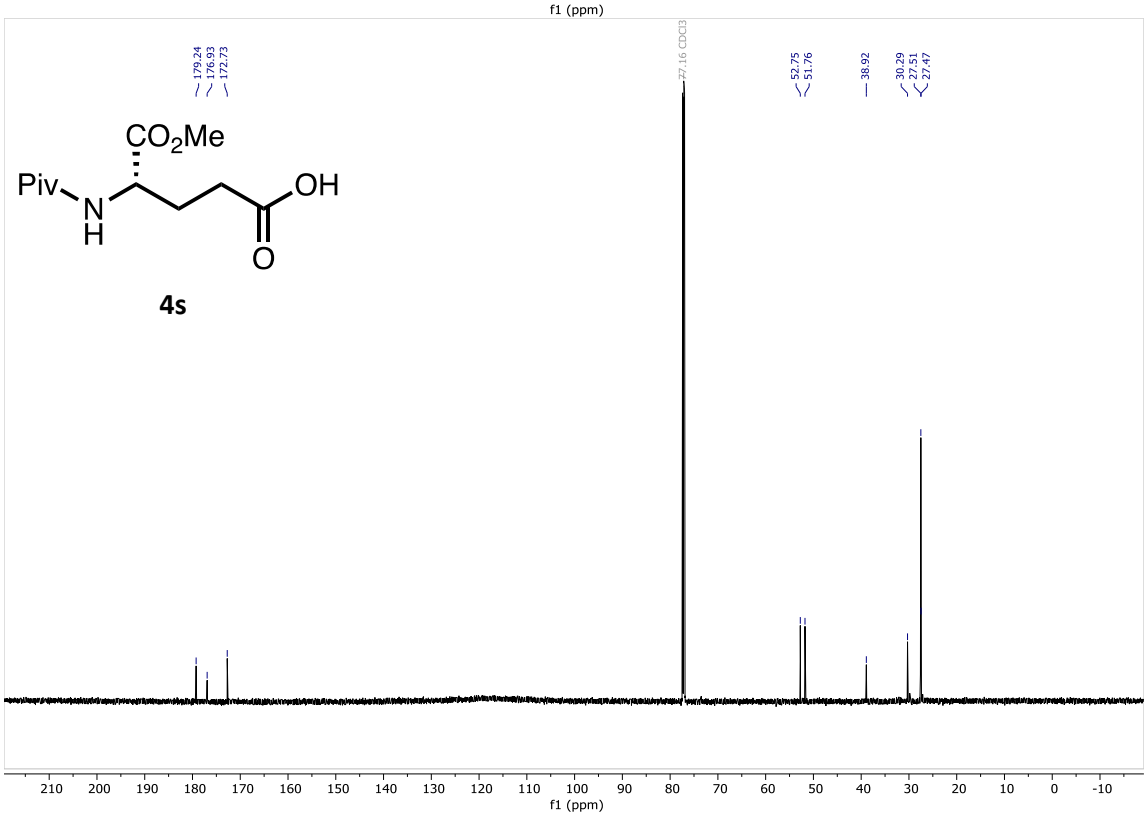

_N_-(5-oxo-5-phenylpentyl)pivalamide

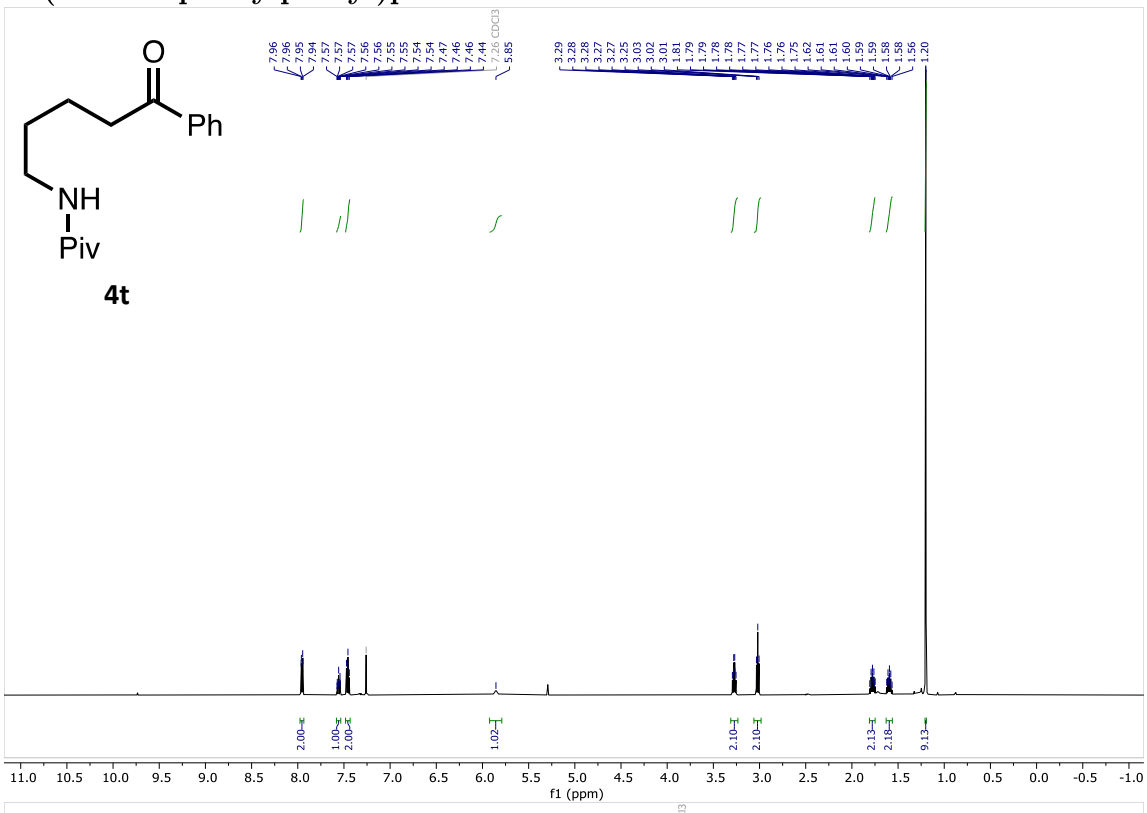

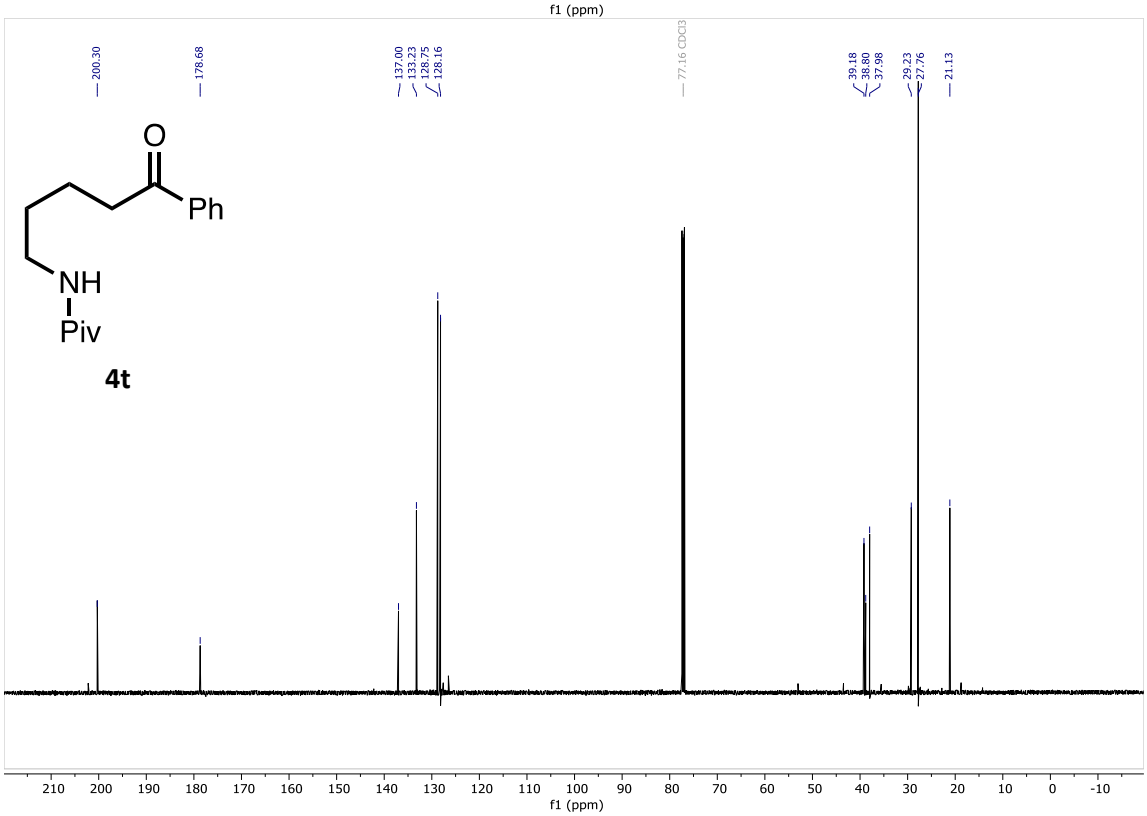

5-oxo-5-phenylpentanoic acid

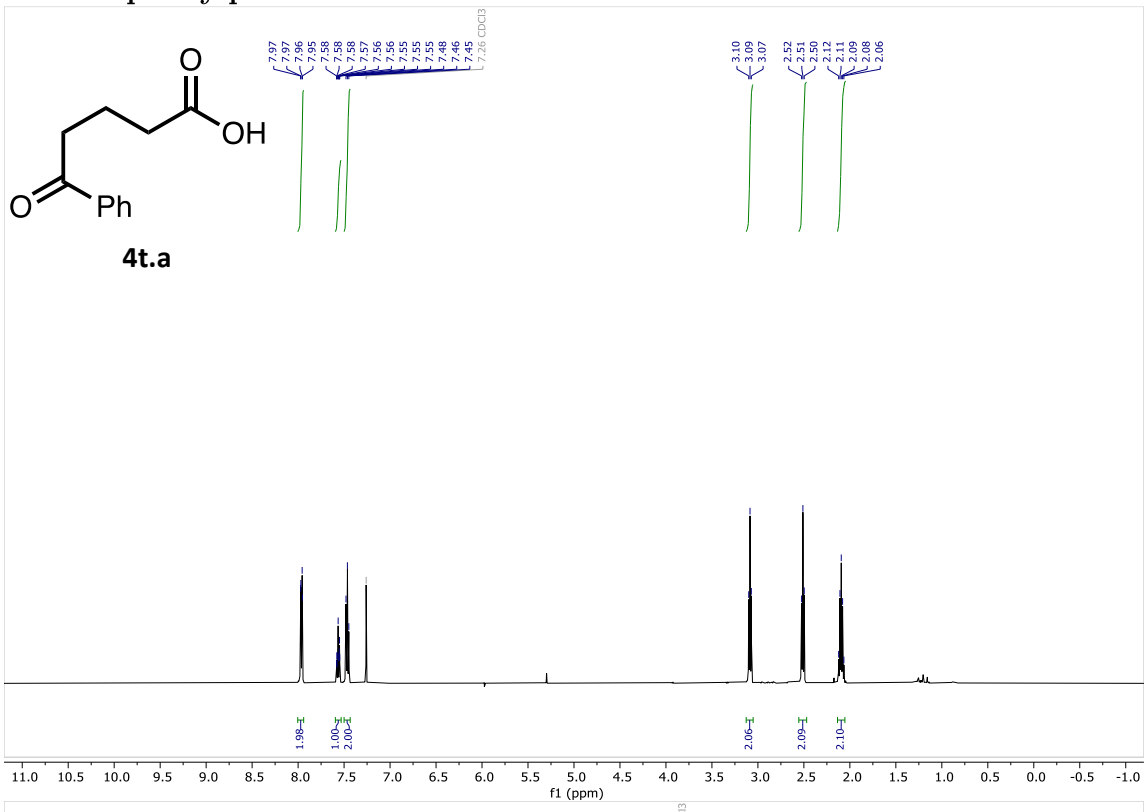

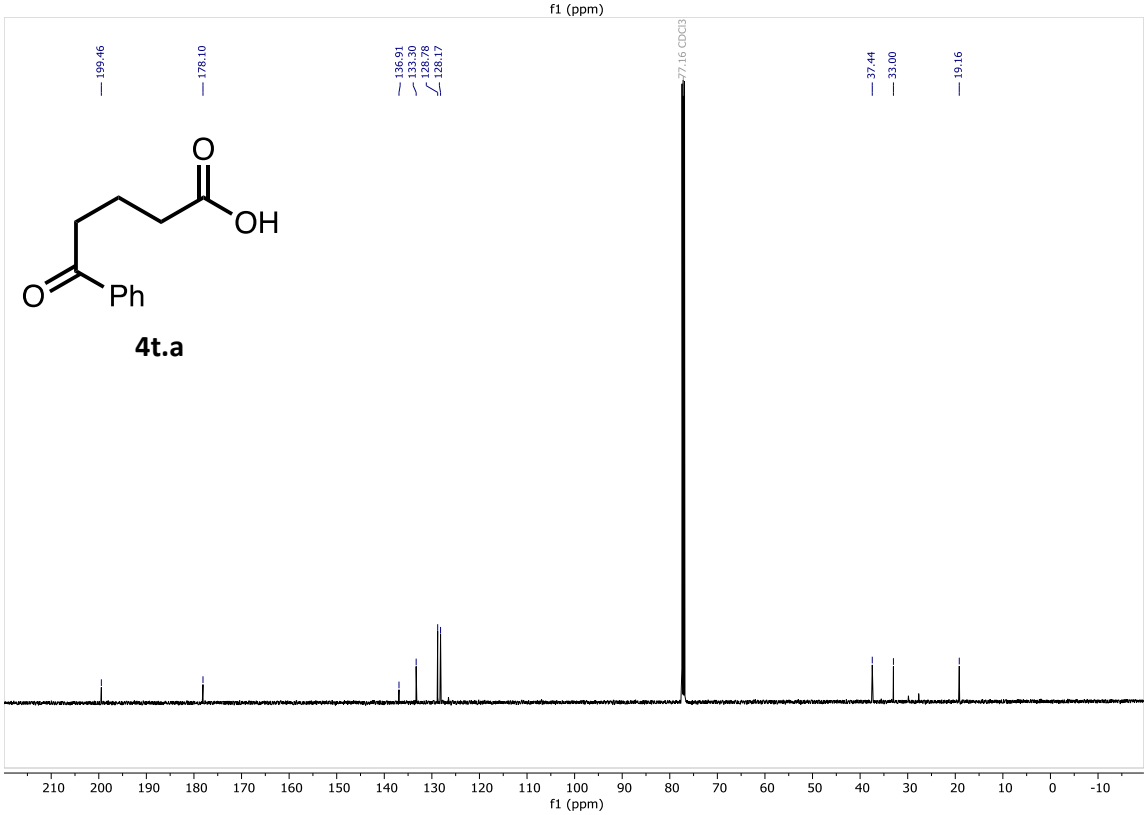

5-oxo-5-phenylpentanoic acid

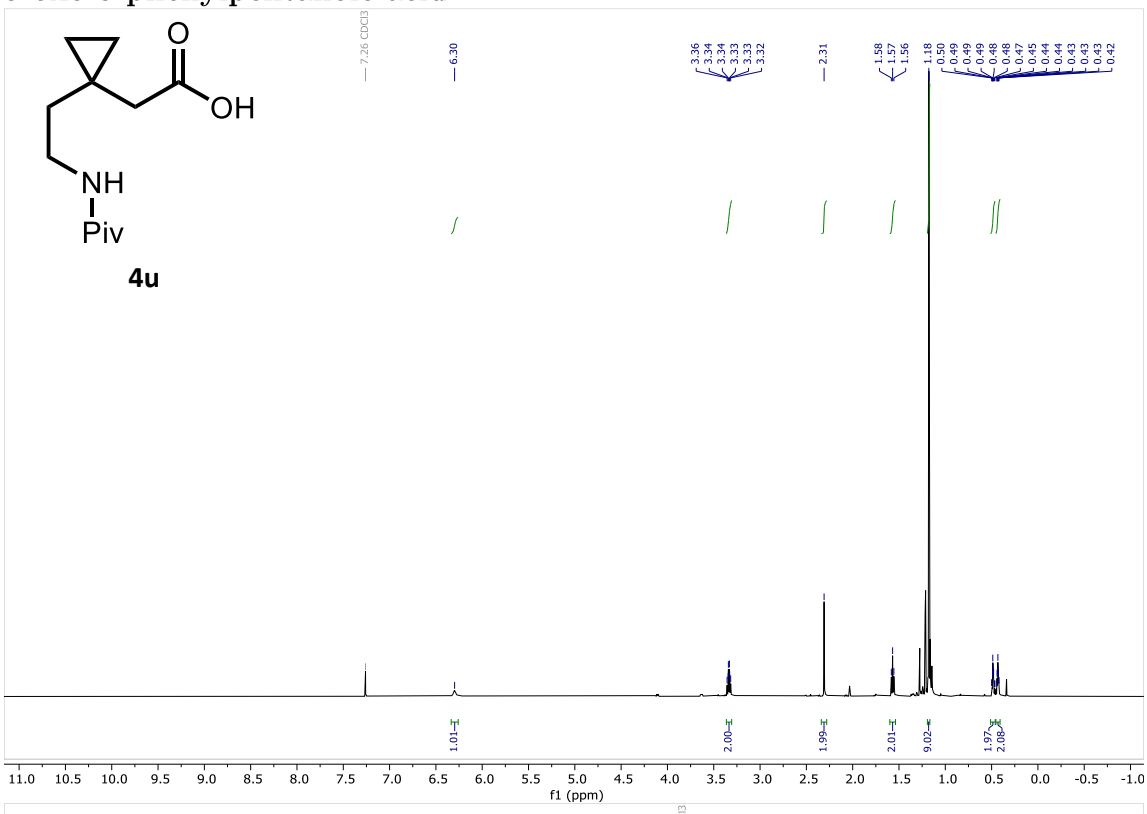

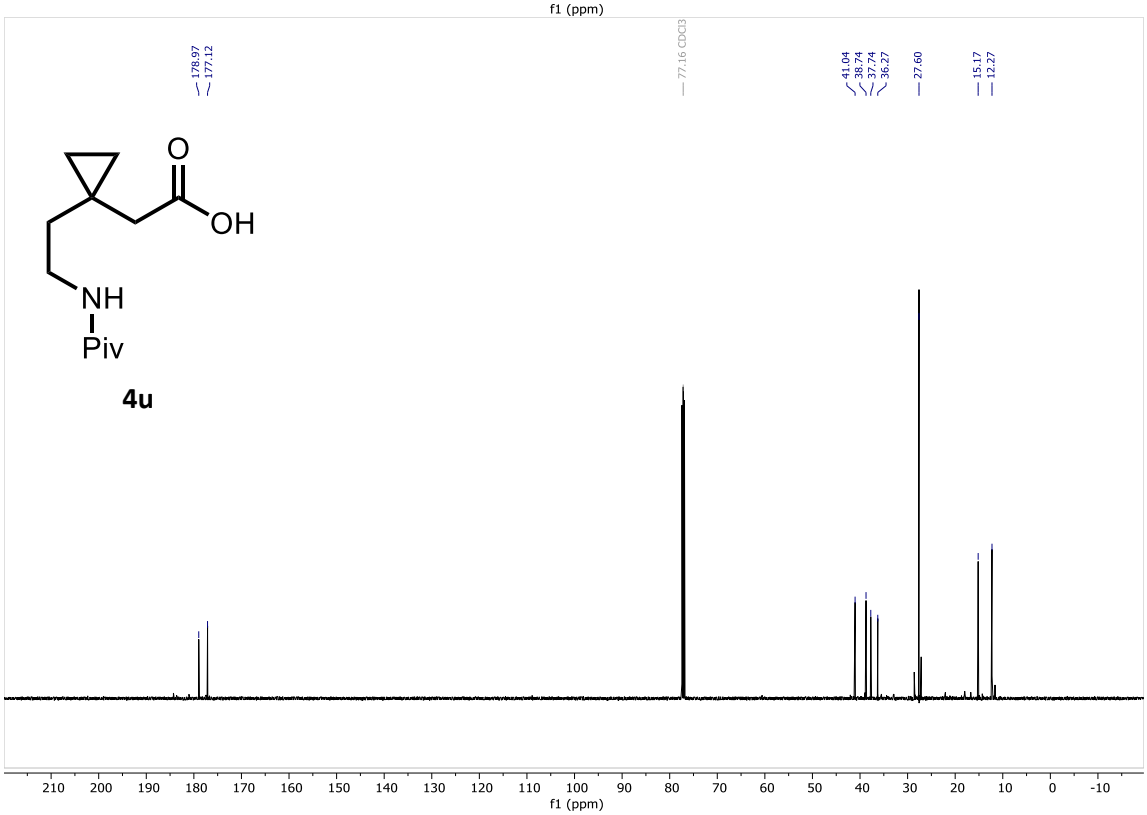

(4*S*)-5-(((3*R*)-3-(*tert*-butoxy)-1-methoxy-1-oxobutan-2-yl)amino)-5-oxo-4-pivalamidopent-anoic acid

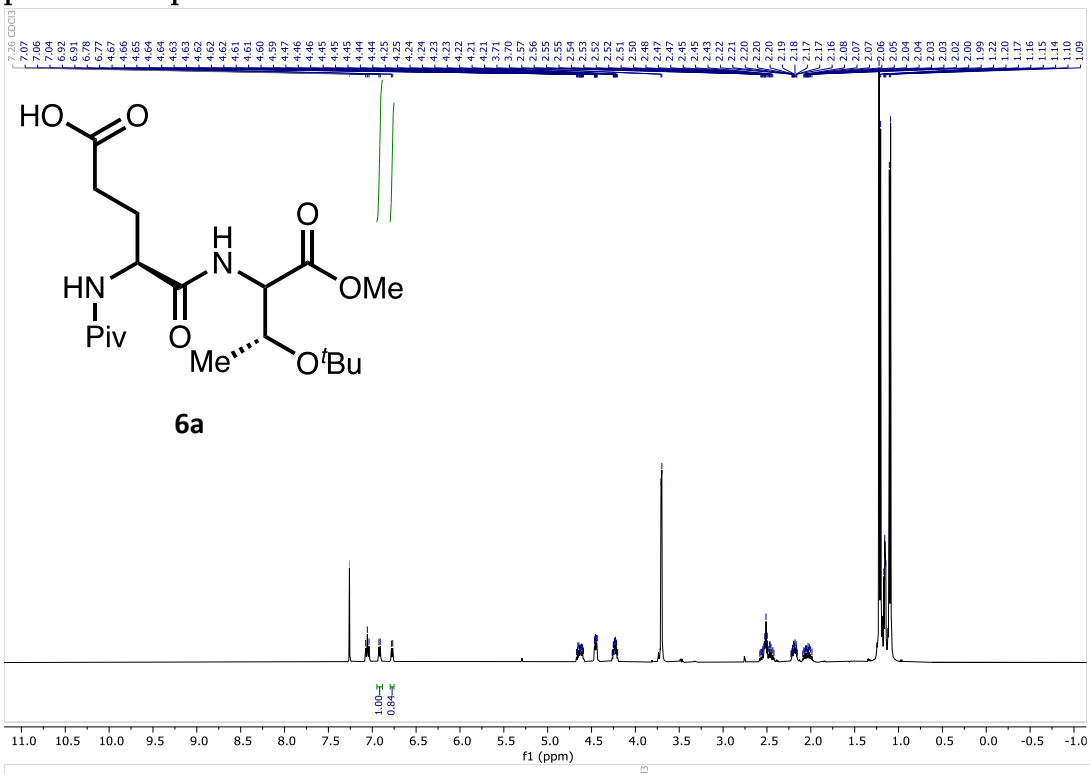

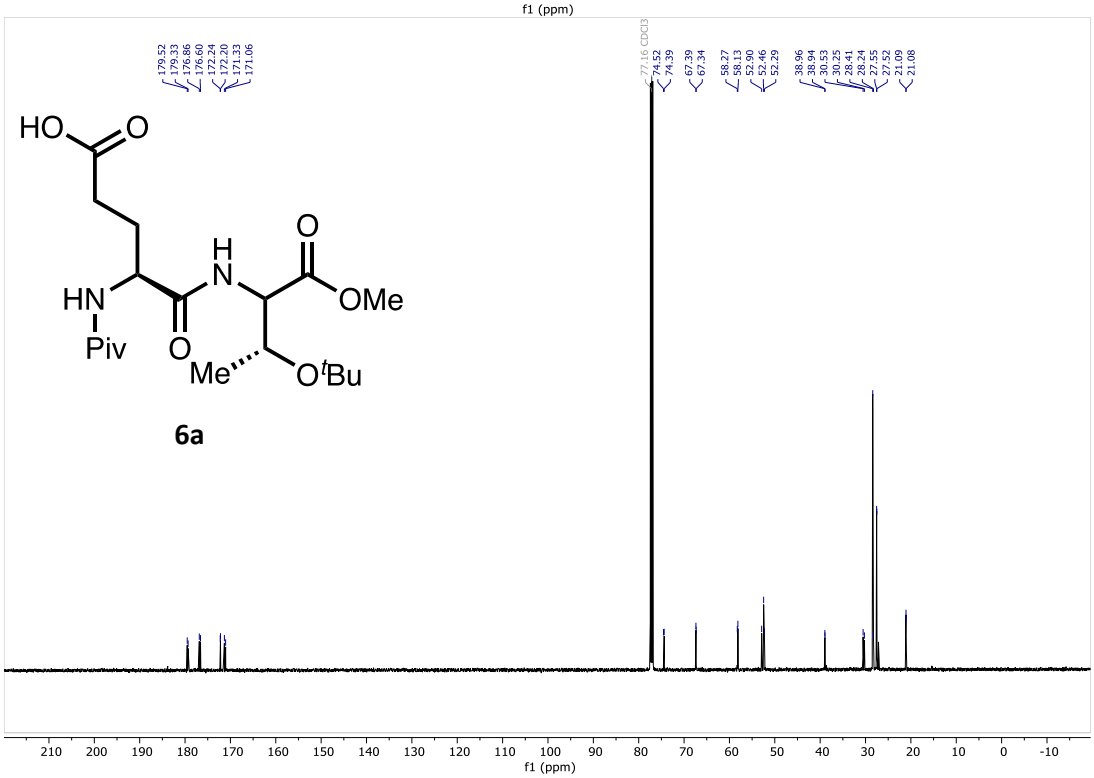

(*S*)-5-(((*S*)-1-methoxy-3-methyl-1-oxobutan-2-yl)amino)-5-oxo-4-pivalamidopentanoic acid

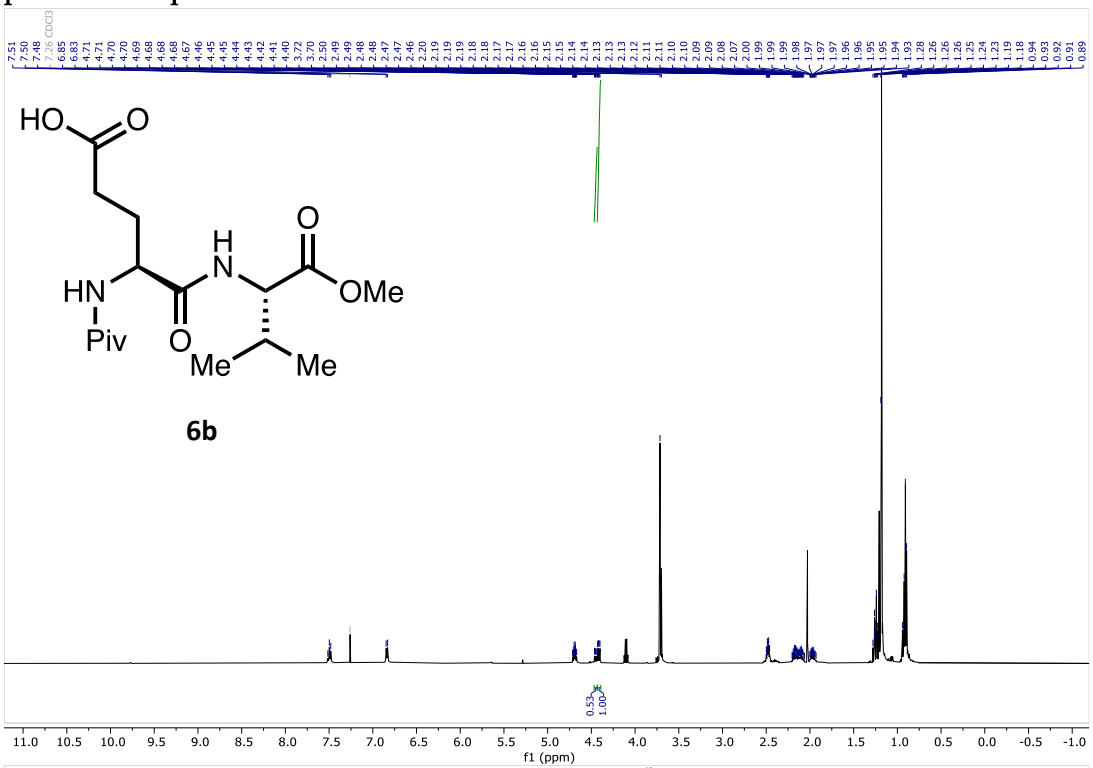

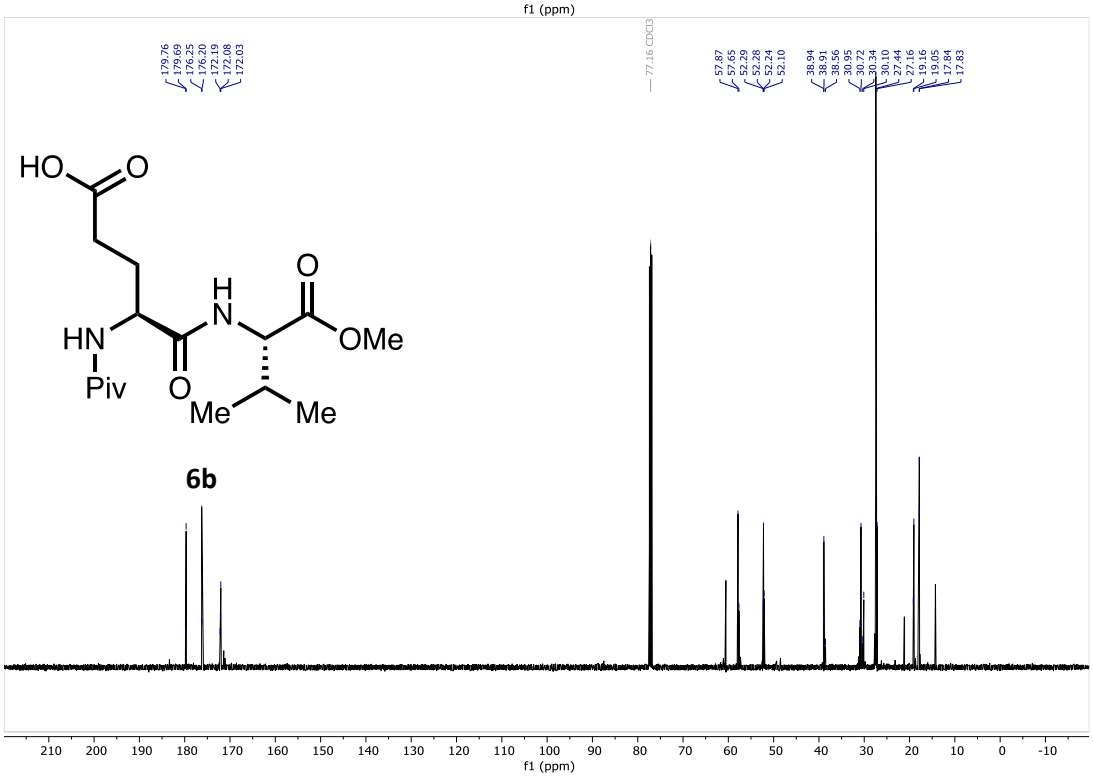

1,3-dioxoisoindolin-2-yl (*S*)-5-(((*S*)-1-methoxy-3-methyl-1-oxobutan-2-yl)amino)-5-oxo-4-pivalamidopentanoate

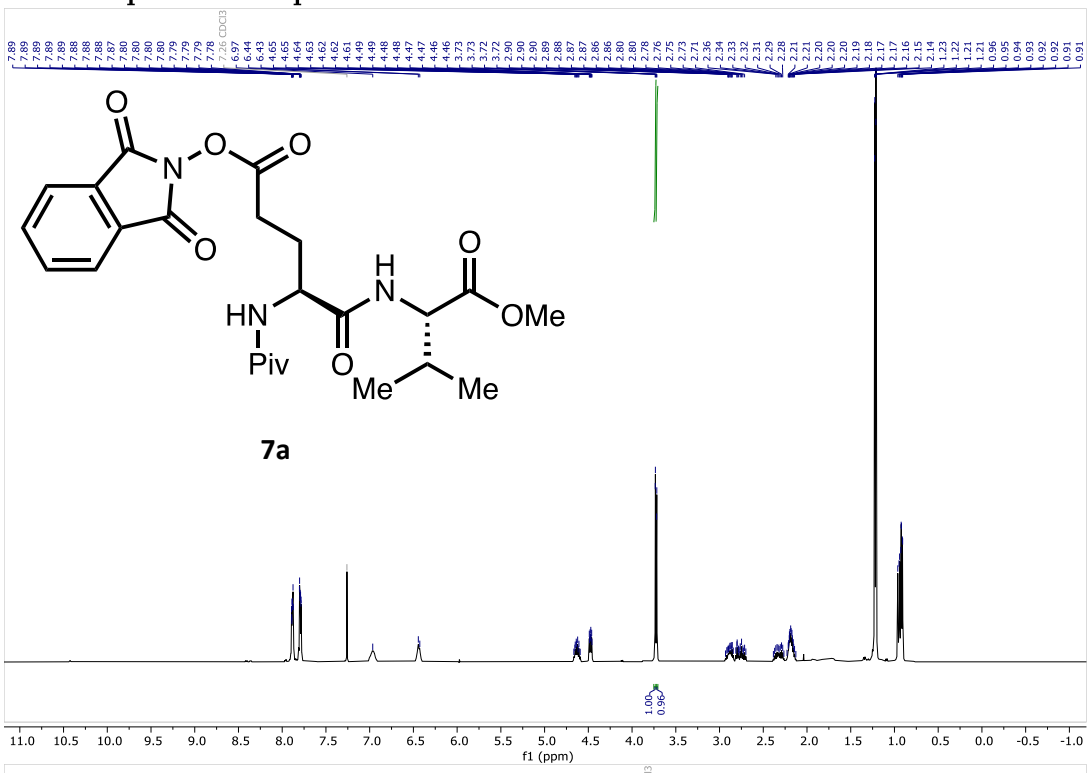

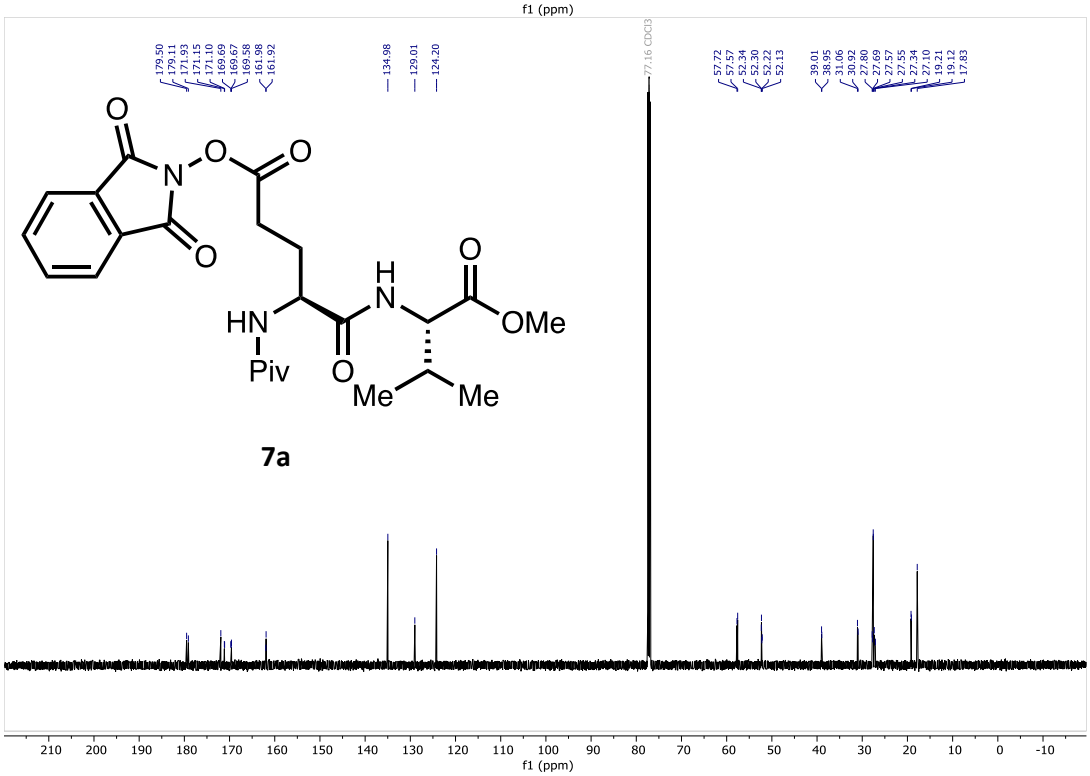

Dimethyl 2,2'-(((*S*)-2-pivalamidopentanedioyl)bis(azanediyl))(2*S*,2'*S*)-bis(3-methylbutanoate)

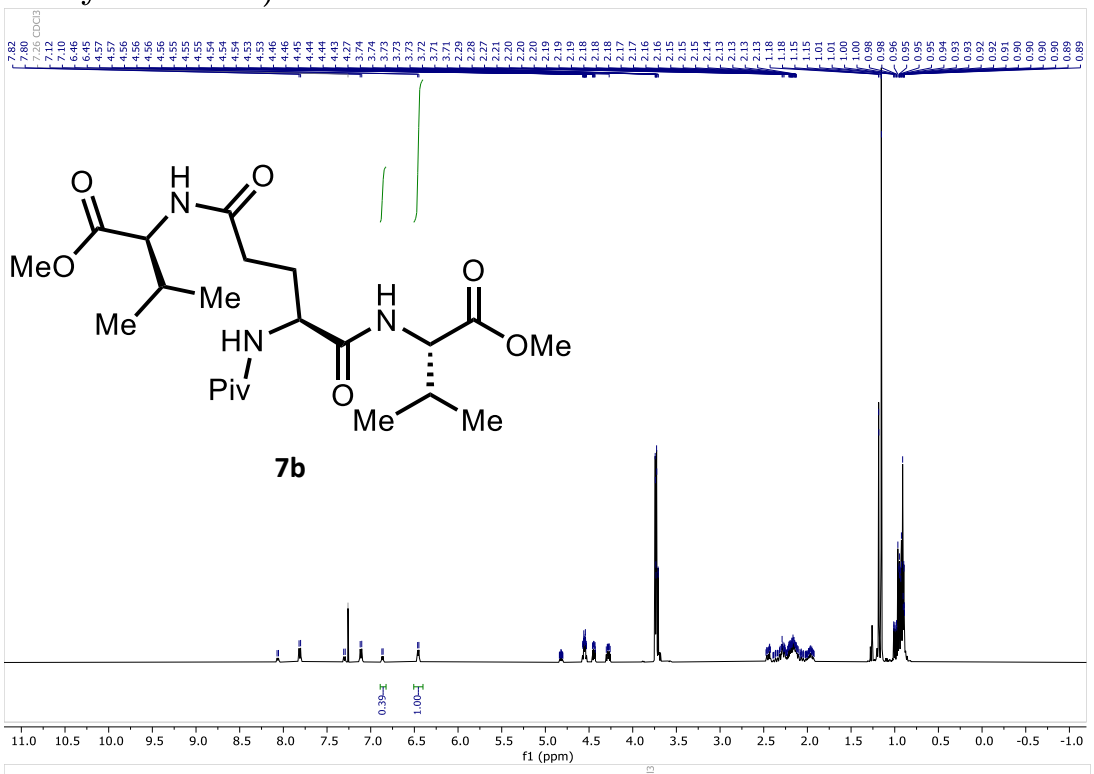

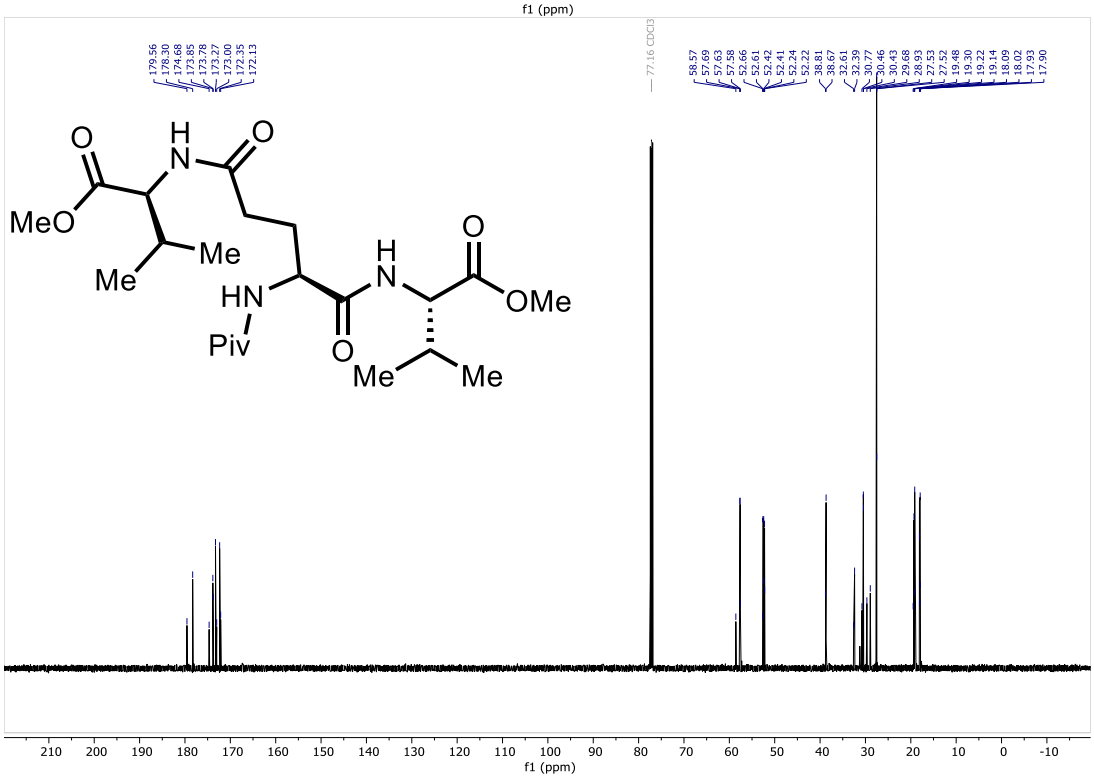

Computational Coordinates and Vibrational Frequencies

Table 1.4.11: Cartesian coordinates (in Å) of all calculated structures for the riboflavin and copper(I) oxidation reactions.

Na_2SO_4
O -0.83724700 -2.60478100 -1.19689300
Na -4.09655100 -4.68065400 -0.44750400
S -2.02264500 -3.30178700 -1.84032300
O -2.02830200 -4.77595300 -1.47741600
O -3.32385800 -2.69881300 -1.34213100
O -1.90034800 -3.12796100 -3.34366900
Na 0.06257000 -1.92300200 -3.21157100

HSO_4__1min
O -1.56928000 -2.19594600 -0.93216000
S -2.09534900 -3.24272600 -2.12780700
O -2.09854800 -4.58211600 -1.49366100
O -3.43360800 -2.69149400 -2.42267400
O -1.10820900 -3.10375100 -3.22448000
H -0.68275500 -2.49111700 -0.66877800

SO_4__minus
O -1.67668000 -2.32464200 -0.91454800
S -2.02818900 -3.28715100 -2.06255000
O -2.20590400 -4.67250300 -1.57908200
O -3.37715400 -2.61451100 -2.37014800
O -1.08387400 -3.15906300 -3.19227200

$NaHSO_4$
O -0.84364300 -2.71477400 -1.16892100
S -1.93361200 -3.45523600 -1.86965300
O -2.07257200 -4.86392000 -1.46080900
O -3.34513700 -2.70345500 -1.44001300
O -1.89945700 -3.20572300 -3.33515400
Na -0.03018500 -1.71982800 -3.16793500
H -3.52334700 -2.91757700 -0.50889600

1a
N -1.48973100 1.18530800 0.57649100
C -0.50213800 1.37469200 -0.50409900
C -0.42329800 2.84673300 -0.93089900
C -1.82708600 3.45952300 -0.95637200
C -2.42978800 3.47251000 0.46687200
C -1.77629300 2.39468800 1.34908000
H 0.47962400 0.99882600 -0.18708000
H 0.21996300 3.41698200 -0.25056400
H -1.80591100 4.47012400 -1.37486400
H -2.27317800 4.44497900 0.94634000
H -2.39994600 2.16309800 2.20372100
H -3.51114000 3.30834800 0.41857500
H -0.82709100 2.76720400 1.75332600
H -2.45830300 2.85608400 -1.61956500
H 0.04794500 2.89425600 -1.91746500
H -0.82178200 0.75634200 -1.34577200
C -1.95376700 -0.08535900 0.76395100
O -1.49696500 -1.00064400 0.06410400
C -3.04754500 -0.40437800 1.81883600
C -4.31900700 0.44757100 1.61257100
H -5.11084200 0.07763400 2.27190100
H -4.18403000 1.50658100 1.83274500
H -4.67571400 0.36217800 0.58118100
C -3.44869800 -1.87991800 1.63016100
H -2.59087300 -2.54288600 1.75684200
H -4.20983300 -2.14429500 2.37101300
H -3.86050800 -2.05305500 0.63275000
C -2.48566500 -0.25634800 3.25057000
H -1.60178100 -0.88904900 3.37993700
H -2.20378000 0.76591500 3.50835300
H -3.24105000 -0.58240400 3.97294300

1.A
N -1.68274700 1.30592400 0.51590600
C -1.29523400 1.41346600 -0.71435500
C -1.10977000 2.69185200 -1.43211000
C -1.16029700 3.92986800 -0.53429800
C -2.22823400 3.73919000 0.54275100
C -1.93726100 2.49881000 1.37731500
H -0.17319800 2.60954300 -1.99667600
H -0.18289100 4.08017800 -0.06483100
H -2.26292800 4.59497400 1.22112300
H -2.77056900 2.26244300 2.03018800
H -3.21835900 3.64381400 0.08392100
H -1.04347800 2.61971500 1.99584200
H -1.37040700 4.81354700 -1.13982300

H -1.89728900 2.70733900 -2.20212800
H -1.10984100 0.48012000 -1.23902600
C -1.75415900 -0.10105200 1.06809200
O -0.84080000 -0.81771100 0.76562500
C -2.98320400 -0.50919500 1.87242300
C -4.27047200 0.09378800 1.27429800
H -5.12491200 -0.30871600 1.82412900
H -4.32177600 1.18115100 1.34739000
H -4.38350000 -0.18500800 0.22307200
C -3.06290000 -2.04783000 1.79226000
H -2.16960500 -2.51333300 2.21223200
H -3.93301000 -2.38325000 2.36166700
H -3.17479800 -2.38379800 0.75819700
C -2.79842300 -0.11179300 3.35964100
H -1.87121700 -0.52984500 3.75979700
H -2.79116400 0.96567800 3.52835200
H -3.63539000 -0.52958000 3.92533500

1a_OH
N -1.43566600 1.18260000 0.61171800
C -0.44309000 1.38299000 -0.43627200
C -0.48712000 2.82941900 -0.95774700
C -1.92201500 3.36421200 -0.93393200
C -2.42296000 3.44867200 0.52266500
C -1.71673300 2.39061800 1.39206200
H 0.15920500 3.45176200 -0.32765800
H -1.98172600 4.34085800 -1.42234700
H -2.21300000 4.43672700 0.94640300
H -2.29544400 2.15354700 2.27627000
H -3.50733000 3.30575800 0.55727500
H -0.75467800 2.77528600 1.74668700
H -2.56229900 2.68410700 -1.50774400
H -0.06703600 2.85112400 -1.96808900
H -0.69153400 0.68408700 -1.23933200
C -1.97553200 -0.07657400 0.73729900
O -1.58566300 -0.98149900 -0.00709100
O 0.83368300 1.05735700 0.11607400
H 1.49422300 1.22650200 -0.57068700
C -3.06505400 -0.38230100 1.79918500
C -4.30131800 0.53151000 1.65089900
H -5.10474300 0.15118500 2.28957200
H -4.12402000 1.56714300 1.93946100
H -4.66475000 0.52594600 0.61836900
C -2.46706900 -0.30933000 3.22202600
H -2.12506300 0.68781900 3.50378500
H -3.22524300 -0.61661800 3.94942800
H -1.61669600 -0.99236000 3.31344100
C -3.53521900 -1.83106200 1.56700800
H -2.70531800 -2.53529500 1.64832000
H -4.28943400 -2.08867100 2.31698600
H -3.97852200 -1.94869300 0.57502400

$Na_2S_2O_8$
S 1.62960000 2.08771400 -5.89558900
O 0.70032800 3.10867100 -5.35698100
O 0.99701800 1.19925700 -6.89813400
O 2.98644100 2.54504200 -6.21053600
S 0.74807400 -0.96887500 -3.54144200
O 0.92503700 -1.68173200 -4.82869500
O -0.60581200 -1.02156300 -2.97171900
O 1.87546000 -1.11171200 -2.61362200
Na 0.99865200 -1.05055800 -6.98683900
Na -0.53182400 2.63685500 -3.44496800
O 0.71857600 0.70894400 -3.95828500
O 1.99911100 1.09863500 -4.54952800

$K_2S_2O_8$
S 1.64186700 2.07693400 -5.78680500
O 1.48475300 3.36651800 -5.09729700
O 0.35345100 1.45584300 -6.19332100
O 2.72063300 1.96051700 -6.78334300
S 0.78866500 -0.81056400 -3.45713200
O 0.75815500 -1.33886600 -4.83427100
O -0.53809100 -0.54550700 -2.85607300
O 1.78575100 -1.43231100 -2.57526600
K 1.30854200 -0.87143400 -7.37190400
K -1.42993200 1.83622800 -4.10374900
O 1.27506600 0.85089300 -3.58518500
O 2.29180000 1.00242800 -4.61199200

(2.A.m), SINGLET
C -10.49493900 -0.18817900 -0.06030800
C -9.84257500 -0.75029700 1.01751500
C -8.71001000 -0.14349700 1.60353200
C -8.21474500 1.07891900 1.06822100
C -8.88376900 1.65262100 -0.02571700
C -10.00036800 1.04334200 -0.58563600
N -8.13298200 -0.74466000 2.68157400
N -7.10245100 1.65099800 1.66874700
C -6.52211900 1.08036100 2.77675400
C -7.10175100 -0.16840600 3.23345200
C -6.47482900 -0.81446600 4.42076800

O -6.85001400 -1.87087300 4.91094400
N -5.41454000 -0.09456600 4.92288900
C -4.90299300 1.12765600 4.43558000
N -5.50368200 1.69430600 3.33913400
H -10.18548400 -1.68105100 1.45700100
H -8.56250700 2.60045900 -0.43258600
H -4.94211900 -0.47904800 5.73317900
O -3.94593500 1.63285500 5.01240800
C -10.69498500 1.69711400 -1.74820300
H -10.20465300 2.63001600 -2.03172500
H -10.70662400 1.03446000 -2.62065700
H -11.74065900 1.91707500 -1.50596400
C -11.70438000 -0.84945500 -0.66486700
H -12.58184600 -0.19518500 -0.61576100
H -11.54253100 -1.08470600 -1.72265300
H -11.94276300 -1.77795900 -0.14232100
C -6.57600600 2.95405400 1.22762400
H -5.49959700 2.94150700 1.39285400
H -6.76442200 3.06663200 0.16309300
C -7.17870200 4.10004000 2.03320700
H -6.95878900 3.97674500 3.09305000
H -6.77302800 5.04642100 1.67268000
O -8.60525700 4.17908500 1.83667900
C -9.39331700 3.53926400 2.73580100
O -8.96363400 2.92890800 3.69461200
C -10.84315300 3.65912900 2.35484100
H -11.04351900 2.96495200 1.53212100
H -11.46948200 3.39361100 3.20570800
H -11.07344500 4.66720600 2.00537900

(2.A.m), TRIPLET

C -10.50250400 -0.13931500 -0.05930700
C -9.86745100 -0.71114800 1.04071600
C -8.72554000 -0.15434700 1.63562800
C -8.20453900 1.06928500 1.05326100
C -8.85741900 1.64427700 -0.05827500
C -9.98540300 1.07257900 -0.62122500
N -8.18764100 -0.77193700 2.72077700
N -7.08997600 1.63959600 1.63231600
C -6.52812100 1.03479200 2.77780400
C -7.10995000 -0.15880800 3.26847000
C -6.49052800 -0.75868400 4.45064700
O -6.86617900 -1.79154100 5.00265700
N -5.39646600 -0.04619200 4.94233200
C -4.87414700 1.12733400 4.42512200
N -5.47907900 1.65374500 3.28991400
H -10.25503300 -1.62294500 1.48163300
H -8.49470000 2.57161300 -0.47757000
H -4.94458200 -0.42296800 5.76738400
O -3.90915700 1.68171000 4.94813000
C -10.65982100 1.71919400 -1.79890200
H -10.14196600 2.63412900 -2.09290200
H -10.68196500 1.04671200 -2.66394600
H -11.70056700 1.97508300 -1.57015300
C -11.72197300 -0.78274500 -0.64554100
H -12.57798200 -0.09855200 -0.61138200
H -11.56433700 -1.02920300 -1.70205800
H -11.98636600 -1.69636600 -0.11118100
C -6.57509000 2.94964300 1.21621900
H -5.50232300 2.95895000 1.39811700
H -6.74244500 3.06908600 0.14885300
C -7.20805100 4.08920600 2.01479500
H -6.97244700 3.98526600 3.07389700
H -6.83379000 5.04199700 1.63729600
O -8.63635700 4.12336400 1.83605900
C -9.39122800 3.46673800 2.75286700
O -8.92625100 2.88153800 3.71069700
C -10.84893500 3.53644200 2.39193900
H -11.03208100 2.86068300 1.55025000
H -11.45299400 3.22255600 3.24226400
H -11.12322300 4.54462100 2.07535100

(2.A.m)_1plus

C -10.48532200 -0.16990300 -0.07289600
C -9.85009100 -0.72774600 1.03532200
C -8.72488500 -0.13787200 1.60776600
C -8.19537600 1.08423400 1.02907600
C -8.85292900 1.65134100 -0.09292800
C -9.96696500 1.05543400 -0.64036100
N -8.17695300 -0.71864700 2.71281200
N -7.10708800 1.64765900 1.61005700
C -6.53764800 1.07079800 2.74506600
C -7.14462300 -0.14433100 3.25198700
C -6.53323900 -0.75787400 4.47382200
O -6.94809800 -1.77518100 4.99420400
N -5.44974900 -0.04899300 4.95451700
C -4.91133900 1.12061800 4.42228200
N -5.50504200 1.66277900 3.27079900
H -10.22411500 -1.63779300 1.48910500
H -8.49936700 2.57572600 -0.52337700
H -4.99376900 -0.41335600 5.78500100
O -3.95109900 1.66308800 4.93689800

C -10.64878400 1.67668900 -1.82066900
H -10.14937400 2.59602700 -2.12727000
H -10.65827900 0.98448700 -2.66936200
H -11.69328200 1.90772300 -1.58621200
C -11.69091100 -0.82175700 -0.66126400
H -12.55046400 -0.14177500 -0.62604800
H -11.52593900 -1.05669600 -1.71924700
H -11.94675300 -1.73936200 -0.13176900
C -6.57734000 2.96084900 1.18111900
H -5.50339200 2.95121500 1.35371900
H -6.75961600 3.07771600 0.11798100
C -7.20431500 4.08915300 2.00301500
H -6.94495600 3.98268500 3.05630300
H -6.83246300 5.03887100 1.61762700
O -8.63304900 4.12838900 1.85176500
C -9.36914500 3.43614100 2.76156600
O -8.87052400 2.73753700 3.62271700
C -10.83886600 3.62195600 2.52018900
H -11.11666100 3.10588500 1.59581400
H -11.40111900 3.19946700 3.35146300
H -11.07567400 4.68020500 2.39236500

(2.A.m)_1minus
C -10.50883600 -0.17275400 -0.06763700
C -9.84799600 -0.75458200 1.00631100
C -8.71103500 -0.17647100 1.61912400
C -8.23062400 1.05928500 1.08748100
C -8.89915100 1.64485500 0.00830300
C -10.02688000 1.05559800 -0.57638700
N -8.14185600 -0.80945500 2.68138500
N -7.09605100 1.63434600 1.68861100
C -6.51917400 1.03930100 2.80545200
C -7.07120200 -0.18953300 3.25357300
C -6.44583800 -0.80662100 4.40973100
O -6.78235300 -1.87286600 4.94808200
N -5.36933800 -0.07992700 4.91652100
C -4.86959800 1.13718300 4.43616600
N -5.48580900 1.68553400 3.35338000
H -10.20006900 -1.69393100 1.42353600
H -8.57631300 2.60268200 -0.37720100
H -4.90408000 -0.47200500 5.72536200
O -3.90058300 1.65521800 5.01324700
C -10.71775900 1.73961900 -1.72856800
H -10.21979900 2.67782200 -1.98602600
H -10.73090300 1.10893200 -2.62607000
H -11.76460800 1.96875400 -1.49419300
C -11.72195200 -0.83403600 -0.67253700
H -12.60553400 -0.18717500 -0.61322900
H -11.57109700 -1.05949500 -1.73511100
H -11.95553100 -1.77029600 -0.15960400
C -6.57699900 2.92902600 1.25339000
H -5.50113200 2.93044800 1.42705600
H -6.75372000 3.04369700 0.18457800
C -7.17626400 4.09194400 2.03776800
H -6.97287800 3.97138900 3.10119600
H -6.76379900 5.03765700 1.67980600
O -8.60230200 4.17676100 1.82304300
C -9.40901000 3.58806000 2.73547000
O -9.01560900 3.08789200 3.77092800
C -10.84160200 3.61388400 2.27435400
H -10.97400500 2.81824600 1.53350900
H -11.50527100 3.43284300 3.11950100
H -11.08204300 4.56355900 1.79265000

(2.A.t), with two acetates
C -10.88276600 -0.48173900 -0.00614700
C -9.88349300 -0.96896800 0.81092200
C -8.68674500 -0.25326900 1.03385800
C -8.49372500 1.00365600 0.39458000
C -9.51389300 1.50051600 -0.43288900
C -10.68751500 0.78410000 -0.63583600
N -7.75522200 -0.78593500 1.87394500
N -7.30787700 1.68303000 0.63719000
C -6.36737700 1.18205900 1.50650300
C -6.66281700 -0.10989500 2.09585600
C -5.64773700 -0.68035800 3.02546600
O -5.75727100 -1.76132300 3.58770100
N -4.55666000 0.14166500 3.19460300
C -4.33322300 1.40065600 2.59677200
N -5.28836400 1.89562400 1.74325900
H -9.98878900 -1.92249800 1.31754600
H -9.42013400 2.46924200 -0.90167200
H -3.82703100 -0.18670500 3.81703900
O -3.29803600 2.00050400 2.86515500
C -11.76063400 1.35727200 -1.51966800
H -11.46829100 2.32857800 -1.92239500
H -11.97629100 0.68664800 -2.35888200
H -12.69832600 1.48133100 -0.96667000
C -12.15331900 -1.25873700 -0.22396700
H -13.02958100 -0.68785900 0.10270900
H -12.30196200 -1.48939200 -1.28467100
H -12.13457400 -2.19956500 0.32958700

C -7.05629800 3.01695000 0.07386300
H -5.98570600 3.10461300 -0.09827300
H -7.57481000 3.10702100 -0.87800800
C -7.48298900 4.11654700 1.04760600
H -6.95272800 3.98848100 1.99177700
O -8.90353400 4.04483100 1.28517900
C -9.32416300 3.36980700 2.38816700
O -8.56998200 2.83182300 3.17217700
C -10.82503600 3.35481900 2.45979000
H -11.20090800 2.63976400 1.72079600
H -11.14142200 3.04200300 3.45402300
H -11.23567700 4.33596700 2.21427600
C -7.23604300 5.50423700 0.47647600
H -7.58377700 6.26832200 1.17598500
H -7.75427700 5.64277700 -0.47665700
O -5.81581600 5.61152300 0.28632600
C -5.38108900 6.75565800 -0.29192700
O -6.13070900 7.65087300 -0.62367500
C -3.88508000 6.74278200 -0.45229200
H -3.55683800 7.67647500 -0.90673800
H -3.40725600 6.61337000 0.52274900
H -3.58661500 5.89780900 -1.07921300

(2.A.th), with three acetates

C -10.78353500 -0.43055800 -0.54791100
C -9.94942500 -0.82210900 0.47874800
C -8.82364700 -0.05825600 0.85789700
C -8.52954000 1.14780700 0.16126900
C -9.38035600 1.54547300 -0.88280200
C -10.48679900 0.78325200 -1.23795100
N -8.06110900 -0.49471100 1.89982100
N -7.42143900 1.88030900 0.56653600
C -6.65241200 1.47422700 1.63299000
C -7.03769000 0.22638000 2.26349700
C -6.21097700 -0.23590800 3.41376900
O -6.41015900 -1.27065000 4.03503700
N -5.18545500 0.63073600 3.71748400
C -4.86862000 1.84268200 3.06754700
N -5.64783300 2.23560900 2.00700600
H -10.13694200 -1.73328700 1.03691100
H -9.21018700 2.47291000 -1.41003300
H -4.58540000 0.37637500 4.49391500
O -3.91383700 2.49448200 3.47539000
C -11.38068900 1.25113000 -2.35286800
H -11.02756300 2.19193200 -2.77854700
H -11.42919300 0.50601900 -3.15467300
H -12.40635900 1.39736600 -1.99642200
C -11.98340600 -1.25538000 -0.92909000
H -12.91036700 -0.68072100 -0.82423900
H -11.92751000 -1.58001000 -1.97404600
H -12.06103100 -2.14418500 -0.29987300
C -7.09069300 3.18121800 -0.03490700
H -6.00906000 3.28191500 -0.02841900
H -7.44012900 3.20439800 -1.06361400
C -7.70542700 4.30527200 0.80308400
H -7.31031300 4.24447200 1.81724200
O -9.13830200 4.12411200 0.84190400
C -9.68483300 3.55440900 1.94383400
O -9.03646100 3.20225700 2.90955000
C -11.17236200 3.42048400 1.78479000
H -11.38427200 2.73274800 0.96073100
H -11.60719900 3.03787800 2.70679900
H -11.61073200 4.38858500 1.53012300
C -7.48897900 5.69500500 0.19250400
H -8.26469200 5.87725000 -0.55365000
O -6.20279500 5.69443200 -0.45641500
C -6.06414700 6.49118500 -1.55127000
O -6.94928100 7.21061400 -1.96211200
C -4.69205300 6.33744600 -2.14483700
H -4.58199400 7.01043000 -2.99381600
H -3.93314600 6.55749300 -1.38934100
H -4.54515400 5.30259200 -2.46717200
C -7.45967500 6.81216300 1.23832700
H -6.55225700 6.72565300 1.83696100
H -7.49257600 7.78386500 0.74374100
O -8.61412300 6.73258700 2.09214100
C -8.40983500 6.37097500 3.38551900
O -7.31780300 6.11292600 3.84946200
C -9.70515100 6.31380600 4.14909400
H -10.53775800 6.70706000 3.56678700
H -9.90055600 5.26951300 4.40775000
H -9.59682900 6.87444700 5.08019700

(2.A.f), with four acetates

C -10.66493300 -0.19968400 -0.70290900
C -9.92297400 -0.66203900 0.36436200
C -8.80622100 0.04676600 0.85939400
C -8.42338900 1.26927500 0.23905600
C -9.18135500 1.74040600 -0.84488000
C -10.28131000 1.03219100 -1.31371600
N -8.13913900 -0.45625600 1.93625200
N -7.32412200 1.94372900 0.75359300

C -6.65267400 1.47139200 1.85784700
C -7.12515900 0.21503200 2.40646400
C -6.40489800 -0.31805800 3.59696700
O -6.68388900 -1.36760100 4.15987200
N -5.37914800 0.50104200 4.01229200
C -4.97463200 1.72459500 3.43729600
N -5.65569700 2.18257300 2.33592700
H -10.17994700 -1.58877100 0.86642600
H -8.94383000 2.68345400 -1.31534800
H -4.84992500 0.19765200 4.82192500
O -4.03558200 2.32867800 3.94339200
C -11.07488800 1.57810600 -2.46840700
H -10.66200900 2.52385000 -2.82378700
H -11.08641700 0.87064600 -3.30494800
H -12.11927600 1.74383300 -2.18167100
C -11.85667500 -0.96750200 -1.20855200
H -12.77186500 -0.36844200 -1.14515200
H -11.73255000 -1.24746700 -2.26050400
H -12.00692700 -1.88037000 -0.62885900
C -6.90391300 3.25030000 0.22884100
H -5.82271600 3.30701300 0.32359400
H -7.17387700 3.32303200 -0.82172700
C -7.53764500 4.36966900 1.05939800
H -7.21090400 4.26468400 2.09321500
O -8.97351600 4.24589700 0.99080800
C -9.61482900 3.66137700 2.03132000
O -9.04278300 3.23203800 3.01439100
C -11.09485300 3.61843300 1.78328600
H -11.29446200 3.02442000 0.88675200
H -11.59837500 3.17697800 2.64181000
H -11.46986900 4.62913800 1.60232400
C -7.22661700 5.75913000 0.49557000
H -7.87273000 5.93082800 -0.36742800
O -5.85441600 5.78536300 0.05981800
C -5.60934000 5.99229800 -1.26163600
O -6.48027600 6.04821700 -2.10477400
C -4.13600600 6.15389200 -1.50104600
H -3.93338700 6.14775400 -2.57097700
H -3.81174500 7.10665400 -1.07098900
H -3.57820700 5.35869500 -1.00108300
C -7.35500900 6.89609400 1.52985700
H -6.39948200 6.97981100 2.04968200
O -8.38718900 6.62147900 2.49516700
C -7.99359600 6.25953300 3.74940900
O -6.83520400 6.06654700 4.05312300
C -9.17585600 6.10320300 4.66365900
H -10.00828400 6.73306400 4.34902400
H -9.49473700 5.05719000 4.63021700
H -8.87495800 6.34126700 5.68433200
C -7.76408200 8.21948400 0.89516700
H -8.75583900 8.14000900 0.44545500
H -7.77947600 9.01305900 1.64699800
O -6.79171800 8.53394700 -0.11564300
C -7.22060800 9.28419900 -1.16113800
O -8.34694000 9.72861500 -1.24135500
C -6.13292200 9.44947100 -2.18658400
H -6.04752100 8.51680500 -2.75286000
H -6.38891700 10.26231900 -2.86518500
H -5.17139700 9.64117500 -1.70597200

(2.A.m)-[$K_2S_2O_4$], SINGLET

S -0.08250500 -0.95435300 -4.71253200
O -0.60439500 -1.62436400 -5.91212700
O 0.37494200 -1.86710200 -3.64568600
O 0.76060200 0.23392500 -4.93787600
S -2.96104000 -0.61743800 -2.06519700
O -1.76556600 -0.73168600 -1.18729400
O -3.98117700 -1.65218100 -1.85916600
O -3.44209100 0.76787200 -2.23199200
K -0.27682600 -3.01647300 -1.34865600
K -2.42355500 2.47062100 -4.11380600
O -2.44044900 -1.09078500 -3.62312900
O -1.43811400 -0.11473100 -4.04814700
C 5.38628900 0.58780300 -3.19281400
N 4.26202200 1.50620500 -3.44311200
H 6.06648900 0.62647000 -4.03960400
C 6.09265200 0.91951400 -1.88243800
C 4.42844000 2.67032200 -4.18096600
C 3.07157000 1.22994000 -2.81988700
H 5.39766700 0.84423200 -1.04682900
H 6.92881000 0.23357300 -1.73947700
O 6.66621100 2.24215400 -1.92229300
C 3.31653200 3.55084700 -4.30223900
C 5.64055100 3.03050700 -4.79293900
C 2.00024800 2.18306700 -3.02443000
N 2.98135000 0.14354200 -2.08027600
C 5.91966900 3.25912000 -1.42499000
C 3.45647800 4.74822600 -5.03735700
N 2.11537400 3.28052500 -3.71725000
C 5.76019500 4.21508800 -5.50939300
H 6.51690500 2.40751800 -4.68863900
C 0.69070200 1.86133000 -2.40193300

C 1.78406000 -0.16066400 -1.49483600
O 4.81730700 3.10948600 -0.93594800
C 6.62357200 4.57585600 -1.60392600
C 4.64656300 5.09807600 -5.64137700
H 2.58468700 5.39079300 -5.10375900
C 7.07919300 4.56891500 -6.13923200
O -0.31252800 2.56351200 -2.52541900
N 0.69213900 0.70602200 -1.67296800
O 1.62149500 -1.17009400 -0.80279600
H 6.51523000 4.88680800 -2.64823800
H 6.16678600 5.32648400 -0.95992200
H 7.69002000 4.48178000 -1.39162100
C 4.77405900 6.38333900 -6.41427300
H 7.82973500 3.79952500 -5.94990500
H 6.97593700 4.69041600 -7.22321100
H 7.45612000 5.52114400 -5.74972200
H -0.21648700 0.35945400 -1.34909700
H 5.54820900 7.02975200 -5.98614800
H 5.05759100 6.19542000 -7.45575000
H 3.83154300 6.93436700 -6.41229500
H 4.97433100 -0.41779100 -3.12185800

(2.B*.m)-[$K_2S_2O_4$], TRIPLET, T_1'
S -0.27200200 -1.02571700 -4.75667500
O -0.87859100 -1.75342900 -5.88082700
O 0.28618500 -1.88861200 -3.69492200
O 0.52695900 0.16492600 -5.09436200
S -2.97544500 -0.61432700 -1.92989000
O -1.73206600 -0.72647700 -1.11940300
O -3.99783300 -1.62411500 -1.63257400
O -3.44110400 0.77392900 -2.11116400
K -0.32986500 -3.05919000 -1.39646800
K -2.43164300 2.44439100 -4.04321700
O -2.55020800 -1.14494600 -3.49791100
O -1.58334100 -0.17879100 -4.01789000
C 5.43331300 0.60940700 -3.19118500
N 4.31099700 1.50360600 -3.49950300
H 6.13856300 0.63263900 -4.01787300
C 6.10480500 0.97917400 -1.86841000
C 4.47307500 2.67110600 -4.21433400
C 3.06355500 1.24197300 -2.89177100
H 5.39761400 0.88076000 -1.04484900
H 6.96374000 0.32593600 -1.70777700
O 6.62553500 2.32101100 -1.90362400
C 3.33626900 3.56796700 -4.32638800
C 5.70255300 3.02769700 -4.81059100
C 2.01529800 2.17722900 -3.06370400
N 2.98455100 0.11574800 -2.20811200
C 5.82587200 3.30860300 -1.42725800
C 3.52783700 4.75798600 -5.04111700
N 2.11838500 3.32791100 -3.76849200
C 5.86174700 4.21176000 -5.50880000
H 6.56104300 2.38016500 -4.70615800
C 0.73594000 1.83962500 -2.45054200
C 1.78216200 -0.21505700 -1.60140600
O 4.72053100 3.11209800 -0.96254300
C 6.47992800 4.65167900 -1.59477100
C 4.74463900 5.09994900 -5.62999300
H 2.67849800 5.42801100 -5.11779200
C 7.18875600 4.56155700 -6.12232300
O -0.28225900 2.53939300 -2.52745600
N 0.71788000 0.64932200 -1.74408200
O 1.67366500 -1.25970600 -0.94862400
H 6.43915500 4.92953000 -2.65296300
H 5.94493400 5.39640900 -1.00690200
H 7.53077600 4.61123000 -1.30149800
C 4.88373300 6.39051800 -6.37728100
H 7.92507500 3.77768300 -5.93532700
H 7.10297600 4.69740600 -7.20631300
H 7.57983800 5.50071800 -5.71487800
H -0.19476600 0.32001700 -1.41201400
H 5.66730700 7.01544600 -5.93286600
H 5.18402800 6.20980800 -7.41609100
H 3.94926000 6.95330300 -6.37849900
H 5.03969000 -0.40136800 -3.10536200

(2.A.m)–(1a)__1plus,
C -10.53619500 -1.38696200 2.30897800
C -9.24832400 -1.06709300 2.70508200
C -8.42437500 -0.23383800 1.93381000
C -8.93684500 0.33189500 0.71065200
C -10.26264900 0.03375600 0.33136000
C -11.05094500 -0.81108400 1.09109900
N -7.16190300 0.02195800 2.37813500
N -8.11044900 1.13849300 -0.02528700
C -6.80754600 1.38430800 0.39513000
C -6.38783200 0.75039600 1.63419500
C -4.97598200 0.97277200 2.06905000
O -4.48968800 0.46841200 3.06680800
N -4.27277600 1.79848600 1.22164200
C -4.74768300 2.40930100 0.05434300
N -6.06556800 2.16746000 -0.32972900

H -8.83387700 -1.46528700 3.62331200
H -10.69095000 0.47038400 -0.55821200
H -3.30463500 1.98604200 1.46022000
O -4.01398700 3.12775900 -0.60246100
C -12.44578600 -1.13109600 0.64620100
H -12.69413300 -0.61641000 -0.28239800
H -12.56177100 -2.20897900 0.48913400
H -13.17295800 -0.84202100 1.41238900
C -11.38743100 -2.29965000 3.13605300
H -12.29340400 -1.78453800 3.47487500
H -11.71657000 -3.16473800 2.55047700
H -10.84369000 -2.65809700 4.01065700
C -8.60565300 1.92781700 -1.17383400
H -7.78151400 2.03424100 -1.87638400
H -9.40922700 1.38177500 -1.65790300
C -9.05701900 3.31451500 -0.71899100
H -8.22461300 3.86370400 -0.27963500
H -9.44852000 3.85387600 -1.58210900
O -10.14073500 3.22958800 0.22395000
C -9.81644600 3.21915200 1.54259600
O -8.67015400 3.22448500 1.94767300
C -11.05102100 3.16151700 2.39609800
H -11.55128900 2.20118500 2.23746200
H -10.77596300 3.26056300 3.44493700
H -11.75045000 3.94937600 2.10736500
O -5.58028400 -1.30457900 -0.00643300
C -6.20850200 -2.29906300 0.37311500
N -7.42810600 -2.53946800 -0.25055800
C -7.65081100 -1.84595900 -1.53517100
C -8.46801300 -3.46802500 0.17190200
C -8.96518900 -2.26249600 -2.18089000
H -7.59363600 -0.76736200 -1.37542500
H -6.80564900 -2.09339900 -2.18791000
C -8.82979700 -4.47645500 -0.93237300
H -8.16807000 -3.97022200 1.08264800
H -9.35683400 -2.87190800 0.42235000
C -9.05034000 -3.78985800 -2.30249100
H -9.81217100 -1.87690200 -1.60378600
H -9.01845200 -1.78952500 -3.16512300
H -9.73007700 -4.99983800 -0.59922000
H -8.03034500 -5.21901900 -1.00092600
H -10.01792900 -4.07332100 -2.72406200
H -8.28454200 -4.12462300 -3.00966600
C -5.60991500 -3.26319600 1.42130100
C -6.33133600 -3.17953600 2.78518400
H -7.37680100 -3.49110700 2.75187500
H -5.81684500 -3.84132200 3.48801900
H -6.28899500 -2.16185900 3.17864600
C -5.59611100 -4.71143300 0.88086400
H -4.99493700 -5.32805700 1.55479500
H -6.58398900 -5.16900600 0.82243300
H -5.13913900 -4.75554300 -0.11230200
C -4.14819900 -2.82571100 1.64466800
H -4.09369700 -1.81589800 2.05322200
H -3.68212800 -3.51368800 2.35565100
H -3.57819800 -2.85258600 0.71280200

(2.A.m)–(1a), singlet

C -10.78948900 -1.29715400 2.36253700
C -9.47990800 -1.06581100 2.73505900
C -8.62058300 -0.25145500 1.96798500
C -9.10841500 0.36170400 0.78238800
C -10.44430700 0.13732900 0.41195800
C -11.27539300 -0.67745000 1.17379100
N -7.33217900 -0.08844300 2.38534500
N -8.23379300 1.15592400 0.05087200
C -6.92583700 1.31677000 0.44122900
C -6.52903500 0.62496800 1.65308200
C -5.10525900 0.74757400 2.06901700
O -4.62351000 0.19436900 3.04971200
N -4.37045400 1.55502600 1.23535900
C -4.81957400 2.20774100 0.06851300
N -6.13967700 2.07643300 -0.28684500
H -9.06362500 -1.51653200 3.62958400
H -10.86163100 0.61359400 -0.46328400
H -3.38743900 1.66825100 1.45472800
O -4.01504400 2.87002600 -0.57790300
C -12.69575100 -0.90207300 0.73428300
H -12.91828300 -0.35815100 -0.18532600
H -12.88594100 -1.96681500 0.55917900
H -13.40182500 -0.57799400 1.50667900
C -11.68242500 -2.18579600 3.18578400
H -12.56775700 -1.64533400 3.53838900
H -12.04274300 -3.03821400 2.59926200
H -11.15012400 -2.57304100 4.05677600
C -8.68967600 1.92187400 -1.12085200
H -7.85013800 1.99088700 -1.81113500
H -9.49641800 1.37892800 -1.60632700
C -9.11493400 3.33083100 -0.72221100
H -8.28119800 3.86636600 -0.26892300
H -9.47090400 3.86622100 -1.60348400
O -10.22593100 3.29128500 0.19623800

C -9.93926600 3.32980100 1.52127400
O -8.81216600 3.42652800 1.96479200
C -11.19196800 3.19285600 2.34192700
H -11.49380300 2.14017800 2.33918600
H -10.99524300 3.50431700 3.36713400
H -12.00793000 3.77562000 1.91079000
O -5.25243200 -1.43846400 -0.19360300
C -5.94270000 -2.37707400 0.23578700
N -7.16534600 -2.59904900 -0.33070300
C -7.47841300 -1.79986400 -1.53361700
C -8.26453500 -3.42282900 0.17728400
C -8.78930100 -2.25434400 -2.17809700
H -7.50731000 -0.73801700 -1.28569600
H -6.65109800 -1.92994000 -2.23907800
C -8.75788600 -4.42574400 -0.87480100
H -7.95789500 -3.93409700 1.08170100
H -9.08313700 -2.75460200 0.46776900
C -8.82680100 -3.78205600 -2.28140100
H -9.64742000 -1.89067100 -1.60140800
H -8.86049700 -1.79110100 -3.16709800
H -9.74509900 -4.78003700 -0.55943000
H -8.09604300 -5.29746900 -0.89229300
H -9.72402200 -4.11227400 -2.81314400
H -7.96836300 -4.10840600 -2.88026400
C -5.36682400 -3.32346500 1.32415800
C -6.05266800 -3.13339400 2.69523300
H -7.11477300 -3.38578700 2.69377700
H -5.56206200 -3.78330300 3.42792500
H -5.95567400 -2.09900200 3.03016500
C -5.43498200 -4.79528900 0.86097400
H -4.88146100 -5.42051300 1.56889900
H -6.44977600 -5.19052200 0.80416000
H -4.97247700 -4.91388500 -0.12419600
C -3.87991800 -2.95883900 1.50437900
H -3.76659400 -1.93084500 1.85073500
H -3.43635700 -3.62911400 2.24787900
H -3.32815300 -3.06868600 0.56732500

(2.B*.m)–(1a)_triplet

C -10.54261300 -1.32573900 2.32149500
C -9.25602200 -1.00021100 2.72514300
C -8.39972900 -0.18345500 1.96090200
C -8.92823800 0.35950100 0.72424000
C -10.24299000 0.04311200 0.33461200
C -11.05135000 -0.79098200 1.09147000
N -7.14927100 0.05826500 2.41977600
N -8.10793500 1.18293600 -0.02605200
C -6.78242900 1.40363600 0.40093900
C -6.35611800 0.80359600 1.61136400
C -4.95840100 0.98997400 1.98630100
O -4.42053700 0.51333400 2.98687400
N -4.23388900 1.78207700 1.09925700
C -4.71367400 2.37805300 -0.05662400
N -6.04094600 2.15159500 -0.39245700
H -8.86016900 -1.39021200 3.65558200
H -10.65467700 0.46051400 -0.57302800
H -3.25962900 1.94269300 1.32608100
O -3.98407500 3.07649200 -0.75897300
C -12.43958200 -1.12962100 0.62648500
H -12.66746500 -0.63447100 -0.31932700
H -12.55571400 -2.20991200 0.48215500
H -13.19296700 -0.82578600 1.36200000
C -11.39559600 -2.22873000 3.16187100
H -12.31966100 -1.72440700 3.46716500
H -11.69695300 -3.11802500 2.59657000
H -10.86491200 -2.55256500 4.05853500
C -8.61852700 1.98307000 -1.14564000
H -7.80036700 2.13336100 -1.84711000
H -9.40445600 1.42733100 -1.65072800
C -9.11538000 3.34956700 -0.67683200
H -8.29929000 3.91912600 -0.23182100
H -9.53419000 3.89318800 -1.52508700
O -10.18591100 3.21012000 0.27661000
C -9.85095200 3.22128400 1.59092900
O -8.71596300 3.37940000 1.99495100
C -11.05969300 2.97439600 2.45046400
H -11.33482200 1.91770200 2.37070600
H -10.82651700 3.20817700 3.48842200
H -11.90958700 3.56589300 2.10414700
O -5.45428400 -1.44510900 -0.11420300
C -6.16784400 -2.36057600 0.32153200
N -7.38480200 -2.56493800 -0.27731900
C -7.61998600 -1.81598100 -1.52888700
C -8.46316300 -3.45819600 0.14470300
C -8.92436600 -2.24133300 -2.19843200
H -7.60454400 -0.74357700 -1.32693300
H -6.77466100 -2.01311800 -2.19784000
C -8.84509100 -4.45661500 -0.95681900
H -8.17594400 -3.97941300 1.04919600
H -9.33225600 -2.84362700 0.40670400
C -8.98459100 -3.76645800 -2.33792100
H -9.78350200 -1.87581300 -1.62574800

H -8.97525200 -1.75805100 -3.17898500
H -9.78491500 -4.93239400 -0.65856000
H -8.08874900 -5.24618400 -1.00440000
H -9.91590400 -4.06604700 -2.82722300
H -8.16765100 -4.08580100 -2.99495000
C -5.63052300 -3.29507600 1.43861300
C -6.40794800 -3.16739000 2.76656200
H -7.44466200 -3.50216000 2.70489700
H -5.91160900 -3.78223600 3.52482000
H -6.41114800 -2.12805300 3.10132500
C -5.60650000 -4.75806800 0.94127700
H -5.07950000 -5.37673500 1.67454900
H -6.59897600 -5.18983600 0.80543900
H -5.07130600 -4.83671200 -0.01055600
C -4.17586100 -2.87101900 1.72214400
H -4.12882900 -1.84577900 2.09279000
H -3.75364900 -3.53770100 2.48100800
H -3.56038000 -2.93782300 0.82173000

(2.A.m)-[$K_2S_2O_8$]–(1a), Singlet, S_0
S 2.06451200 -0.68474600 -5.86102100
O 0.97567600 -1.33129000 -6.60835200
O 2.31413900 -1.26774100 -4.52214900
O 3.27854900 -0.35611100 -6.63045500
S 0.15733800 1.80695100 -3.57989000
O 1.14613500 1.22174300 -2.64539700
O -1.25416600 1.58013400 -3.23444600
O 0.50475700 3.17375500 -4.02445500
K 1.75973100 -1.30308600 -1.96109500
K 0.90805500 5.46078600 -2.68090400
O 0.19989800 0.85093700 -4.98925200
O 1.53356400 0.92643400 -5.58566100
C 5.22355900 0.14133500 -4.18954600
N 4.54378300 1.42823200 -3.94445200
H 5.13375800 -0.10076900 -5.24271000
C 6.66853500 0.19939800 -3.71226300
C 4.50165600 2.41861500 -4.91486100
C 4.05468600 1.65701500 -2.68875100
H 6.71785700 0.41671900 -2.64530800
H 7.15615500 -0.75374700 -3.92225100
O 7.41414000 1.19563500 -4.44451700
C 3.95129800 3.68446500 -4.56179600
C 4.99478700 2.24274500 -6.21801600
C 3.56060200 2.98566500 -2.41805200
N 4.05763500 0.66962000 -1.80838500
C 7.50204100 2.43313600 -3.90073600
C 3.88920800 4.71274900 -5.52857400
N 3.50413600 3.94265900 -3.30367200
C 4.92613600 3.26398300 -7.15513500
H 5.43276600 1.30289400 -6.51472100
C 3.07943200 3.27100800 -1.04271700
C 3.51980000 0.88343300 -0.57348600
O 7.02067700 2.73427800 -2.82549600
C 8.22758500 3.37237600 -4.82435500
C 4.35782100 4.53000600 -6.81196900
H 3.46463200 5.66181300 -5.21787100
C 5.45721200 3.03063400 -8.54248000
O 2.65079400 4.36504500 -0.68315200
N 3.14769600 2.18922600 -0.20404800
O 3.31929100 -0.03216600 0.23155500
H 7.54172400 3.66616200 -5.62597600
H 8.53715400 4.26131100 -4.27591300
H 9.08807500 2.88261400 -5.28371900
C 4.28235400 5.63694600 -7.82855700
H 5.86100200 2.02226300 -8.64830200
H 4.66908000 3.16650000 -9.29144700
H 6.24983700 3.74699900 -8.78536600
H 2.76775200 2.30350000 0.72879300
H 5.27811900 5.90793500 -8.19640200
H 3.69254400 5.33526500 -8.70114400
H 3.82311200 6.52975100 -7.39930000
H 4.68472800 -0.62019600 -3.63181700
O -0.45661700 4.64002400 -0.59977500
C -0.36774200 4.39887400 0.61918700
N -0.59617900 3.12980700 1.04645600
C 0.02019100 5.53947000 1.59621200
C -0.87306500 2.13365800 -0.01181900
C -0.76293900 2.64872300 2.42021300
C -1.18090600 5.92904900 2.48757800
C 1.26968700 5.17286100 2.42824400
C 0.38935100 6.77594600 0.75330900
C -1.05744300 0.73205500 0.56791200
H -1.74949600 2.44281300 -0.58907200
C 0.13706800 1.43846600 2.69672100
H -0.55036800 3.44238000 3.12506300
H -1.81546200 2.37568300 2.56594900
H -1.50809800 5.13238800 3.15726200
H -0.90772800 6.78969200 3.10647200
H -2.03681500 6.21805500 1.86895800
H 1.59140000 6.05120200 2.99741300
H 1.10774500 4.36622300 3.14408800
H 2.08291900 4.87915300 1.75969900

H -0.43177900 7.07409600 0.09814500
H 0.61924200 7.61004200 1.42360700
H 1.27256800 6.57987300 0.14098200
C 0.06646000 0.39215900 1.55305300
H -2.03214800 0.64338500 1.06176500
H -1.07036600 0.02624300 -0.26849800
H -0.17469400 1.00096100 3.65078900
H 1.16748500 1.78588200 2.83248600
H -0.08221600 -0.61238500 1.96166400
H 1.01961700 0.36822800 1.01630900
H -0.02819100 2.13329100 -0.70263500

(2.B*.m)-[$K_2S_2O_8$]–(1a), triplet, T_1
S -2.21606500 -1.27804600 -4.75422700
O -3.06938700 -2.38223000 -5.21780400
O -0.96339000 -1.70689900 -4.09402000
O -2.09496100 -0.11335900 -5.64889000
S -2.77282400 -0.75817900 -1.01782800
O -1.29949300 -0.83681100 -1.19074700
O -3.32967000 -1.71816600 -0.05602300
O -3.29516600 0.62042500 -0.96053700
K -0.31768000 -3.24115800 -1.98956100
K -2.61071900 2.31034700 -3.03762100
O -3.43242000 -1.41781300 -2.45325700
O -3.14145100 -0.48121800 -3.53164900
C 5.83442000 0.78609900 -3.08366000
N 4.70764500 1.52576600 -3.66618200
H 6.69807700 0.89082500 -3.73569600
C 6.14611300 1.24393100 -1.65897200
C 4.87927400 2.70726700 -4.35395300
C 3.39591400 1.09374600 -3.36567900
H 5.28298200 1.08746500 -1.01198600
H 7.00390400 0.68300100 -1.28541200
O 6.53508300 2.63154800 -1.62273800
C 3.69589300 3.43102100 -4.77925100
C 6.15853700 3.23615000 -4.63845100
C 2.30578800 1.88324900 -3.80661800
N 3.30213200 -0.04196700 -2.69737600
C 5.56249500 3.53832400 -1.36531800
C 3.89092300 4.63805400 -5.45751500
N 2.42096300 3.01649900 -4.53352400
C 6.32212900 4.43447900 -5.31067800
H 7.04382500 2.71619400 -4.30255800
C 0.97361900 1.42349600 -3.43094900
C 2.04195800 -0.52452000 -2.37673300
O 4.40414900 3.23084100 -1.15967300
C 6.09250000 4.94262600 -1.41794700
C 5.15955500 5.15537500 -5.73267700
H 3.00390200 5.18052700 -5.76501100
C 7.69878900 4.97315600 -5.58315000
O -0.07392600 2.01753100 -3.70649100
N 0.94539100 0.24414400 -2.70235500
O 1.90775400 -1.61524100 -1.80665200
H 6.11811100 5.26011700 -2.46561100
H 5.42504600 5.60436900 -0.86676400
H 7.10807600 4.99739200 -1.02344000
C 5.29924800 6.45775600 -6.45710900
H 8.46577900 4.30405700 -5.18883100
H 7.87238400 5.09583600 -6.65811700
H 7.83734700 5.95858100 -5.12444700
H 0.02721200 -0.11929000 -2.43444100
H 5.84437200 7.18597500 -5.84481800
H 5.88077000 6.33147100 -7.37787900
H 4.32628500 6.87845100 -6.71422300
H 5.55634900 -0.26530400 -3.04972700
O -1.31550400 4.12515100 -1.55446600
C -0.21283500 4.28699100 -0.99384500
N 0.24252400 3.31759800 -0.15741000
C 0.57738300 5.59685100 -1.24917500
C -0.66927600 2.17500800 0.05873600
C 1.55464400 3.22859500 0.50079700
C 0.95966000 6.30643100 0.06751500
C 1.81730500 5.32312600 -2.12949100
C -0.34606600 6.54785300 -2.03553600
C -0.22648000 1.32139800 1.24017000
C 2.11197400 1.80723500 0.38207600
H 2.25141000 3.91101000 0.03020600
H 1.46150200 3.51650500 1.55590000
H 1.69850400 5.76498800 0.65776400
H 1.38339400 7.28859000 -0.16566100
H 0.07565700 6.46432200 0.69433700
H 2.28144800 6.27840800 -2.39892100
H 2.58136300 4.71318000 -1.64645900
H 1.53023800 4.81318600 -3.05276500
H -1.25214600 6.78262700 -1.47070200
H 0.18919900 7.48147000 -2.23519600
H -0.64731300 6.10809000 -2.98827500
C 1.18121100 0.74901200 1.01803000
H -0.25421600 1.92384600 2.15583900
H -0.95348500 0.51498300 1.36966400
H 3.10731600 1.78979400 0.83365100
H 2.25979400 1.60643800 -0.68076200

H 1.59027100 0.39976400 1.97194600
H 1.11595400 -0.12445800 0.36182300
H -1.67786700 2.56292600 0.20906700
H -0.69917300 1.55736900 -0.84163100

(2.C.m)-[$K_2S_2O_8$]_1min, doublet
S -0.83257000 -1.26260000 -4.88232000
O -1.43624800 -2.22308300 -5.81903300
O -0.04499700 -1.87658300 -3.79572100
O -0.26175000 -0.03766300 -5.47513700
S -3.09195000 -0.64078600 -1.75320400
O -1.74939300 -0.68733500 -1.11861200
O -4.08012600 -1.55893500 -1.17258300
O -3.55496900 0.72471300 -2.06872600
K -0.29058000 -2.97482300 -1.40560300
K -2.38641200 2.22512700 -4.10571300
O -2.91113700 -1.40697800 -3.27835300
O -2.16744700 -0.48099800 -4.12215700
C 5.52440600 0.66571000 -3.17233900
N 4.39483300 1.54008500 -3.48410700
H 6.25131700 0.71972200 -3.98133200
C 6.16562000 1.00588400 -1.83038800
C 4.57003000 2.73522800 -4.20671200
C 3.15982400 1.23913400 -2.92837800
H 5.43323900 0.91212000 -1.02923300
H 7.01544700 0.34628000 -1.64324300
O 6.70065800 2.34724700 -1.84264900
C 3.43146500 3.57835600 -4.38930400
C 5.80197000 3.12726400 -4.73907500
C 2.09087200 2.14222900 -3.16653900
N 3.08097100 0.11069600 -2.21356000
C 5.91908500 3.33629800 -1.35075600
C 3.61260600 4.77641700 -5.11953400
N 2.19820200 3.29343000 -3.88735000
C 5.95677800 4.32100500 -5.45287000
H 6.68414900 2.52392900 -4.57277200
C 0.81179800 1.79637500 -2.58976300
C 1.88477100 -0.23714700 -1.67851100
O 4.84674800 3.15111400 -0.80942300
C 6.54574600 4.68229400 -1.59687000
C 4.83622900 5.16209000 -5.64955200
H 2.73684700 5.40673600 -5.24668900
C 7.31162000 4.70119000 -5.99298100
O -0.23899400 2.46648900 -2.69748100
N 0.79971300 0.61599300 -1.86833200
O 1.71319400 -1.28583200 -1.01812500
H 6.36433200 4.95562900 -2.64177000
H 6.08889400 5.42697400 -0.94558000
H 7.62586900 4.64664400 -1.44276700
C 4.96939100 6.45641400 -6.41182000
H 8.06097000 3.94485000 -5.74680400
H 7.29466600 4.81560900 -7.08374400
H 7.65454600 5.65965000 -5.58457200
H -0.11116900 0.29052300 -1.54400900
H 5.69611000 7.12854900 -5.94011400
H 5.32045600 6.28625700 -7.43663700
H 4.01196500 6.98025900 -6.46617200
H 5.14994600 -0.35585800 -3.11575600

MSX-1
MSX (T_1)/S_0 (E = -4260.04863529 a.u.)

S	-3.503613	-2.164740	-1.883975
O	-4.702348	-2.916057	-2.285555
O	-2.999836	-2.489400	-0.531766
O	-2.471323	-1.962057	-2.914119
S	-4.606331	0.816891	0.307742
O	-3.481823	0.216266	1.075295
O	-5.862060	0.928147	1.059812
O	-4.216712	1.972651	-0.519837
K	-4.115921	-2.335740	1.892365
K	-2.282209	1.646245	-2.438642
O	-5.085853	-0.388079	-0.810382
O	-4.025175	-0.514631	-1.803437
C	3.369324	-3.196634	1.736088
N	2.716026	-2.578460	0.577618
H	4.321551	-3.609873	1.400860
C	3.559072	-2.296331	2.954783
C	3.436448	-1.888241	-0.436280
C	1.369710	-2.307151	0.608321
H	2.605880	-1.887631	3.283952
H	4.012734	-2.885786	3.753276
O	4.486145	-1.213180	2.712237
C	2.760577	-1.555563	-1.669656
C	4.792314	-1.602848	-0.329800
C	0.866298	-1.766159	-0.638063
N	0.663258	-2.356837	1.701332
C	3.959172	-0.033146	2.318445
C	3.481324	-0.889789	-2.689811
N	1.498287	-2.085584	-1.862546
C	5.483836	-0.931405	-1.347467
H	5.335127	-1.869873	0.566272
C	-0.122376	-0.702420	-0.503164

C	-0.600156	-1.761425	1.662614
O	2.767489	0.143514	2.151718
C	5.022303	1.000451	2.074557
C	4.812503	-0.555868	-2.549123
H	2.941255	-0.642233	-3.597343
C	6.937673	-0.608937	-1.157591
O	-0.418530	0.109285	-1.378790
N	-0.831994	-0.796471	0.687152
O	-1.448253	-2.003907	2.518149
H	5.203683	1.050958	0.996476
H	4.660255	1.977549	2.397359
H	5.955332	0.749067	2.578257
C	5.542300	0.178604	-3.640314
H	7.299290	-0.963547	-0.191079
H	7.549006	-1.065468	-1.944246
H	7.110125	0.471968	-1.215656
H	-1.746420	-0.330862	0.717590
H	5.923833	1.140125	-3.279078
H	6.404754	-0.391354	-4.001613
H	4.881841	0.373591	-4.487298
H	2.742691	-4.034573	2.050659
O	-0.624267	3.375501	-1.278119
C	0.274817	3.237848	-0.423536
N	-0.084241	3.066882	0.874445
C	1.757217	3.287397	-0.878715
C	-1.535911	3.144697	1.152927
C	0.788838	2.824087	2.031566
C	2.573794	4.336003	-0.092693
C	2.393837	1.883715	-0.795924
C	1.773375	3.707293	-2.361744
C	-1.818398	3.198568	2.649424
C	0.224966	1.717483	2.928302
H	1.769099	2.512404	1.692905
H	0.910688	3.755370	2.599224
H	2.763295	4.058564	0.943737
H	3.546161	4.466323	-0.577633
H	2.066588	5.306372	-0.095949
H	3.422466	1.926909	-1.168887
H	2.421347	1.464694	0.210271
H	1.836476	1.191794	-1.429640
H	1.339468	4.700562	-2.503585
H	2.809535	3.728123	-2.713659
H	1.211058	3.001898	-2.976573
C	-1.237213	1.974231	3.366228
H	-1.405081	4.121761	3.072623
H	-2.902891	3.249452	2.789714
H	0.889793	1.623527	3.791815
H	0.304041	0.778924	2.379535
H	-1.300751	2.115690	4.450063
H	-1.849793	1.099978	3.122538
H	-1.935381	4.025807	0.643853
H	-2.036369	2.277886	0.716332

(2.E.m)-[$K_2S_2O_8$]–(1a'), triplet, (T)–1

S	-1.50451100	-1.06447400	-4.83061000
O	-2.48311500	-1.84530900	-5.60347800
O	-0.61987200	-1.87438800	-3.96784500
O	-0.85794600	0.05734100	-5.53060600
S	-2.88769200	-0.54723000	-1.27011400
O	-1.41841300	-0.67263400	-1.10175800
O	-3.68330700	-1.56622500	-0.57306900
O	-3.38023800	0.84349000	-1.18281500
K	-0.26331100	-3.05094700	-1.61805300
K	-2.64140200	2.66021900	-3.07031700
O	-3.20868500	-1.02233900	-2.87786900
O	-2.46779700	-0.11387200	-3.74867900
C	5.73544500	0.75983200	-3.44956100
N	4.57818400	1.56675000	-3.85471200
H	6.52746300	0.88353300	-4.18484300
C	6.21166100	1.11272200	-2.04295900
C	4.74243800	2.79390900	-4.52458500
C	3.33407000	1.16910800	-3.39942200
H	5.41982400	0.92835300	-1.31769100
H	7.09433900	0.52060100	-1.79592600
O	6.62472100	2.49371600	-1.96902500
C	3.60529700	3.58850400	-4.81477300
C	5.99339100	3.28841100	-4.91530500
C	2.22793200	1.99008900	-3.69636000
N	3.23414500	0.04151600	-2.70624000
C	5.70898800	3.39261800	-1.53505000
C	3.74151000	4.81797800	-5.47107300
N	2.37024100	3.13549300	-4.41554500
C	6.13340700	4.51320000	-5.56728300
H	6.89089400	2.73544100	-4.67971900
C	0.92929700	1.66175800	-3.17077700
C	2.00940600	-0.34237400	-2.24200000
O	4.59292900	3.09086700	-1.16000000
C	6.24353700	4.79522800	-1.62425700
C	4.98679600	5.29615000	-5.85389300
H	2.84674800	5.40003800	-5.66982800
C	7.50499700	5.00196000	-5.94995200
O	-0.05847300	2.39309900	-3.34941900

N 0.90473200 0.49966400 -2.44208800
O 1.83818700 -1.40494300 -1.62262200
H 6.11262400 5.14587600 -2.65349100
H 5.67977400 5.44527300 -0.95563300
H 7.30873300 4.82851400 -1.39037900
C 5.11374000 6.62428500 -6.55041700
H 8.27602200 4.28678700 -5.65652200
H 7.58184900 5.16218900 -7.03131900
H 7.73070900 5.96193700 -5.47193400
H 0.00841200 0.18901800 -2.05551400
H 5.74461800 7.31346100 -5.97799100
H 5.58031400 6.51258500 -7.53559000
H 4.13672700 7.09209700 -6.68780800
H 5.42414000 -0.28423200 -3.45345600
O -1.53630900 4.02842400 -1.06721500
C -0.36600000 4.14135000 -0.65374100
N 0.11258000 3.18318800 0.21953400
C 0.49725000 5.34291700 -1.11127600
C -0.67457000 2.07913800 0.51587200
C 1.39533100 3.22167500 0.94554200
C 0.54413100 6.39109400 0.02405200
C 1.93208200 4.95828200 -1.56196700
C -0.22177800 5.96798600 -2.32370600
C -0.15424300 1.07321400 1.48036600
C 2.15420600 1.90648800 0.74667700
H 1.98935900 4.05883500 0.60715400
H 1.17521100 3.38142800 2.00750600
H 1.03698400 6.00815400 0.92167300
H 1.09828600 7.27383700 -0.31169100
H -0.46643700 6.70839500 0.30028500
H 2.22918600 5.57789400 -2.41332000
H 2.68606100 5.11221000 -0.78891300
H 2.00074100 3.91665500 -1.87253300
H -1.24404900 6.25923000 -2.07807000
H 0.33091200 6.85407600 -2.65060900
H -0.26107700 5.25584200 -3.15300100
C 1.31420800 0.68021800 1.18171700
H -0.20907000 1.45907100 2.51279400
H -0.79757500 0.19116100 1.44366900
H 3.09152600 1.96636500 1.30767500
H 2.43348400 1.83480300 -0.30718000
H 1.74643600 0.21508800 2.07416600
H 1.32521400 -0.07267100 0.39109700
H -1.60750900 1.98467600 -0.01229200
H 1.53136000 3.68792700 -4.56337100

(2.F.m)-[$K_2S_2O_8$]–(1.A), singlet, (S)–1

S -1.45083900 -1.07829900 -4.80801700
O -2.44883400 -1.86417500 -5.54930600
O -0.61900500 -1.86582000 -3.87605300
O -0.74429000 -0.02862700 -5.56063700
S -2.96935900 -0.32171200 -1.35239900
O -1.57133800 -0.73007900 -1.05580400
O -4.00825400 -1.11217400 -0.68453400
O -3.14841400 1.14847700 -1.34200700
K -0.28013500 -3.03634900 -1.52528000
K -2.59174500 2.74271700 -3.50040000
O -3.26776000 -0.79627600 -2.95803500
O -2.38901200 -0.01032100 -3.81662600
C 5.59469800 0.62523300 -3.58524900
N 4.42492900 1.42726600 -3.93201100
H 6.36620900 0.78477400 -4.33904500
C 6.13662100 0.88407600 -2.17995600
C 4.57804200 2.73673600 -4.48030900
C 3.20144200 1.06967800 -3.36574000
H 5.35930000 0.69720100 -1.44108400
H 6.99901900 0.24046200 -1.99245700
O 6.62380800 2.23848400 -2.03557000
C 3.42655100 3.51114800 -4.74681600
C 5.82368400 3.29293800 -4.77497100
C 2.09122400 1.87150900 -3.62155100
N 3.16871600 -0.03498900 -2.59984000
C 5.78942600 3.14932700 -1.49142800
C 3.56845400 4.80582400 -5.24535400
N 2.16470500 2.94365600 -4.54635600
C 5.96771800 4.58670800 -5.29981700
H 6.72550300 2.73851500 -4.55554400
C 0.90069500 1.62455500 -2.92535600
C 1.99754200 -0.38769500 -2.02102300
O 4.69199700 2.88294600 -1.03927400
C 6.37823100 4.53254900 -1.55003100
C 4.82117100 5.36166400 -5.53173600
H 2.66868900 5.38953600 -5.42492800
C 7.34612000 5.13199800 -5.58117900
O -0.11767700 2.37841100 -2.94719600
N 0.90913800 0.47847600 -2.13893300
O 1.84831400 -1.44093700 -1.35247000
H 6.11639000 4.96653300 -2.52073900
H 5.94866400 5.14840800 -0.75971100
H 7.46611200 4.50672400 -1.47249500
C 4.92474100 6.76553100 -6.07189800
H 8.11735500 4.39625400 -5.33929900

H 7.46639700 5.40966800 -6.63539400
H 7.55097900 6.03594700 -4.99452900
H 0.00721500 0.13660300 -1.80728000
H 5.52032400 7.40752700 -5.41178900
H 5.41544800 6.78545200 -7.05245400
H 3.93715200 7.22069100 -6.18113000
H 5.30184500 -0.42479500 -3.62528300
O -1.49587000 4.26225400 -1.04095400
C -0.30839700 4.28218800 -0.83340000
N 0.20115600 3.23398900 0.09823600
C 0.65240100 5.31464200 -1.42251000
C -0.43259200 2.09782500 0.12169600
C 1.34109000 3.40528100 1.03596700
C 0.67784500 6.53256000 -0.46244500
C 2.07867600 4.78250000 -1.67731600
C 0.02847300 5.75844400 -2.76298300
C -0.04829700 1.04688600 1.08272300
C 2.25118400 2.17964200 0.93486200
H 1.85868800 4.32491200 0.79796000
H 0.90973300 3.50833000 2.03664300
H 1.08461100 6.28620100 0.52147000
H 1.31442100 7.30373500 -0.90491300
H -0.32549800 6.94503800 -0.32797900
H 2.53583100 5.37440700 -2.47406800
H 2.73808000 4.86141100 -0.81387500
H 2.08126600 3.74370000 -2.00266200
H -0.97471200 6.16434600 -2.62184600
H 0.66095700 6.52858700 -3.21071300
H -0.03573000 4.90767400 -3.44449700
C 1.48516200 0.88988800 1.27740100
H -0.50404400 1.36948500 2.03398600
H -0.53410800 0.11488700 0.79934000
H 3.09719300 2.32616100 1.61022400
H 2.65994000 2.13921300 -0.07606100
H 1.66250400 0.59875800 2.31488900
H 1.82119100 0.07006400 0.63992900
H -1.27908000 1.97837800 -0.54917100
H 1.39942800 3.59825200 -4.44289900

MSX-2

MSX (T)-1/S_0 (E = -4260.09988392 a.u.)

S	-3.440243	-2.529157	-1.760539
O	-4.565622	-3.252686	-2.372140
O	-3.233890	-2.816719	-0.326570
O	-2.215750	-2.411485	-2.568632
S	-4.897781	0.500650	0.087166
O	-3.840705	-0.038648	0.978904
O	-6.247067	0.533591	0.663923
O	-4.471686	1.705454	-0.658152
K	-3.965764	-2.426381	2.186491
K	-2.632404	1.546451	-2.660527
O	-5.156168	-0.689169	-1.106934
O	-3.906848	-0.859300	-1.840435
C	3.337024	-2.742865	1.776735
N	2.876492	-2.007677	0.597826
H	4.178774	-3.372157	1.492939
C	3.694831	-1.818511	2.938225
C	3.788327	-1.572111	-0.392834
C	1.552214	-1.593727	0.569709
H	2.820661	-1.248601	3.250821
H	4.081122	-2.405360	3.773544
O	4.754660	-0.910574	2.564710
C	3.313451	-0.804783	-1.486002
C	5.154735	-1.862373	-0.346810
C	1.118412	-0.821967	-0.517950
N	0.754993	-1.958311	1.575692
C	4.396386	0.321804	2.133505
C	4.204933	-0.354879	-2.465217
N	1.971019	-0.510828	-1.555528
C	6.046329	-1.422448	-1.330666
H	5.560455	-2.411245	0.490580
C	-0.219620	-0.337543	-0.551330
C	-0.547215	-1.566831	1.556215
O	3.252712	0.733191	2.131842
C	5.588385	1.084896	1.627435
C	5.564705	-0.650107	-2.408562
H	3.812448	0.240151	-3.284542
C	7.508617	-1.767550	-1.222194
O	-0.659396	0.388102	-1.470115
N	-0.985979	-0.721094	0.530814
O	-1.363952	-1.913866	2.433790
H	5.806429	0.742593	0.610502
H	5.359081	2.149650	1.604446
H	6.469458	0.892268	2.241397
C	6.497590	-0.144615	-3.476953
H	7.706762	-2.366274	-0.330555
H	7.852001	-2.336260	-2.094315
H	8.131060	-0.866702	-1.171151
H	-1.975350	-0.467158	0.527643
H	7.286493	0.486236	-3.051857
H	6.999485	-0.971331	-3.992576
H	5.959597	0.443782	-4.223317

H	2.522008	-3.389605	2.101206
O	-1.301217	3.327247	-1.085654
C	-0.346142	3.277453	-0.311374
N	-0.618126	2.891337	1.028039
C	1.077771	3.627020	-0.784683
C	-1.847871	2.421733	1.325223
C	0.311243	3.013806	2.174015
C	1.413150	5.068957	-0.335335
C	2.164490	2.628754	-0.306572
C	1.041205	3.590066	-2.325997
C	-2.208197	2.144558	2.733034
C	0.304025	1.714257	2.980903
H	1.304309	3.238381	1.812967
H	-0.028135	3.857406	2.785237
H	1.440762	5.173684	0.751975
H	2.397353	5.348412	-0.724031
H	0.678787	5.778217	-0.727816
H	2.918074	2.511691	-1.090160
H	2.692460	2.956779	0.589202
H	1.753996	1.642079	-0.097746
H	0.297250	4.279937	-2.726924
H	2.025681	3.868022	-2.712237
H	0.797226	2.583630	-2.676766
C	-1.104774	1.370421	3.503880
H	-2.378457	3.110553	3.238945
H	-3.155675	1.605940	2.751224
H	1.018466	1.817852	3.801469
H	0.687891	0.921012	2.336903
H	-1.194139	1.612738	4.566832
H	-1.286522	0.299527	3.393623
H	-2.545674	2.316507	0.508464
H	1.606033	0.096829	-2.277883

(2.F.m)-[$K_2S_2O_8$]_1min, singlet, (S)–2

S 0.70859200 -1.38917000 -4.78163700
O 0.27261700 -2.35334700 -5.80296700
O 1.44212600 -1.98182200 -3.64768200
O 1.23909800 -0.10258500 -5.28294400
S -1.71427700 -0.92455600 -1.76857400
O -0.42751100 -1.01699200 -1.03923200
O -2.77346500 -1.81904600 -1.27886100
O -2.11548000 0.45575800 -2.10616600
K 1.32274200 -3.04648000 -1.25030800
K -0.38605100 1.97637200 -3.83769800
O -1.44903100 -1.68227700 -3.29616500
O -0.73756300 -0.72550200 -4.12752200
C 5.77264600 0.63839900 -4.35628900
N 4.66384000 1.55011400 -4.10064500
H 6.08827500 0.74799800 -5.39441900
C 6.95264700 0.81717200 -3.40394000
C 4.59481500 2.82400200 -4.72891900
C 3.80609600 1.26255400 -3.03927000
H 6.62264200 0.69085000 -2.37397300
H 7.73562700 0.09323800 -3.64116500
O 7.56475600 2.11774500 -3.55873500
C 3.50006100 3.67510600 -4.46112600
C 5.57520300 3.27893300 -5.61524600
C 2.75354300 2.13200000 -2.77315400
N 4.04076200 0.13180800 -2.35131900
C 7.17871000 3.09700100 -2.71095600
C 3.44254300 4.92991900 -5.06520200
N 2.45595900 3.24120500 -3.62160500
C 5.51187600 4.53690200 -6.23190700
H 6.44660200 2.66865500 -5.80847600
C 1.84937700 1.82457300 -1.74129200
C 3.17760100 -0.22416500 -1.37168500
O 6.41717700 2.93129800 -1.77801900
C 7.79442200 4.41455800 -3.10051600
C 4.42770800 5.38264400 -5.94982700
H 2.59257800 5.56929500 -4.83742800
C 6.61205000 4.96878600 -7.16974900
O 0.82388800 2.50648100 -1.46023400
N 2.14301300 0.65348100 -1.04973300
O 3.25955900 -1.30383600 -0.73657800
H 7.20010200 4.83780100 -3.91710900
H 7.77279100 5.09758500 -2.25151200
H 8.81563600 4.28108600 -3.46187800
C 4.32055600 6.74974400 -6.57664000
H 7.37602100 4.19297400 -7.26459700
H 6.22733100 5.18536100 -8.17377300
H 7.10545400 5.88382900 -6.82014700
H 1.41261900 0.30217600 -0.44165800
H 5.18178100 7.37881200 -6.32101500
H 4.29145300 6.69059800 -7.67133400
H 3.41703800 7.26702000 -6.24407600
H 5.40425600 -0.37985500 -4.22385300
H 2.01096100 3.99246400 -3.10345600

(2.F.m)-[$K_2S_2O_8$]_1min, triplet, (S)–2 (t)

S -1.03893400 -1.58330500 -4.39262600
O -1.81078500 -2.63327000 -5.07422100
O 0.21126700 -2.04352500 -3.76013400

O -0.95987800 -0.27720600 -5.08119200
S -1.64597800 -1.24921800 -0.59634200
O -0.16613000 -1.18764200 -0.68371800
O -2.16979600 -2.23346200 0.35991900
O -2.29634100 0.07612700 -0.61605500
K 1.13121100 -3.37085000 -1.67207500
K -1.79917100 1.68980400 -2.84684900
O -2.16650300 -2.01670500 -2.04704800
O -2.05538700 -1.03287100 -3.11103300
C 6.40840400 0.84628000 -4.37197800
N 5.17794900 1.63569700 -4.38020200
H 6.97567600 1.05036200 -5.27842100
C 7.24847000 1.11012900 -3.12433500
C 5.13322900 2.88818300 -4.97299500
C 4.11313600 1.14454700 -3.62714900
H 6.67686600 0.86898700 -2.22849600
H 8.16476600 0.51701700 -3.15818900
O 7.66615800 2.48905300 -3.07907800
C 3.93018000 3.68054200 -4.85695500
C 6.20069200 3.46718500 -5.70060800
C 2.92553000 1.95011700 -3.52990500
N 4.19215000 -0.09672500 -3.06743000
C 6.89134400 3.35060900 -2.37408700
C 3.85084900 4.94194600 -5.45806600
N 2.87227700 3.16457600 -4.13612500
C 6.11509700 4.72094300 -6.28486100
H 7.14144800 2.93825900 -5.77911900
C 1.81652700 1.49823000 -2.77146700
C 3.16380300 -0.55389000 -2.35415200
O 5.97804100 3.00681700 -1.64786800
C 7.31936300 4.77052700 -2.62499300
C 4.90543500 5.48949500 -6.17573600
H 2.92534800 5.50349300 -5.34637300
C 7.29672900 5.28011200 -7.03485500
O 0.74040800 2.14850700 -2.64103800
N 2.01193100 0.27298300 -2.15793200
O 3.12535100 -1.69014600 -1.80289600
H 7.00486500 5.05170600 -3.63626800
H 6.85124800 5.43278000 -1.89729600
H 8.40711800 4.86137000 -2.57846100
C 4.79271000 6.85302300 -6.80353900
H 8.13989200 4.58458500 -7.01993000
H 7.04983500 5.48706300 -8.08407300
H 7.63710700 6.23050500 -6.60497900
H 1.20844000 -0.15687800 -1.70669700
H 5.54229400 7.55316100 -6.41042600
H 4.94168200 6.82289400 -7.89118800
H 3.80643300 7.28746800 -6.61748100
H 6.12413600 -0.20625100 -4.36826700
H 2.01528300 3.69353000 -4.01692500

(2.A.m)-[KSO_4_$KHOSO_3$]_1min, singl, (S)–3

S 0.79040800 -0.14383300 -5.48741200
O 1.28892800 -0.68484800 -6.79388200
O 1.74241700 -0.52184400 -4.35831100
O 0.64354400 1.36142300 -5.54249800
S -1.50377000 -0.39589900 -0.49535300
O -1.17770400 1.15474400 -0.13195700
O -2.57707500 -0.76816400 0.43629900
O -1.88697900 -0.41244500 -1.93922800
K 0.10921800 -2.17637600 -2.96121100
K -1.42627900 1.53213700 -3.82115200
O -0.21629400 -1.14104100 -0.28370800
O -0.57574600 -0.74117900 -5.14290600
C 6.10849800 0.52438500 -4.17531400
N 4.88045700 1.32669500 -4.05202900
H 6.52069700 0.66127900 -5.17164300
C 7.11811800 0.88631100 -3.09132700
C 4.72770800 2.52844200 -4.73341600
C 3.93683200 0.90096300 -3.15360100
H 6.69417800 0.71033400 -2.10320800
H 8.02236900 0.29057000 -3.22418700
O 7.52932200 2.26406000 -3.20694100
C 3.56149700 3.30091500 -4.47565700
C 5.67746800 3.02787000 -5.63985900
C 2.77428400 1.75137000 -2.99256800
N 4.15001600 -0.21796400 -2.49432000
C 6.86062900 3.17809100 -2.46164800
C 3.38807500 4.53577100 -5.13619600
N 2.60379800 2.89132900 -3.59550200
C 5.48892700 4.24598300 -6.28232900
H 6.59304300 2.48743500 -5.83202000
C 1.73900700 1.27813500 -2.05164300
C 3.17619500 -0.68287100 -1.65877100
O 5.96679300 2.89503200 -1.68853100
C 7.34886100 4.56918300 -2.75858500
C 4.31909800 5.02229900 -6.03177800
H 2.48565100 5.09396000 -4.90895300
C 6.53466500 4.74849700 -7.23977400
O 0.66408700 1.88306200 -1.87525700
N 2.05571200 0.14199500 -1.38466500

O 3.21297800 -1.78690800 -1.11770600
H 6.90950300 4.89378800 -3.70760000
H 7.02923600 5.24707400 -1.96789500
H 8.43457900 4.58821800 -2.86846500
C 4.11227500 6.34341700 -6.72312000
H 7.36891000 4.04935900 -7.32088000
H 6.11196200 4.89777400 -8.23960400
H 6.92868800 5.71845800 -6.91654700
H 1.32102100 -0.28540600 -0.80221800
H 4.92261100 7.04425900 -6.49335400
H 4.09481800 6.22467700 -7.81221500
H 3.16969900 6.80082200 -6.41562500
H 5.82662500 -0.52059000 -4.05362400
H -0.44400100 1.46107300 -0.74285900

[K_2SO_4]
S 0.91129800 1.02441100 -2.92941400
O 2.25782500 0.32963700 -2.85716800
O 0.20460500 0.92835000 -1.59049700
O 1.10117800 2.49117200 -3.26718700
K 1.86317900 -1.46929600 -4.77790800
K -0.05154700 3.53475000 -1.10768500
O 0.08008900 0.34887800 -4.00380400

$CuBF_4$
Cu 0.33323200 1.23640300 -4.27284500
B -1.35375900 1.16291400 -2.18718400
F -2.62346200 1.68166900 -2.23302700
F -0.38601600 2.18894700 -2.53212700
F -1.03069200 0.60025400 -0.97807100
F -1.17735400 0.18924300 -3.25036900

(LH)– $CuBF_4$
N -1.41176200 1.43913400 0.39947200
C -0.50534400 1.81399000 -0.71681700
C -0.57992900 3.31496900 -1.01029000
C -2.03966300 3.78014000 -0.98710400
C -2.64707200 3.58381800 0.42213700
C -1.83802000 2.56732400 1.23974800
H 0.51308000 1.49291700 -0.46914100
H 0.01276400 3.88646000 -0.28763600
H -2.11796800 4.82580700 -1.29672200
H -2.65225800 4.52511900 0.98073900
H -2.39912900 2.21365000 2.09468300
H -3.68620100 3.24983900 0.34407400
H -0.92770100 3.03142100 1.63206900
H -2.60415400 3.19051500 -1.71872200
H -0.12695000 3.48678500 -1.99097700
H -0.82101900 1.24593700 -1.59330700
C -1.69042900 0.14211200 0.55427500
O -1.15946500 -0.66050200 -0.28104500
Cu 0.02979300 -2.04849700 0.17018000
B 1.30860700 -3.68091000 2.05056500
F 0.87390800 -4.96455200 2.28240300
F 2.58812100 -3.44624600 2.49508100
F 1.29456600 -3.46012300 0.57830400
F 0.39957900 -2.72572800 2.55393400
C -2.64107000 -0.40472800 1.64280700
C -2.01758600 -0.22111000 3.04655000
H -1.85359000 0.82084100 3.32401600
H -2.68935800 -0.66066500 3.79000200
H -1.06085500 -0.74733700 3.10417100
C -2.83623300 -1.91964400 1.42653400
H -3.58309700 -2.27811800 2.14036200
H -3.18652200 -2.14390600 0.41688600
H -1.91512100 -2.47805800 1.61474400
C -4.03931300 0.24735000 1.52899600
H -4.05231100 1.31624100 1.73785900
H -4.45159900 0.09508700 0.52695800
H -4.71057800 -0.23327700 2.24605700

($Na_2S_2O_4$)– $CuBF_4$
Cu 0.71627900 2.20603500 -3.60792300
B 0.82203700 2.78723200 -6.35935300
F 0.79545400 3.94031700 -7.08833100
F 0.41124300 1.66666200 -7.09514400
F 2.04745800 2.55581900 -5.72873900
F -0.16416800 2.90130100 -5.24738900
S 0.83999900 -0.08619900 -1.81495400
O -0.14270900 -0.06186600 -3.22685000
O 1.43255900 1.29239400 -2.05668100
O -0.07307000 -0.15309200 -0.67494200
O 1.81720300 -1.16643200 -1.95942200
O -1.09876100 -1.16593200 -3.19083900
Na -1.54781300 0.94527600 -6.06771200
S -0.85423400 -2.14692000 -4.58948800
O -2.04013400 -2.99853100 -4.42555600
O -0.90489300 -1.19002900 -5.72427500
O 0.45355900 -2.79982000 -4.42315800
Na 2.74651300 -0.67144500 -5.31849900

[(LH)–($NaSO_4$)]–[$NaSO_4$–$CuBF_4$], trip

Cu 1.56805400 1.88684300 -4.03361100
B -0.75175900 1.62220900 -2.44245600
F -1.91794500 2.32075600 -2.15707800
F 0.39502300 2.46610000 -2.32523300
F -0.61397000 0.47797500 -1.67975700
F -0.79171800 1.24241800 -3.83587600
S 2.67922500 -0.45099900 -4.39463900
O 2.60066300 0.78768600 -5.34662500
O 4.06609100 -0.84438700 -4.11993100
O 1.99672600 0.21933700 -3.14027400
O 1.79194400 -1.54653800 -4.86135200
O -2.21904000 -1.27760900 -4.52571700
Na -3.15007800 1.70963400 -4.11608600
S -2.45850100 -0.87705500 -5.93427400
O -3.30818500 -1.90510700 -6.68517000
O -3.02156500 0.49309600 -6.04755000
O -1.21420100 -1.05393800 -6.80598600
Na -0.14655900 -1.17649800 -3.48283200
O 1.21940600 3.51453000 -4.95948100
C 0.12066200 4.01058000 -5.38317600
C -0.31743700 5.34929200 -4.74653600
C 0.73828500 5.74542400 -3.69372500
H 0.81977400 4.98595500 -2.91418600
H 1.72307000 5.88470100 -4.14456600
H 0.43193300 6.68793200 -3.23149700
C -1.66210700 5.19349900 -3.99635600
H -2.50479400 4.93146500 -4.63684400
H -1.58152400 4.43055500 -3.21948800
H -1.90056900 6.14513500 -3.51234500
C -0.36854700 6.47464300 -5.80502400
H -0.54251300 7.42642000 -5.29512300
H 0.58530800 6.54688600 -6.33616400
H -1.15887500 6.35152000 -6.54542900
N -0.55947500 3.39189700 -6.34778900
C -0.05074600 2.14975700 -6.97079900
C -1.81445300 3.83821800 -6.98352200
C 0.21828800 2.37389000 -8.46154700
H -0.81756100 1.38548500 -6.83134200
H 0.85410000 1.82758700 -6.46884800
C -1.59069500 4.11947000 -8.47233200
H -2.53467900 3.02206800 -6.86490300
C -1.03374000 2.88184300 -9.18290200
H 0.56148700 1.42759600 -8.89216900
H 1.03553700 3.09747800 -8.56975300
H -2.54471500 4.42889400 -8.91106300
H -0.89393500 4.95984300 -8.57594200
H -0.80871200 3.11023500 -10.22936400
H -1.79650600 2.09215900 -9.18225700
H -2.21039600 4.70704100 -6.47606800

[(LH)–($NaSO_4$)]–[$NaSO_4$–$CuBF_4$], sing
Cu -0.59056000 2.04520600 -2.02829500
B 2.49659100 2.45591300 -2.46560600
F 3.19257000 3.56783500 -2.03045400
F 3.29934100 1.64069500 -3.29872200
F 1.98159900 1.71365400 -1.39674300
F 1.38265800 2.87121400 -3.29136700
S -1.16277100 -0.27047300 -3.89583200
O 0.26280500 0.20171400 -4.72337800
O -0.71358200 0.18793500 -2.52872900
O -2.24121400 0.52806500 -4.48343100
O -1.25688000 -1.72456000 -3.99792000
O 0.15846500 -0.27881800 -6.10025800
Na 1.98782500 1.90235600 -5.26115100
S 1.63039700 -1.12209600 -6.44312300
O 1.35310300 -1.42464700 -7.85309400
O 2.66941700 -0.08788400 -6.19799900
O 1.68903400 -2.26532500 -5.51899800
Na 2.26297400 -1.52110700 -2.39852500
O -0.80878800 3.79419200 -1.30232100
C -0.13342000 4.82912500 -1.59829500
C -0.55093400 5.64043900 -2.85032700
C -1.61539700 4.82516600 -3.61274500
H -1.19958000 3.88651600 -3.99134000
H -2.47373900 4.58978000 -2.98150500
H -1.96096500 5.41182600 -4.46856000
C 0.61376600 5.89289200 -3.83799700
H 0.19153200 6.23860700 -4.78625900
H 1.32024100 6.65497500 -3.50992100
H 1.16459700 4.96983000 -4.01957800
C -1.20586300 6.96701300 -2.39832500
H -2.05916500 6.77241600 -1.74145100
H -0.51670900 7.62778800 -1.86926400
H -1.57140100 7.50360900 -3.27893200
N 0.85866500 5.19800000 -0.78044700
C 1.22131600 4.35155700 0.37447600
C 1.68669000 6.40891500 -0.85848900
C 1.03629700 5.12234700 1.68206500
H 2.26897700 4.06727700 0.23514400
H 0.61559600 3.45190900 0.34482800
C 1.54350800 7.24017500 0.42172100
H 2.72314700 6.08030900 -0.99717400

H 1.41015300 7.00132600 -1.71988100
C 1.86283400 6.41315900 1.67132600
H 1.32990300 4.47728500 2.51692600
H -0.02770400 5.35769800 1.80998400
H 2.20568100 8.10892600 0.34661700
H 0.51509500 7.61816400 0.47883700
H 1.67460300 7.00102200 2.57550100
H 2.93057000 6.15648600 1.67191400

TS(H-transf), trip

Cu 1.41768100 1.62681600 -3.93997500
B -0.62969000 1.65544800 -1.58385200
F -1.75075400 2.44930000 -1.87655300
F 0.52357700 2.27373800 -2.23400600
F -0.38905900 1.54198100 -0.24595000
F -0.82571000 0.39466900 -2.20038700
S 2.65621500 -0.61332700 -4.49368800
O 2.44087000 0.68484100 -5.34734100
O 4.08000200 -0.90047500 -4.28614900
O 1.96036100 -0.08365800 -3.17756200
O 1.84751400 -1.74136600 -5.01671600
O -1.70512100 -0.61117800 -4.82234700
Na -2.79071100 1.14116700 -3.52355300
S -2.42467100 -0.24937400 -6.09060400
O -3.16820500 -1.38426300 -6.68727200
O -3.23977400 0.98036900 -5.85320700
O -1.34473400 0.07252000 -7.21295900
Na -0.07614100 -1.49513400 -3.48314300
O 0.96135800 3.29269600 -4.84532100
C 0.01674700 3.90562100 -5.40594300
C -0.42197300 5.25288800 -4.78061900
C 0.57332000 5.59052100 -3.64706600
H 0.57956000 4.81694300 -2.87776600
H 1.59134000 5.70663700 -4.02822800
H 0.26892700 6.53597800 -3.18939800
C -1.82492200 5.11474700 -4.13016000
H -2.62720600 4.90695100 -4.83984100
H -1.81923800 4.32324000 -3.37622900
H -2.06503100 6.05822400 -3.63031800
C -0.36327400 6.41189700 -5.80670700
H -0.56138800 7.34929200 -5.27881100
H 0.63326100 6.48420200 -6.25308800
H -1.09042700 6.33788700 -6.61543900
N -0.51713600 3.39943300 -6.55885800
C 0.08674400 2.25728100 -7.18191200
C -1.77624400 3.85092500 -7.20973600
C 0.23780500 2.36806400 -8.70109300
H -0.63796300 1.29682800 -7.03360300
H 1.00994100 1.97715300 -6.68261100
C -1.57965200 4.09602600 -8.70805500
H -2.50552100 3.05045200 -7.04363300
C -1.03972600 2.83987700 -9.39785200
H 0.56527800 1.39520500 -9.07912000
H 1.05702000 3.07750900 -8.88913300
H -2.54603700 4.39051900 -9.12977000
H -0.89122100 4.93719300 -8.85433000
H -0.83959900 3.03577900 -10.45590100
H -1.79237400 2.04359100 -9.35314100
H -2.14394500 4.74028600 -6.71604100

[L-OSO_3Na]–[$NaHSO_4$–$CuBF_4$], singlet

Cu 1.45386500 1.78398500 -4.29552300
B -1.29284700 1.80989600 -2.13612300
F -2.66943000 2.06298500 -2.25657600
F -0.61543700 2.83687000 -1.52273700
F -1.07480700 0.57268000 -1.50094900
F -0.81018500 1.66077700 -3.49883200
S 2.80591500 -0.77457000 -3.74333100
O 3.69988400 -0.17265000 -4.74486300
O 3.39994200 -1.61579500 -2.70458300
O 1.86032100 0.27597500 -3.13895400
O 1.77196300 -1.76781500 -4.53281200
O -1.51046300 -0.65265800 -5.17912400
Na -2.81848800 1.34117800 -4.58762500
S -0.84103000 -0.26040700 -6.45171200
O -1.33036900 -0.94753400 -7.65092800
O -1.32601000 1.32440300 -6.55277400
O 0.65044300 -0.19952100 -6.34230700
Na -0.29391700 -0.84829400 -3.14304100
O 1.12250700 3.23541300 -5.49117600
C 0.08520800 3.92142000 -5.68820800
C -0.14580500 5.16774800 -4.80790500
C 0.91657700 5.16310400 -3.68885100
H 0.77927000 4.30931400 -3.02093100
H 1.92964400 5.13733500 -4.09332000
H 0.80091100 6.07598400 -3.09795800
C -1.52682100 5.15046600 -4.11092900
H -2.37330600 5.27857100 -4.78292400
H -1.66452900 4.22289000 -3.55301000
H -1.55462000 5.97591900 -3.39377600
C 0.06579000 6.44726000 -5.65274900
H -0.03729000 7.31932600 -5.00094500

H 1.07287000 6.45948300 -6.07994900
H -0.64665800 6.55968400 -6.47143800
N -0.74427600 3.55770300 -6.70294700
C -0.49437000 2.26194400 -7.31909800
C -2.01643300 4.22374200 -7.06394700
C -0.82455200 2.20439100 -8.80158000
H 0.54155400 1.99643800 -7.14059400
C -2.25646100 4.21719400 -8.57197400
H -2.84151500 3.71171800 -6.55820800
C -2.19357000 2.79582600 -9.12742700
H -0.74363300 1.16148800 -9.11760200
H -0.04193000 2.76682700 -9.32428400
H -3.23335600 4.67515400 -8.75429800
H -1.50242400 4.84456900 -9.06225100
H -2.35735600 2.79046100 -10.20861500
H -2.98265500 2.18280100 -8.67526700
H -1.99059700 5.24402800 -6.70508600
H 1.39588200 -1.26221800 -5.31031400

[(LOH)–$CuBF_4$]–[$NaHSO_4$]$_2$, singlet
Cu 0.91141300 1.31715900 -4.50014300
B -1.91163000 1.58561100 -1.92620300
F -3.23166900 1.87584400 -2.31381200
F -1.30905000 2.65150100 -1.29888500
F -1.86744900 0.41889400 -1.14289600
F -1.19578300 1.27914100 -3.15425100
S 2.48810100 -1.08332800 -3.96937300
O 2.88266000 -0.52383900 -5.27807200
O 3.57555200 -1.46579800 -3.06335500
O 1.46200000 -0.16404100 -3.29234500
O 1.66871900 -2.45792700 -4.23043100
O -2.83768400 -0.51795200 -5.21549400
Na -2.98265500 1.67419200 -4.64634600
S -1.57326000 -1.15090400 -5.67023100
O -1.68472700 -1.92898600 -6.90939300
O -0.52686500 0.07647700 -5.96271400
O -0.87864600 -1.87499600 -4.55232700
Na -0.56111200 -0.95157400 -2.45262100
O 0.88683200 2.90953200 -5.60133900
C 0.00630000 3.79815200 -5.74244000
C -0.07419200 4.93991600 -4.70474800
C 1.09327700 4.76518900 -3.71283600
H 1.02150600 3.81726600 -3.17423000
H 2.06070100 4.80130800 -4.21870100
H 1.05302000 5.57627100 -2.98038800
C -1.37865700 4.89981000 -3.87448300
H -2.29257500 4.88317400 -4.46907800
H -1.38029100 4.02909700 -3.21842400
H -1.41331300 5.79076700 -3.24015800
C 0.11629800 6.30242100 -5.41339200
H 0.21101800 7.08185200 -4.65220000
H 1.03209500 6.30170800 -6.01206200
H -0.71182500 6.58108400 -6.06518900
N -0.75703600 3.77797300 -6.86442700
C -0.44663200 2.78966100 -7.89519800
C -1.99585000 4.54504100 -7.10779400
C -0.45250900 3.41596700 -9.28724200
H 0.53404300 2.37955700 -7.66617400
C -1.97337200 5.22548000 -8.47520300
H -2.82907600 3.83533300 -7.05545800
C -1.73483200 4.19713600 -9.58290200
H -0.27786700 2.62395000 -10.02390500
H 0.41331700 4.08586000 -9.33560400
H -2.92622000 5.74407800 -8.61857000
H -1.18020700 5.98282600 -8.48886400
H -1.65540100 4.68516100 -10.55835500
H -2.58869900 3.51118700 -9.63620800
H -2.13533000 5.27074700 -6.31842100
H 0.73755300 -2.24128600 -4.52365500
O -1.43184200 1.73677200 -7.77267300
H -1.54626400 1.30500000 -8.63227400
H -0.89398900 0.65898600 -6.69775000

[(LNHCO)–$CuBF_4$]–[$NaHSO_4$]$_2$, singlet
Cu 0.79563400 1.46916000 -4.51065500
B -1.49587000 0.48813000 -1.23160300
F -2.83600800 0.86651900 -1.44588000
F -0.95606200 1.11834900 -0.13534100
F -1.39189100 -0.91540300 -1.13496600
F -0.77057300 0.86416700 -2.42638300
S 2.17451500 -0.90822500 -5.54809000
O 1.96137000 0.02830900 -6.67264700
O 3.52912900 -1.44418700 -5.39204400
O 1.63231900 -0.30227300 -4.24706100
O 1.24151100 -2.20926900 -5.79111300
O -3.25998600 -0.33528300 -4.58269700
Na -2.68938800 1.80843000 -3.56497000
S -2.00621000 -0.47369200 -5.35390300
O -2.35952900 -0.82663800 -6.86852500
O -1.24303600 0.81797500 -5.38664000
O -1.17057200 -1.62576600 -4.87832500
Na 0.07139700 -1.38515500 -2.85899600

O 0.46425000 3.36546600 -4.44368300
C -0.26561300 4.13849800 -5.12314200
C -0.39361900 5.59370400 -4.64124500
C 0.61864700 5.82266500 -3.50373800
H 0.45369200 5.13016600 -2.67653500
H 1.64577100 5.69439000 -3.85553400
H 0.50691200 6.84493500 -3.13153500
C -1.82073000 5.76873400 -4.06808700
H -2.59928300 5.64455700 -4.82356700
H -2.00406000 5.04430400 -3.26793400
H -1.91846200 6.77356200 -3.64694200
C -0.10871300 6.63301500 -5.74527400
H -0.07092800 7.62481000 -5.28576700
H 0.85986600 6.44852200 -6.21967100
H -0.87279300 6.66632100 -6.52073800
N -0.95944300 3.64030100 -6.15891400
C -0.47267700 1.29522500 -8.35299600
C -1.77868300 4.29132500 -7.18555400
C 0.22358600 2.46237700 -8.96932800
H 0.17157900 0.51462300 -7.92036400
C -0.99504800 4.70012000 -8.44620700
H -2.56702900 3.58083800 -7.44620300
C -0.68388800 3.59462400 -9.46581500
H 0.81672600 2.03341300 -9.79171900
H 0.97767900 2.80714900 -8.24770500
H -1.58845300 5.46664900 -8.95779600
H -0.06209300 5.18421800 -8.13947100
H -0.19814100 4.06907500 -10.32362100
H -1.61837600 3.16087200 -9.83689400
H -2.26901800 5.16312100 -6.75733300
H 0.29175100 -1.97320000 -5.58864100
O -1.69909400 1.18650300 -8.30654500
H -0.93673900 2.62528800 -6.19581600
H -2.15504900 -0.02105100 -7.46561300

[($NaHSO_4$)$_2$–$CuBF_4$]
Cu 2.27429600 0.98275300 -3.78130100
B 0.98186700 1.82372100 -1.39640100
F 1.13831200 2.43666600 -0.18972900
F 2.13449500 2.14780800 -2.25080700
F 0.96644500 0.41883600 -1.28543800
F -0.16069200 2.26000000 -2.08159100
S 0.81917100 -0.74203300 -5.69786900
O -0.16441300 0.58448900 -5.68391300
O 0.84536100 -1.27398300 -7.05413300
O 2.17108400 -0.22391100 -5.25642600

LNHCO
O -0.40862400 6.47387600 -6.50172600
C -0.90856100 5.35570700 -6.33939000
C -0.98632900 4.72595700 -4.93380300
C 0.46656900 4.44847300 -4.49276300
H 0.92915800 3.69318300 -5.13446900
H 1.06016400 5.36510000 -4.54130300
H 0.47877400 4.07970900 -3.46171200
C -1.80216400 3.42461300 -4.87420800
H -2.83665000 3.57900000 -5.20119400
H -1.34808100 2.63033400 -5.47334900
H -1.83984900 3.06938500 -3.83972400
C -1.62164800 5.77372000 -4.00039800
H -1.61202100 5.40856700 -2.96862500
H -1.06840700 6.71384100 -4.04658400
H -2.66172200 5.97266400 -4.28080500
N -1.37668600 4.63191600 -7.39144000
C 0.38910300 2.40153100 -7.96593000
C -1.47045200 5.20857000 -8.73369200
C 1.29959100 3.37545300 -8.66792300
O 0.57604100 1.96641700 -6.84392900
C -0.12473100 5.41544400 -9.43765500
H -2.10660100 4.54239100 -9.32316500
C 0.65453400 4.15186800 -9.82673400
H 2.11532400 2.75339400 -9.06713100
H 1.75416000 4.03779700 -7.92372100
H -0.33679300 5.98068000 -10.35336600
H 0.49875800 6.05815300 -8.80935900
H 1.45179200 4.45201100 -10.51427900
H 0.00546700 3.47407900 -10.39878700
H -1.97789700 6.17745200 -8.66203100
H -0.46732400 2.03355100 -8.57244500
H -1.90879800 3.79838100 -7.19822700

O 0.18435700 -1.59178800 -4.65996200
O -1.96076800 -0.61545400 -2.47650100
Na -1.47862200 1.41674300 -3.72671600
S -3.01970200 -1.06402300 -3.44768000
O -4.24048700 -1.58207100 -2.82101800
O -3.21803000 -0.01417700 -4.48651600
O -2.39371000 -2.36723400 -4.21164900
Na 0.14459200 -1.43931300 -2.28681700
H -1.50937400 -2.11396100 -4.56936600
H 0.09422000 1.18832400 -6.40265200

References

(1) Blakemore, D. C.; Castro, L.; Churcher, I.; Rees, D. C.; Thomas, A. W.; Wilson, D. M.; Wood, A. *Nat. Chem.* **2018**, *10*, 383–394.

(2) Cernak, T.; Dykstra, K. D.; Tyagarajan, S.; Vachal, P.; Krska, S. W. *Chem. Rev.* **2016**, *45*, 546–576.

(3) Corey, E. J.; Howe, W. J.; Orf, H. W.; Pensak, D. A.; Petersson, G. *J. Am. Chem. Soc.* **1975**, *97*, 6116–6124.

(4) Hoffmann, R. W., *Elements of Synthesis Planning*; Springer: 2009.

(5) Huigens, R. W.; Morrison, K. C.; Hicklin, R. W.; T. A. Flood, J.; Richter, M. F.; Hergenrother, P. J. *Nat. Chem.* **2013**, *5*, 195–202.

(6) Hu, Y.; Stumpfe, D.; Bajorath, J. *J. Med. Chem.* **2017**, *60*, 1238–1246.

(7) Vitaku, E.; Smith, D. T.; Njardarson, J. T. *J. Med. Chem.* **2014**, *57*, 10257–10274.

(8) Lamberth, C. *Pest Manag. Sci.* **2013**, *69*, 1106–1114.

(9) Roque, J. B.; Kuroda, Y.; Göttemann, L. T.; Sarpong, R. *Science* **2018**, *361*, 171–174.

(10) Roque, J. B.; Kuroda, Y.; Göttemann, L. T.; Sarpong, R. *Nature* **2018**, *564*, 244–248.

(11) Jurczyk, J.; Lux, M. C.; Adpressa, D.; Kim, S. F.; Lam, Y.; Yeung, C. S.; Sarpong, R. *Science* **2021**, *373*, 1004–1012.

(12) Onomura, O.; Moriyama, A.; Fukae, K.; Yamamoto, Y.; Maki, T.; Matsumura, Y.; Demizu, Y. *Tetrahedron Lett.* **2008**, *49*, 6728–6731.

(13) Yamamoto, K.; Toguchi, H.; Harada, T.; Kuriyama, M.; Onomura, O. *Heterocycles* **2020**, *101*, 486–495.

(14) He, K.; Zhang, T.; Zhang, S.; Sun, Z.; Zhang, Y.; Yuan, Y.; Jia, X. *Org. Lett.* **2019**, *21*, 5030–5034.

(15) Ito, R.; Umezawa, N.; Higuchi, T. *J. Am. Chem. Soc.* **2005**, *127*, 834–835.

(16) Kaname, M.; Yoshifuji, S.; Sashida, H. *Tetrahedron Lett.* **2008**, *49*, 2786–2788.

(17) Osberger, T. J.; Rogness, D. C.; Kohrt, J. T.; Stepan, A. F.; White, M. C. *Nature* **2016**, *537*, 214–219.

(18) Sperry, J. *Synthesis* **2011**, 3569–3580.

(19) Latimer, W. M., *The oxidation states of the elements and their potentials in aqueous solutions*; Prentice-Hall: 1938.

(20) Minisci, F.; Citterio, A.; Giordano, C. *Acct. Chem. Res.* **1983**, *16*, 27–32.

(21) Mandal, S.; Bera, T.; Dubey, G.; Saha, J.; Laha, J. K. *ACS Catal.* **2018**, *8*, 5085–5144.

(22) Batista, V. F.; Galman, J. L.; Pinto, D. C. G. A.; Silva, A. M. S.; Turner, N. J. *ACS Catal.* **2018**, *8*, 11889–11907.

(23) Cibulka, R.; M. W. Fraaije, E., *Flavin-Based Catalysis: Principles and Applications*; Wiley-VCH: 2021.

(24) Lee, J.; von Gunten, U.; Kim, J.-H. *Environ. Sci. Technol.* **2020**, *54*, 3064–3081.

(25) Metzler, D. E.; Cairns, W. L. *J. Am. Chem. Soc.* **1971**, *93*, 2772–2777.

(26) Kino, K.; Kobayashi, T.; Arima, E.; Komori, R.; Kobayashi, T.; Miyazawa, H. *Bioorg. Med. Chem. Lett.* **2009**, *19*, 2070–2074.

(27) Smith, E. C.; Metzler, D. E. *J. Am. Chem. Soc.* **1963**, *85*, 3285–3288.

(28) Crist, R. H. *J. Am. Chem. Soc.* **1932**, *54*, 3939–3942.

(29) Liu, R.-H.; He, Y.-H.; Yu, W.; Zhou, B.; Han, B. *Org. Lett.* **2019**, *21*, 4590–4594.

(30) Faheem; Kumar, B. K.; Sekhar, K. V. G. C.; Chander, S.; Kunjiappan, S.; Murugesan, S. *RSC Adv.* **2021**, *11*, 12254–12287.

(31) Faheem; Kumar, B. K.; Sekhar, K. V. G. C.; Chander, S.; Kunjiappan, S.; Murugesan, S. *Expert Opin. Drug Discov.* **2021**, *16*, 1119–1147.

(32) Jin, J.; MacMillan, D. W. C. *Angew. Chem. Int. Ed.* **2015**, *54*, 1565–1569.

(33) Kaledin, A. L.; Huang, Z.; Geletii, Y. V.; Lian, T.; Hill, C. L.; Musaev, D. G. *J. Phys. Chem. A* **2009**, *114*, 73–80.

(34) Cismesia, M. A.; Yoon, T. P. *Chem. Sci.* **2015**, *6*, 5426–5434.

(35) Vanýsek, P. Electrochemical Series. In Handbook of Chemistry and Physics 103rd Edition, Rumble, J. R., ed. `https://hbcp.chemnetbase.com/faces/contents/ContentsSearch.xhtml` (accessed 10/18/2021).

(36) Mülhdorf, B.; Wolf, R. *Chem. Commun.* **2015**, *51*, 8425–8428.

(37) Maza, J. C.; Ramsey, A. V.; Mehare, M.; Krska, S.; Parish, C. A.; Francis, M. B. *Org. Biomol. Chem.* **2020**, *18*, 1881–1885.

(38) Hoyt, E. A.; Oliveira, B. L.; Bernardes, G. J. L. *Nat. Rev. Chem.* **2019**, *3*, 147–171.

(39) Li, S. C.; Goto, N. K.; Williams, K. A.; Deber, C. M. *Pro. Natl. Acad. Sci. USA* **1996**, *93*, 6676–6681.

(40) Jacob, J.; Duclohier, H.; Cafiso, D. S. *Biophys. J.* **1999**, *76*, 1367–1376.

(41) Morgan, A. A.; Rubenstein, E. *PLoS ONE* **2013**, *8*, e53785.

(42) Murarka, S. *Adv. Synth. Catal.* **2018**, *360*, 1735–1753.

(43) Roque, J. B.; Sarpong, R.; Musaev, D. G. *J. Am. Chem. Soc.* **2021**, *143*, 3889–3900.

(44) Kaledin, A. L.; Roque, J. B.; Sarpong, R.; Musaev, D. G. *Top. Catal.* **2021**, *65*, 418–432.

(45) Pitts, C. R.; Bloom, S.; Woltornist, R.; Auvenshine, D. J.; Ryzhkov, L. R.; Siegler, M. A.; Lectka, T. *J. Am. Chem. Soc.* **2014**, *136*, 9780–9791.

(46) Subbaraman, L. R.; Santappa, M. *Z. Phys. Chem.* **1966**, *48*, 172–178.

(47) Xie, W.; Zhao, M.; Cui, C. *Organometallics* **2013**, *32*, 7440–7444.

(48) Topczewski, J. J.; Cabrera, P. J.; Saper, N. I.; Sanford, M. S. *Nature* **2016**, *531*, 220–224.

(49) Seebach, D.; Lohmann, J.-J.; Syfrig, M. A.; Yoshifuji, M. *Tetrahedron* **1983**, *39*, 1963–1974.

(50) Rao, Y.; Li, X.; Danishefsky, S. J. *J. Am. Chem. Soc.* **2009**, *131*, 12924–12926.

(51) Metternich, J. B.; Sagebiel, S.; Lückener, A.; Lamping, S.; Ravoo, B. J.; Gilmour, R. *Chem. Eur. J.* **2018**, *24*, 4228–4233.

(52) Vasilopoulos, A.; Krska, S. W.; Stahl, S. S. *Science* **2021**, *372*, 398–403.

(53) Frisch, M. J. et al., *Gaussian 16*; Revision C.01: 2016.

(54) Hay, P. J.; Wadt, W. R. *J. Chem. Phys.* **1985**, *82*, 270–283.

(55) Hay, P. J.; Wadt, W. R. *J. Chem. Phys.* **1985**, *82*, 299–310.

(56) Wadt, W. R.; Hay, P. J. *J. Chem. Phys.* **1985**, *82*, 284–298.

(57) Becke, A. D. *Phys. Rev. A* **1988**, *38*, 3098–3100.

(58) Lee, C.; Yang, W.; Parr, R. G. *Phys. Rev. B* **1988**, *37*, 785–789.

(59) Becke, A. D. *J. Chem. Phys.* **1993**, *98*, 1372–1377.

(60) Grimme, S.; Antony, J.; Ehrlich, S.; Krieg, H. A. *J. Chem. Phys.* **2010**, *132*, 154104.

(61) Becke, A. D.; Johnson, E. R. *J. Chem. Phys.* **2005**, *123*, 154101.

(62) Becke, A. D.; Johnson, E. R. *J. Chem. Phys.* **2005**, *122*, 154104.

(63) Johnson, E. R.; Becke, A. D. *J. Chem. Phys.* **2006**, *124*, 174104.

(64) Barone, V.; Cossi, M. *J. Chem. Phys. A* **1998**, *102*, 1995–2001.

(65) Cossi, M.; Rega, N.; Scalmani, G.; Barone, V. *J. Comput. Chem.* **2003**, *24*, 669–681.

(66) Burke, K.; Werschnik, J.; Gross, E. K. U. *J. Chem. Phys.* **2005**, *123*, 062206.

(67) Haines, B. E.; Musaev, D. G. *ChemCatChem* **2021**, *13*, 1201–1206.

(68) McLarney, B. D.; Hanna, S.; Musaev, D. G.; France, S. *ACS Catal.* **2019**, *9*, 4526–4538.

(69) Sperger, T.; Sanhueza, I. A.; Kalvet, I.; Schoenebeck, F. *Chem. Rev.* **2015**, *115*, 9532–9586.

(70) Ahn, S.; Hong, M.; Sundararajan, M.; Ess, D. H.; Baik, M.-H. *Chem. Rev.* **2019**, *119*, 6509–6560.

Chapter 2

Cyclic Amines as Latent Alkyl Radicals for Molecular Remodeling*

2.1 Introduction

The development of new drugs often relies on testing derivatives of a lead compound. Therefore, the ability to effectively generate structural analogs of a lead compound is central to drug discovery.[1–3] These analogs are typically made by synthesizing each compound through its own unique reaction sequence. However, a much more efficient synthetic strategy would be possible if a single drug candidate could be elaborated to many desired analogs through selective structural remodeling.[4] In this way, only a single synthetic route is required to create a potential drug candidate which can be used as a common intermediate for the generation of several more. Since saturated cyclic aliphatic amines are prevalent in F.D.A.-approved drugs,[5,6] our laboratory has initiated a program aimed at selective structural modification of cyclic amines that would enable the rapid generation of analogs for drug development.[7–9]

Our laboratory has previously demonstrated ring opening and halogenation of cyclic amines to form linear alkyl halides (Figure 2.1, previous work).[8] This process involved sequential C–N and C–C bond cleavage resulting in an alkyl radical that could be halogenated. The alkyl halide served as a functional handle for further structural diversification, including carbon–carbon bond formation. While the overall transformation achieves the desired structural reconfiguration, we wondered whether the alkyl radical intermediate could be utilized directly for bond formation (Figure 2.1, this work). To this end, we envisioned that the radical could be engaged by a radical acceptor or transition metal that would promote value-added bond formation.

Herein, we present the utilization of an alkyl radical arising from the deconstructive functionalization of cyclic amines for skeletal remodeling and heterocycle replacement. Specifically, we have developed a deconstructive Minisci reaction, enabling direct carbon–carbon

*Part of this chapter is adapted from previously published work: *J. Am. Chem. Soc.* **2023**, *145*, 11245–11257.

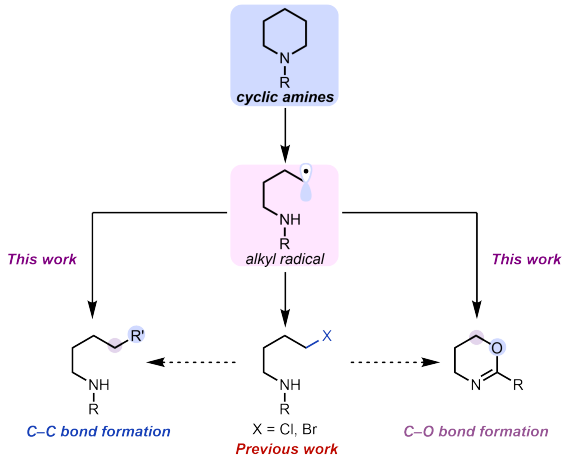

Figure 2.1: Formation of primary alkyl radical through deconstructive functionalization of cyclic amines. Previous work: Formation of alkyl halides as versatile intermediates for structural diversification. This work: Direct use of the alkyl radical for skeletal remodeling.

bond formation following the deconstructive ring opening of cyclic amines, as well as the transformation of cyclic amines into oxazines, constituting a replacement of the *N*-heterocycle. These forms of structural diversification, ring opening and heterocycle replacement,[10,11] are important for structural analog studies because they alter the conformational freedom of a given molecule and add or remove hydrogen bond acceptors and donors, two properties that affect the biological activity of potential drug candidates.[12] Therefore, the described transformations encompass desirable transformations that may provide direct access to structural analogs.

2.2 Results and Discussion

Ring-Opening Minisci Reaction

We envisioned a structural reconfiguration of cyclic amines by combining our deconstructive process with a coupling reaction in a one-pot sequence. To this end, we turned toward Csp^3–Csp^2 bond formation using a radical decarboxylation process and addition of the resulting alkyl radical to a heterocycle acceptor. We have previously demonstrated access to a proposed primary alkyl radical through a series of oxidations with a Ag(I) salt and persulfate oxidant (Scheme 2.1).[8] Therefore, we hypothesized that this radical might engage a coupling partner in carbon-carbon bond forming processes. This type of Csp^3–Csp^2 bond formation has recently been demonstrated in radical additions to quinones through a silver-mediated deconstructive process.[13] Since the conditions for the deconstructive process that lead to an alkyl radical are somewhat acidic (as a result of the formation of hydrogen sulfate ions and

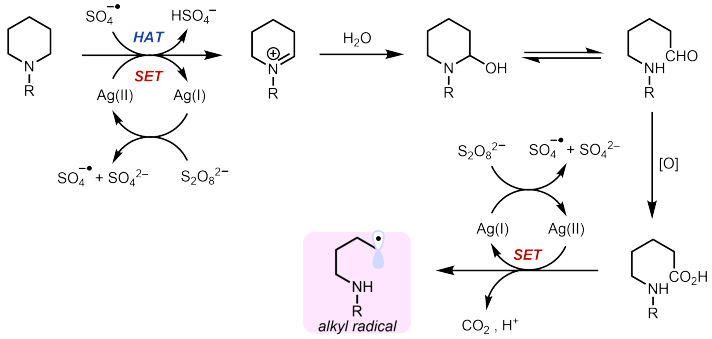

Scheme 2.1: Proposed mechanism for the formation of a primary alkyl radical from cyclic amines through a Ag(I)/persulfate oxidation sequence.

carbonic acid over the course of the reaction sequence), we hypothesized that these conditions would be amenable to Minisci-type reactions,[14] which proceed more favorably upon protonation of a heteroarene acceptor.

Following optimization of the reaction conditions, treatment of Piv-protected piperidine **1a** with the Ag(I)/persulfate conditions and 4-trifluoromethylpyridine under acidic conditions (trifluoroacetic acid) afforded the corresponding amino-alkyl substituted pyridine in 50% yield (Figure 2.2). Pyridines bearing electron donating/withdrawing substituents were also competent in this coupling reaction, forming the desired products (**9a**–**9c**) in moderate yet useful yields (50–67%). We next subjected cyclic amines of various ring sizes (**9d**–**9f**) to the same conditions, again providing the alkylation products in moderate yield (39–62%). A 2-methyl substituted piperidine derivative also underwent the expected ring opening selectively away from the substituted side of the ring (**9g**), selectivity that was also observed with our mild ring-opening oxidation conditions (see Chapter 1) and previous studies.[7,8,13]

Autocyclization Using Cu(II) Oxidation

We also investigated the interception of the proposed alkyl radical intermediate with other transition metals. Particularly, since De La Mare, Kochi, and coworkers[15,16] previously reported the formation of alkenes from alkyl radicals through an oxidation by Cu(II) followed by an elimination, we wondered whether we could gain access to terminal olefins from the primary radical generated by the deconstructive process (Scheme 2.1). However, upon the addition of a Cu(II) source to the Ag(I)/persulfate reagents for the deconstructive functionalization of Piv-protected pyrrolidine, we did not detect any of the expected alkene product. Instead, we observed the formation of an oxazine in 85% yield (Figure 2.3). This heterocycle may arise from oxidation of the alkyl radical by Cu(II) and intramolecular nucleophilic trapping by the amide carbonyl oxygen instead of elimination to generate an olefin. The structure of **10m** was unambiguously confirmed by X-ray crystallography. The formation

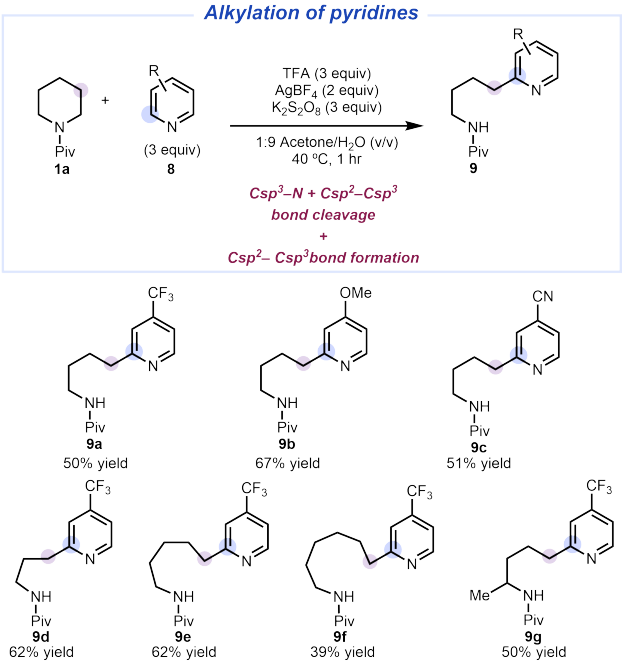

Figure 2.2: Deconstructive Minisci reaction scope. Only isolated yields are shown. See Section 2.4 for full details.

of these oxazine heterocycles has previously been reported from the autocyclization of γ-bromo alkyl amides.[17] We extended the transformation to the ring opening and subsequent cyclization of N-Bz-pyrrolidine (**1v**) to provide phenyl-substituted oxazine **10v** in 40% yield. The transformation of pyrrolidines to oxazines represents an effective strategy to access new chemical space in medicinal chemistry.

Since the formation of the oxazines did not align with our initial hypothesis, we embarked upon an examination of the mechanism for their formation using DFT calculations, as summarized in Figure 2.4.† We have previously investigated a mechanism for the generation of an alkyl radical from a cyclic amine using Ag(I) and persulfate.[8,18] Here, we propose that the alkyl radical is similarly formed prior to interacting with Cu(II) to form complex **11**, although the exact details continue to be investigated. While the combination of a carbon-centered radical with Cu(II) is often depicted as a Cu(III) intermediate,[19,20] we recognize that these types of copper complexes may have an electronic structure that reflects a Cu(I) center, in which a formal reduction of Cu(II) occurs.[21] Our calculations suggest that deprotonation to form the alkene has an associated barrier of 9.7 kcal/mol, while the competing intramolecular cyclization is essentially barrierless. Even though **11** is hydrated and the concentration of H_2O is 500 times higher than the copper complex, calculations

†Calculations were performed by Bohyun Park and Mu-Hyun Baik at the Korea Advanced Institute of Science and Technology (KAIST) Department of Chemistry, Daejeon 34141 Korea.

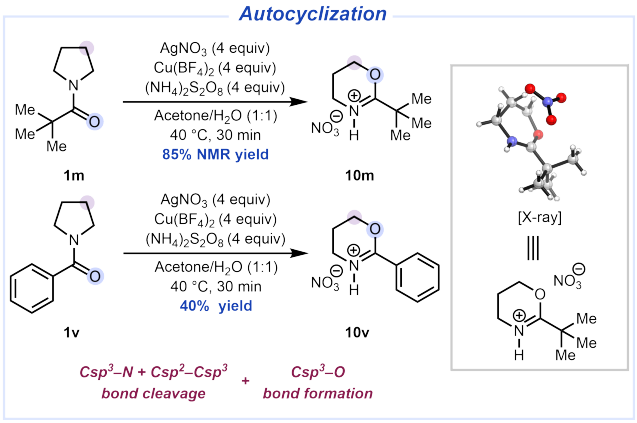

Figure 2.3: Autocyclization of cyclic amines. Isolated yields are shown unless otherwise noted. See Section 2.4 for full experimental details and crystallographic data.

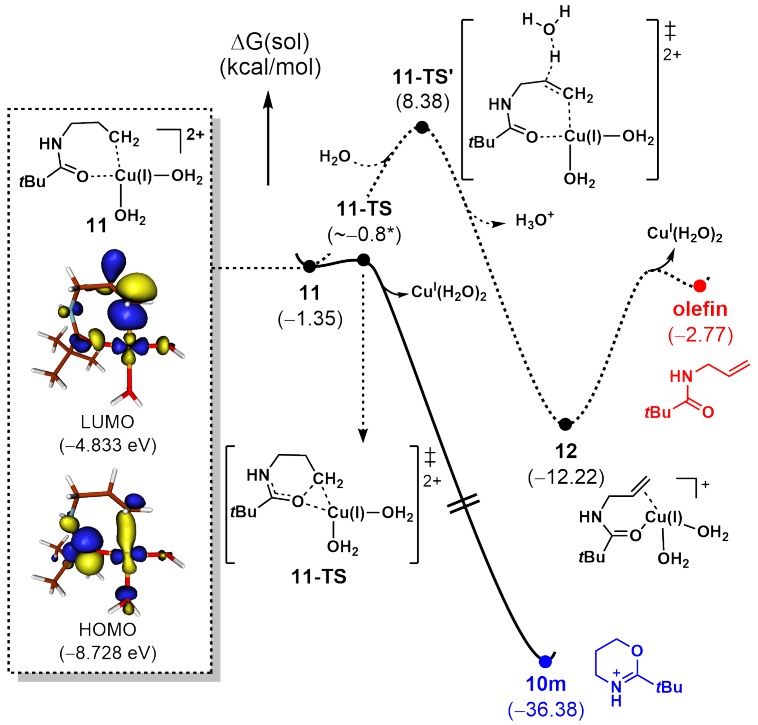

Figure 2.4: Free energy profile for oxazine formation by Cu(II) oxidation. See Section 2.4 for full computational details.

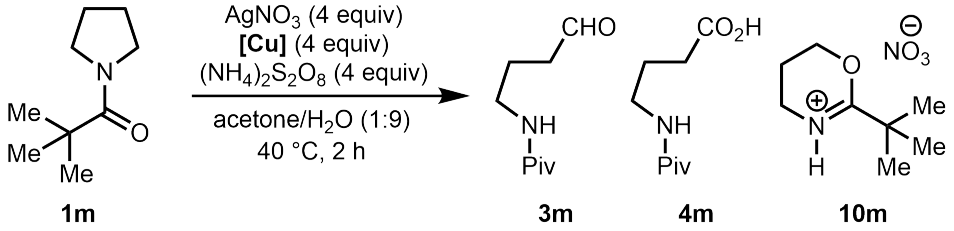

[Cu]	recovered 1m [%]	3m yield [%]	4m yield [%]	10m yield [%]
$CuCl_2$	33	3	5	—
$CuBr_2$	69	3	3	—
$Cu(OAc)_2{\cdot}H_2O$	16	9	15	3
$CuSO_4{\cdot}5H_2O$	—	—	13	12
$Cu(MeCN)_4BF_4$	—	—	46	6

Table 2.1: Product distribution for the autocyclization reaction with various copper salts. Conversion and yields were determined by ^{1}H NMR integration using Ph_3CH as an internal standard.

suggest that the intrinsic reaction rate of cyclization should be about 5×10^6 times faster than deprotonation (see Section 2.4 for details). Therefore, the cyclization should be the dominant pathway. Indeed, a screen of various copper salts, which would otherwise lead to products such as olefination and halogenation of primary alkyl radicals,[16] revealed that only the linear aldehyde **3m**, carboxylic acid **4m**, and cyclization product **10m** could be obtained (see Table 2.1). The rapid cyclization can also be rationalized on the basis of the frontier molecular orbitals of **11**. While the orbitals of **11** are all interacting, there is a prominent interaction between the HOMO and LUMO orbitals that informs the observed cyclization to oxazine **10m**. As shown in Figure 2.4, the shape of the nucleophilic HOMO on the amidyl oxygen and the low energy LUMO on the primary alkyl in **11** are reasonably well matched for the favorable intramolecular HOMO–LUMO interaction.[22]

2.3 Conclusion

We have developed a ring-opening C–C bond formation process that takes advantage of a decarboxylative Csp^3–Csp^2 Minisci coupling reaction. While our laboratory previously reported the formation of alkyl halides through a similar transformation that could serve as precursors for C–C bond formation,[8] the Minisci process reported here provides direct access to value-added C–C coupled products. A second study aimed at a one-pot, multi-metallic, decarboxylative transformation led to the formation of oxazines. Additional investigations to expand the scope of oxazine formation from cyclic amines are ongoing in our lab.

In the studies presented here, persulfate emerged as a versatile oxidant that could be

tuned by pairing with various oxidation mediators to selectively oxidize various substrates. The multiple means by which the peroxy bond can be homolyzed, in combination with the oxidation potential and H-atom abstraction ability of the sulfate radical anion, allow for many different oxidative processes. The versatility of cyclic amines as substrates for late-stage diversification as reported here rests on their ability to serve as latent alkyl radicals. These studies, as well as previous reports from our laboratories and others, demonstrate high potential for skeletal modification of cyclic amines by the generation of an alkyl radical through oxidative ring opening. Other pathways for structural diversification of cyclic aliphatic amines are currently under investigation in our lab.

2.4 Experimental Section

Solvents and Reagents

Tetrahydrofuran (THF) and triethylamine (Et_3N) were sparged with argon and dried by passing through alumina columns using argon in a Glass Contour solvent purification system. Dichloromethane (CH_2Cl_2) was freshly distilled over calcium hydride under a N_2 atmosphere prior to each use. DMF was purchased in Aldrich Sure/Seal™ bottles. N-Boc-piperidine (**1a.a**) was obtained from Aldrich and used as received. Reagents were purchased from commercial vendors as follows: Riboflavin (RTA, 98%) was purchased from Alfa Aesar. Silver nitrate ($AgNO_3$, ≥99%) was purchased from Sigma-Aldrich. Ammonium persulfate ($(NH_4)_2S_2O_8$, ACS Reagent) was purchased from J. T. Baker Chemicals, potassium persulfate ($K_2S_2O_8$, ACS Reagent) was purchased from Fisher Scientific, and sodium persulfate ($Na_2S_2O_8$, 98+%) was purchased from Acros Organics. Acetonitrile (HPLC), acetone (HPLC) and water (HPLC) were purchased from Fisher Scientific.

Experimental Procedures

Unless otherwise noted in the experimental procedures, reactions were carried out in flame or oven-dried glassware under a positive pressure of N_2 in anhydrous solvents using standard Schlenk techniques. Reaction temperatures above room temperature (22–23 °C) were controlled by an IKA® temperature modulator and monitored using glass thermometers. Reaction progress was monitored using a combination of LC/MS analysis (using a Shimadzu LCMS-2020 (UFLC) equipped with the LC-20AD solvent delivery system, a SPD-20AV prominence UV/Vis detector (SPD-M20A Photo Diode Array), and a Thermo Scientific Hypersil GOLD HPLC column (5 µm particle size, 4.6 × 50 mm)), and thin-layer chromatography (TLC) on Macherey-Nagel (MN) silica gel plates (glass backed, 60 Å, 0.25 mm thickness, UV254 manganese-activated zinc silicate fluorescence indicator). Visualization of the developed plates was performed under UV-light (254 nm) irradiation, and then gently heated with *p*-anisaldehyde or cerium ammonium molybdate (CAM) stain. Flash column chromatography was performed with either glass columns using Silicycle silica gel (40–63 μm particle size) or using a Yamazen Smart Flash EPCLC W-Prep 2XY (dual channel) automated flash chromatography system on prefilled, premium, universal columns using ACS grade solvents. Preparative thin layer chromatography was performed on SiliCycle Siliaplates (glass backed, extra hard layer, 60 Å, 250 μm thickness, F254 indicator).

Analytical Instrumentation

^{1}H NMR and ^{13}C NMR data were recorded on Bruker AVQ-400, AVB-400, AV-600, and AV-700 spectrometers using $CDCl_3$ as solvent, typically at 20–23 °C. Chemical shifts (δ) are reported in ppm relative to the residual solvent signal (δ 7.26 for ^{1}H NMR, δ 77.16 for ^{13}C NMR in $CDCl_3$). ^{19}F NMR spectra were acquired on an AVQ-400 spectrometer and internally referenced to $CFCl_3$ (δ 0.00). Data for ^{1}H and ^{13}C spectroscopy are reported as follows; chemical shift (δ ppm), multiplicity (s = singlet, d = doublet, t = triplet, q = quartet, quint = quintet, hept = heptet, m = multiplet, br = broad), coupling constant (Hz), integration. High-resolution mass spectra (HRMS) were analyzed as MeOH solutions (30–50 μM) using a Finnigan LTQ FT mass spectrometer (Thermo). Solutions were injected

directly into the ion source via syringe pump with 5 uL/min flow rate. Xcalibur software (version 2.0.7, Thermo) was used for both spectra acquisition and data analysis.

Preparation of *N*-Protected Cyclic Amines

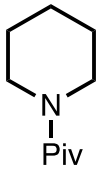

1a

2,2-dimethyl-1-(piperidin-1-yl)propan-1-one (**1b**) was prepared according to a published procedure.[23] Spectral data were in full agreement with the reported literature values.

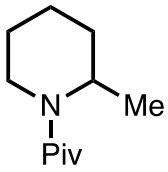

1g

2,2-dimethyl-1-(2-methylpiperidin-1-yl)propan-1-one (**1g**) was prepared according to a published procedure.[8] Spectral data were in full agreement with the reported literature values.

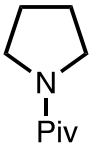

1m

2,2-dimethyl-1-(pyrrolidin-1-yl)propan-1-one (**1m**) was prepared according to a published procedure.[24] Spectral data were in full agreement with the reported literature values.

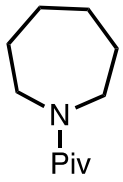

1n

1-(azepan-1-yl)-2,2-dimethylpropan-1-one (**1n**) was prepared according to a published procedure.[8] Spectral data were in full agreement with the reported literature values.

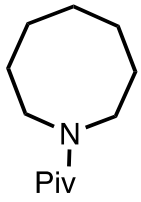

1o

1-(azocan-1-yl)-2,2-dimethylpropan-1-one (**1o**) was prepared according to a published procedure.[8] Spectral data were in full agreement with the reported literature values.

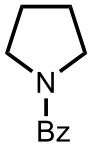

1v

phenyl(pyrrolidin-1-yl)methanone (**1v**) was prepared according to a published procedure.[25] Spectral data were in full agreement with the reported literature values.

Procedure for Deconstructive Minisci Reaction

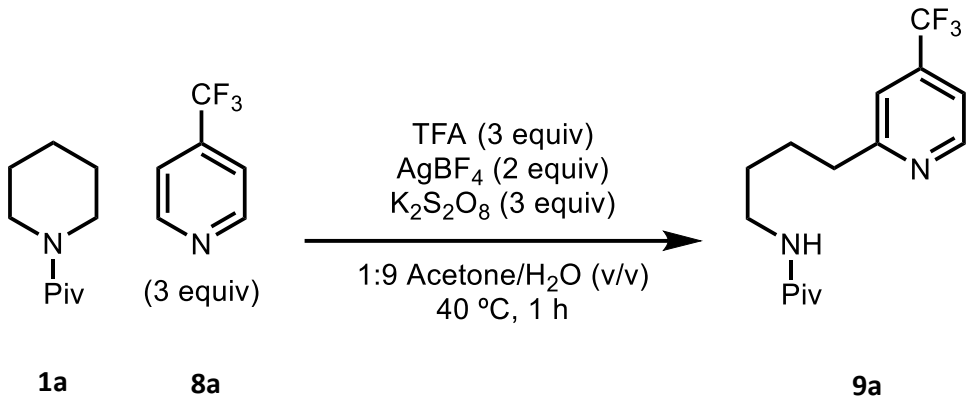

A 1-dram vial was charged with **1a** (33.9 mg, 0.20 mmol), **8a** (88.3 mg, 0.60 mmol), and 2.0 mL of a 1:9 acetone:H_2O solution by volume. Trifluoroacetic acid (46 µL, 0.60 mmol) was added to the mixture, and the contents were allowed to stir for 5 min. Potassium persulfate (162 mg, 0.60 mmol) and silver tetrafluoroborate (78 mg, 0.40 mmol) were added and the mixture was allowed to stir at 40 °C. After 1 h, CH_2Cl_2 (2.0 mL) was added and the phases were separated. The aqueous layer was extracted with CH_2Cl_2 (2.0 mL × 3). The combined organic layers were dried over Na_2SO_4, filtered, and concentrated under reduced pressure. The resulting crude mixture was purified by preparative thin-layer chromatography (50% EtOAc/hexanes) to provide *N*-(4-(4-(trifluoromethyl)pyridin-2-yl)butyl)pivalamide (**9a**) (29 mg, 48%) as a yellow oil.

^{1}H NMR (700 MHz, $CDCl_3$) δ 8.71 (d, J = 5.2 Hz, 1H), 7.40 (s, 1H), 7.37 (d, J = 5.2 Hz, 1H), 5.84 (s, 1H), 3.28 (td, J = 7.0, 5.7 Hz, 2H), 2.92 (t, J = 7.7 Hz, 2H), 1.84 – 1.75 (m, 2H), 1.57 (p, J = 7.2 Hz, 2H), 1.17 (s, 9H).

^{13}C NMR (176 MHz, $CDCl_3$) δ 178.7, 163.4, 149.8, 139.3 (q, J = 34.2 Hz), 122.9 (q, J = 273.3 Hz), 118.9 (q, J = 3.7 Hz), 117.2 (q, J = 3.4 Hz), 39.3, 38.8, 37.4, 29.2, 27.7, 26.9.

^{19}F NMR (376 MHz, $CDCl_3$) δ -64.07 (s, 3F).

HRMS (ESI): Calc'd for $C_{15}H_{22}F_3N_2O$ $[M+H]^+$: 303.1679, found: 303.1687.

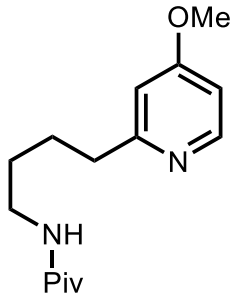

9b

N-(4-(4-Methoxypyridin-2-yl)butyl)pivalamide (**9b**): The title compound was prepared according to the representative procedure using **1a** and **8b**. Purification by preparative thin-layer chromatography (8% MeOH/CH_2Cl_2) provided the title compound (35.7 mg, 67%) as a yellow oil.
^{1}H NMR (700 MHz, $CDCl_3$) δ 8.4 (d, J = 5.6 Hz, 1H), 6.7 (dt, J = 8.1, 2.4 Hz, 2H), 5.9 (s, 1H), 3.9 (s, 3H), 3.3 (td, J = 6.9, 5.5 Hz, 2H), 2.8 (t, J = 7.6 Hz, 2H), 1.8 – 1.8 (m, 2H), 1.6 (p, J = 7.2 Hz, 2H), 1.2 (s, 9H);
^{13}C NMR (126 MHz, $CDCl_3$) δ 178.6, 166.3, 163.5, 150.3, 108.9, 107.7, 55.2, 39.5, 38.8, 37.8, 29.0, 27.8, 27.1;
HRMS (ESI): Calc'd for $C_{15}H_{25}N_2O_2$ $[M+H]^+$: 265.1911, found: 265.1910.

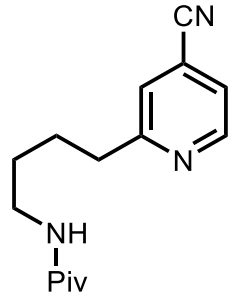

9c

N-(4-(4-cyanopyridin-2-yl)butyl)pivalamide (**9c**): The title compound was prepared according to the representative procedure using **1a** and **8c**. Purification by preparative thin-layer chromatography (5% MeOH/CH_2Cl_2) provided the title compound (26.7 mg, 51%) as a colorless oil.
^{1}H NMR (400 MHz, $CDCl_3$) δ 8.73 (dd, J = 5.1, 0.9 Hz, 1H), 7.43 (s, 1H), 7.39 (dd, J = 5.0, 1.5 Hz, 1H), 5.88 (s, 1H), 3.30 (td, J = 6.9, 5.6 Hz, 2H), 2.91 (t, J = 7.6 Hz, 2H), 1.79 (tt, J = 8.9, 6.9 Hz, 2H), 1.64 – 1.39 (m, 2H), 1.21 (s, 9H).

^{13}C NMR (101 MHz, $CDCl_3$) δ 178.8, 163.6, 150.1, 124.7, 122.7, 121.0, 116.7, 39.2, 38.7, 37.5, 29.1, 27.7, 26.7.
HRMS (ESI): Calc'd for $C_{15}H_{22}N_3O$ $[M+H]^+$: 260.1758, found: 260.1758.

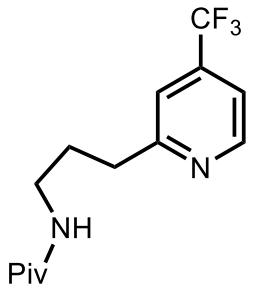

9d

N-(3-(4-(trifluoromethyl)pyridin-2-yl)propyl)pivalamide (**9d**): The title compound was prepared according to the representative procedure using **1m** and **8a**. Purification by preparative thin-layer chromatography (50% EtOAc/hexanes) provided the title compound (35.8 mg, 62%) as a yellow oil.
^{1}H NMR (500 MHz, $CDCl_3$): δ 8.69 (d, J = 5.2 Hz, 1H), 7.37 (s, 1H), 7.34 (d, J = 5.2 Hz, 1H), 6.11 (s, 1H), 3.31 (q, J = 6.6 Hz, 2H), 2.92 (t, J = 7.4 Hz, 2H), 1.99 (p, J = 7.1 Hz, 2H), 1.17 (s, 9H);
^{13}C NMR (126 MHz, $CDCl_3$) δ 178.7, 163.1, 150.3, 138.9 (q, J = 33.9 Hz), 122.9 (q, J = 273.1 Hz), 118.7 (q, J = 3.6 Hz), 117.0 (q, J = 3.5 Hz), 39.2, 38.8, 35.7, 28.9, 27.7.
^{19}F NMR (470 MHz, $CDCl_3$) δ -64.85 (s, 3F);
HRMS (ESI): Calc'd for $C_{14}H_{20}F_3N_2O$ $[M+H]^+$: 289.1522, found: 289.1531.

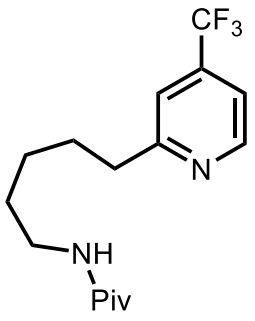

9e

N-(5-(4-(Trifluoromethyl)pyridin-2-yl)pentyl)pivalamide (**9e**): The title compound was prepared according to the representative procedure using **1n** and **8a**. Purification by

preparative thin-layer chromatography (50% EtOAc/hexanes) provided the title compound (32.8 mg, 52%) as a yellow oil.

^{1}H NMR (500 MHz, $CDCl_3$) δ 8.68 (d, J = 5.1 Hz, 1H), 7.34 (s, 1H), 7.32 (dd, J = 5.1, 1.6 Hz, 1H), 5.62 (s, 1H), 3.23 (td, J = 7.2, 5.7 Hz, 2H), 2.92 – 2.79 (m, 2H), 1.85 – 1.73 (m, 2H), 1.54 (p, J = 7.3 Hz, 2H), 1.43 – 1.33 (m, 2H), 1.16 (s, 9H).

^{13}C NMR (126 MHz, $CDCl_3$) δ 178.5, 163.8, 150.3, 138.7 (q, J = 33.7 Hz), 123.0 (q, J = 273.1 Hz), 118.4 (q, J = 3.6 Hz), 116.8 (q, J = 3.6 Hz), 39.4, 38.8, 38.3, 29.6, 29.3, 27.7, 26.6.

^{19}F NMR (470 MHz, $CDCl_3$) δ -64.82 (s, 3F).

HRMS (ESI): Calc'd for $C_{16}H_{24}F_3N_2O$ $[M+H]^+$: 317.1836, found: 317.1835.

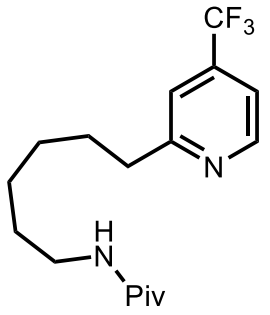

9f

N-(6-(4-(Trifluoromethyl)pyridin-2-yl)hexyl)pivalamide (**9f**): The title compound was prepared according to the representative procedure using **1o** and **8a**. Purification by preparative thin-layer chromatography (50% EtOAc/hexanes) provided the title compound (26.1 mg, 39%) as a yellow oil.

^{1}H NMR (500 MHz, $CDCl_3$) δ 8.71 (d, J = 5.2 Hz, 1H), 7.37 (s, 1H), 7.34 (d, J = 4.9 Hz, 1H), 5.62 (s, 1H), 3.22 (td, J = 7.3, 5.7 Hz, 2H), 2.90 – 2.84 (m, 2H), 1.76 (p, J = 7.3 Hz, 2H), 1.51 (p, J = 7.3 Hz, 2H), 1.38 (qd, J = 9.8, 9.3, 4.1 Hz, 4H), 1.19 (s, 9H).

^{13}C NMR (151 MHz, $CDCl_3$) δ 178.5, 164.0, 150.2, 138.8, 126.2 – 119.8 (m), 118.5 (q, J = 4.0, 3.5 Hz), 116.9 (q, J = 3.4 Hz), 39.6, 38.8, 38.3, 31.1, 29.6, 29.0, 27.8, 26.7.

^{19}F NMR (376 MHz, $CDCl_3$) δ -64.01 (s, 3F).

HRMS (ESI): Calc'd for $C_{17}H_{26}F_3N_2O$ $[M+H]^+$: 331.1992, found: 331.1991.

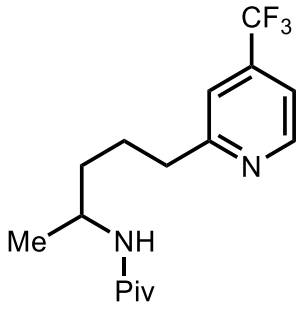

9g

N-(5-(4-(Trifluoromethyl)pyridin-2-yl)pentan-2-yl)pivalamide (**9g**): The title compound was prepared according to the representative procedure using **1g** and **8a**. Purification by preparative thin-layer chromatography (50% EtOAc/hexanes) provided the title compound (31.8 mg, 50%) as a yellow oil.

^{1}H NMR (500 MHz, $CDCl_3$) δ 8.61 (d, J = 5.2 Hz, 1H), 7.27 (s, 1H), 7.24 (dd, J = 5.2, 1.6 Hz, 1H), 5.42 – 5.32 (m, 1H), 3.95 (dq, J = 8.4, 6.6 Hz, 2H), 2.80 (qdd, J = 13.9, 8.7, 6.6 Hz, 2H), 1.68 (dddt, J = 18.3, 13.9, 8.9, 6.6 Hz, 2H), 1.47 – 1.35 (m, 2H), 1.09 (s, 9H), 1.03 (d, J = 6.6 Hz, 3H).

^{13}C NMR (126 MHz, $CDCl_3$) δ 177.9, 163.6, 150.2, 138.8 (q, J = 33.6 Hz), 123.0 (q, J = 273.1 Hz), 118.6 (q, J = 3.5 Hz), 116.9 (q, J = 3.5 Hz), 44.8, 38.7, 38.0, 36.6, 27.7, 26.2, 21.1.

^{19}F NMR (470 MHz, $CDCl_3$) δ -64.84 (s, 3F).

HRMS (ESI): Calc'd for $C_{16}H_{24}F_3N_2O$ $[M+H]^+$: 317.1835, found: 317.1836.

Procedure for Autocyclization Reaction

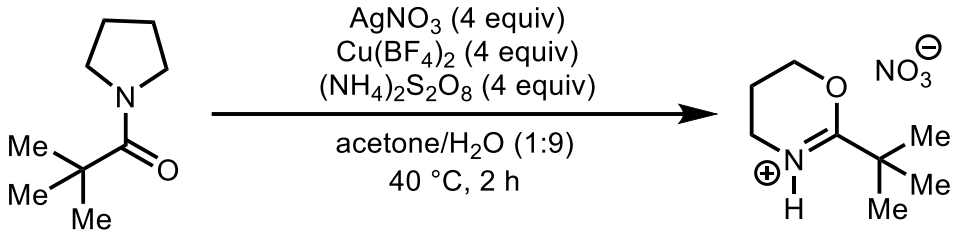

1m **10m**

2-(*tert*-Butyl)-5,6-dihydro-4*H*-1,3-oxazine (10m): To a 1-dram vial was added, sequentially, cyclic amine **1m** (31.1 mg, 0.20 mmol, 1 equiv), silver nitrate (136 mg, 0.80 mmol, 4 equiv), copper(II) tetrafluoroborate (190 mg, 0.80 mmol, 4 equiv), ammonium persulfate (183 mg, 0.80 mmol, 4 equiv) and 1 ml of a 1:1 acetone:H_2O solution. The resulting mixture was then stirred at 40 °C for 2 h. The reaction mixture was diluted with water (0.5 mL) and extracted with 3 x 3 mL of diethylether and the organic layers were discarded. The aqueous layer was then extracted with DCM (3 x 3 mL) and the combined DCM layers were dried over Na_2SO_4, filtered, and concentrated under reduced pressure, affording the title compound as a white solid (26.5 mg, 65%).

^{1}H NMR (500 MHz, $CDCl_3$) δ 10.1 (s, 1H), 4.7 (t, J = 5.5 Hz, 2H), 3.7 (d, J = 5.9 Hz, 2H), 2.2 (p, J = 5.7 Hz, 2H), 1.3 (d, J = 1.3 Hz, 9H).
^{13}C NMR (126 MHz, $CDCl_3$) δ 182.0, 70.0, 39.4, 39.1, 26.3, 18.7.
HRMS (ESI): Calc'd for $C_8H_{16}NO$ $[M+H]^+$: 142.1226, found: 142.1227.

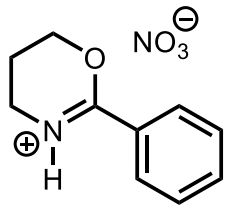

10v

2-phenyl-5,6-dihydro-4*H*-1,3-oxazine (10v): The title compound was prepared according to the representative procedure using phenyl(piperidin-1-yl)methanone (**1m**). Preparative TLC (1:1 Et_2O/DCM) afforded the title compound **10v** (18.0 mg, 40%) as a white solid.

^{1}H NMR (500 MHz, $CDCl_3$) δ 11.54 (s, 1H), 8.01 – 7.93 (m, 2H), 7.67 (td, J = 7.4, 1.2 Hz, 1H), 7.51 (t, J = 8.0 Hz, 2H), 4.81 (t, J = 5.4 Hz, 2H), 3.83 (t, J = 6.0 Hz, 2H), 2.30 (p, J = 5.8 Hz, 2H).
^{13}C NMR (126 MHz, $CDCl_3$) δ 168.9, 135.7, 129.5, 128.5, 125.4, 70.2, 39.6, 19.1.
HRMS (ESI): Calc'd for $C_{10}H_{12}NO$ $[M+H]^+$: 162.0913, found: 162.0914.

Computational Details

General Computational Considerations for Computations in Figure 2.4

All calculations were conducted using DFT[26] implemented in the Gaussian 09 suite[27] of ab initio quantum chemistry programs with Becke's three-parameter exchange functional B3LYP including Grimme's D3 dispersion correction with Becke-Johnson damping levels of theory.[28–34] Geometry optimizations were conducted using Pople's 6-31G(d,p) basis set for main group elements.[35–40] Copper was modeled using the Los Alamos ECP plus DZ basis (LANL2DZ) that includes relativistic effective core potentials.[41] The energies of the optimized structures were reevaluated by additional single-point calculations on each optimized geometry using the same functional and Pople's 6-311++G(d,p) basis set.[42–45] Copper was remodeled for single-point calculations using Stuttgart group effective core potential SDD.[46] Solvation effects were adopted at the same level of single-point calculations and at the self-consistent reaction field polarizable continuum model (IEF-PCM) with a dielectric constant of 78.3553 for water.[47] The Gibbs free energies were computed with the following equations.

$$G(sol) = \varepsilon(sol) + G(corr) \quad (1)$$

$$G(corr) = H(corr) - TS(tot) \quad (2)$$

$$H(corr) = E(tot) + k_BT \quad (3)$$

$$E(tot) = E(t)+E(r)+E(v)+E(e) \quad (4)$$

$$S(tot) = S(t)+S(r)+S(v)+S(e) \quad (5)$$

$$\Delta E(SCF) = \Sigma E(SCF) \text{ for products} - \Sigma E(SCF) \text{ for reactants} \quad (6)$$

$$\Delta G(sol) = \Sigma G(sol) \text{ for products} - \Sigma G(sol) \text{ for reactants} \quad (7)$$

E(sol) is the electronic energy in solution phase computed from the SCF (self-consisted field) procedure with the IEF-PCM calculations; G(sol) is the free energy in solution phase; G(corr) is the thermal correction to the free energy; T is the temperature (298.15 K); S(tot) is the entropy; E(tot) is the total internal thermal energy; E(t), E(r), E(v), and E(e) are the internal thermal energies from translation, rotation, vibration, and electronic motions, respectively; S(t), S(r), S(v), and S(e) are the entropies from translation, rotation, vibration, and electronic motions, respectively; The entropy we refer to is specifically of the solute(s), and the entropy of the solvent is implicitly comprised in the continuum solvation model.

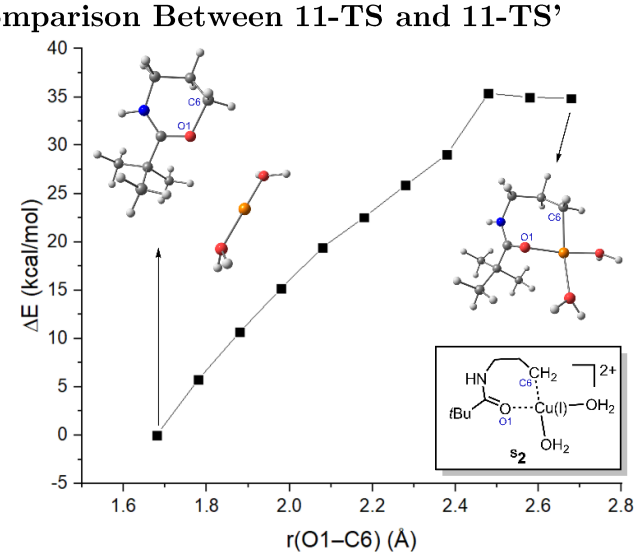

Figure 2.4.1: Electronic energy surface plot for the cyclization of **11** toward dihydro-oxazine (**10m**) with respect to the O1–C6 distance.

To investigate the reaction rate for the cyclization of **11** toward the cyclized product, dihydro-oxazine (**10m**), we have conducted a potential energy surface scan from **11** to **10m** with respect to the O1–C6 bond length as shown in Figure 2.4.1. However, despite our efforts with various methods, the transition state calculations for the cyclization did not converge. Instead, we assumed that the transition might require free energy of about 0.5 kcal/mol, which is the electronic energy difference between two points at r(O1–C6) = 2.68 Å (**11**) and at r(O1–C6) = 2.48 Å (**11-TS** in Figure 2.4.1). Because of this uncertainty, we denoted the $\Delta G(sol)$ for **11-TS** as ~–0.8 in Figure 2.4.1.

More significant is the relative reaction rate for the cyclization as compared to the rate of deprotonation. On the basis of transition state theory, the equilibrium constant for the quasi-equilibrium, $K^{\ddagger}$, can be written as,

$$K^{\ddagger} = \exp(-\Delta G^{\ddagger}/RT)$$

The ratio [**11-TS**]/[**11**] is then estimated to be $\exp(-(0.5\times4182\ J)/(8.3145\ J\cdot K^{-1}\times298.15\ K))\fallingdotseq0.43$. Whereas, for the deprotonation, the ratio [**11-TS'**]/[**11**] is calculated to be $[H_2O]\times\exp(-(9.73\times4182\ J)/(8.3145\ J\cdot K^{-1}\times298.15\ K))\fallingdotseq4.13\times10^{-6}$, where $[H_2O] = 55.6$. The rate constant $k^{\ddagger}$ for the bimolecular reaction is known to be generally much lower than that of the unimolecular reaction, we posit that the cyclization of **11** is at least 10^5 times faster than the deprotonation.

3.9 Energy Components for Optimized Structures in Figure 2.4

Table 2.4.1: Computed energy components for optimized structures.

	E(sol)(SCF)/(Hartree)	**Thermal Correction to G/(Hartree)**
	B3LYP-D3 /6-311++G(d,p)/SDD	B3LYP-D3 /6-31G(d,p)/LANL2DZ
$Cu^{I}(H_2O)_2$	-350.17225	0.01968
H_2O	-76.26704	0.00371
H_3O^+	-76.85586	0.01528
CO	-113.35032	-0.01411
11	-794.62020	0.23612
11-TS'	-871.08488	0.25297
12	-794.25191	0.22776
olefin	-444.04010	0.18358
10m	-444.48969	0.20236

X-ray Crystallographic Data

X-ray Analysis of 10m

A colorless block 0.12 x 0.08 x 0.05 mm in size was mounted on a Cryoloop with Paratone oil. Data were collected in a nitrogen gas stream at 100(2) K using omega scans. Crystal-to-detector distance was 30.23 mm and exposure time was 0.50 seconds per frame at low and 2.00 seconds at high angles, using a scan width of 0.5°. Data collection was 100% complete to 74.000° in θ. A total of 61459 reflections were collected covering the indices -21<=h<=21, -21<=k<=21, -8<=l<=8. 1204 reflections were found to be symmetry independent, with an R_{int} of 0.0652. Indexing and unit cell refinement indicated a primitive, tetragonal lattice. The space group was found to be P 42/m b c (No. 135). The data were integrated using the CrysAlis^{Pro} 1.171.40.68a software program and scaled using the SCALE3 ABSPACK scaling algorithm. Solution by intrinsic phasing (SHELXT-2015) produced a heavy-atom phasing model consistent with the proposed structure. All non-hydrogen atoms were refined anisotropically by full-matrix least-squares (SHELXL-2014). All hydrogen atoms were placed using a riding model. Their positions were constrained relative to their parent atom using the appropriate HFIX command in SHELXL-2014.

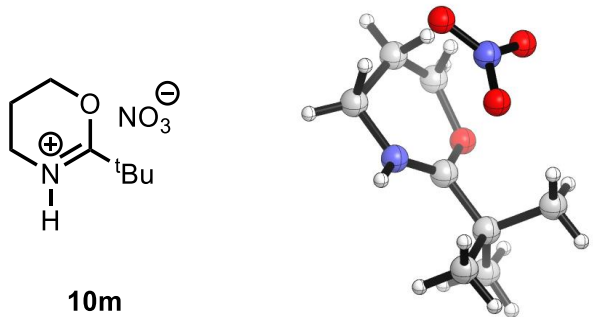

10m

This crystal structure has been deposited at the Cambridge Crystallographic Data Center under CCDC 2128702.

Table 2.4.2: Crystal data and structure refinement for JRoque_David.

Identification code	JRoque_David	
Empirical formula	C8 H16 N2 O4	
Formula weight	204.23	
Temperature	150(2) K	
Wavelength	1.54184 Å	
Crystal system	Tetragonal	
Space group	P 42/m b c	
Unit cell dimensions	a = 17.20020(10) Å	a= 90°.

	b = 17.20020(10) Å	b= 90°.
	c = 6.94210(10) Å	g = 90°.
Volume	2053.80(4) Å^3	
Z	8	
Density (calculated)	1.321 Mg/m^3	
Absorption coefficient	0.893 mm^{-1}	
F(000)	880	
Crystal size	0.120 x 0.080 x 0.050 mm^3	
Theta range for data collection	3.634 to 79.180°.	
Index ranges	-21<=h<=21, -21<=k<=21, -8<=l<=8	
Reflections collected	61459	
Independent reflections	1204 [R(int) = 0.0652]	
Completeness to theta = 74.000°	99.8 %	
Absorption correction	Semi-empirical from equivalents	
Max. and min. transmission	1.00000 and 0.55325	
Refinement method	Full-matrix least-squares on F^2	
Data / restraints / parameters	1204 / 0 / 99	
Goodness-of-fit on F^2	1.175	
Final R indices [I>2sigma(I)]	R1 = 0.0598, wR2 = 0.1451	
R indices (all data)	R1 = 0.0608, wR2 = 0.1457	
Extinction coefficient	n/a	
Largest diff. peak and hole	0.278 and -0.359 e.Å^{-3}	

Table 2.4.3: Atomic coordinates (x 10^4) and equivalent isotropic displacement parameters (Å^{2}x 10^3) for jroque_david. U(eq) is defined as one third of the trace of the orthogonalized U^{ij} tensor.

	x	y	z	U(eq)
O(1)	7080(1)	5330(1)	5000	34(1)
N(1)	8120(1)	4507(1)	5000	33(1)
N(2)	8130(2)	4606(1)	0	43(1)
O(4)	8791(1)	4837(1)	0	73(1)
O(2)	8016(1)	3891(1)	0	87(1)
C(4)	7382(1)	4630(1)	5000	28(1)
O(3)	7588(2)	5080(1)	0	83(1)
C(7)	8711(2)	5137(2)	5000	41(1)
C(2)	6768(1)	3996(2)	5000	34(1)
C(1)	7127(2)	3191(2)	5000	47(1)
C(3)	6268(2)	4101(1)	3207(5)	67(1)
C(6)	8324(2)	5882(2)	4215(6)	37(1)
C(5)	7600(2)	5995(2)	5361(10)	36(2)

Table 2.4.4: Bond lengths [Å] and angles [°] for jroque_david.

O(1)-C(4)	1.310(3)
O(1)-C(5)	1.474(4)
N(1)-C(4)	1.286(3)
N(1)-C(7)	1.485(3)
N(1)-H(1)	0.88(4)
N(2)-O(4)	1.205(3)
N(2)-O(3)	1.239(3)
N(2)-O(2)	1.246(3)
C(4)-C(2)	1.518(3)
C(7)-C(6)	1.544(4)
C(7)-H(7A)	0.9900
C(7)-H(7B)	0.9900
C(2)-C(1)	1.517(4)
C(2)-C(3)	1.523(3)
C(2)-C(3)#1	1.523(3)
C(1)-H(1A)	0.99(3)
C(1)-H(1B)	1.02(3)
C(3)-H(3A)	0.9800
C(3)-H(3B)	0.9800
C(3)-H(3C)	0.9800
C(6)-C(5)	1.490(6)
C(6)-H(6A)	0.9900
C(6)-H(6B)	0.9900
C(5)-H(5A)	0.9900
C(5)-H(5B)	0.9900
C(4)-O(1)-C(5)	118.2(2)
C(4)-N(1)-C(7)	123.7(2)
C(4)-N(1)-H(1)	124(2)
C(7)-N(1)-H(1)	112(2)
O(4)-N(2)-O(3)	119.6(3)
O(4)-N(2)-O(2)	118.3(3)
O(3)-N(2)-O(2)	122.1(3)
N(1)-C(4)-O(1)	122.8(2)
N(1)-C(4)-C(2)	124.6(2)
O(1)-C(4)-C(2)	112.5(2)
N(1)-C(7)-C(6)	108.1(2)
N(1)-C(7)-H(7A)	110.1
C(6)-C(7)-H(7A)	110.1
N(1)-C(7)-H(7B)	110.1

C(6)-C(7)-H(7B)	110.1
H(7A)-C(7)-H(7B)	108.4
C(1)-C(2)-C(4)	111.9(2)
C(1)-C(2)-C(3)	109.71(16)
C(4)-C(2)-C(3)	107.95(15)
C(1)-C(2)-C(3)#1	109.71(16)
C(4)-C(2)-C(3)#1	107.95(15)
C(3)-C(2)-C(3)#1	109.6(3)
C(2)-C(1)-H(1A)	107.1(19)
C(2)-C(1)-H(1B)	110.9(13)
H(1A)-C(1)-H(1B)	109.4(16)
C(2)-C(3)-H(3A)	109.5
C(2)-C(3)-H(3B)	109.5
H(3A)-C(3)-H(3B)	109.5
C(2)-C(3)-H(3C)	109.5
H(3A)-C(3)-H(3C)	109.5
H(3B)-C(3)-H(3C)	109.5
C(5)-C(6)-C(7)	106.3(3)
C(5)-C(6)-H(6A)	110.5
C(7)-C(6)-H(6A)	110.5
C(5)-C(6)-H(6B)	110.5
C(7)-C(6)-H(6B)	110.5
H(6A)-C(6)-H(6B)	108.7
O(1)-C(5)-C(6)	108.3(3)
O(1)-C(5)-H(5A)	110.0
C(6)-C(5)-H(5A)	110.0
O(1)-C(5)-H(5B)	110.0
C(6)-C(5)-H(5B)	110.0
H(5A)-C(5)-H(5B)	108.4

Symmetry transformations used to generate equivalent atoms:
#1 x,y,-z+1

Table 2.4.5: Anisotropic displacement parameters ($Å^2$x 10^3)for jroque_david. The anisotropic displacement factor exponent takes the form: $-2p^2[h^2a^{*2}U^{11} + ... + 2 h k a^* b^* U^{12}]$

	U^{11}	U^{22}	U^{33}	U^{23}	U^{13}	U^{12}
O(1)	26(1)	21(1)	56(1)	0	0	-2(1)
N(1)	25(1)	23(1)	51(1)	0	0	-1(1)
N(2)	41(1)	26(1)	61(2)	0	0	6(1)
O(4)	39(1)	39(1)	143(3)	0	0	-3(1)
O(2)	44(1)	26(1)	191(4)	0	0	4(1)
C(4)	26(1)	22(1)	37(1)	0	0	-2(1)
O(3)	51(2)	36(1)	162(3)	0	0	18(1)
C(7)	24(1)	28(1)	71(2)	0	0	-6(1)
C(2)	23(1)	23(1)	54(2)	0	0	-4(1)
C(1)	31(1)	23(1)	87(3)	0	0	-3(1)
C(3)	62(2)	42(1)	96(2)	11(1)	-41(2)	-18(1)
C(6)	35(2)	26(2)	49(2)	3(2)	-2(2)	-6(1)
C(5)	35(2)	21(1)	53(6)	-3(2)	0(2)	-7(1)

Table 2.4.6: Hydrogen coordinates (x 10^4) and isotropic displacement parameters ($Å^2$x 10^3) for jroque_david.

	x	y	z	U(eq)
H(7A)	9157	4989	4176	49
H(7B)	8904	5226	6325	49
H(3A)	6001	4604	3268	100
H(3B)	5883	3682	3142	100
H(3C)	6599	4084	2059	100
H(6A)	8675	6334	4370	44
H(6B)	8198	5822	2831	44
H(5A)	7727	6027	6749	44
H(5B)	7341	6485	4975	44
H(1A)	6692(19)	2813(19)	5000	40(9)
H(1B)	7459(15)	3108(13)	3810(40)	58(8)
H(1)	8330(20)	4050(20)	5000	48(10)

Table 2.4.7: Torsion angles [°] for jroque_david.

C(7)-N(1)-C(4)-O(1)	0.0
C(7)-N(1)-C(4)-C(2)	180.0
C(5)-O(1)-C(4)-N(1)	-11.1(3)
C(5)-O(1)-C(4)-C(2)	168.9(3)
C(4)-N(1)-C(7)-C(6)	-21.79(18)
N(1)-C(4)-C(2)-C(1)	0.0
O(1)-C(4)-C(2)-C(1)	180.0
N(1)-C(4)-C(2)-C(3)	-120.80(18)
O(1)-C(4)-C(2)-C(3)	59.20(18)
N(1)-C(4)-C(2)-C(3)#1	120.80(18)
O(1)-C(4)-C(2)-C(3)#1	-59.20(18)
N(1)-C(7)-C(6)-C(5)	51.9(3)
C(4)-O(1)-C(5)-C(6)	44.2(5)
C(7)-C(6)-C(5)-O(1)	-63.1(4)

Symmetry transformations used to generate equivalent atoms:
#1 x,y,-z+1

NMR Spectral Data

NMR Spectra – Minisci Products

N-(4-(4-(trifluoromethyl)pyridin-2-yl)butyl)pivalamide

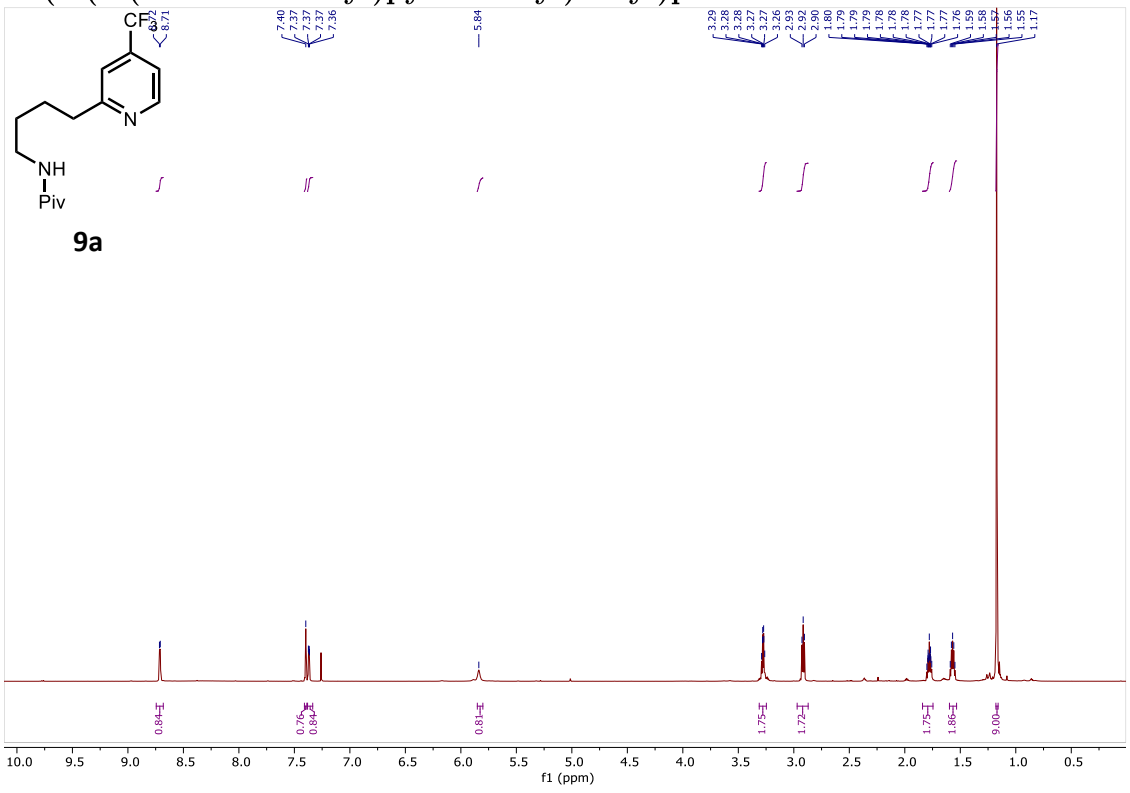

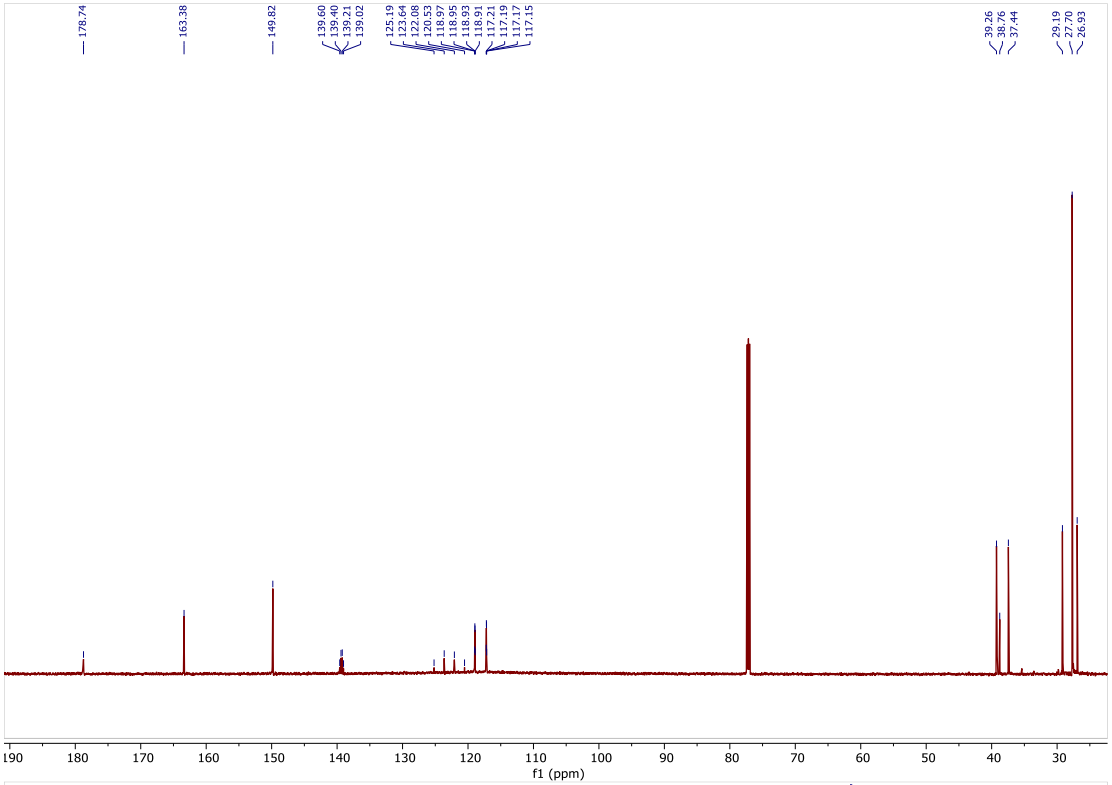
178.74
163.38
149.82
139.60
139.40
139.21
139.02
125.19
123.64
122.08
120.53
118.97
118.95
118.93
118.91
117.21
117.19
117.17
117.15
39.26
38.76
37.44
29.19
27.70
26.93
f1 (ppm)

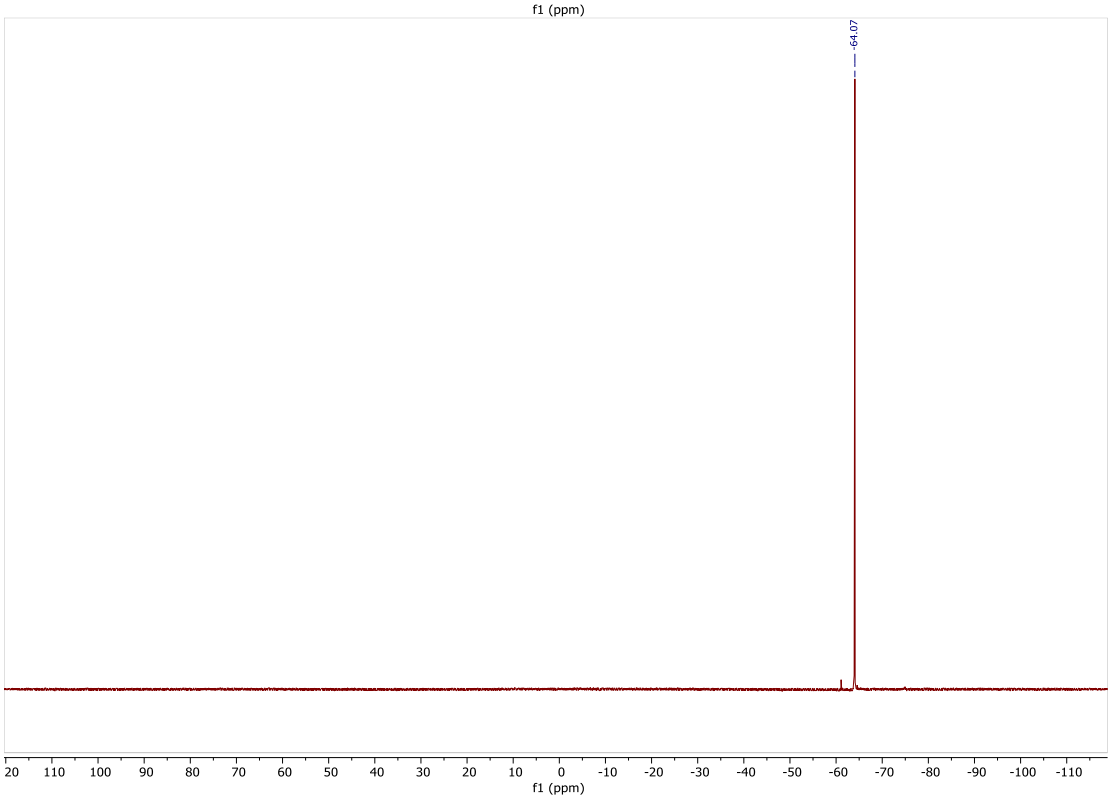
-64.07
f1 (ppm)

N-(4-(4-methoxypyridin-2-yl)butyl)pivalamide

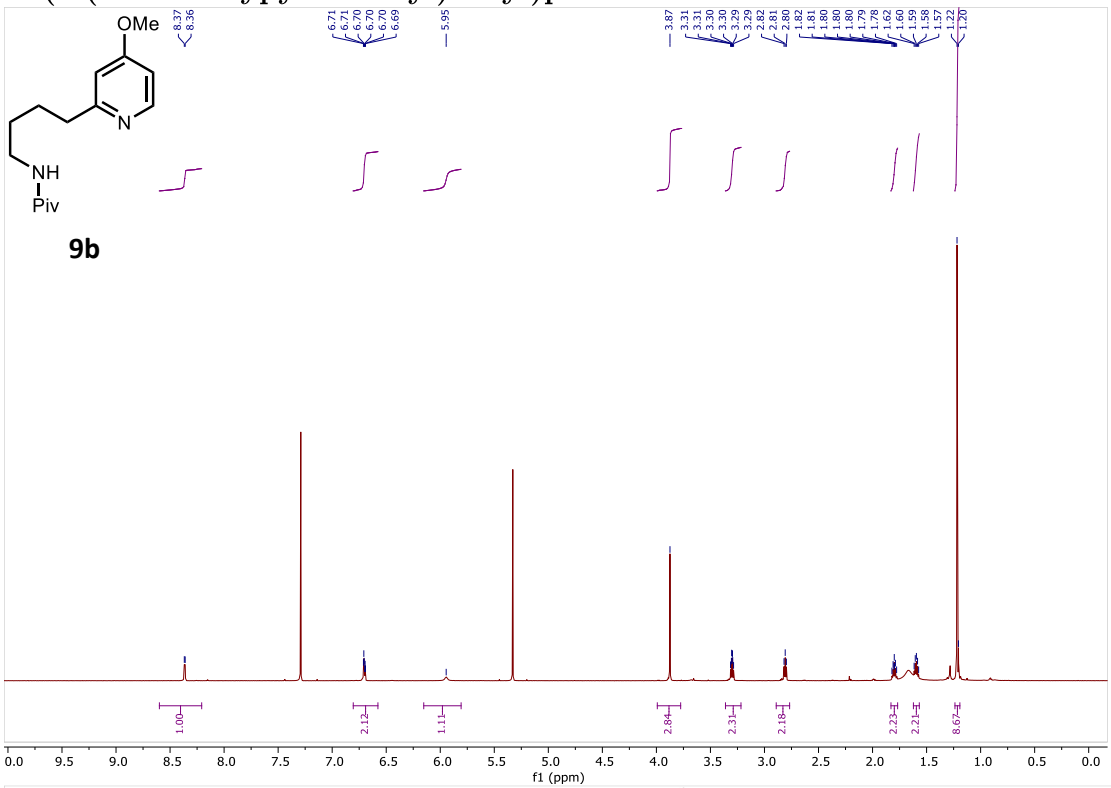

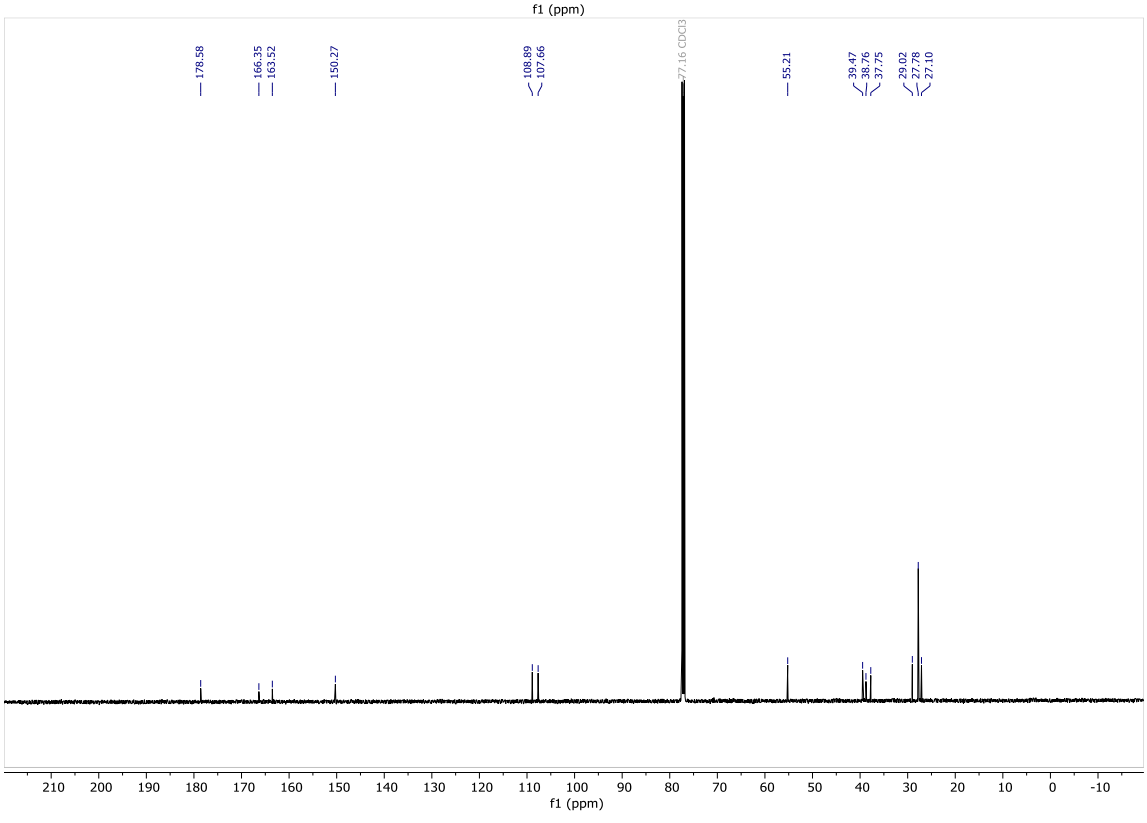

N-(4-(4-cyanopyridin-2-yl)butyl)pivalamide

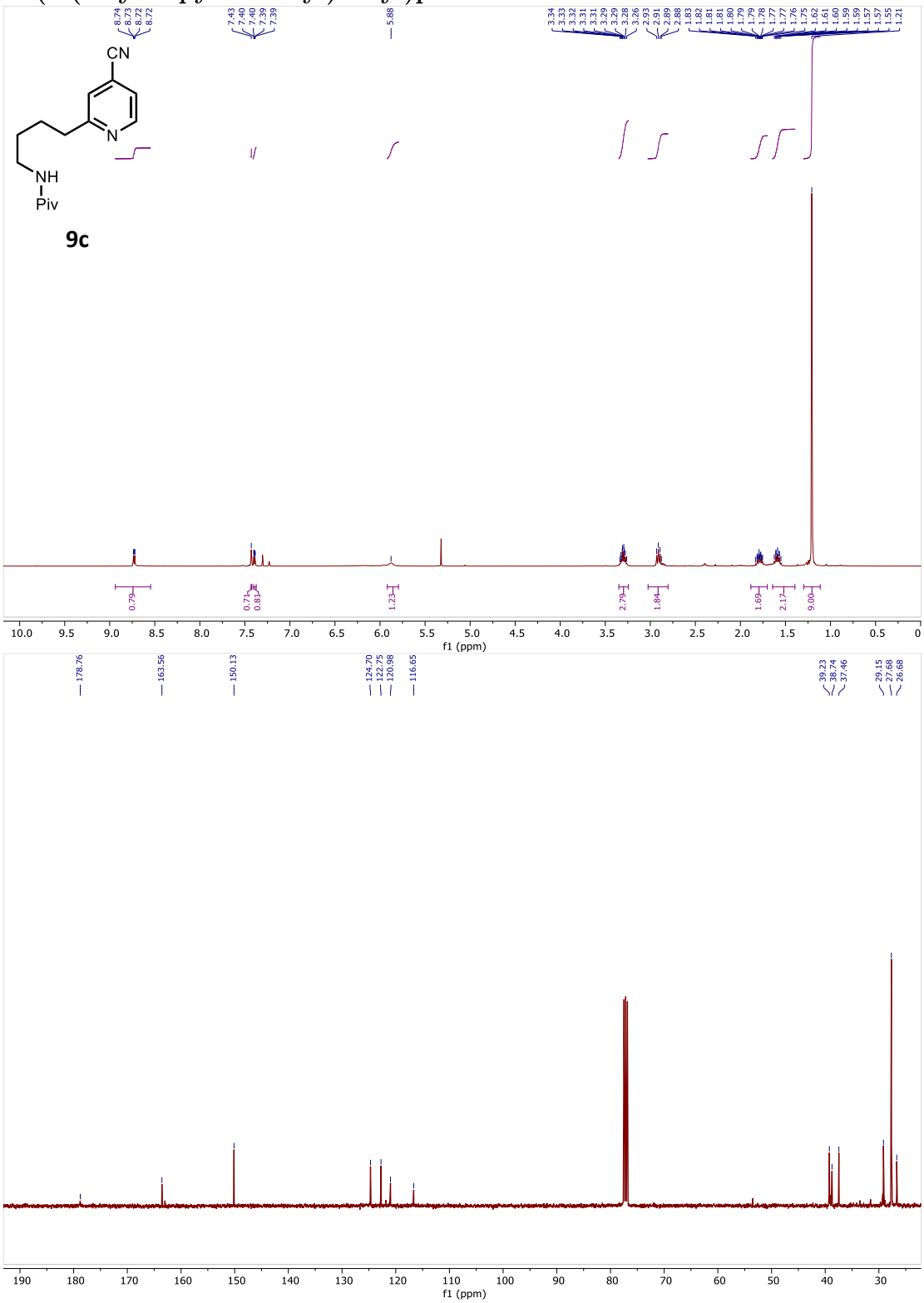

N-(3-(4-(trifluoromethyl)pyridin-2-yl)propyl)pivalamide

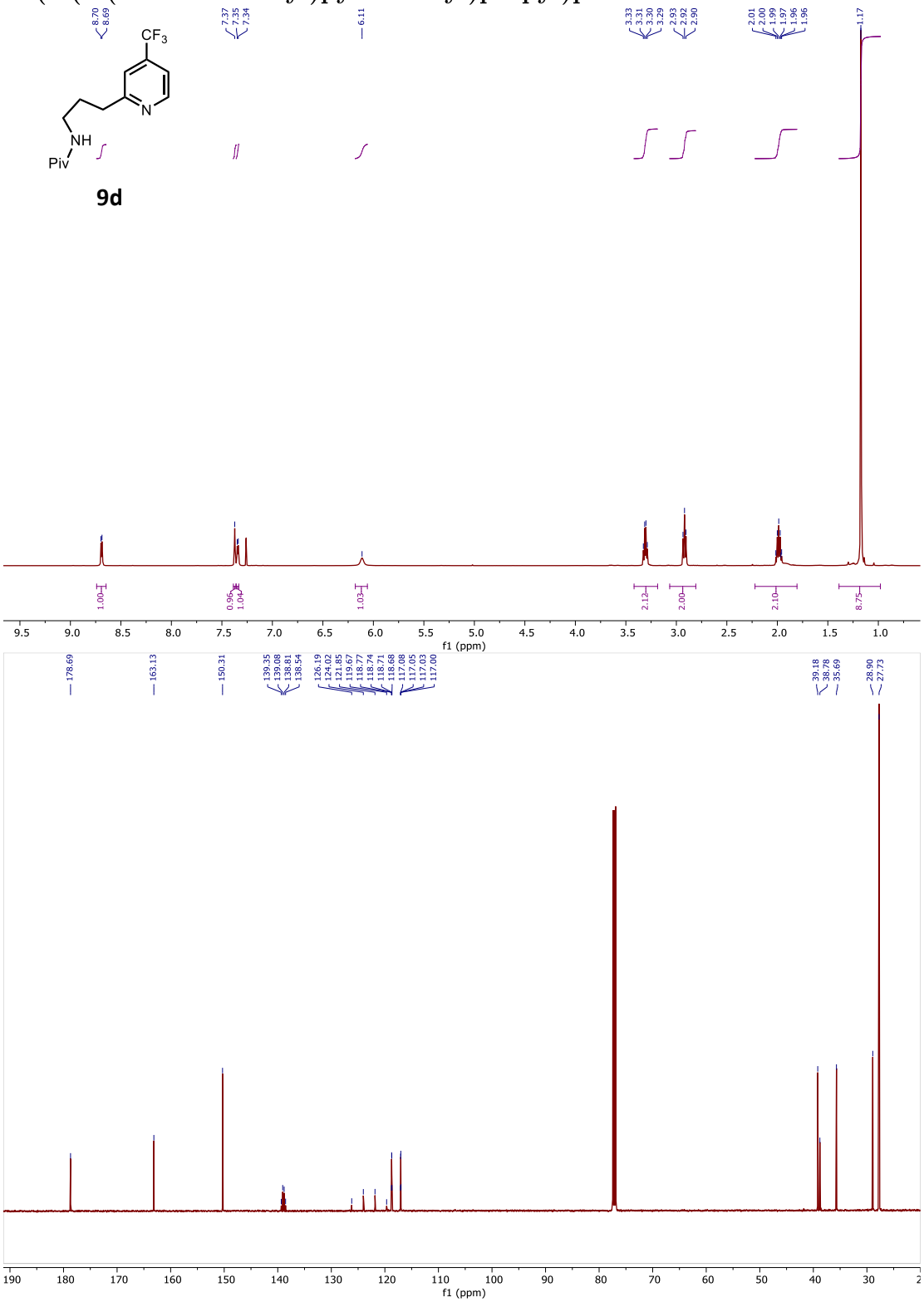

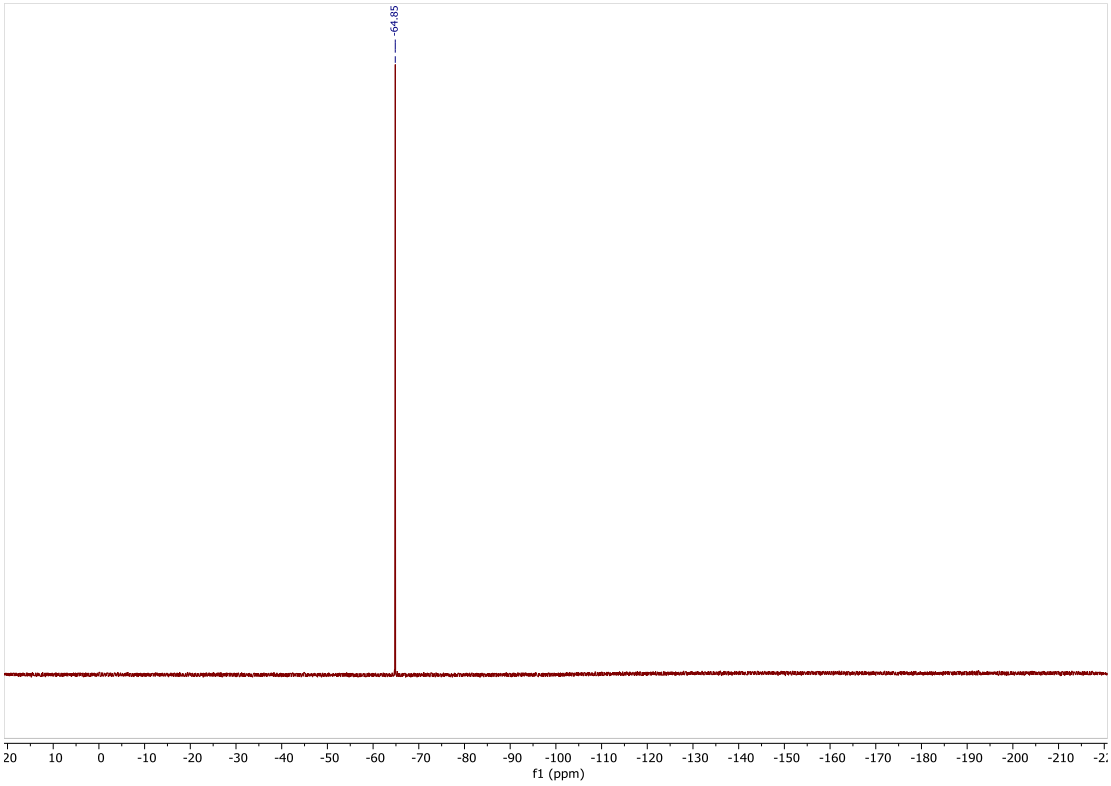
-64.85
20 10 0 -10 -20 -30 -40 -50 -60 -70 -80 -90 -100 -110 -120 -130 -140 -150 -160 -170 -180 -190 -200 -210
f1 (ppm)

N-(5-(4-(trifluoromethyl)pyridin-2-yl)pentyl)pivalamide

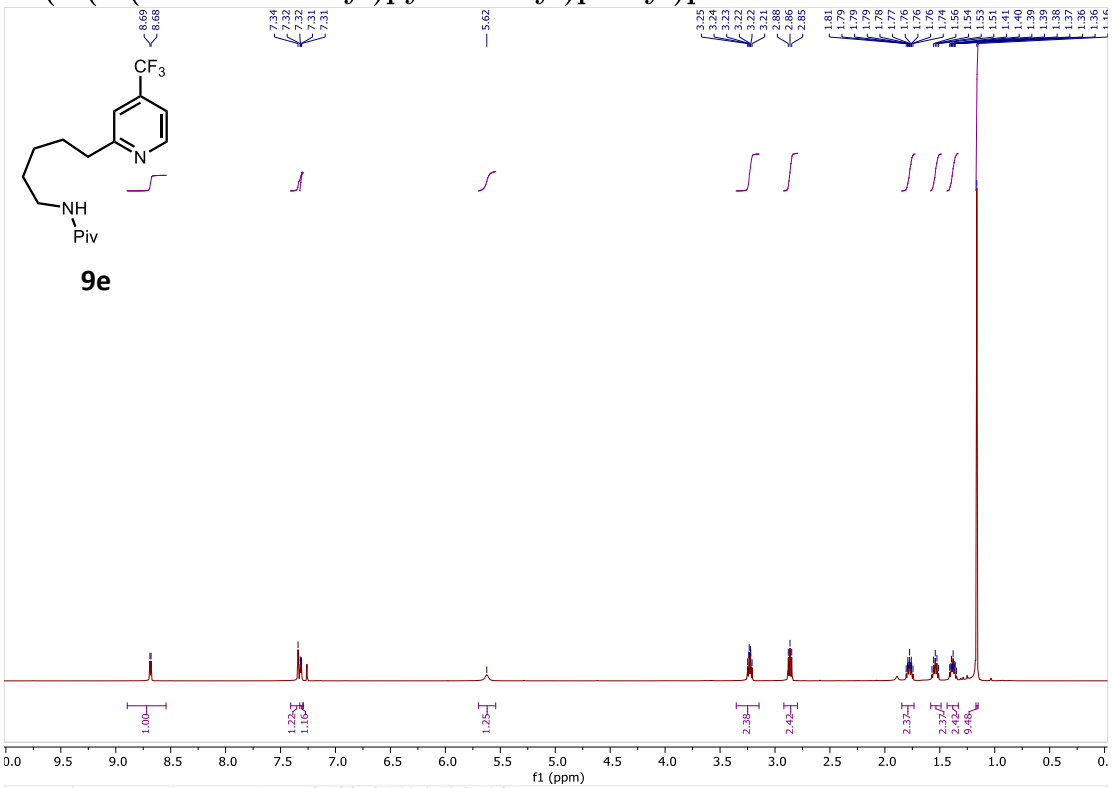

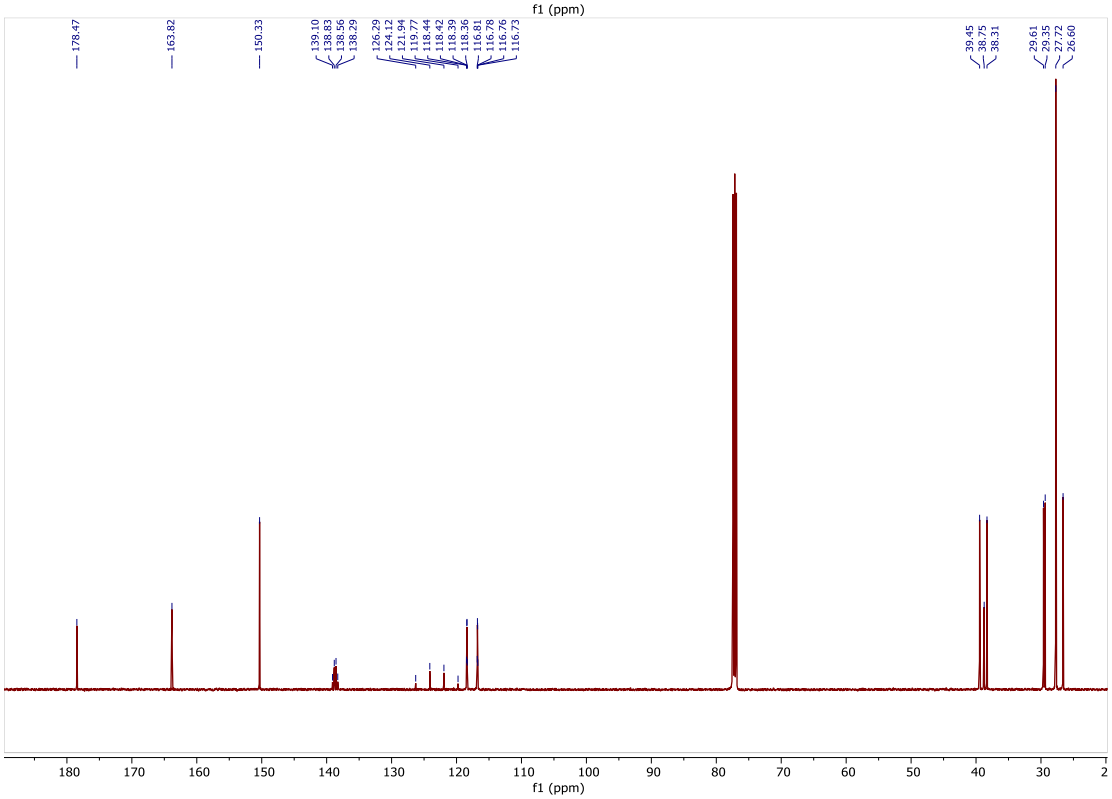

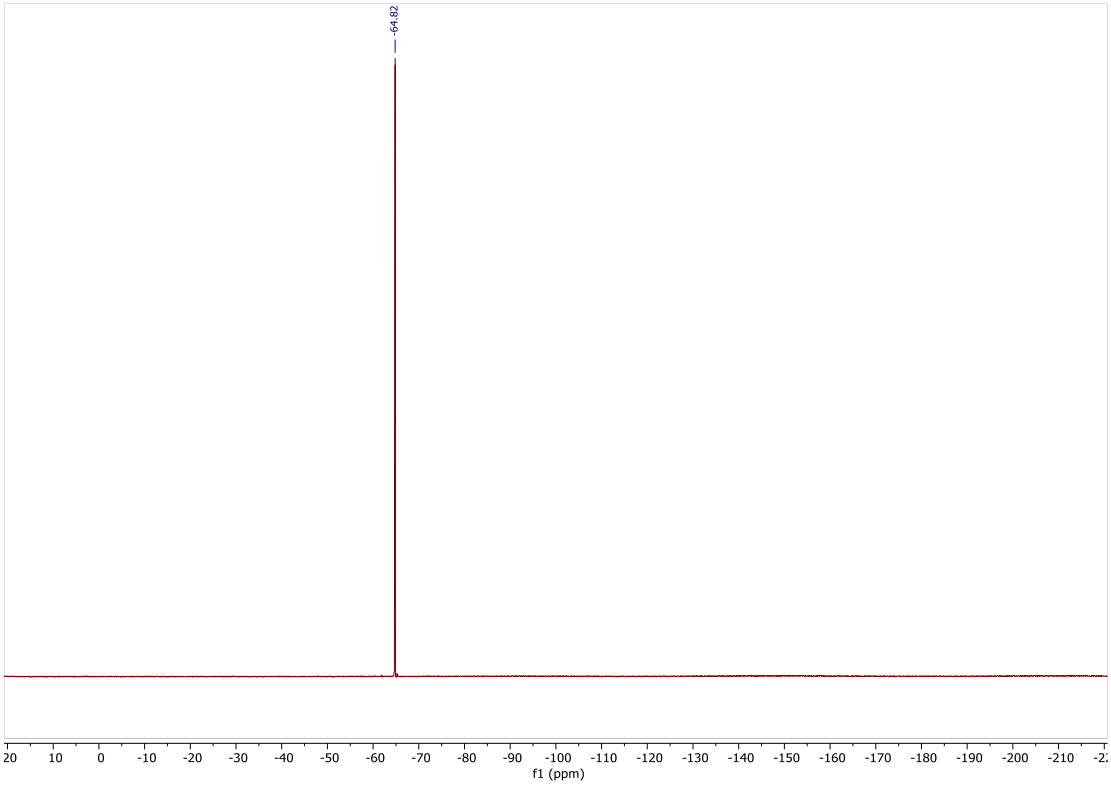
-64.82
20 10 0 -10 -20 -30 -40 -50 -60 -70 -80 -90 -100 -110 -120 -130 -140 -150 -160 -170 -180 -190 -200 -210
f1 (ppm)

N-(6-(4-(trifluoromethyl)pyridin-2-yl)hexyl)pivalamide

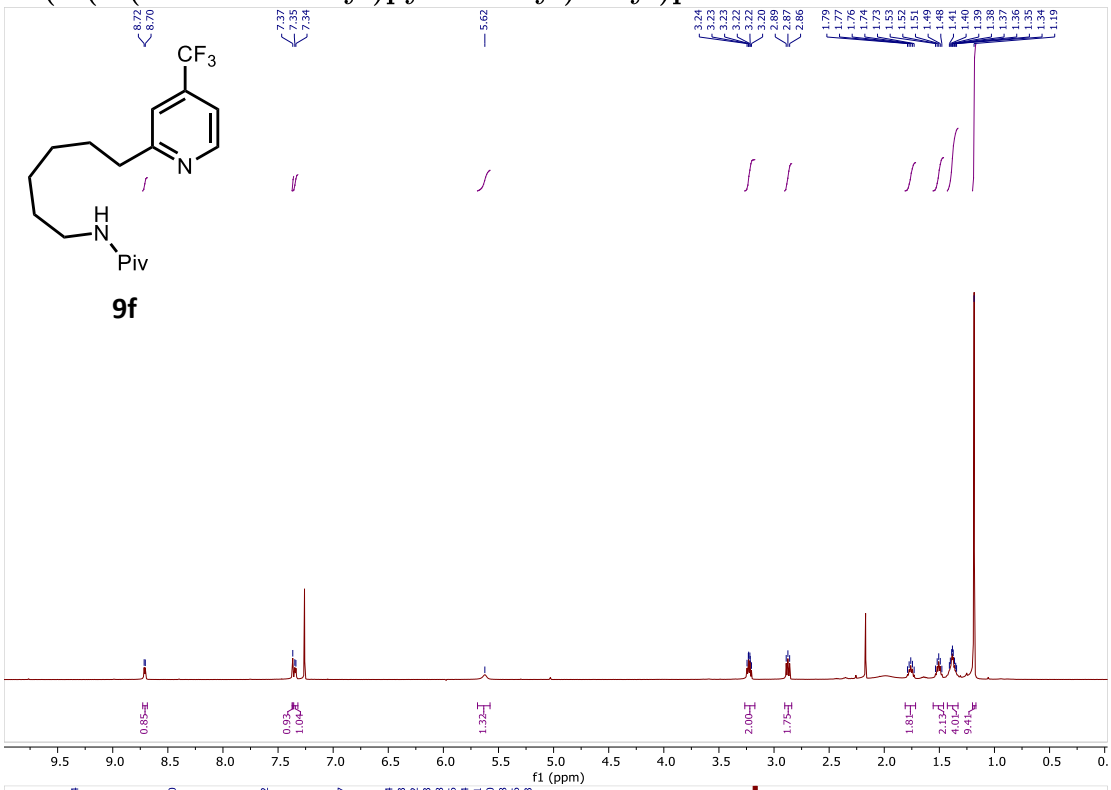

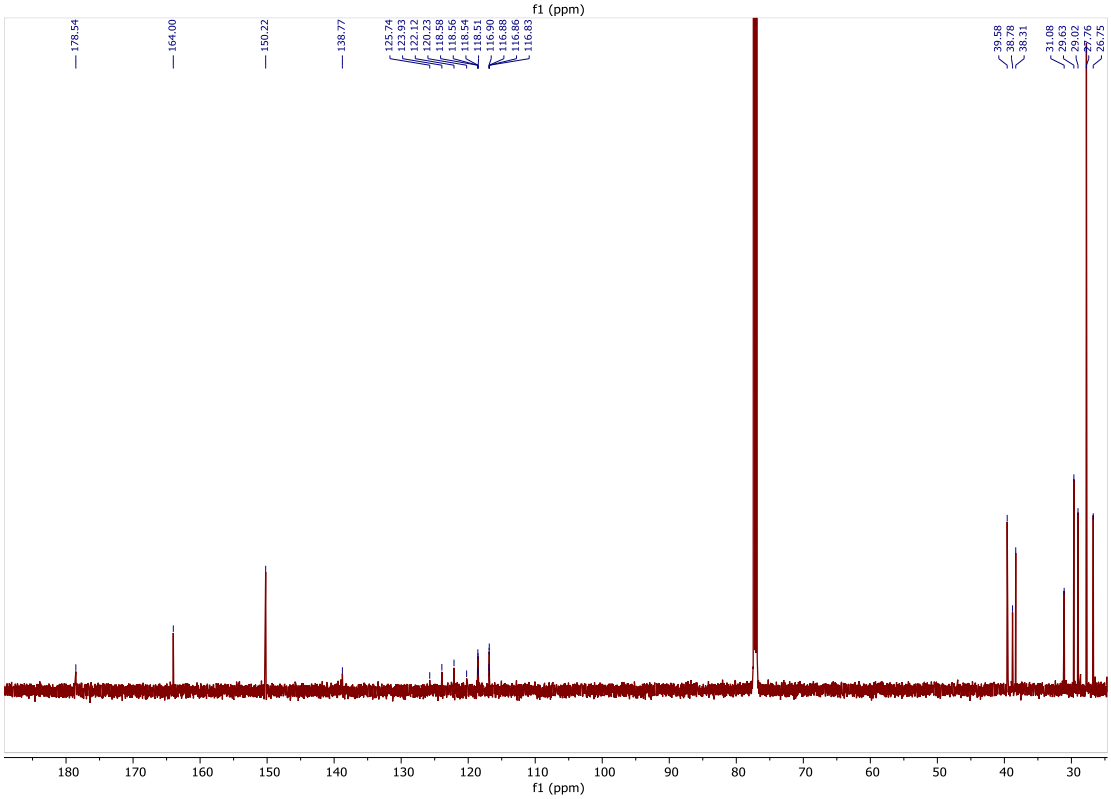

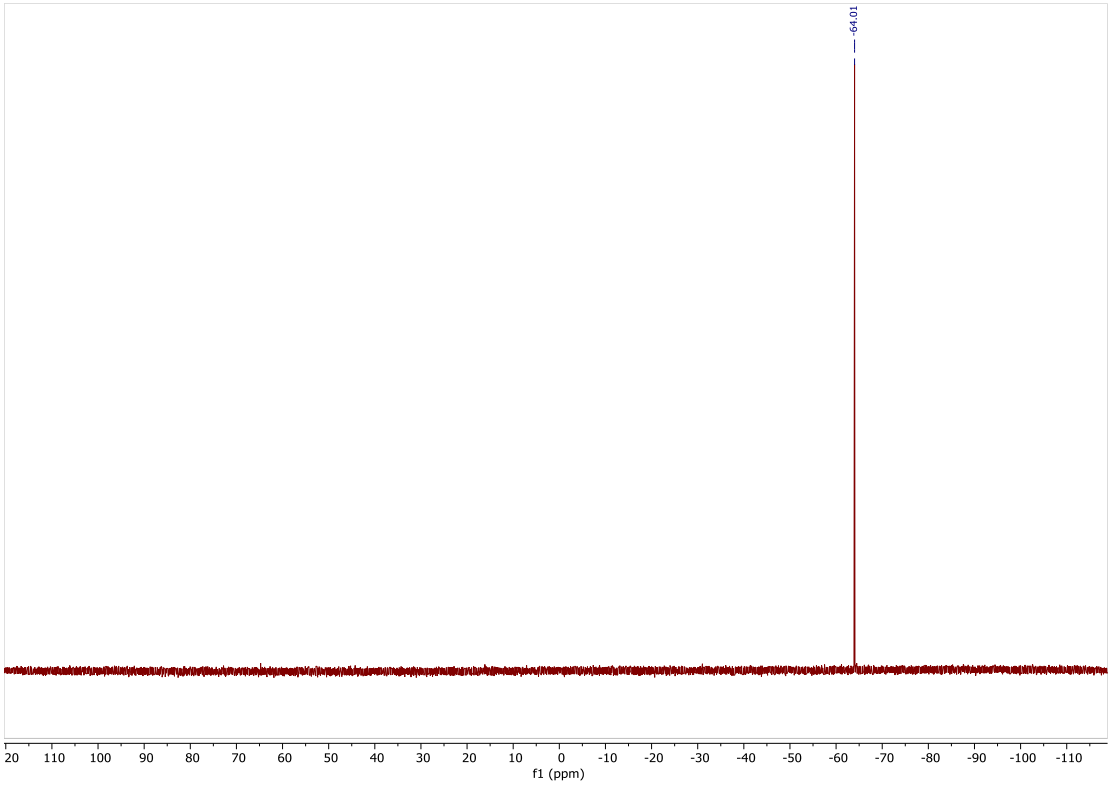
-64.01
20 110 100 90 80 70 60 50 40 30 20 10 0 -10 -20 -30 -40 -50 -60 -70 -80 -90 -100 -110
f1 (ppm)

N-(5-(4-(trifluoromethyl)pyridin-2-yl)pentan-2-yl)pivalamide

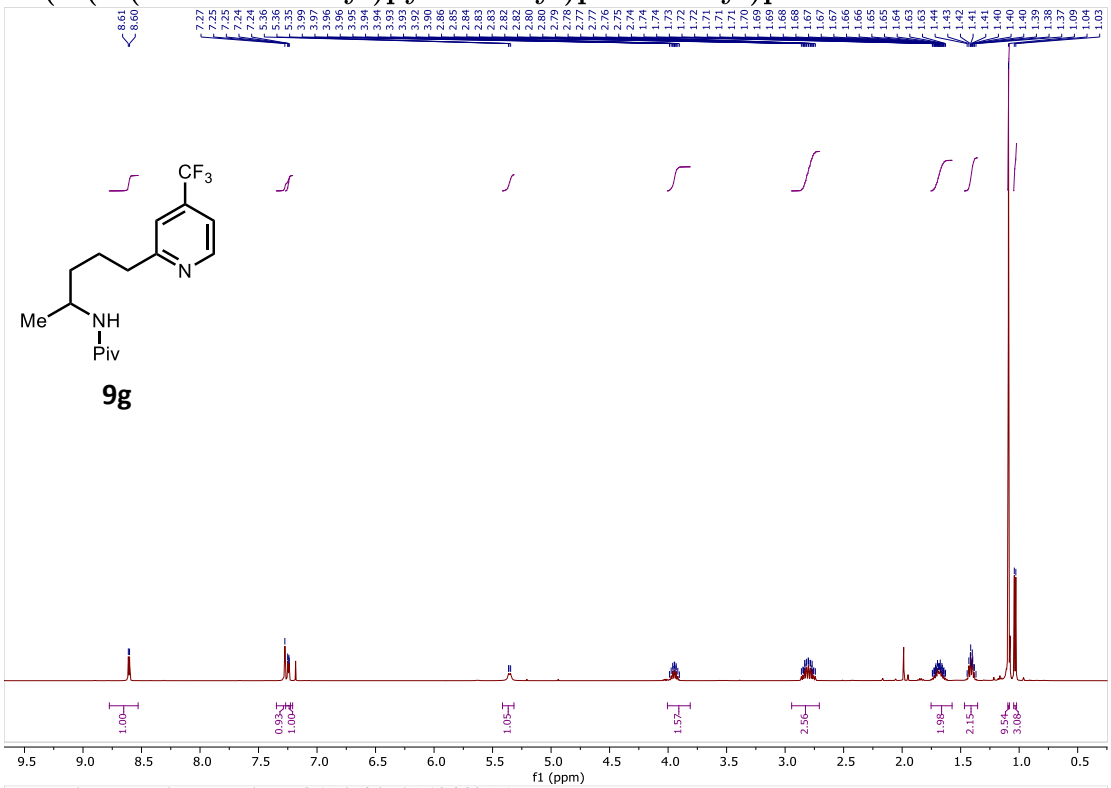

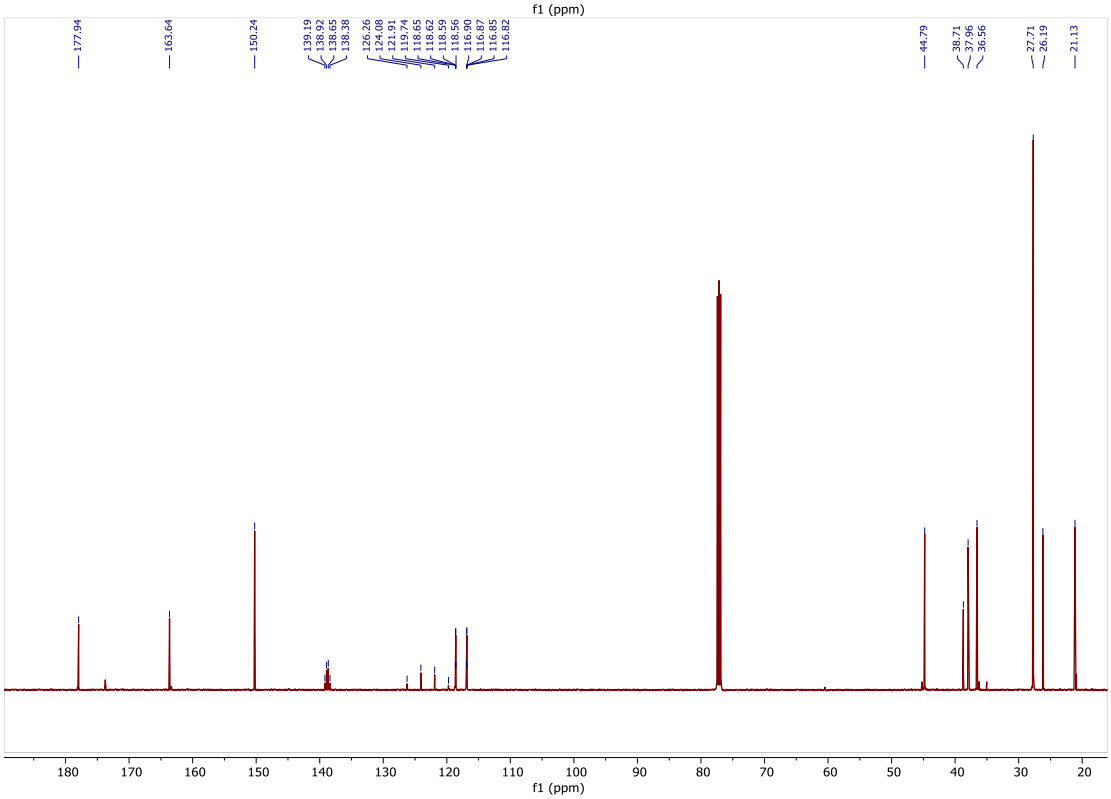

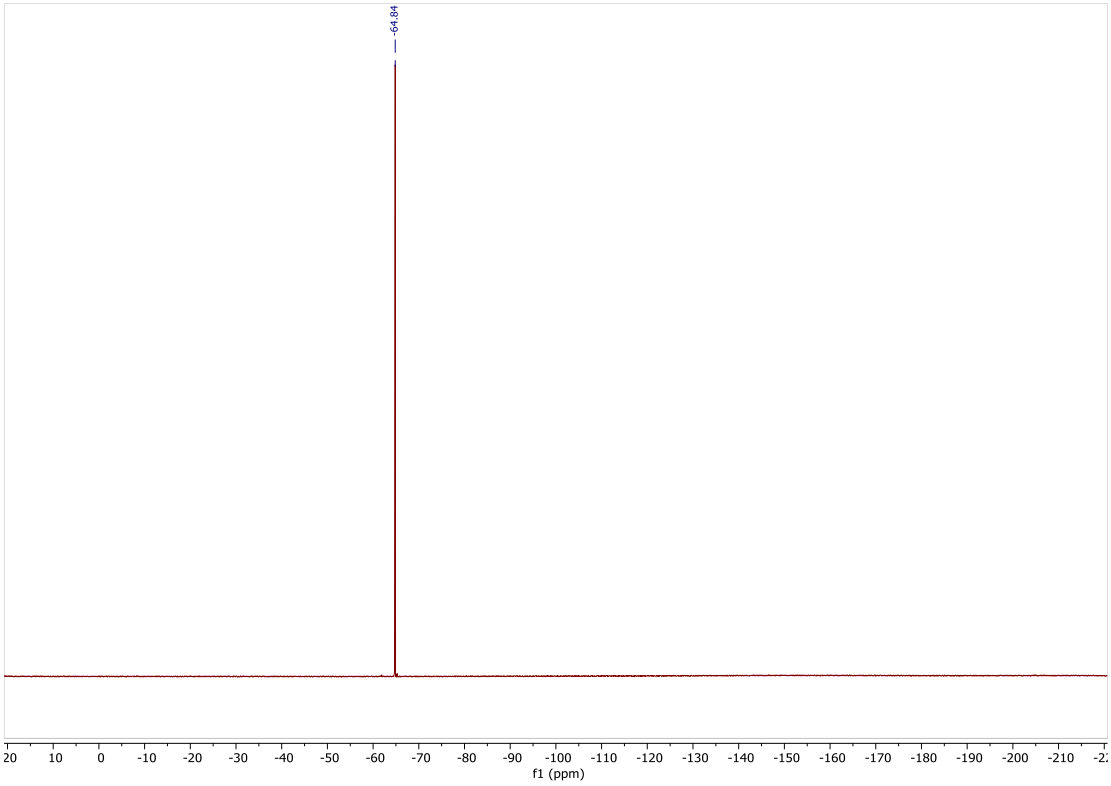
-64.84
20 10 0 -10 -20 -30 -40 -50 -60 -70 -80 -90 -100 -110 -120 -130 -140 -150 -160 -170 -180 -190 -200 -210
f1 (ppm)

NMR Spectra – Autocyclization Products

2-(*tert*-butyl)-5,6-dihydro-4*H*-1,3-oxazine

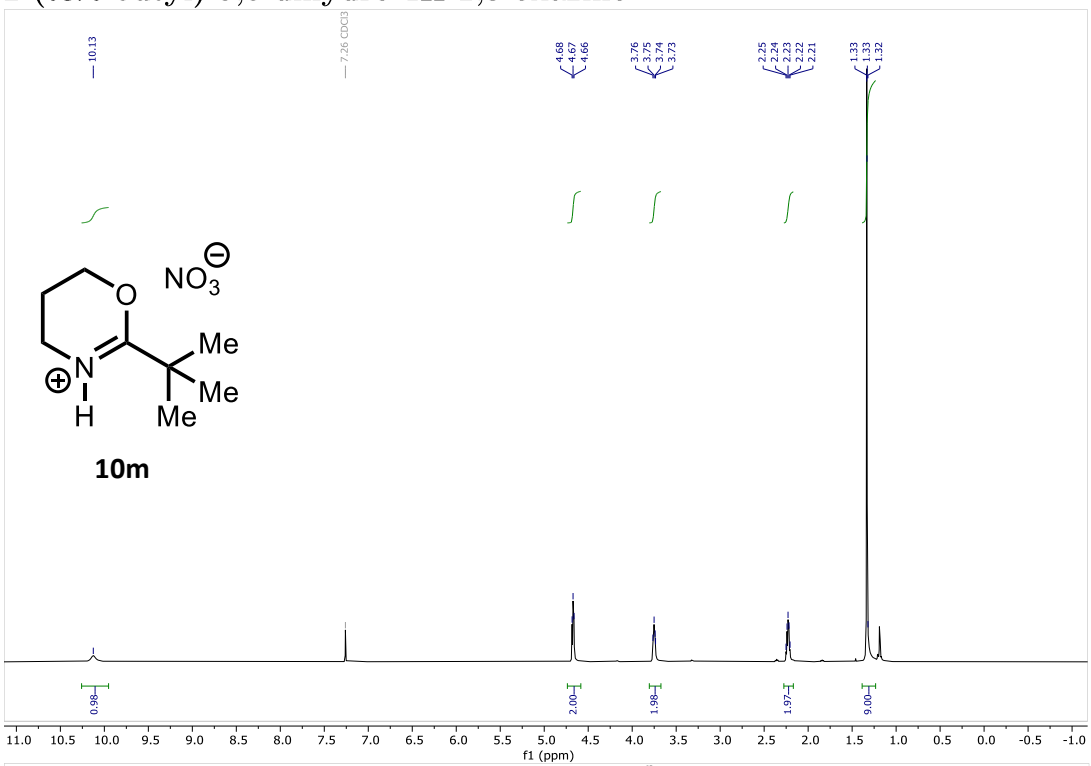

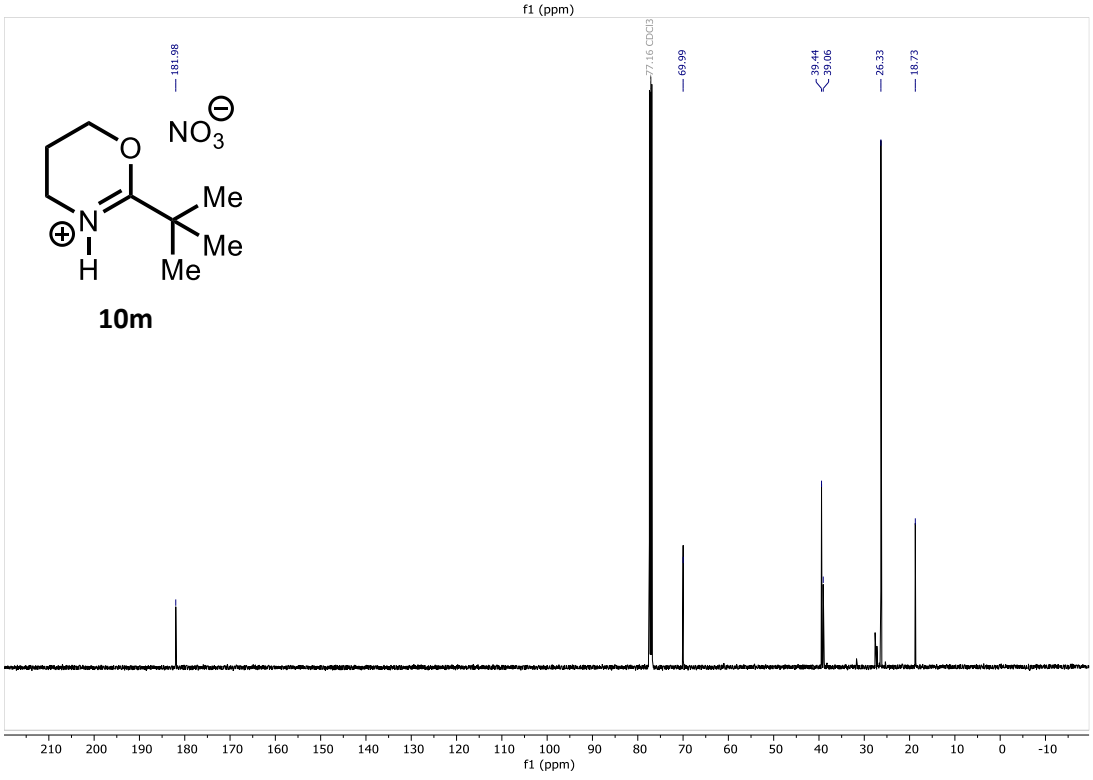

2-phenyl-5,6-dihydro-4*H*-1,3-oxazine

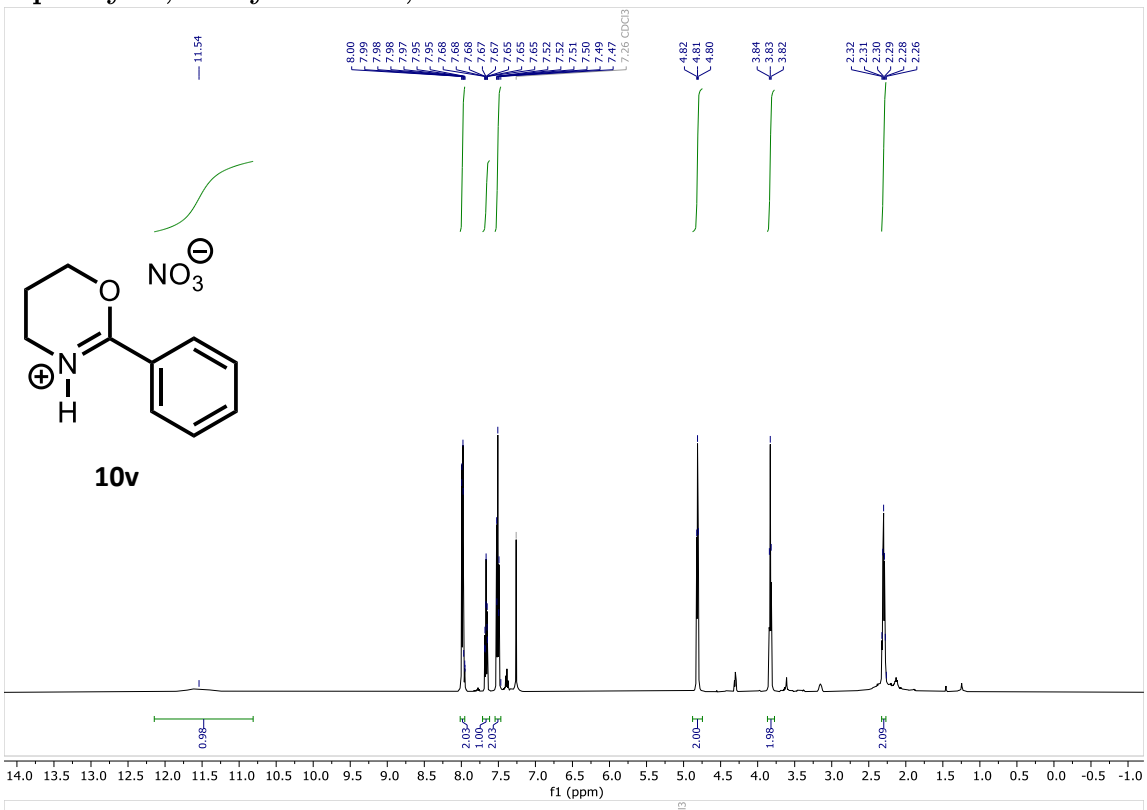

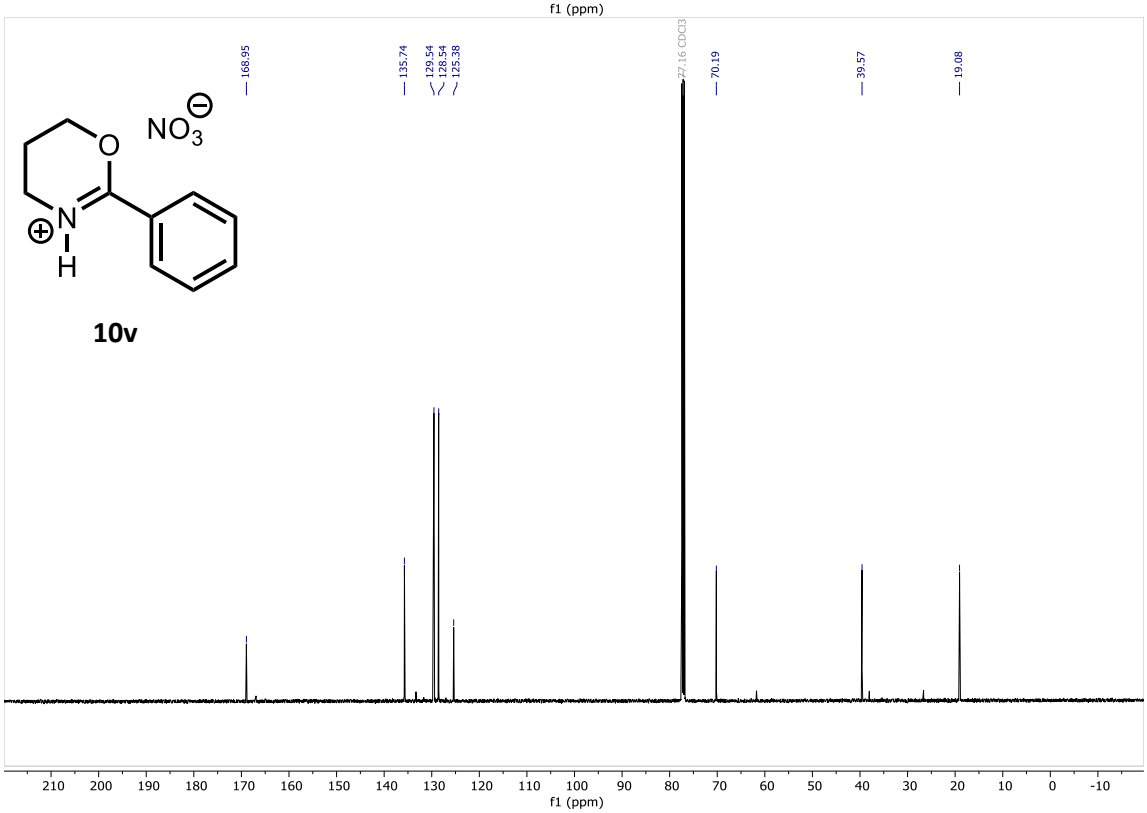

Computational Coordinates and Vibrational Frequencies

Table 2.4.8: Cartesian coordinates of the optimized geometries for the autocyclization process. The cartesian coordinates of optimized geometries are given below in the standard XYZ format, and units are in Å.

$Cu^{I}(H_2O)_2$			
Cu	-0.000001	-0.015904	-0.000001
O	-1.916053	-0.041990	0.045146
H	-2.466433	-0.497143	-0.607432
H	-2.459021	0.619412	0.496257
O	1.916053	-0.041999	-0.045135
H	2.459003	0.619319	-0.496388
H	2.466446	-0.497008	0.607532

H_2O			
O	0.000000	0.000000	0.119237
H	0.000000	0.759322	-0.476819
H	0.000000	-0.759322	-0.476819

H_3O^+			
O	-0.000003	0.000000	-0.070534
H	-0.479665	-0.817077	0.187333
H	-0.467790	0.823925	0.187333
H	0.947428	-0.006848	0.187344

CO			
C	0.000000	0.000000	-0.650254
O	0.000000	0.000000	0.487690

11			
C	-0.643701	2.688618	0.315671
C	-1.731084	1.806837	-0.110986
H	-3.916441	-1.014316	0.481151
N	1.556332	1.664027	-0.133181
C	0.638462	2.718980	-0.543607
C	2.561999	-1.604793	-0.978134
C	2.227635	-0.696826	0.230147
C	1.274533	0.377327	-0.255007
C	3.518959	-0.104202	0.818534
C	1.477039	-1.511548	1.313316
O	0.167627	0.062695	-0.839786
H	-0.429938	2.611425	1.387534
H	-1.126373	3.687038	0.198105
H	-1.942717	1.729989	-1.179628
H	-2.576872	1.676123	0.562794
H	0.391375	2.599735	-1.602309
H	1.151854	3.671224	-0.413376
H	3.092530	-1.053594	-1.759043
H	3.207509	-2.418326	-0.639712
H	1.659031	-2.039289	-1.412205
H	4.172877	-0.919528	1.134983
H	4.081257	0.476324	0.079128
H	3.330995	0.510282	1.706290
H	2.143154	-2.284849	1.703191
H	0.599575	-2.016477	0.897537
H	1.175808	-0.882576	2.158696
O	-3.174503	-0.569526	0.922679
Cu	-1.455840	-0.366317	-0.046435
O	-1.520679	-2.324635	-0.822258
H	-1.869974	-3.162916	-0.487339
H	-0.963454	-2.535235	-1.585888
H	2.446529	1.920672	0.280592
H	-3.227755	-0.781899	1.868409

11-TS'			
C	2.211283	-0.831218	0.428157
C	2.350518	0.487886	0.004497
H	0.483978	3.976199	0.408292
N	0.165381	-2.077492	-0.115260
C	1.557296	-1.877891	-0.486647
C	-3.071010	-1.284074	-1.187728
C	-2.226441	-1.464650	0.096619
C	-0.785180	-1.150368	-0.276482
C	-2.401565	-2.891425	0.642945
C	-2.666525	-0.438515	1.165127
O	-0.468801	-0.034211	-0.788835
H	2.049384	-0.987997	1.498865
H	3.479207	-1.116543	0.335396
H	2.433203	0.707005	-1.059764
H	2.655517	1.269926	0.697336

H	1.618033	-1.552656	-1.529320
H	2.065544	-2.838362	-0.395598
H	-2.785254	-2.006155	-1.957733
H	-4.124074	-1.447259	-0.946401
H	-2.958704	-0.278007	-1.596854
H	-3.455133	-3.056338	0.878352
H	-2.125222	-3.653774	-0.093724
H	-1.843383	-3.056633	1.571780
H	-3.706482	-0.629786	1.439742
H	-2.600419	0.580318	0.777023
H	-2.061853	-0.518516	2.075225
O	1.139631	3.334334	0.084389
Cu	0.156281	1.637844	-0.196014
O	-1.527462	2.971804	0.507495
H	-1.963245	2.872683	1.367039
H	-2.230851	3.214381	-0.113828
H	-0.110200	-2.974256	0.264988
H	1.662124	3.778281	-0.600528
O	4.663016	-1.846890	0.280270
H	5.124345	-2.002471	1.120927
H	5.329462	-1.607226	-0.384639

==========

12

==========

C	-1.281993	1.785136	0.681301
C	-2.608470	1.753735	0.328333
H	-2.697062	-2.320667	-0.704102
N	1.091111	1.602308	-0.057207
C	-0.192546	2.283750	-0.248026
C	3.049685	-0.989119	-1.370055
C	2.708777	-0.278654	-0.038647
C	1.282794	0.277317	-0.175507
C	3.758999	0.807004	0.260289
C	2.684429	-1.308049	1.117832
O	0.333945	-0.515367	-0.400809
H	-0.998648	1.666544	1.725898
H	-2.942685	2.053520	-0.659692
H	-3.376164	1.600921	1.077290
H	-0.515543	2.198858	-1.294582
H	-0.009041	3.340843	-0.044024
H	3.085139	-0.274344	-2.207931
H	4.031290	-1.459453	-1.291861
H	2.303496	-1.759739	-1.601166
H	4.745522	0.341879	0.350133
H	3.833256	1.545950	-0.548629
H	3.567821	1.329513	1.209077
H	3.679515	-1.745482	1.237775
H	1.990796	-2.130379	0.897641
H	2.403710	-0.845626	2.071282
O	-2.874882	-1.455946	-1.118237
Cu	-1.697373	-0.151969	-0.025519
O	-1.354717	-2.087545	1.090559
H	-1.476459	-2.278975	2.029229
H	-0.401951	-2.121285	0.913105
H	1.902608	2.177832	0.095796
H	-2.766378	-1.572837	-2.073976

==========

olefin

==========

C	2.946537	0.009109	-0.502506
C	4.116289	0.584329	-0.222507
N	0.707200	0.103518	0.479392
C	2.008584	-0.550683	0.535695
C	-2.789904	-0.414465	0.861194
C	-1.726189	0.271425	-0.024536
C	-0.429307	-0.557392	0.097167
C	-1.575630	1.744428	0.389585
C	-2.160057	0.190793	-1.509472
O	-0.432459	-1.763622	-0.143479
H	2.607965	-0.074213	-1.538700
H	4.470387	0.682687	0.807213
H	4.768835	0.970782	-1.002447
H	1.805193	-1.616405	0.350055
H	2.441413	-0.449790	1.540356
H	-2.518134	-0.342799	1.922135
H	-3.761933	0.063827	0.724903
H	-2.868396	-1.471832	0.597862
H	-2.543039	2.254677	0.297297
H	-1.255499	1.842338	1.434312
H	-0.866034	2.281561	-0.249299
H	-3.122197	0.687055	-1.648305
H	-2.252153	-0.857133	-1.815722
H	-1.424548	0.674692	-2.163712
H	0.679484	1.103636	0.602416

==========

10m

==========

C	-2.699482	-0.055645	0.421723
C	-2.008492	-1.238029	-0.228435
N	-0.655543	1.149285	-0.138839
C	-2.129494	1.237346	-0.151444
C	2.072951	-0.790560	-1.188204
C	1.543031	0.006776	0.027662
C	0.032262	0.034120	-0.067526
C	2.134264	1.425327	0.027381
C	1.910454	-0.721244	1.343505
O	-0.550683	-1.130651	-0.070758
H	-2.553213	-0.087610	1.505671
H	-3.773768	-0.109228	0.229696

H	-2.195542	-1.296473	-1.303844
H	-2.256336	-2.190931	0.235797
H	-2.459824	1.407246	-1.180832
H	-2.413313	2.104756	0.447351
H	1.817945	-0.298938	-2.131681
H	3.161715	-0.847335	-1.120476
H	1.675862	-1.806979	-1.201352
H	3.221071	1.351808	0.098354
H	1.915941	1.967583	-0.899500
H	1.800939	2.015757	0.887990
H	2.998829	-0.775047	1.419421
H	1.513509	-1.737597	1.360130
H	1.536293	-0.180712	2.217915
H	-0.120983	2.009325	-0.147260

Vibrational Frequencies of the Optimized Geometries

Table 2.4.9: Vibrational Frequencies (in cm^{-1}) of the Optimized Geometries for the autocyclization reaction.

==========

$Cu^{I}(H_2O)_2$

==========

114.12 114.21 132.46 183.89 185.02 378.55
509.56 618.25 619.05 1648.19 1649.56 3799.01
3802.21 3894.29 3894.30

==========

H_2O

==========

1665.28 3799.59 3912.80

==========

H_3O^+

==========

783.27 1668.62 1668.78 3583.76 3702.64 3702.85

==========

CO

==========

2208.63

11

==========

18.13 29.01 55.98
65.38 71.43 101.43 116.88 147.15 163.26
174.39 202.14 209.89 226.45 256.30 259.21
264.10 295.26 303.91 317.65 324.01 329.69
352.86 367.67 377.43 388.66 402.64 437.66
476.54 522.46 535.21 579.93 630.16 686.56
717.96 745.76 790.16 793.10 853.82 907.26
940.62 951.46 975.18 978.01 999.07 1041.18
1047.37 1068.37 1112.31 1157.49 1203.71 1222.35
1236.56 1248.52 1297.61 1333.98 1380.28 1383.68
1409.76 1411.19 1414.43 1451.52 1480.15 1490.11
1493.11 1493.66 1498.51 1515.59 1523.78 1532.91
1542.64 1614.65 1647.59 1652.46 2897.29 3044.02
3047.55 3069.33 3090.21 3101.65 3113.24 3116.47
3118.06 3144.47 3148.34 3148.97 3156.41 3173.35
3228.90 3589.29 3752.80 3785.31 3844.54 3882.39

==========

11-TS'

==========

-385.93 19.72 26.83
48.44 58.52 66.12 75.67 86.56 100.66
116.18 117.63 124.22 155.24 183.79 207.77
219.26 241.19 250.99 276.97 286.93 298.89
317.04 325.03 329.88 336.14 373.59 382.70
398.99 417.99 426.88 438.53 444.48 456.86
508.94 535.22 557.06 585.71 647.52 651.80
689.97 726.93 784.28 794.71 867.42 909.04
944.17 948.76 954.09 978.67 1000.67 1028.99

1047.90 1056.79 1069.55 1124.49 1150.66 1228.43
1241.22 1258.20 1284.30 1301.74 1333.50 1391.03
1394.63 1410.16 1414.96 1444.13 1450.81 1487.41
1493.01 1500.36 1502.15 1515.77 1525.31 1537.83
1573.46 1593.19 1611.88 1640.01 1651.03 1657.67
3042.81 3054.25 3067.40 3089.78 3112.47 3115.47
3131.14 3134.33 3143.47 3146.19 3151.94 3157.25
3159.92 3241.20 3616.55 3735.20 3738.19 3775.42
3846.29 3847.08 3869.92

==========

12

==========

42.43 50.49 62.40 77.49 82.56 98.25
115.27 154.10 159.29 204.27 233.34 245.74
267.06 274.49 290.77 301.04 311.06 320.50
331.48 338.27 348.67 363.04 370.95 385.27
401.00 408.53 470.12 519.46 532.62 541.43
544.73 609.00 642.61 670.00 776.79 800.04
861.50 899.74 943.80 947.61 953.87 985.23
1000.31 1022.36 1044.21 1051.13 1078.33 1149.13
1231.76 1242.58 1257.77 1282.81 1292.96 1322.66
1363.15 1411.70 1418.33 1448.79 1450.75 1487.18
1495.02 1503.59 1508.93 1517.94 1527.19 1540.45
1576.54 1600.22 1612.37 1641.13 1664.75 3011.05
3016.04 3031.40 3042.44 3080.77 3088.81 3100.37
3117.58 3121.89 3129.08 3148.04 3172.07 3177.46
3273.95 3680.40 3709.25 3765.64 3845.85 3893.26

==========

olefin

==========

47.26 65.69 71.56 140.68 222.72 231.00
266.03 282.90 301.80 311.65 337.97 366.71
371.12 392.10 443.49 510.83 520.93 579.90
689.28 771.00 792.14 871.36 934.72 938.41
951.82 964.24 973.17 1014.14 1044.65 1049.53
1050.62 1084.69 1167.89 1215.66 1233.08 1260.38
1278.60 1305.71 1323.90 1378.48 1400.77 1406.54
1438.62 1468.14 1490.65 1500.43 1509.40 1510.63
1513.89 1524.40 1542.62 1547.12 1727.08 1747.89
3015.95 3022.68 3036.66 3040.68 3063.36 3087.88
3099.57 3106.90 3108.41 3117.10 3124.06 3139.57
3150.67 3206.54 3658.62

==========

10m

==========

31.59 103.02 168.25
210.50 216.41 263.41 269.85 311.59 313.90
332.52 339.11 387.92 468.20 503.70 516.07
603.90 700.19 755.17 793.35 841.03 878.75
899.97 920.17 942.21 956.11 974.55 979.70
1047.43 1050.63 1074.49 1093.94 1145.74 1224.14
1227.35 1238.21 1250.33 1263.27 1306.28 1326.15
1358.07 1401.90 1410.84 1415.09 1419.19 1454.40
1492.08 1493.12 1499.23 1502.44 1505.32 1516.05
1522.11 1524.91 1538.94 1570.20 1680.90 3041.73
3063.01 3065.20 3080.64 3085.79 3100.84 3111.28

3138.80 3140.50 3141.46 3146.29 3148.03 3158.76
3162.39 3182.76 3609.13

References

(1) Blakemore, D. C.; Castro, L.; Churcher, I.; Rees, D. C.; Thomas, A. W.; Wilson, D. M.; Wood, A. *Nat. Chem.* **2018**, *10*, 383–394.

(2) Gerry, C. J.; Schreiber, S. L. *Nat. Rev. Drug Discov.* **2018**, *17*, 333–352.

(3) Brown, D. G.; Boström, J. *J. Med. Chem.* **2016**, *59*, 4443–4458.

(4) Campos, K. R.; Coleman, P. J.; Alvarez, J. C.; Dreher, S. D.; Garbaccio, R. M.; Terrett, N. K.; Tillyer, R. D. *Science* **2019**, *363*, eaat0805.

(5) Vitaku, E.; Smith, D. T.; Njardarson, J. T. *J. Med. Chem.* **2014**, *57*, 10257–10274.

(6) Shearer, J.; Castro, J. L.; Lawson, A. D. G.; MacCoss, M.; Taylor, R. D. *J. Med. Chem.* **2022**, *65*, 8699–8712.

(7) Roque, J. B.; Kuroda, Y.; Göttemann, L. T.; Sarpong, R. *Science* **2018**, *361*, 171–174.

(8) Roque, J. B.; Kuroda, Y.; Göttemann, L. T.; Sarpong, R. *Nature* **2018**, *564*, 244–248.

(9) Jurczyk, J.; Lux, M. C.; Adpressa, D.; Kim, S. F.; Lam, Y.; Yeung, C. S.; Sarpong, R. *Science* **2021**, *373*, 1004–1012.

(10) Huigens, R. W.; Morrison, K. C.; Hicklin, R. W.; T. A. Flood, J.; Richter, M. F.; Hergenrother, P. J. *Nat. Chem.* **2013**, *5*, 195–202.

(11) Hu, Y.; Stumpfe, D.; Bajorath, J. *J. Med. Chem.* **2017**, *60*, 1238–1246.

(12) Sun, H.; Tawa, G.; Wallqvist, A. *Drug Discov. Today* **2012**, *17*, 310–324.

(13) Liu, R.-H.; He, Y.-H.; Yu, W.; Zhou, B.; Han, B. *Org. Lett.* **2019**, *21*, 4590–4594.

(14) Minisci, F.; Citterio, A.; Giordano, C. *Acct. Chem. Res.* **1983**, *16*, 27–32.

(15) Mare, H. E. D. L.; Kochi, J. K.; Rust, F. F. *J. Am. Chem. Soc.* **1963**, *85*, 1437–1449.

(16) Kochi, J. K. *Science* **1967**, *155*, 415–424.

(17) Reddy, D. N.; Prabhakaran, E. N. *J. Org. Chem.* **2010**, *76*, 680–683.

(18) Roque, J. B.; Sarpong, R.; Musaev, D. G. *J. Am. Chem. Soc.* **2021**, *143*, 3889–3900.

(19) Gu, Q.-S.; Li, Z.-L.; Liu, X.-Y. *Acc. Chem. Res.* **2019**, *53*, 170–181.

(20) Li, Z.-L.; Fang, G.-C.; Gu, Q.-S.; Liu, X.-Y. *Chem. Soc. Rev.* **2020**, *49*, 32–48.

(21) DiMucci, I. M.; Lukens, J. T.; Chatterjee, S.; Carsch, K. M.; Titus, C. J.; Lee, S. J.; Nordlund, D.; Betley, T. A.; MacMillan, S. N.; Lancaster, K. M. *J. Am. Chem. Soc.* **2019**, *141*, 18508–18520.

(22) Zhuo, L.-G.; Liao, W.; Yu, Z.-X. *Asian J. Org. Chem.* **2012**, *1*, 336–345.

(23) Xie, W.; Zhao, M.; Cui, C. *Organometallics* **2013**, *32*, 7440–7444.

(24) Rao, Y.; Li, X.; Danishefsky, S. J. *J. Am. Chem. Soc.* **2009**, *131*, 12924–12926.

(25) Otani, Y.; Nagae, O.; Naruse, Y.; Inagaki, S.; Ohno, M.; Yamaguchi, K.; Yamamoto, G.; Uchiyama, M.; Ohwada, T. *J. Am. Chem. Soc.* **2003**, *125*, 15191–15199.

(26) Parr, R. G.; Weitao, Y., *Density-Functional Theory of Atoms and Molecules (International Monographs on Chemistry #16)*; Oxford University Press: New York, 1995.

(27) Frisch, M. J. et al., *Gaussian 09*; Revision D.01: 2013.

(28) Becke, A. D. *Phys. Rev. A* **1988**, *38*, 3098–3100.

(29) Lee, C.; Yang, W.; Parr, R. G. *Phys. Rev. B* **1988**, *37*, 785–789.

(30) Grimme, S.; Antony, J.; Ehrlich, S.; Krieg, H. A. *J. Chem. Phys.* **2010**, *132*, 154104.

(31) Slater, J. C., *Quantum Theory of Molecules and Solids, Vol. 4.* McGraw-Hill: New York, NY, 1974.

(32) Vosko, S. H.; Wilk, L.; Nusair, M. *Can. J. Phys.* **1980**, *58*, 1200–1211.

(33) Becke, A. D. *J. Chem. Phys.* **1993**, *98*, 5648–5652.

(34) Grimme, S.; Ehrlich, S.; Goerigk, L. *J. Comput. Chem.* **2011**, *32*, 1456–1465.

(35) Ditchfield, R.; Hehre, W. J.; Pople, J. A. *J. Chem. Phys.* **1971**, *54*, 724–728.

(36) Hehre, W. J.; Pople, J. A. *J. Chem. Phys.* **1972**, *56*, 4233–4234.

(37) Binkley, J. S.; Pople, J. A. *J. Chem. Phys.* **1977**, *66*, 879–880.

(38) Hariharan, P. C.; Pople, J. A. *Theor. Chim. Acta* **1973**, *28*, 213–222.

(39) Hehre, W. J.; Ditchfield, R.; Pople, J. A. *J. Chem. Phys.* **1972**, *56*, 2257–2261.

(40) Francl, M. M.; Pietro, W. J.; Hehre, W. J.; Binkley, J. S.; Gordon, M. S.; DeFrees, D. J.; Pople, J. A. *J. Chem. Phys.* **1982**, *77*, 3654–3665.

(41) Hay, P. J.; Wadt, W. R. *J. Chem. Phys.* **1985**, *82*, 270–283.

(42) Clark, T.; Chandrasekhar, J.; Spitznagel, G. W.; Schleyer, P. V. R. *J. Comput. Chem.* **1983**, *4*, 294–301.

(43) Frisch, M. J.; Pople, J. A.; Binkley, J. S. *J. Chem. Phys.* **1984**, *80*, 3265–3269.

(44) Krishnan, R.; Binkley, J. S.; Seeger, R.; Pople, J. A. *J. Chem. Phys.* **1980**, *72*, 650–654.

(45) McLean, A. D.; Chandler, G. S. *J. Chem. Phys.* **1980**, *72*, 5639–5648.

(46) Küchle, W.; Dolg, M.; Stoll, H.; Preuss, H. *J. Chem. Phys.* **1994**, *100*, 7535–7542.

(47) Cancès, E.; Mennucci, B.; Tomasi, J. *J. Chem. Phys.* **1997**, *107*, 3032–3041.